Suspended sediment behaviour of a reallocation pilot study in the port of Rotterdam

Gaining insight into the dynamics of a sediment reallocation pilot study, using model hindcasts and measurements

D.Deckers

TU Delft Delft University of Technology

Port of Rotterdam

Suspended sediment behaviour of a reallocation pilot study in the port of Rotterdam

Gaining insight into the dynamics of a sediment reallocation pilot study, using model hindcasts and measurements

by

D. (Daan) Deckers

in partial fulfillment of the requirements to obtain the degree of
Master of Science
in Hydraulic Engineering

at the Delft University of Technology,

to be defended publicly on Thursday October 8, 2020 at 13:00.

Student number:	4213297	
Project duration:	October, 2019 - October, 2020	
Thesis committee:	Prof. dr. ir. J. D. Pietrzak,	TU Delft
	ir. L. Hulsen,	Port of Rotterdam
	dr. A. Kirichek,	Deltares
	dr. C. Chassagne,	TU Delft
	dr. ir. M. A. de Schipper	TU Delft

An electronic version of this thesis is available at `http://repository.tudelft.nl/`.

TU Delft

Port of Rotterdam

Abstract

The port of Rotterdam is located within the Rhine-Meuse estuary where a substantial amount of fine sediment transport takes place. Therefore, the port of Rotterdam is subject to significant siltation, requiring maintenance dredging to guarantee a sufficient nautical depth of fairways and harbour basins.

To optimise the dredging strategy in the port of Rotterdam, a pilot study has been carried out wherein sediment is reallocated in the Rotterdam Waterway, during ebb, instead of offshore in the North Sea. Between May and November 2019, 210,000 tons of sediment has been reallocated. This pilot study has been carried out in the context of the larger EU-Interreg Sediment Uses as Resources in Circular and Territorial Economies (*SURICATES*) project. The main goals are to re-use the sediment as a resource and to reduce the sailing time of the dredging vessels. Both ideas comply with the Building with Nature philosophy; a concept gaining popularity over recent years in The Netherlands focusing on, amongst others the optimisation of dredging strategies [Baptist et al., 2017, Van Eekelen et al., 2016]. It is expected that the reallocated sediment is mainly transported offshore, while at the same time some of the sediment will nourish the river banks of the Rotterdam Waterway enhancing its flood resilience.

This thesis focuses on understanding the fine sediment behaviour of the SURICATES pilot project on two different scales. This is done by analysing measurements and model hindcasts. The measurement campaign is set-up by *Deltares* and the *Port of Rotterdam*. For the model hindcasts an operational hydrodynamic and sediment model is used. On the small scale this is done by focusing on the behaviour of a single disposal over a tidal cycle. The large scale focuses on the cumulative long term behaviour of all sediment reallocations.

For the small scale two measurement surveys are analysed. In both surveys it is found that a sediment reallocation executed by bow coupling is subject to mixing up to halfway the water column. Subsequently, the sediment plume is advected around and below the pycnocline. Further measurements in the mid field are lacking, but it is hypothesised that the majority of the sediment settles during subsequent low water slack. For the other execution method, drawing the bottom doors, which is used to reallocate the majority of the sediment, useful measurement are absent. It is hypothesised that the majority of this reallocated sediment is confined in the salt wedge and therefore mainly transported upstream over time.

To assess the long term behaviour of the cumulative behaviour of all sediment reallocations, a different measurement campaign is set-up. In this measurement campaign, bed samples are collected prior to and during the pilot study to determine the change of the bed composition. In this campaign an indication for increased sedimentation related to the pilot study is found for nearly all the sample locations.

The short term model study is set-up to enhance the understanding of the short term behaviour of a sediment plume, to derive an accurate source term for the sediment disposals and to carry out a sensitivity analysis. This sensitivity analysis is executed to derive the influence of differences in disposal method, timing of disposal, and uncertainties in the model. It is found that the execution method has the largest influence on the critical sediment fluxes on the short term, followed by the timing of disposal.

From the long term model hindcast, in which the entire pilot study is hindcasted, it is found that 27% of the total amount of reallocated sediment flows downstream from the location of disposal and 73% upstream. These estimations are in line with the hypothesis and long term measurement results, but a thorough calibration of the results is lacking.

To conclude, in this thesis a pilot study utilising a different sediment reallocation strategy in the port of Rotterdam has been investigated. This study shows that majority of the sediment disposed, in the current set-up of the pilot study, is estimated to flow upstream. In the sensitivity analysis, it is predicted that this might be caused by the timing of disposal or method of execution. It is also found that the initial behaviour of the sediment plume and the long term measurement contain a large amount of uncertainties. As most important recommendation for future work an expansion of the current measurement survey is proposed with at least two fixed locations: one downstream and one upstream of the location of disposal. In this way sediment fluxes can be established, which can also be used to verify and calibrate the sediment model.

Preface

In front of you lies my master thesis concluding seven very pleasant years at Delft University of Technology, characterised by valuable experiences inside and outside of my studies. I would like to use this preface to reflect on those seven years and to thank the people who made this possible.

When looking for a study I wanted to combine physics and mathematics from a practical point of view, work on large projects and this all preferably in an international setting; logically I started to study Civil Engineering. And this study, the university and Delft as city didn't disappoint me. The atmosphere in Delft encouraged me to seek opportunities outside my studies, such as working in committees and to be in charge of an association during a full time board year. Next to this, TU Delft and Civil Engineering encourages students to go abroad. Over the years I took these opportunities with both hands, allowing me to work in Indonesia, Argentina and Peru on a wide range of projects, gaining valuable experience abroad. Within my studies I discovered a particular interest in understanding natural systems: coastal regions, estuaries and rivers, and how engineering can enhance such natural systems.

The journey of writing my master thesis started over a year ago. By coincidence, I went to a collaborative session between the TU Delft and the Port of Rotterdam. Here my attention was drawn to the research opportunities regarding the improvement of dredging strategies within the port, as it combines a thorough understanding of the system and how engineers can improve this system.

Granting the thesis topic was not straightforward as I did not follow the most applicable courses. I therefore want to thank the Port of Rotterdam, with Lambèr in particular and Prof. dr. ir. Julie Pietrzak, for their confidence beforehand. Apart from the confidence I also want to thank Julie Pietrzak for chairing my graduation committee and for her valuable feedback writing this thesis. The same goes towards the rest of my graduation committee, dr. Alex Kirichek, dr. Claire Chassagne and dr. ir. Matthieu de Schipper for guiding me throughout the process. A special acknowledgement goes towards my daily supervisor, ir. Lambèr Hulsen: I am very grateful for the extensive support in the set-up of the model hindcasts and the very valuable feedback on my process and thesis in general.

Writing this thesis has been done mostly from the Port of Rotterdam office. The pleasant working environment and the colleagues here, who were always willing to help out with Python, made the office feel like a new home. Another acknowledgment goes towards Marco Wensveen and Gerrit van der Sanden, who provided me the measurement data and invited me to join the measurement survey on November 5, 2019. A special note goes towards Marlein Geraeds, my fellow graduate student, who was always available for serious discussions about the subject, but also for moments of distraction during the multiple lunch and coffee breaks.

The last word goes towards my friends and family. First of all, my fellow roommates, Chris and Viktor, who took me on a trip to Norway by camper mid August, while I was experiencing the largest stress working towards the end of this thesis. The trip allowed me to let go the thesis stress for at least two weeks. A different note goes towards the friends I made over the years, from my hometown friends, the guys from the football team, MDP 271, the friends at Civil Engineering, my old roommates at the Drosovilla and the friends from LAGA; there was never a dull moment over these seven years. My last word goes towards my brother, Jeroen, and my parents, Hans and Anja: I can't be grateful enough for the Scotland year and the unconditional support over the years.

D. Deckers
Rotterdam, September 2020

Contents

List of Symbols

B_{j0}	Initial buoyancy flux buoyant jet	m^5/s^2
c	Wave celerity	m/s
c_f	Friction coefficient	-
C	Sediment concentration	g/l (kg/m^3)
D	Deposition	m^2/s
D_{j0}	Initial diameter jet	m
D_p	Particle diameter	m
D_f	Floc diameter	m
E	Erosion	m^2/s
f_w	Friction coefficient	-
g	Gravitational acceleration	m^2/s
$g^{'}$	Reduced gravity	m^2/s
h	Water depth	m
l_m	Momentum length scale buoyant jet	m
M	Rate of erosion	m^2/s
n_f	Fractal dimension	-
N	Buoyancy frequency	s^{-1}
Q_{j0}	Initial discharge buoyant jet or overflow	m^3/s
Re_f	Fluid Reynolds number	-
Re_p	Particle Reynolds number	-
Ri	Richardson number	-
Ri_f	Flux Richardson number	-
u	Horizontal stream wise velocity	m/s
u_{orb}	Orbital wave velocity	m/s
u_{cf}	Crossflow velocity	m/s
v	Horizontal lateral velocity	m/s
w	Vertical velocity	m/s
w_s	Settling velocity	m/s
W_{j0}	Initial vertical velocity of buoyant jet or overflow plume	m/s
z_B	Buoyancy length scale buoyant JICF	m
z_C	Transition to bent over plume length scale buoyant JICF	m
z_M	Momentum length scale JICF	m
$\Delta\rho_0$	Specific density	-
ϵ	Dissipation rate of turbulent kinetic energy	-
ζ	Velocity factor	-
η	Wave height	m
λ	Kolmogorov length scale	m^2/s
μ	Dynamic viscosity	$Pa\,s$
ν	Kinematic viscosity	m^2/s^3
ρ	Density	kg/m^3
ρ_s	Density solid	kg/m^3
ρ_w	Density water	kg/m^3
ρ_{cf}	Density ambient water	kg/m^3
τ	Bed shear stress	N/m^2
τ_b	Induced shear stress	N/m^2
τ_d	Critical deposition shear stress	N/m^2
τ_e	Critical erosion shear stress	N/m^2

Glossary

Column The column is a device used to obtain the top layer of sediment from the bed. It consist of a PVC pipe with a copper lit with additional weight. It is accelerated into the bed under its own weight, as vacuum is created between the sediment and the lit, the sediment can be collected. 44, 75

Cross flow The cross flow velocity is the superposition of the velocity of the dredging vessel and the local flow velocity [de Wit, 2015]. 30

Deposition Deposition is the gross flux of sediment on the river bed [Winterwerp and Kesteren, 2004]. 17

Eulerian frame of reference A frame of reference which is fixed at a certain location in time. 21

Grabber The grabber is a device used to scrape of the top layer of the bed. Subsequently this sample is brought on-board. 44, 75

Hindered settling Hindered settling is the reduction of the settling velocity of particles due to its surrounding concentration. As the concentration increases, particles will collide with one another reducing its settling velocity [Winterwerp and van Prooijen, 2015].. 17, 129

Lagrangian frame of reference A frame of reference which moves in the direction of the observer and therefore changes in time. 42, 63

Lutocline The lutocline is the location with the sharpest gradient in turbidity. 20

Mud A sediment mixture containing clay, silt and sand. Its properties are mainly determined by the ratio of this composition. e.g. the larger the clay composition the larger the cohesion of the mud [Winterwerp and van Prooijen, 2015]. 2, 16

Non-Newtonian fluid A fluid which exhibits non-Newtonian behaviour has a viscosity which depends on the stress applied on the fluid. Due to the applied stress the viscosity may increase or decrease. For Newtonian fluids the viscosity is independent of the stress applied on the fluid [Winterwerp and Kesteren, 2004]. 18

Operationeel Stromings Model (OSR) The Operationeel Stromings model is a model developed by the Port of Rotterdam which contains the forecast and measured data of, for example, salinity, water levels and currents at several locations within the port.. 47, 60

Residual current The net current averaged over an arbitrary period of time, e.g. a tidal cycle [Bosboom and Stive, 2015]. 15

Settling Settling are the particles falling through the water column [Winterwerp and Kesteren, 2004]. 16

Slack water The moment the tidal currents reverse in direction. i.e. flow reversal from ebb to flood happens around Low Water (LW) and is therefore called Low water slack (LWS). During high water slack, flow reverses from flood to ebb and happens after high water. The slack water period is the time frame in which flow velocities are below a certain threshold value [Bosboom and Stive, 2015]. 17, 146, 147

TSHD Trailing Suction Hopper Dredgers (TSHD) are a type of dredging vessel used for large maintenance dredging or land reclamation projects. Through a large pipe, equipped with a suction head, sediment is removed from the bed. Material can be released by opening the doors of the barge or by bow coupling. 27

Acronyms

ADCP Acoustic Doppler Current Profiler. 42

CFD Computational Fluid Dynamics. 50

HvH Hook of Holland. 64

HW High Water. 13

HWS High Water Slack. 14

JICF Jet in Cross Flow. 30

LW Low Water. 13

LWS Low Water Slack. 14

OBS Optical Backscatter. 42

PSU Practical Salinity Unit. 155

RANS Reynolds Averaged Navier-Stokes equation. 47

ROFI Region of Freshwater Influence. 2

SPM Suspended Particulate Matter. 2, 11, 13

SSC Suspended Sediment Concentration. 139

TDM Ton Dry Matter. 3

1

Introduction

The port of Rotterdam is located within the Rhine-Meuse estuary where a substantial amount of fine sediment transport takes place. In order to keep the port and its waterways accessible, large volumes of sediment are dredged and reallocated in the North Sea every year. As this reallocation strategy is both expensive and non sustainable, new reallocation strategies are being developed. *SURICATES*, which stands for Sediment Uses as Resources In Circular And Territorial EconomieS, is an EU Interreg (inter-regional) project, which aims to increase sediment reuse to reduce erosion and increase flood protection in ports, waterways and coastlines. One of the SURICATES projects has been executed in the port of Rotterdam from May until November 2019. During this pilot study, 209,000 ton of clean dredged sediment has been released in the Rotterdam Waterway during ebb discharges, using the natural current to transport the sediment towards the sea [PortofRotterdam, 2018].

Dredging volumes in the port of Rotterdam increased since the most recent expansion of the port, Maasvlakte 2, finished in 2011. Since this expansion, the amount of required dredging, in areas operated by Port of Rotterdam, increased from roughly 5.2 to 8.9 million cubic metres per year with a current peak value of 11.3 million cubic metres in 2016 [de Bruijn, 2018]. Due to the increased dredging quantities, the Port of Rotterdam authority has launched an initiative to stimulate innovation within this context; *Program Innovative Sediment MAnagement* (*PRISMA*). Within this program the effect of sediment traps has been investigated by Tempel [2019] and the modelling of fine sediment has been improved by de Groot [2018]. Currently, experiments with water injection dredging are carried out as well. As the SURICATES program also aims at reducing maintenance dredging costs, the SURICATES pilot study is adopted by the Port of Rotterdam.

This pilot study is set up, in the context of the broader SURICATES program, by the *Port of Rotterdam* in cooperation with *Deltares*, *Rijkswaterstaat* and *Bureau de Recherches Géologiques et Minières*. For this pilot study, executed over the course of half a year, fine sediment from the harbour basins has been disposed in the Rotterdam Waterway instead of offshore in the North Sea. It is estimated that by releasing the dredged sediment during ebb tide, the return flow towards the harbour basins is limited and accretion of the river banks is accelerated. The goal of the pilot study (in the latter referred to as *SURICATES* pilot study or *SURICATES*) is two-fold: disposing sediment in the Rotterdam Waterway reduces the sailing time of the hoppers and nourishes the river banks. The sailing time is reduced with approximately 3 hours per cycle which leads to a cut in fuel consumption. Thus a reduction in dredging costs and combustion of exhaust fumes. By disposing the sediment at the allocated location, it is expected that accretion takes places at the river banks of the Rotterdam Waterway. This accretion is used for the creation of a tidal park, called '*Groene Poort Zuid*'. This tidal park and other inter tidal areas can be used by wildlife or for recreational purposes. Moreover, flood resilience is improved as the natural foreshore of the river banks is extended.

In this chapter, some background on the area is given at fist. In the subsequent section additional information regarding the execution of the SURICATES pilot study is given. This is followed by the problem statement, the objective and approach of this research.

1.1. Background information

The port of Rotterdam roughly stretches over a length of 40 kilometres from the mouth at Hook of Holland in the west to the bifurcation between the New Meuse and Hollandse IJssel in the east, see fig. 1.1 and fig. A.1. The port can be split in two parts, with the harbour basins lining the Rotterdam Waterway and New Meuse in the north, such as the Botlek and Eemhaven, and the harbour basins lining the Calandkanaal and Beerkanaal towards the south, such as the Maasvlakte and Europoort. These two different parts of the port are subject to different siltation processes; the harbour basins in the north are subject to siltation induced by fluvial sediment, whereas the basins located in the south are subject to siltation induced by marine sediment [de Nijs, 2012].

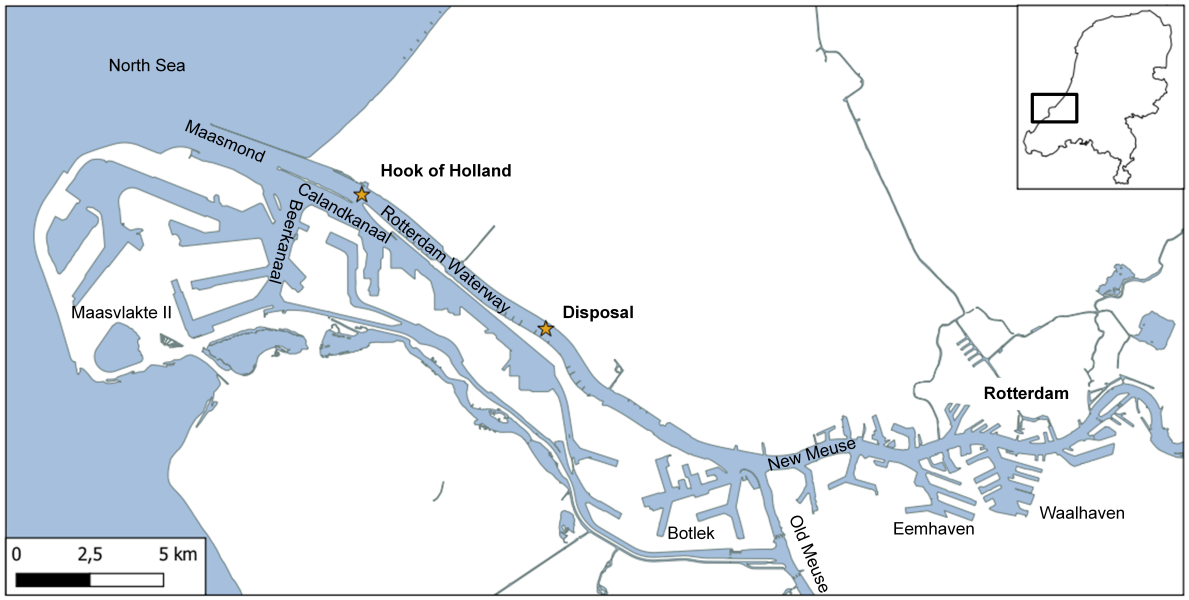

Figure 1.1: An overview of the port of Rotterdam with its main features. The disposal location in the bend of Maassluis and Hook van Holland are indicated with a star.

The Rhine-Meuse estuary is signified by substantial tidal influence; the tide at Hook of Holland has a mean spring tidal range of 2.00 m and a mean neap tidal range of 1.20 m, with maximum tidal currents exceeding 1 m/s. The salinity in the Rotterdam Waterway alternates between partially mixed during flood and stratified conditions during ebb. During low river discharges salt water intrusion can be significant and may be detected at the bifurcation of the New Meuse and the Hollandse IJssel. The river discharge through the Rotterdam Waterway originates for 80 % from the Rhine upstream and is regulated through the Haringvliet sluices. For low freshwater discharges ($< 1700\ m^3/s$) the sluices are closed such that all the fresh water is discharged trough the Rotterdam Waterway to limit salt intrusion. For high freshwater discharges ($> 1700\ m^3/s$), the Haringvliet sluices are (partly) opened. The Rotterdam Waterway ends up in the North Sea creating a large Region of Freshwater Influence (ROFI), hereafter referred to as the Rhine-ROFI. The bed of the Rotterdam Waterway mainly consists of sand, whereas the dredged material from the basins mainly consists of Mud [de Nijs et al., 2008].

de Nijs [2012] has contributed for a large extent to the current understanding of the hydrodynamics and subsequent trapping of sediment in the Rotterdam Waterway. In de Nijs [2012], the emphasis has been put on the advection of the salt wedge and estuarine turbidity maximum, in order to describe the observed transport and trapping of Suspended Particulate Matter (SPM). It has been found that fluvial sediment from upstream rains out in the Rotterdam Waterway and subsequent advection of the salt wedge in the upstream direction induces the siltation of the harbour basins of the Rotterdam Waterway and New Meuse. This emphasises the importance of the understanding of the governing hydrodynamics to describe the sediment dynamics within the Rotterdam Waterway.

However, since de Nijs [2012], several projects have altered the bathymetry and shape of the port, such as the construction of Maasvlakte 2 and the deepening of the Rotterdam Waterway. For the increase of the total

Time:	May - Nov. 2019
# Disposals:	125
Total disposed:	209,000 TDM
	582,000 m^3
Average disposal:	1,650 TDM
	4,600 m^3
Average concentration:	360 g/l
Average density:	1,300 kg/m^3

(a) Summary of SURICATES pilot study

Daily:			
	Flood:	-3,600 TDM	
	Ebb:	+5,000 TDM	
	Gross:	8,600 TDM	19 %
	Net:	+1,400 TDM	100 %
Annual:			
	Inflow:	-1.3 M TDM	
	Outflow:	+1.8 M TDM	
	Gross:	3.1 - 3.4 M TDM	15 %
	Net:	+0.5 - 0.7 M TDM	71 %

(b) Estimated sediment fluxes in the Rotterdam Waterway

Figure 1.2: a) Key data of the SURICATES pilot study. b) Estimated sediment fluxes on daily timescales de Nijs et al. [2010] and yearly timescale van Dreume [1995] in the Rotterdam Waterway. A positive flux is seaward directed, while a negative flux is landward directed. The percentages in the utmost right column indicate the significance of the pilot study.

dredging volumes within the port of Rotterdam the construction of Maasvlakte 2, in 2011, is considered to be the main cause [de Bruijn, 2018]. Whereas for the hydrodynamics of the Rotterdam Waterway its deepening, finished in 2019, is considered to have the most effect, see appendix A.1. Therefore, Geraeds [2020] has executed a study, as part of the SURICATES study, to verify whether the processes described by de Nijs [2012] are still governing in the Rotterdam Waterway.

1.1.1. SURICATES

The aim of SURICATES, as stated in the work plan, is to reuse sediment within the Rotterdam Waterway to reduce erosion and improve flood resilience by nourishing the river banks. Moreover, the sailing time of the dredging vessel is reduced. Over the course of the pilot study 209,000 Ton Dry Matter (TDM) ($\pm$ 582,000 m^3) has been disposed in the bend near Maassluis around High Water Slack (HWS) instead of at the North Sea (Loswallen), see fig. 1.1 for the disposal site. This pilot study lasted for 16 weeks, from the end of May until mid November 2019. The amount of sediment disposed is equal to approximately 12 - 16 % of the total dredging budget of $\pm$ 3 - 4 million m^3 per year in the Rotterdam Waterway. The total amount of sediment dredged in the entire port equals $\pm$ 15 million m^3 per year.

The significance of the size of the pilot study is further illustrated in fig. 1.2, where the size of the pilot study is compared with estimated sediment fluxes in the Rotterdam Waterway.

1.1.2. Sediment fluxes

Annually 4.9 million TDM (3.4 million TDM mud and 1.5 million TDM fine sand) is transported from the Rhine and Meuse towards the Rhine-Meuse estuary, of which 75% remains inside the Hollandsdiep-Haringvliet basin and harbour basins lining the Rotterdam Waterway and New Meuse. Hence $\pm$ 0.9 million TDM is transported towards the North Sea [Spanhoff and Verlaan, 2000]. van Dreume [1995] found very similar fluxes and estimated that approximately 0.7 million TDM mud reaches the North Sea through the Rotterdam Waterway. In de Nijs et al. [2010] the flux of SPM at Hook of Holland is estimated at 3,640 tons during flood and 5,030 tons during ebb, hence a net transport of 1,390 tons per tide.[1] If this is extrapolated to a full year the gross flux equals 3.2 million TDM and a net seaward flux of 0.5 million TDM, which is in the same order as found by Spanhoff and Verlaan [2000] and van Dreume [1995]. The SURICATES pilot study therefore has a limited size in terms of the total sediment fluxes; $\pm$ 28 % if corrected for the duration of the study. Moreover, it should be noted that all fluxes mentioned are depth-averaged fluxes, e.g. in the near-bed region at Hook of Holland and at Maassluis a net landward transport is observed when averaged over the tidal cycle, whereas the depth-averaged flux is seaward directed [de Nijs et al., 2010].

In de Nijs et al. [2010] is stated that 50 % of the annual import of fluvial sediment from the upstream river boundary is transported towards the North Sea, this is in agreement with the flux estimates in Hendriks and

[1] The measurements are executed on April 14, 2005 under high discharge conditions

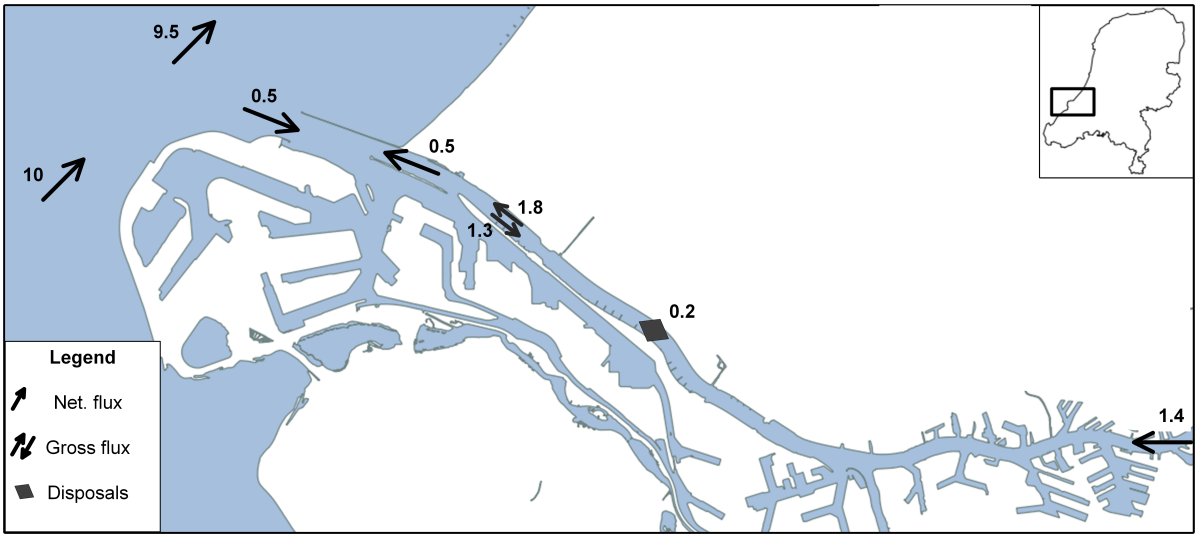

Figure 1.3: Estimation of annual sediment fluxes in the port of Rotterdam [de Nijs et al., 2010, Hendriks and Schuurman, 2017, Spanhoff and Verlaan, 2000, van Dreume, 1995].

Schuurman [2017], Spanhoff and Verlaan [2000] and van Dreume [1995]. Moreover, in de Nijs et al. [2010] is hypothesized that the majority of the inflow of sediment at Hook of Holland into the Rotterdam Waterway is most likely to be attributed to recirculated fluvial SPM rather than marine sediment being imported.

In short, all four approximations of the sediment flux in the Rotterdam Waterway are largely in agreement with one another. Moreover, it is stressed that the SURICATES pilot study has an impact of 28 % on the gross fluxes in the Rotterdam Waterway over the time of execution.

1.2. Problem statement

The re-use of sediment on the scale of the SURICATES pilot study has been executed before in 2008 and 2009, however, on a different scale, see appendix A.2. Therefore, the foreknowledge on the behaviour is limited. Although sediment behaviour in the Rotterdam Waterway is generally considered to be well understood, it has to be investigated to what extent this knowledge can be conveyed to the behaviour of the sediment plumes. For example, the effect of differences in hydrodynamic forcing (river discharge, tide, wind) is well understood in terms of hydrodynamics and sediment dynamics. But, the effect on the execution of the pilot study is unknown.

Over the course of the pilot study two different methods of disposal (by using bow coupling and drawing the bottom doors) have been used to reallocate the sediment. From observations by the surveyors, it is noticed that the behaviour of a sediment plume for both methods is different. The difference in behaviour has to be quantified, both for the initial behaviour of the plume, but also for the effect on the cumulative behaviour of all disposals.

To model the hydrodynamics and sediment behaviour within the port of Rotterdam, operational hydrodynamic models and sediment models are used. The performance of the hydrodynamic model has been assessed multiple times, e.g. by Rotsaert and Collard [2009], de Nijs and Pietrzak [2012] and Geraeds [2020]. From these studies, deficiencies are found in the hydrodynamic models. The effect of these deficiencies on the behaviour of the SURICATES pilot study must be assessed.

Apart from deficiencies in the hydrodynamic modelling, assumptions and simplifications need be made to be able to hindcast the SURICATES pilot study. To model the entire period of the SURICATES pilot study, a simplification of the hydrodynamics is required. The effect of the simplification in the hydrodynamic forcing must to be investigated. Next to this, the effect of simplifications in the sediment reallocations have to be verified. At last, it has to be derived to what extent the sediment models are applicable to hindcast the SURICATES pilot study on different time and spatial scales.

1.3. Research objective

The SURICATES pilot study is one of the first projects reusing dredged sediment for the accretion of river banks, while at the same time reducing sailing times and dredging costs. This thesis focuses on the fulfilment of the latter mentioned goal: an estimation of the SURICATES sediment fluxes to determine the efficiency of the pilot study as it has been executed.

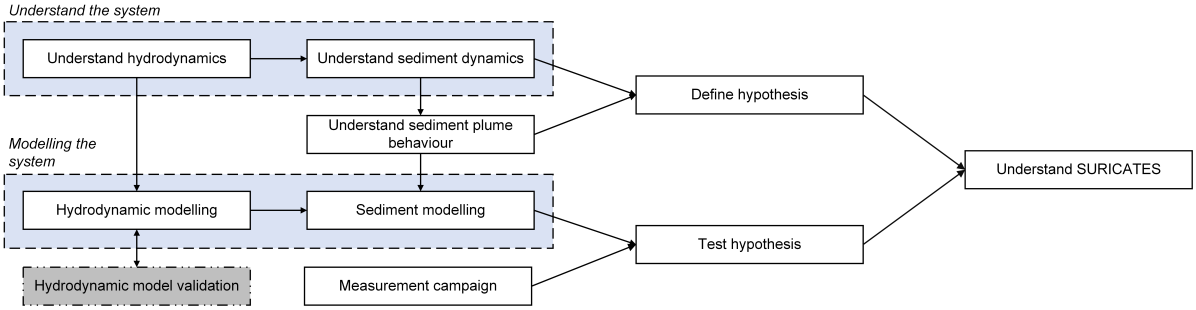

Figure 1.4: Approach of this thesis, with the box in grey indicating work by Geraeds [2020].

In order to derive the performance of this project the behaviour of the reallocated sediment plumes has to be understood. Therefore both a thorough understanding of the governing hydrodynamics, sediment dynamics and behaviour of a sediment plume in specific is required. Subsequently, a hypothesis can be formulated based on the latter, for the behaviour of the sediment plume on the short term. The hypothesis and the understanding of the system, can be used to assess the effect of the sediment plumes on the long term. This hypothesis is then compared with the results of the measurement campaign (as part of the SURICATES pilot study) and the modelling study; both based on the short term and long term results. This approach is shown in fig. 1.4. Altogether the following research objective has been formulated:

> **Use the results obtained from the measurement campaign and operational sediment models, to hindcast the behaviour of the SURICATES pilot study on different spatial and time scales.**

To support the research objective the following main research question is stated:

> *What governs the behaviour of sediment plumes disposed in the port of Rotterdam, in the context of the SURICATES pilot study, on different spatial and time scales, based on field measurements and model results?*

In support of the main question, sub-questions have been defined. These are stated below, accompanied with the approach to answer them.

1. **Which processes govern the hydrodynamics and the sediment behaviour in the port of Rotterdam?**
   Existing literature on the hydrodynamics and sediment dynamics of estuaries in general are discussed. Subsequently, this knowledge is applied to understand the behaviour in the port of Rotterdam.
2. **What is the expected behaviour of sediment plumes in the system?**
   Using the knowledge of the system and by assessing existing literature on the behaviour of sediment plumes, a hypothesis is drawn on the behaviour of the pilot study on the short and long term.
3. **How is the reallocated sediment distributed in time and space on different spatial and time scales?**
   The results of the measurement surveys on November 5 and September 11, 2019 are analysed to gather insight in the short term behaviour of a sediment disposal. The results from the long term measurement campaign are used to analyse the long term impact of the pilot study.
4. **Which assumptions and simplifications have to be made to model the SURICATES pilot study on different time and spatial scales?**
   In this chapter the required assumptions and simplifications for the set-up of the sediment model are analysed.
5. **To what extent can current models reproduce the sediment distribution as found in the data analysis?**

In the last chapter, the model results are discussed. At first the inaccuracies in the hydrodynamic modelling based on Geraeds [2020] and other literature, and its effect on the sediment model is defined. The model results are interpreted based on the hypothesis formulated and compared with the measurement results.

1.3.1. Scope of the research

This thesis is part of a series covering multiple complexities involved in the SURICATES pilot study. As stated previously the SURICATES pilot study has multiple goals: induce accretion at the river banks for wetland creation and to increase flood resilience. However, this thesis will focus on the understanding of sediment fluxes in the direction of the flow only; lateral accretion is not investigated.

As shown in fig. 1.4, five prerequisites are required to understand SURICATES. In Geraeds [2020], a measurement survey (not part of SURICATES) has been conducted on August 13, 2019 to verify and conclude that the dominant hydrodynamic processes as found by de Nijs [2012] are still governing the hydrodynamics, despite different human interventions, see appendix A.1. In Geraeds [2020] also the predictive capabilities of the hydrodynamic models is assessed, In this thesis the effect of the inaccuracies in the hydrodynamic model on sediment behaviour is discussed.

In this research, unraveling the behaviour of the SURICATES pilot study is continued, by adding sediment plume behaviour to the research. This is done by adding the understanding of sediment plume behaviour to the literature work and include sediment disposals in the sediment models.

The data analysis in this research focuses on the near field to mid field (short term) behaviour of the sediment plume upon disposal and the long term by analysis of the grab samples taken. For the short term analysis multiple surveys have been conducted, of which the November 5 and September 11, 2019 survey have been covered in this thesis. This imposes a sharp scope of the research in terms of applicability of the measurement results. The execution of the pilot study is influenced by a number of boundary conditions imposed by both the environmental conditions and conditions imposed by the execution of the disposal. The most important parameters are listed below and lead to multiple possible combinations of *disposal boundary conditions* and *environmental boundary conditions*. Both measurement surveys only cover one specific combination of boundary conditions.

Disposal boundary conditions :

- Disposal method
- Location of disposal
- Time of disposal
- Material disposed

Environmental boundary conditions:

- River discharge
- Tide
- Wind and set-up

1.3.2. Approach and thesis outline

This thesis consists of four different parts and nine different chapters with supporting information in the appendices.

  - **Chapter 1: Introduction**
    In this chapter an introduction to this thesis is given. This introduction contains background information on the port of Rotterdam and the SURICATES pilot study. Next to this, the approach, problem statement, scope and research questions are discussed.

- **Part I:** The first part contains a literature study focusing on the dynamics of the system and sediment plume behaviour in specific used to derive a hypothesis.

  - **Chapter 2: Understanding the system**
    In chapter 2, a brief literature review is given as an introduction to understand the system. This covers hydrodynamic processes occurring in estuaries in general, split into large and small scale processes. Subsequently, this information is used to describe the hydrodynamic phenomena occurring in the Rhine-Meuse estuary and Rhine-ROFI specifically, such as salt wedge advection.

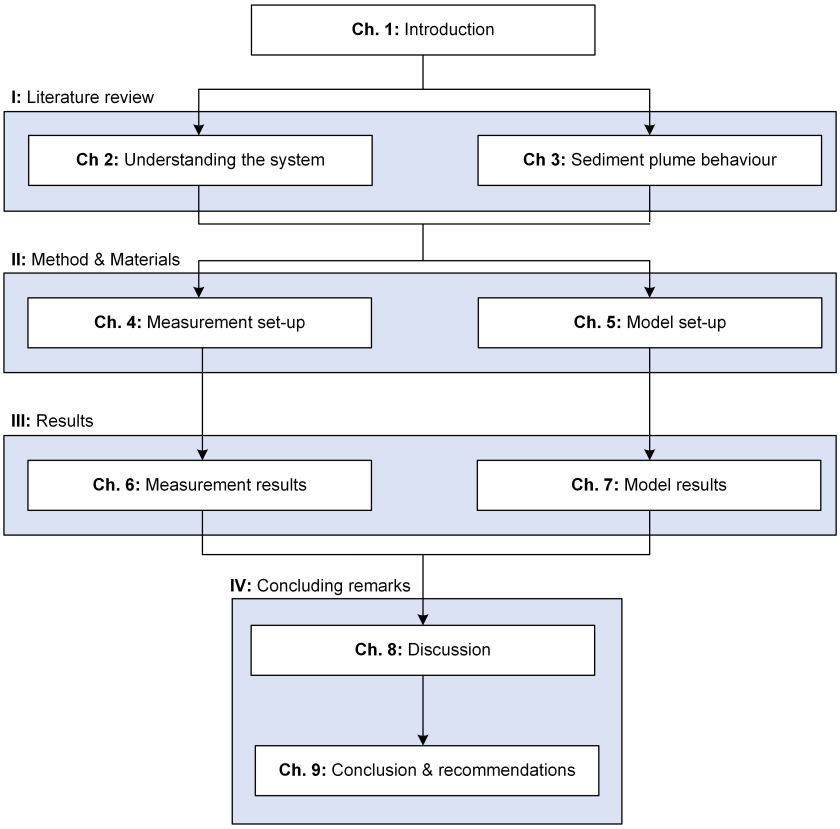

Figure 1.5: A flowchart indicating the outline of this thesis and the relation between different parts (I to IV) and chapters of this thesis.

This is followed by an introduction into sediment dynamics in general such as erosion and sedimentation processes. Finally, this information is used to describe processes going on in the Rotterdam Waterway, such as harbour siltation.

- **Chapter 3: Sediment plume dynamics**
  In chapter 3, the literature review is extended with an introduction into sediment plume behaviour. In this chapter an analogy with plume behaviour in general is drawn and to what extent this theory is valid for sediment plumes in water. Based on the understanding of both the system and plume dynamics, a hypothesis is drawn on the expected behaviour of the sediment plume on different spatial and time scales.

- **Part II:** This second part focuses on the method and materials. In this part the set-up and materials used in the measurement campaign and model hindcasts are discussed.

  - **Chapter 4: Measurement set-up**
    In chapter 4, the set-up of the measurement campaign is discussed. To unravel the behaviour of the SURICATES pilot study on the short term and long term, two different measurement campaigns have been set-up, consisting of different measurement surveys. The set-up and materials used for both measurement campaigns are discussed in this chapter.

  - **Chapter 5: Model set-up**
    In the subsequent chapter, chapter 5, the set-up of the computational models to hindcast the SURICATES pilot study on the short and long term is discussed. At first, the different set-ups for the hydrodynamic models are discussed, which generates the input of the sediment model. Subsequently, the set-up of the two different sediment models is discussed, this includes the implementation of the disposals and sediment parameters. This is concluded with the limitations and assumptions made to be able to hindcast the pilot study.

- **Part III:** The third part focuses on the results of the measurement campaign and model simulations.

  - **Chapter 6: Measurement results**
    In chapter 6, the results of the measurement campaign are analysed. Over the course of the pilot study several surveys have been carried out, split into surveys gathering data for a short term and long term analysis. In this chapter, the survey executed on September 11 and November 5, 2019 are analysed first to verify the hypothesis drawn on near and midfield behaviour first. Subsequently, the results of the long term measurement campaign are analysed. Over the course of the pilot study several surveys have been carried out to analyse the long term influence of the pilot study. These results are interpreted and discussed based on the understanding of the system, short term results and hypothesis, linking chapter 6 with chapter 2 and chapter 3.
  - **Chapter 7: Model results**
    In chapter 7, the results of the model on the short and long term are interpreted using the understanding of the system, chapter 2 and chapter 3. At first, the short term results are used to derive the sensitivity of different model parameters and variations in execution of the pilot study. Subsequently, the model results of the November 5 simulation run are compared with the data from the November 5 survey. The long term results, hindcasting the entire period of the SURICATES pilot study are discussed and compared with the long term data discussed in chapter 6. This chapter is concluded with a discussion on the applicability of these models to hindcast the SURICATES pilot study.

- **Part IV:** The last part comprises of a discussion, conclusion and recommendations following the research.
  - **Chapter 8: Discussion**
    Over the course of the thesis different assumptions and simplifications have been made. In most cases these have been discussed when appropriate, however in this chapter the overall effect of these assumptions and simplifications is discussed.
  - **Chapter 9: Conclusion and recommendations**
    This thesis is concluded with a final chapter, chapter 9, in which the main research question is answered and recommendations for future work are given.

- **Part V:** The appendices in support of this thesis are added as part V.

I

Literature review

2

Understanding the system

As is described in the introduction the Rotterdam Waterway is part of the larger Rhine-Meuse estuary. As for most estuaries the hydrodynamics are governed by the interaction between the tide, freshwater discharge and wind. In section 2.1 estuarine hydrodynamics on the large and small scale is explained, as well as how these process affect the hydrodynamics in the natural system. Moreover, estuaries are characterized by high concentrations of Suspended Particulate Matter (SPM) [de Nijs et al., 2010]. The behaviour of SPM on the small scale, large scale and in the natural system is discussed in section 2.2.

2.1. Hydrodynamics

Estuarine hydrodynamics are complex due to a combination of different forces driving the competition between fresh water and seawater. The overall flow pattern therefore strongly varies in time and space due to a combination of tidal forcing, freshwater discharge and density differences. The main pattern which arises depends mainly on the competition between stratification and mixing. To fully understand estuarine circulation flow both small scale and large scale processes are treated and at last these processes are placed in the context of the Rotterdam Waterway and Rhine ROFI.

2.1.1. Large scale processes

In the following section the hydrodynamics for estuaries in general are explained on a larger scale; i.e. not on the scale of individual particles. The most important processes are *Estuarine circulation* and *tidal straining*.

Estuarine circulation

The classical view of estuarine circulation is the tide-averaged *gravitation circulation* or *exchange flow* caused by the density differences between fresh water and seawater. Since seawater is denser than fresh water, a water level gradient is required to compensate for the density differences. Moreover, the density difference and water level gradient causes an imbalance in the net pressure in the water column: in the upper part of the water column the freshwater pressure is higher and in the lower part of the water column the pressure from the denser water is larger, as is shown in fig. 2.1a for an arbitrary cross-section. This pressure difference and water level gradient drives a baroclinic flow (caused by density differences) in which the fresh water is advected towards the denser water in the upper part of the water column and the denser water is advected towards the fresh water in the lower part of the water column. This phenomena is also known as the *'Lock-exchange mechanism'*. For higher freshwater discharges this mechanism increases, increasing peak flood velocities. Since the concentration of SPM increases towards the bed, a net landward transport of Suspended Particulate Matter is induced by the gravitational circulation. This density driven or baroclinic flow is called the *Gravitational circulation or estuarine circulation.* The arising overall flow pattern for an estuary is shown in fig. 2.1b [Pietrzak, 2015] [MacCready and Geyer, 2010].

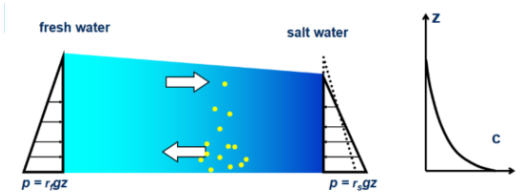

(a) The exchange flow on small scale for an arbitrary cross-section [Winterwerp and van Prooijen, 2015]

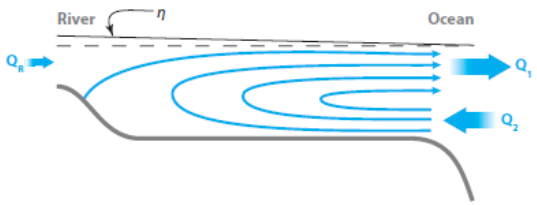

(b) The exchange flow on estuarine scale; Q_R indicates river run-off, Q_1 combined run-off and Q_2 the salt intrusion [MacCready and Geyer, 2010]

Figure 2.1: Schematization of the exchange flow in idealised conditions on different scales.

Tidal straining

In fact the aforementioned idea of the gravitation circulation and exchange flow section 2.1.1, has to be expanded by introducing the tidal forcing. Simpson et al. [1990], found a term, *tidal straining* or *strain-induced periodic stratification* to describe the variation in stratification for Liverpool bay induced by the oscillatory movement of the tides. In general during ebb the entire flow over the water column is seaward directed in which lighter water is advected over denser water close to the bottom. As this process is stable little mixing between the density gradients occurs, hence promoting stratification. During flood conditions denser water from the sea enters the estuary due to the tidal forcing; this denser water repulses the less dense estuarine water, therefore dense water is advected over less dense water at the bottom. As this is unstable, mixing is induced and subsequently reduces the density gradient over the vertical. In short *tidal straining* is the effect of differential advection by a vertical velocity shear induced by the tide acting on a horizontal gradient. [de Boer, 2009].

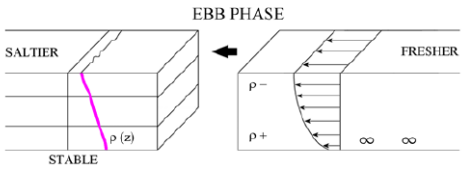

(a) Schematization of tidal straining during ebb

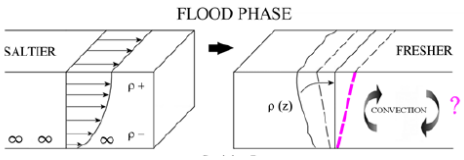

(b) Schematization of tidal straining during flood.

Figure 2.2: Schematization of the exchange flow in idealised conditions [Pietrzak, 2015]

2.1.2. Small scale processes

To fully understand the aforementioned processes on a system scale, small scale effects have to be incorporated as well. The most important of these processes are: turbulence and turbulence damping.

Turbulence

Turbulence are the random fluctuations of the flow velocity which can be seen in three dimensions in the form of so-called eddies. Uijttewaal [2015] uses the following definition for turbulence:

> *"Turbulent fluid motion is an irregular condition of flow in which the various quantities show a random variation with time and space coordinates, so that statistically distinct average values can be discerned".*

Turbulence will appear in conditions where energy can be transferred from the mean motion to turbulent fluctuations. These fluctuations are induced by velocity differences in a flow either between two different fluid bodies (free turbulence) or between the flow and a wall (e.g. a river bed) (wall turbulence). At this interface a mixing layer will arise allowing the exchange of mass and momentum with a length scale defined as Prandtl's mixing length (l_m) and is defined as the length in which the particles conserves its properties.

Turbulence is characterized as a process in which kinetic energy is converted to heat; in other words kinetic energy is dissipated. The turbulence is noticeable as instabilities in the form of the previously mentioned eddies. The mixing property of turbulence is evident to keep SPM in suspension. These eddies are defined by its properties: its length scale, its intensity (eddy viscosity) and its ability to mix momentum and matter in space (eddy diffusivity).

The eddy viscosity is simply defined as the product of the length scale and the velocity gradient and describes the transport of momentum. As the eddy viscosity is a product of the velocity gradient and the mixing length it is a property of the flow and not of the fluid. (The latter may be confusing as viscosity in general is a property of the fluid). Another property is the eddy diffusivity which describes the mixing of matter induced by the turbulent motions in the eddy. [Uijttewaal, 2015].

Turbulence damping

One of the important aspects of stratified flow conditions is *turbulence damping*, due to stratification turbulence development is limited compared to non-stratified conditions. This can be density differences induced by salinity differences or due to differences in SPM concentration. The concept can be explained as following; turbulence tends to distort particles in a random manner and can therefore displace heavier particles upward and lighter particles downward. However, in stratified flow conditions, due to density differences buoyancy forces place the particle back to its original position. Hence the random motion of these particles is limited; *turbulence damping*. Turbulence damping is a very significant process in sediment dynamics as turbulence is required to keep SPM in suspension and is therefore a key driver in the formation of the Estuarine Turbidity Maximum (ETM) at the tip of the salt wedge, see section 2.2.3. [Pietrzak, 2015]

2.1.3. Hydrodynamics of the physical system

In the following section the previously mentioned processes are placed in the context of the Rotterdam Waterway and the Rhine ROFI. An example is the occurrence of *up- and downwelling* in the ROFI due to tidal straining and tidal asymmetry.

Tidal asymmetry

Tidal asymmetry is an asymmetry of the horizontal or the vertical tide (current or water level) and leads to a difference in magnitude and duration of a tidal component. Tidal asymmetry in general is mainly caused by the distortion of the tidal wave as it propagates into shallow waters such as the North Sea or the Rotterdam Waterway. Classical tidal asymmetry is caused by the difference in wave celerity difference at High Water (HW) and Low Water (LW), as the tidal wave celerity is depth dependent in shallow water, see eq. (2.1) [Dronkers, 1986].

$$c = \sqrt{gh} = \sqrt{g(h_0 + \eta)} \tag{2.1}$$

In which h_0 equals the water depth and η the (tidal) wave height which is positive during HW and negative during LW. Hence the tidal wave propagates faster during HW than during LW, leading to asymmetry of the wave: it skews. Due to non-linearity of the bottom friction, the asymmetry is enhanced as LW-waves feel the bottom more than HW-waves. This effect is stronger for relative shallow estuaries such as the Rotterdam Waterway.

The tidal asymmetry encountered in the Rotterdam Waterway is not limited to the classical internal tidal asymmetry, where the flow structure is solemnly determined by the deformation of the tidal wave inside the estuary. In contrast, the internal tidal asymmetry in the Rotterdam Waterway is caused by a combination of the barotropic asymmetry imposed at the mouth and the advection of the salt wedge. The deformation of the tidal wave inside the Rotterdam Waterway is limited, as the generation of M_4 overtides within the estuary is limited [de Nijs et al., 2011a].

At the mouth of the harbour the deformed tidal wave is imposed. As stated by de Nijs et al. [2011a] from the ($M_4 : M_2$) ratio it can be deduced that the tide rises faster than it falls. In combination with the freshwater discharge this leads to a longer ebb than flood period, as is shown infig. 2.3. At the mouth of the Rotterdam Waterway generally the upper part of the water column is ebb dominated, while close to the bed the flow is

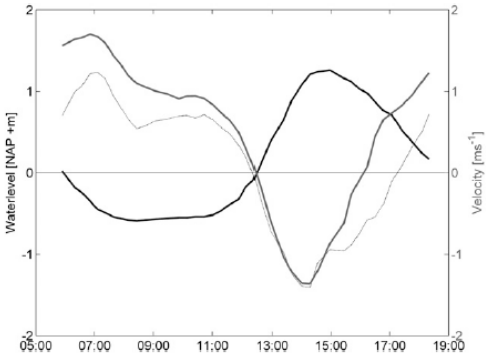

Figure 2.3: Tidal asymmetry in the Rotterdam Waterway, with the water level in black, the velocity close to the bed (2.5m above the bed, (dashed gray)) and close to the surface (12.5m above the bed (thick gray). de Nijs et al. [2011a].

flood dominated. In fig. 2.3 it can be observed that the near-bed velocity is higher during flood than during ebb. Therefore, sediment is generally imported close to the bed. Moving landward, a shift is noticeable, where the effect of the freshwater discharge dominates over the barotropic tidal asymmetry, increasing the ebb period.

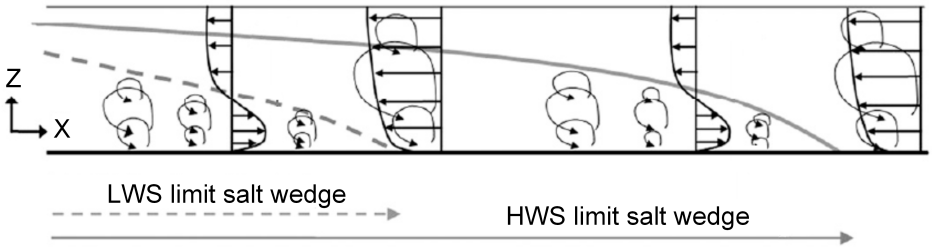

Figure 2.4: A schematisation of the relationship between the advection of the salt wedge and the internal tidal asymmetry. The dashed grey lines indicate the limit of the salt wedge at LWS and the solid lines at HWS. The velocity profiles is landward directed below the salt wedge and down estuary directed above the salt wedge [de Nijs et al., 2011a].

de Nijs et al. [2011a] ascribes the internal tidal asymmetry, or flow structure in general, to the combined effect of barotropic and baroclinic forcing and turbulence damping at the pycnocline. In fig. 2.4 an overview of the flow structure in the Rotterdam Waterway is shown. From fig. 2.4 the relation between the density structure and flow velocity profile is evident, leading to differential advection. The fresh water is being advected down estuary while the salty water is still advected landward. Advection governs the displacement and structure of the salt wedge since turbulent mixing is suppressed. The tidal displacement of the salt wedge controls the height of the pycnocline above the bed at a particular site and therefore also the velocity profile [de Nijs et al., 2011a].

Salt wedge dynamics

The displacement and structure of the salt wedge in the Rotterdam Waterway is governed by its advective properties such as the tidal forcing, wind, wind set-up and freshwater discharge. The structure of the salt wedge generally remains stable throughout a tidal period tide as mixing is inhibited due to turbulence damping. Averaged over a tidal period the salt wedge extends as far as approximately 15 kilometres landward from Hook of Holland. However, this length differs significantly based on the hydrodynamic conditions and tidal phase, at Low Water Slack (LWS) the tip of the salt wedge is located 2 - 11 km landward from Hook of Holland, while during High Water Slack (HWS) this can be 13 - 20 km landward from Hook of Holland [de Nijs et al., 2011b].

In general, wind increases mixing over the vertical and set-up on the North Sea. Storms may lead to a well-mixed state in Rhine ROFI and Rotterdam Waterway. Large wind set-up events increase the barotropic forcing enhancing salt intrusion. Depending on the duration of the set-up event, salt water can be temporarily stored

in the harbour basins lining the Rotterdam Waterway, therefore increasing the tide-averaged salinity. The system is temporarily subject to larger ebb tidal flows and smaller flood flows restoring the system.It takes several tidal periods to restore to equilibrium, depending on the length of the set-up event [de Nijs et al., 2009]. After such storm events the saltwater intrusion limit can even be located in the Maasmond, downstream of Hook of Holland. This is in particular relevant for ETM dynamics, as the width and depth of the Maasmond is much larger, the ETM can lose a large amount of its SPM [de Nijs et al., 2008].

During spring tide the Rotterdam Waterway is generally well-mixed, while during neap tide, conditions can be stratified. Moreover, the salt wedge extends further landward during spring tide than neap tide. Low discharge events lead to a larger intrusion length of the salt wedge. Moreover, the Residual current close to bed is reduced due to a weaker lock-exchange mechanism.

2.2. Fine sediment dynamics

For the SURICATES project the majority of the disposed sediment originates from the harbour basins. This sediment mostly consists of Mud, a cohesive and very fine material. The transport of cohesive material mostly occurs as suspended matter and expresses different behaviour than non-cohesive material such as sand, see appendix B.3.1. To fully understand the behaviour of this cohesive material and how it is transported the small scale processes are described in which is zoomed in on the behaviour of an individual particle. This conveys the knowledge to understand the sediment behaviour on a system scale, the large scale processes. At last it is reflected to what extent these processes occur in the region of interest.

2.2.1. Small scale processes

The fate of sediment particles on the small scale depends on multiple processes. A suspended cohesive particle coagulates to form primary particles. Under Van Der Waals forces these particles aggregate to form flocs. Depending on the amount of turbulence the particle remains in suspension, breaks-up or settles. As it settles it can be eroded and brought back in suspension or stay in the bed and finally consolidate. These different processes are shown in fig. 2.5 and treated in the following separate paragraphs.

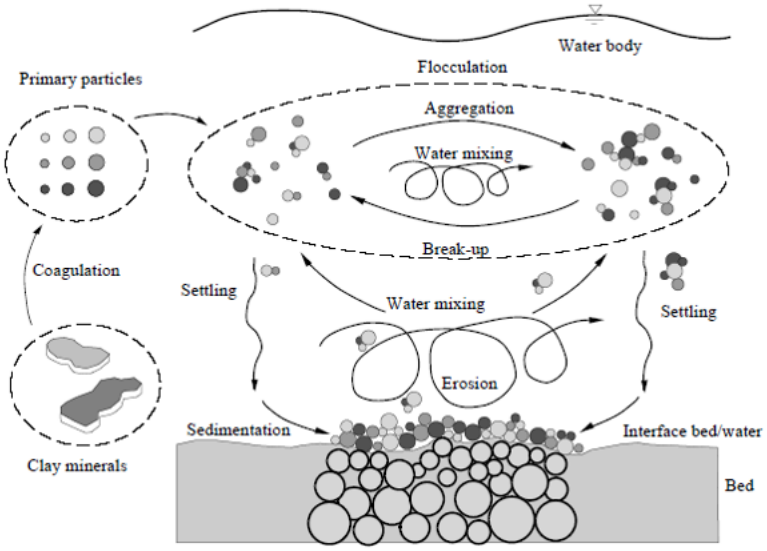

Figure 2.5: Schematization of the fate of a sediment particle in a viscous fluid. [Winterwerp and van Prooijen, 2015]

The cumulative behaviour of particles determine the sediment balance for a cross section in time. The most common formulation is described by Partheniades-Krone:

$$h\frac{dC}{dt} \sim E - D \tag{2.2}$$

In which is stated that the change in SPM concentration ($\frac{dC}{dt}$) multiplied with the water depth (h) is proportional with the difference between eroded (E) and deposited sediment (D) [Winterwerp and van Prooijen, 2015]. In the following two paragraphs, the processes of erosion and deposition are explained in more detail.

Settling

The Settling of non-cohesive particles, such as sand, is described by Stokes' settling velocity. This velocity is based on the assumption of a balance between drag and gravity for a particle settling in a viscous fluid at a constant velocity. Stokes settling velocity may only be applied for spherical parameters and Eucliadian particles with a small particle Reynolds number (Re_p), see appendix B.3.3).

In contrast, the settling of cohesive sediments is governed by the amount of turbulence and the settling velocity of the particles, as turbulence keeps the particles in suspension. In most estuaries the settling velocity of particles increases due to flocculation, as multiple particles bond together increasing their total settling velocity. In the Rotterdam Waterway, however, the effect of flocculation can be neglected, see appendix B.3.4. In contrast, Hindered settling decreases the effective settling velocities of the particles, see appendix B.3.5.

With the settling rate or effective settling velocity the Deposition rate can be determined, this is the flux of sediment settling on the bed. The classic formulation by Krone [1986] is a flux of a concentration (c) multiplied with the settling velocity (w_s). Over time this formulation is expanded with a criterion which includes a threshold value, above this critical deposition shear stress (τ_d) no sediment can be deposited. This extensive formulation for deposition is given in eq. (2.3). [Winterwerp and Kesteren, 2004].

$$\begin{cases} D = w_s c(1 - \frac{\tau_b}{\tau_d}) \text{ for } \tau_b < \tau_d \\ D = 0 \text{ for } \tau_b > \tau_d \end{cases} \tag{2.3}$$

Erosion

In contrast to deposition, *erosion* is defined as the gross amount of sediment that is removed from the bed. In its most generic way it is defined as the difference between forcing defined through the bed shear stress (τ_e) and resistance defined through the critical shear stress (τ_b), scaled with a power (n) for the type of material (cohesive/non-cohesive) and a calibration parameter (M) to scale the rate of erosion. In general $n = 1$ for cohesive material and $n = 1.5$ for non-cohesive material. [Winterwerp and van Prooijen, 2015].

$$E = M(\tau_b - \tau_e)^n \tag{2.4}$$

Which can be rewritten for modelling purposes as following (assuming cohesive sediment; $n = 1$)

$$\begin{cases} E = M\left(\frac{\tau_b}{\tau_e} - 1\right) for\, \tau_b > \tau_e \\ E = 0\, for\, \tau_b < \tau_e \end{cases} \tag{2.5}$$

These formulations, together with eq. (2.2), make up the Partheniades-Krone relation, in which three different states can be distinguished;

- $\tau_b < \tau_d$: *Deposition*
- $\tau_e > \tau_b > \tau_d$: *Stable bed*
- $\tau_e < \tau_b$; *Erosion*

The *erosion* of the bed strongly depends on the bed properties. In general a distinction between the following four bed types is used: a sandy bed, a sandy bed with some fines, a consolidated muddy bed with some sand and a soft muddy bed with some sand. The bed material also defines the dominant transport mode.

For a sandy bed with some fines, such as the Rotterdam Waterway and North-Sea [de Nijs et al., 2008], the mobilization of the fines is governed by the hydrodynamic conditions whereas the entrainment of the fines is determined by the entrainment of sand. This is explained by Van Kessel and Winterwerp; as the sand is coarser than the fines, the fines are 'locked-up' between the sand particles. Therefore the mud particles can only be set to motion if the sand particles surrounding the fines are set to motion. Therefore Van Kessel and Winterwerp, developed a two layer model as displayed in fig. 2.6 which contains a fine top layer, a sand layer underneath with some locked-up finer particles and the interaction between them. The top-layer mainly consists of a thin fluff layer of fine sediment depositions, which is highly dynamic; the particles settle during Slack water and can be resuspended (or entrained) by the tidal currents. In contrast, the second layer has limited dynamics and is only brought in suspension by highly dynamic conditions such as storms or spring tide, while it is capable to store large amounts of fines in the bed [Winterwerp and van Prooijen, 2015].

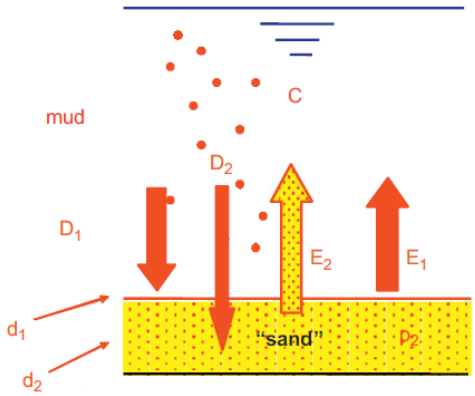

Figure 2.6: A schematization of the two-layer model. In which layer 1 (d_1) represents the thin fluffy layer and layer 2 (d_2) the sand layer with some fines. The deposition fluxes to layer i are represented by D_i and the entrainment fluxes by E_i [Van Kessel and Winterwerp].

Fluid mud

As rapid siltation or liquefaction of mud deposits takes place, a suspension with large concentrations can arise in the order of 10 g/l to 100 g/l. Due to hindered settling and flocculation direct settling is inhibited; a fluid mud layer may arise. A fluid mud layer is a suspension in a transient state, it is slowly consolidating as no mechanism keeps the particles in suspension. A fluid mud layer arises when the rate of sedimentation is larger than the consolidation rate of the bed [Winterwerp and Kesteren, 2004]. It is considered to be a Non-Newtonian fluid and if it is moving, its flow is laminar and independent of the flow characteristics from the water column above. The rate of consolidation is higher for a moving fluid mud layer, as excess pore water is expelled more easy due to shearing in of the moving layer. A fluid mud layer has a SPM concentration at or above the gelling point. The gelling point is the sediment concentration where the mixture of water and sediment flocs form a supportive network in which the flocs supports each other. The gelling concentration is derived by Winterwerp and Kesteren [2004] by using a flocculation model, see appendix B.3.5. The gelling concentration in the Rotterdam Waterway is approximately 60 g/l.

This fluid mud layer forms a two-layer fluid layer with the fluid mud layer close to the bed and the water above. As most turbulence is produced due to bed friction, this turbulence is damped by the SPM concentrations; decreasing the carrying capacity of the flow further. As the carrying capacity is further reduced, more sediment settles enhancing turbulence further. This positive feedback mechanism leads to a destruction of the amount of turbulence and thus concentration profile.

2.2.2. Large scale processes

As the small scale processes merely describe the behaviour of individual particles it is investigated which effects can be distinguished on a system level. This system level is the collective behaviour of more than one individual particle occurring on a larger spatial and time scale. These effects include *lag effects* and *the carrying capacity of the flow*.

Sediment transport capacity

The amount of SPM in suspension is determined by the amount of available sediment and the carrying capacity of the flow. In de Nijs et al. [2008] a vertical SPM concentration profile is derived under stratified conditions, given a Richardson flux number and a mixing coefficient. This concentration profile is given in eq. (2.6) and depends on the following parameters; the Flux Richardson number, see appendix B.1.2, the mixing coefficient induced by turbulence, the velocity profile over the vertical and the hindered settling velocity. This is a qualitative description of the parameters determining for which sediment concentration saturation occurs and needs thorough calibration before it can be applied. This parameter is very relevant in the Rotterdam Waterway, where a sharp pycnocline is noticeable. However due to differential advection of the salt wedge and the river discharge, significant shearing may occur, inducing turbulence. Therefore, in particular

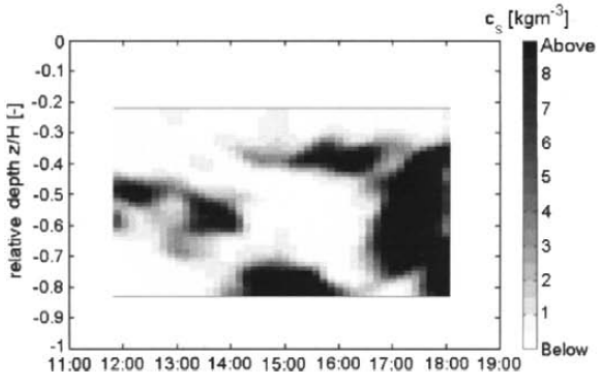

Figure 2.7: Qualitative view on the carrying capacity of the flow changing in time over the vertical [de Nijs et al., 2008].

around the pycnocline it is very relevant to derive the transport capacity as it is a balance between shearing induced turbulence and turbulence damping around the pycnocline.

$$c_s(z) = \frac{Ri_f \rho_s \nu_{t,s} (\frac{\partial u}{\partial z})^2}{\Delta g w_s} \tag{2.6}$$

In which, Ri_f equals the Richardson Flux number (see appendix B.1.2), ρ_s the SPM density, $\nu_{t,s}$, the turbulence viscosity affected by salinity, $\frac{\partial u}{\partial z}$ the vertical velocity shear, Δ the relative excess SPM density , g the gravitional acceleration and w_s the particle settling velocity [de Nijs et al., 2008]. In de Nijs et al. [2008], see fig. 2.7 a qualitative analysis of the carrying capacity of the flow is given. Here it is noted, that the location of the largest carrying capacity, due to aforementioned balance between shearing and turbulence damping, alters between near-bed and close to the surface and the pycnocline. The large carrying capacity over the entire water column after 16:00, is explained by the domination of shearing over turbulence damping. This shearing is induced due to internal tidal asymmetry; HWS near the surface occurs approximately 1 hour before HWS close to the bed.

The concept of concentration profile can be used to predict where the plume sediment transport will take place; if the carrying capacity around the pycnocline is limited after release it is likely that the sediment will settle to lower layers. However, as indicated by de Nijs et al. [2008] the concentration profile should be used for qualitative purposes only as thorough calibration is required to use it for a quantitative analysis.

2.2.3. Sediment dynamics of the system

In this subsection it is described to what extent the small scale and large scale processes can be used to describe the sediment behaviour in the Rotterdam Waterway. These processes are the occurrence of the Estuarine Turbidity Maximum (ETM), the response of the fine sediment to tidal asymmetry and lag effects and the description of the dominant sedimentation processes.

Peak velocity asymmetry

One of the consequences of tidal asymmetry is a difference in the duration of ebb period and flood period. When the ebb period is longer than the flood period, the peak flood velocities are higher due to continuity. This leads to a higher concentration and thus higher transport flux during flood, as transport is proportional to higher powers of the flow velocity. ($S \propto U^3$ for cohesive fractions and $S \propto U^4$ for non-cohesive fractions) It should be noted that the time-lag effect causes a delay and damping between the hydrodynamic forcing and sediment response as the sediment does not respond immediately to a change in its forcing [Winterwerp and van Prooijen, 2015] [Gatto et al., 2017].

From de Nijs et al. [2010] it can be derived that the peak flood velocities are larger than peak ebb velocities. Therefore more sediment is eroded during flood than during ebb, enhancing landward sediment transport.

It should be noted however, that the peak flood velocity is correlated to the lock-exchange mechanism. For higher freshwater discharges, the peak flood velocity increases.

Acceleration asymmetry

Acceleration or slack water asymmetry is associated with a difference in slack water duration. As flow velocities are low during slack water periods, particles have time to settle during these periods. Although the majority of the particles settle around slack water periods, asymmetry of the full acceleration/deceleration period leads to net sediment transport [Gatto et al., 2017].

From fig. 2.3, it can be derived that close to the bed low water slack is shorter than high water slack. Hence particles brought in suspension during ebb have shorter time to settle than particles brought in suspension during flood. Leading to more deposition after flood which enhances landward transport.

ETM dynamics

Although SPM transport is, averaged over the tide, seaward directed, a local peak of SPM can be maintained at the interface between fresh and salt water. This local high concentration of SPM is a distinct feature encountered in multiple estuaries, leading to high turbidity levels and hence called the *Estuarine Turbidity Maximum (ETM)*. This ETM, which may occur at several locations within an estuary, is often the result of accumulated sediment at the tip of the salt wedge. The development and feeding mechanism of the ETM has been described by Jay and Musiak [1994] as following: In the case of strong stratification, turbulence is damped around the pycnocline, as described in section 2.1.2. As the amount of turbulence decreases, the carrying capacity of the flow for SPM decreases as well, since turbulence keeps the SPM in suspension. Subsequently, suspended material rains out through the pycnocline while upward transport is inhibited due to the lack of vertical mixing. Hence SPM is trapped on the landward limit of the salt wedge. This causes high local sediment concentrations (SPM) in the bottom layer and low or almost none SPM in the surface layers during stratified conditions, due to this accumulated SPM [Geyer, 1993]. This trapping mechanism is schematised in fig. 2.8.

In general, the majority of the sediment found in an ETM has fluvial origin, however the trapping process is independent of its source. In Jay and Musiak [1994], it is stated that the formation of the ETM depends mostly on the quality of the supplied material; if the material is too fine it will simply be advected through the estuary as wash load, whereas coarse material will be advected as bed load; both inhibiting the formation of an ETM.

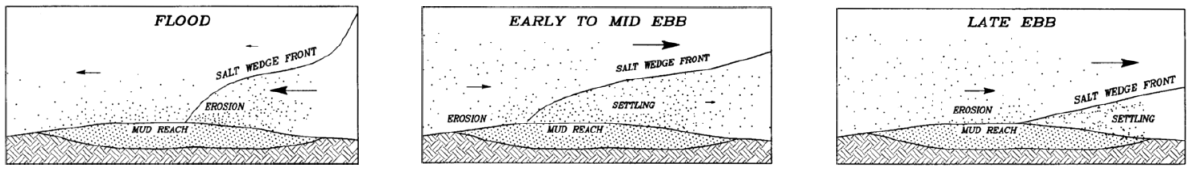

(a) Landward advection of the salt wedge during flood

(b) Seaward retreat of the salt wedge after HWS

(c) Minimum intrusion of the salt wedge before LWS

Figure 2.8: ETM formation and advection over a tidal cycle. During flood the salt wedge is advected landward entrapping SPM from the bed and hence 'feeding' the ETM. Subsequently during early ebb the flow is reversed, but due to tidal straining the salt wedge is advected slower than the less dense surrounding water, allowing fluvial SPM to rain out above the salt wedge. At late ebb or LWS the size of the salt wedge is minimal, with a local peak of accumulated SPM. [Jay and Musiak, 1994]

In the Rotterdam Waterway the trapping mechanism works as following. During flood the salt wedge propagates up estuary, while sediment is resuspended from the bed. Due to turbulence damping at the pycnocline this eroded sediment is entrapped within the salt wedge. During subsequent HWS fresh water, containing fluvial sediment is being advected over the salt wedge. As the fresh water is advected above the salt wedge, inducing vertical velocity shear. Due to this velocity difference vertical transport of SPM into the salt wedge is promoted. During HWS this fluvial sediment may settle around the upstream end of the salt wedge, as indicated in fig. 2.8. Again this settling is induced by the reduction of turbulence above the pycnocline. As the SPM settles again a sharp Lutocline may arise, inducing the possible formation of fluid mud layers [de Nijs et al., 2008]. After ebb, during LWS the entrapped sediment is allowed to settle. During subsequent the the

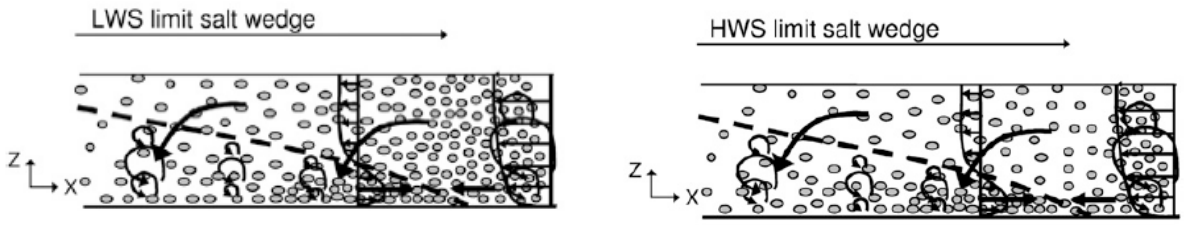

(a) (b)

Figure 2.9: A schematisation of the working principle entrapping fluvial sediment at the tip of the salt wedge. The vertebrae indicate the damping of turbulence at the salt wedge (dashed lines) This working principle acts throughout the tidal cycle, but is most evident around the tip of the salt wedge. Note the difference in fluvial SPM concentration at the end of ebb (LWS) (a) and after flood (HWS) (b) as indication of the entrapping efficiency. [de Nijs et al., 2010]

settled sediment is again resuspended and entrapped within the salt wedge. In fact, based on bed samples, it is found that deposition during LWS and HWS equals the amount of entrainment on subsequent ebb and flood. And the capacity to remobilize the deposited SPM seems sufficient to prevent the long term settling of fine particles in the Rotterdam Waterway. All together this leads to a repetitive pattern of settling, deposition, re-entrainment, advection of SPM, non-capacity transport conditions and the lack of silts in the dredged material explains why the SPM in the ETM is maintained in suspension and does only settle in the basins [de Nijs et al., 2010]. The amount of SPM in the ETM is therefore determined by the length of the salt wedge and not by the strength of the gravitational flow and tidal pumping importing marine SPM.

In the Rotterdam Waterway the appearance of the ETM is stated to be one of the major driving mechanism of the sedimentation of the harbour basins lining the Rotterdam Waterway. as is explained in one of the next paragraphs.

SPM concentrations

The concentration of SPM in the Rotterdam Waterway varies significantly in time and space and is determined by the amount of available sediment and the carrying capacity of the flow. In the measurement campaign, chapter 6, a deviation from the expected background concentration is used as an indication for the advection of a SURICATES sediment plume. Therefore a range of background concentrations has to be found for the Rotterdam Waterway.

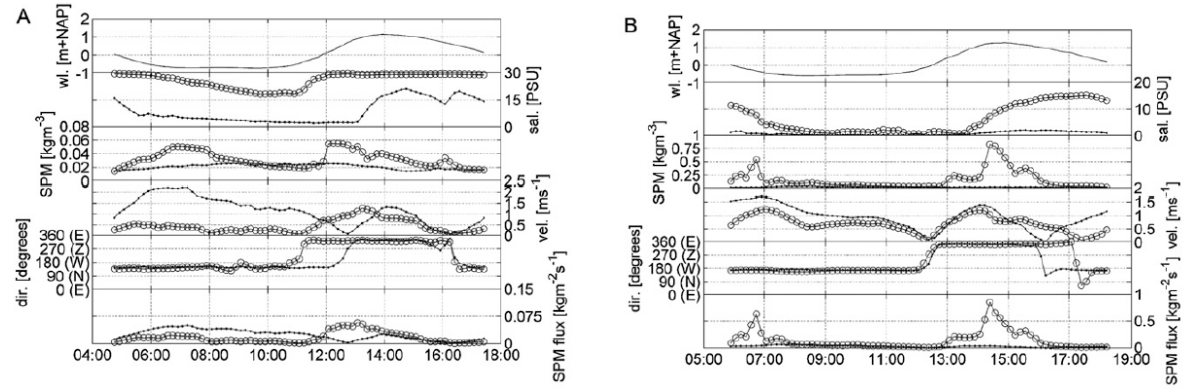

(a) (b)

Figure 2.10: The recorded water level, salinity, SPM concentration ($kg/m^3 = g/l$), velocity magnitude, flow direction, and transport of SPM from in an Eulerian frame of reference at stations Hook of Holland (a, left) and in front of the Botlek (b, right) as recorded on 11 Apr 2006. The data are located at fixed heights NAP -3 m near the surface (dots) and NAP -13 m near the bed (open circles) [de Nijs et al., 2010].

In fig. 2.10 the variation in the concentration of SPM in time is shown at Hook of Holland and the Botlek on

April 11, 2006[1]. It can be observed, that SPM concentrations high in the water column at Hook of Holland are constant at 0.02 g/l, despite the tide. While close to the bed, or below the pycnocline, this varies between 0.02 g/l at LWS to a peak of 0.08 g/l just after LWS. Near the Botlek significantly higher concentrations of SPM are encountered. After LWS and HWS, SPM concentration peaks of 0.5 and 0.75 g/l are encountered. Moreover, it can be observed that SPM concentrations are constantly above 0.25 g/l during flood (13:00 - 16:00) in front of the Botlek. In de Nijs et al. [2010] is stated that peak concentrations are not correlated to peak flood velocities and thus not likely to be caused by resuspension of sediment. It is more likely to be caused by the advection of the local ETM. During high discharge conditions peak values of SPM may reach > 1 g/l.

From the vertical structure of SPM, fig. 2.11 it can be observed that SPM concentrations vary between 0.06 to 0.03 g/l in the top of the water column. Moreover, the importance of the tip of the salt wedge is evident for the distribution of SPM over the vertical. A strong decrease in SPM concentration can be seen above the pycnocline at the onset of ebb. Indicating the efficiency during preceding flood of the assumed trapping mechanism explained in the previous paragraph. Moreover, it can be observed that SPM concentrations above the pycnocline decrease moving seaward at the onset of flood as well. At last the trapping mechanism at the tip of the salt wedge is evident during flood and ebb: especially short after HWS (top) SPM concentrations above the salt wedge decrease rapidly. With peak values of 0.8 g/l at the tip of the salt wedge, explained by the ETM.

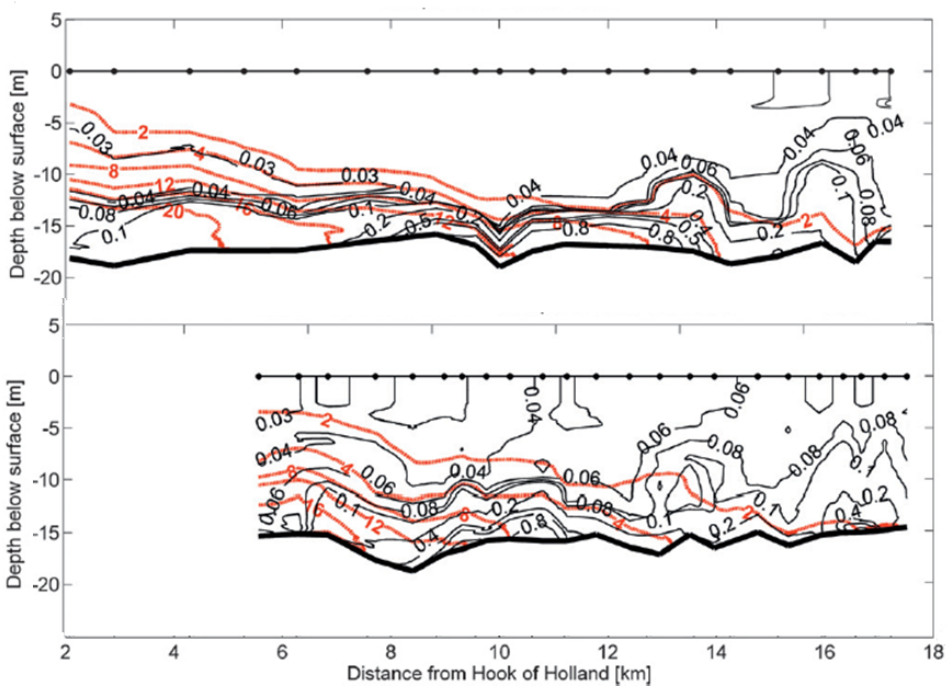

Figure 2.11: Vertical structure of SPM concentrations (g/l) from an Lagrangian FOR in the Rotterdam Waterway during ebb (6:23 - 8:10) (top) (schematized in fig. 2.9a) and flood (12:58 - 14:00) (bottom) (schematized in fig. 2.9b) on April 11, 2006 [de Nijs et al., 2010].

Port sedimentation

The different parts of the port, especially the basins lining the fairways are subject to significant sedimentation. The source of the sediment and the driving processes differ significantly throughout the port as is shown in fig. 2.12. As can be deduced from this figure; a clear distinction can be made between the parts of the port subject to fluvial and marine sediment import. The basins in the 'front' of the port, such as the Maasvlakte and Europoort are subject to marine deposits, whereas the basins lining the Rotterdam Waterway, such as the Botlek, are subject to fluvial sediment deposits. In this section emphasis is put on the sedimentation mechanism in the Rotterdam Waterway. For the driving mechanism towards the Maasmond the reader is referred to appendix B.3.7.

[1] It should be noted that April 11, 2006 is characterized by high discharge conditions, explaining the limited salt intrusion length.

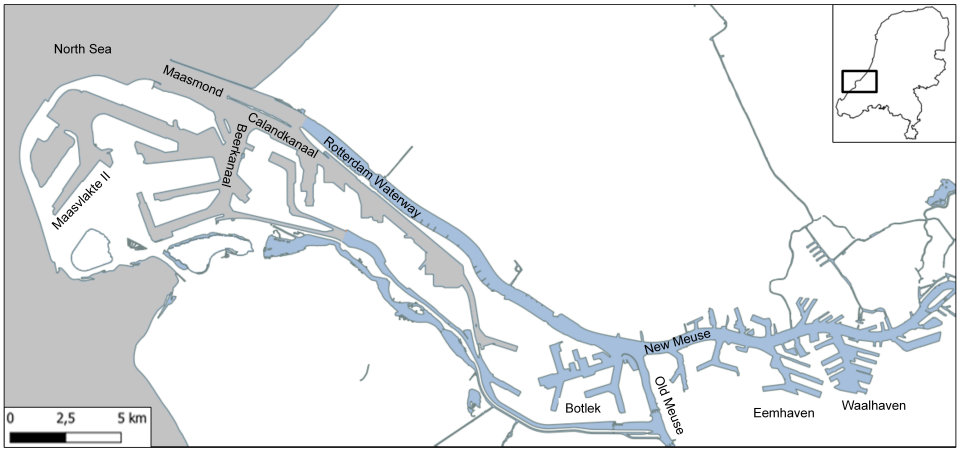

Figure 2.12: Dominant source of sediment in the various parts of the Port of Rotterdam. In the grey areas mainly marine deposits are found, whereas in the blue areas mainly fluvial deposits are found. After de Groot [2018]

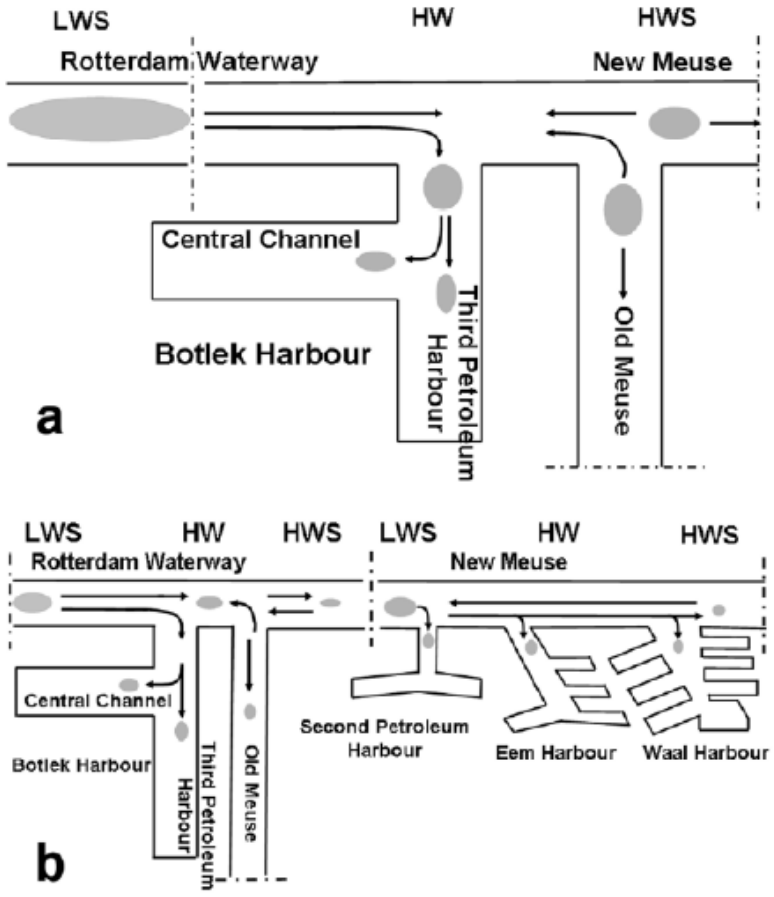

Figure 2.13: A schematization how fluvial sediment is imported into the harbour basins lining the Rotterdam Waterway. a) represent a typical conditions where the ETM oscillates between the junction and the Botlek harbour. b) represent conditions when salt intrusion is promoted and hence advected further upstream. e.g due to spring tide, wind set-up or low river discharges. This caused the ETM to be split between the Old Meuse and New Meuse and allows sediment to be exchanged with basins further upstream. [de Nijs et al., 2009]

In appendix B.3.7 is described how mainly marine sediment is imported into the Maasmond and southern basins. In de Nijs et al. [2008] an absence of significant SPM variations after set-up and storm events in the Rotterdam Waterway is observed. This latter observation supports the fact that the Rotterdam Waterway is not subject to marine import of sediment. Moreover, de Nijs [2012] concluded that the amount of SPM in the ETM is determined by the length of the salt wedge and not by the strength of the gravitational flow and tidal pumping importing marine SPM, supporting the latter observation. The basins lining the Rotterdam Waterway are subject to fluvial sedimentation, as can be seen in fig. 2.12. As explained in section 2.2.3 the salt wedge is constantly supplied with SPM, as SPM transported above the pycnocline slowly rains out and is entrapped herein. As the salt wedge passes harbour basins lining the Rotterdam Waterway and New Meuse during rising tide, water flows into the basins by *tidal filling* and *near-bed density current*. Tidal filling occurs during rising tide and falling tide, driven by the water level differences between the Rotterdam Waterway and harbour basin. During rising tide SPM rich water flows into the harbour basins, while SPM poor water flows out during falling tide. A density current is based on the difference in salinity and SPM concentration between the harbour basin and Rotterdam Waterway. Between LWS and HWS the water in the Rotterdam Waterway is denser, so near the bed a (SPM-enriched) current flows into the basins. As the basins are less dynamic, the carrying capacity of the flow in the basins is less, allowing sediment to settle throughout the tide, with peaks during slack tide. During falling tide, the water in the basins is denser than in the Rotterdam Waterway, however as most SPM has settled in the basins, (near-bed) SPM poor water flows back into the Rotterdam Waterway [de Nijs et al., 2008] [Winterwerp and van Prooijen, 2015].

2.3. Summary

In this chapter existing literature on the hydrodynamics of estuaries and sediment dynamics in estuaries is discussed. This is done for processes on the small scale and larger scale. Subsequently, these processes are used to describe the observed behaviour in the system of interest: Rotterdam Waterway.

Which processes govern the hydrodynamics and the sediment behaviour in the port of Rotterdam?

The most important features governing the hydrodynamics in the Rotterdam Waterway are the advection of the salt wedge, barotropic tidal asymmetry and baroclinic exchange flows and turbulence damping. Due to the advection of the salt wedge and turbulence damping at the pycnocline, 50 % of the provided fluvial sediment from upstream is entrapped within the Rotterdam Waterway. This is advocated by the observation of decreasing SPM concentrations above the pycnocline. The entrapped sediment undergoes a repetitive behaviour of advection, settling, resuspension and accumulation at the tip of the salt wedge in the form of an ETM. When the ETM is located in front of a harbour basin, density currents are driven into the harbour basins leading to siltation of the basins lining the Rotterdam Waterway.

The most important features governing the hydrodynamics in the Rotterdam Waterway are the advection of the salt wedge, barotropic tidal asymmetry, baroclinic exchange flows and turbulence damping. The tidal asymmetry modulates the time scale of the advection of the salt wedge within the estuary. The tidal asymmetry is caused by the deformation of the tidal wave in the North Sea rather than by internal tidal asymmetry of the Rotterdam Waterway [de Nijs et al., 2010]. The associated density differences lead to the observed differential advection of the heavier water near the bed and lighter fresh water on top [de Nijs et al., 2011a]. Moreover, as found by de Nijs et al. [2011a], the flow is ebb dominated upstream (higher ebb velocity and longer ebb period), as the freshwater discharge dominates the barotropic tidal asymmetry. Down estuary, at Hook of Holland, only in the upper part of the water column ebb dominance can be found, while close to the bed the flow is flood dominated.

Above the salt wedge, or pycnocline, SPM rains out throughout the tidal cycle clearing the upper part of the water column from SPM de Nijs et al. [2009]. Due to turbulence damping, this sediment remains entrapped below the pycnocline. This SPM settles during slack water, however most SPM is entrained after tide reversal. Therefore the behaviour of SPM in the ETM is can be summarised by advection, settling, resuspension and

accumulation at the tip of the salt wedge where an ETM can be observed. This theory is supported by the lack of settled fine sediments in the bed of the Rotterdam Waterway.

The location of the ebb end of the salt intrusion limit depends on the river discharge, tidal forcing, wind set-up at sea and the wind. de Nijs et al. [2011a] found that the saltwater intrusion length at LWS is 2 to 11 km from Hook of Holland and at HWS 13 to 20 km. However, in de Nijs et al. [2008] is stated that the saltwater intrusion limit can even be located in the Maasmond, downstream of Hook of Holland. As the width and depth of the Maasmond is much larger, the ETM can lose a large amount of its SPM. During flood, the concentration of SPM and salinity in the Rotterdam Waterway is larger than in the basins, hence a SPM rich density flow is driven into the harbour basins. During subsequent slack water this SPM settles in the harbour basins, resulting in the basins being very effective sediment traps. Hence the SPM distribution is determined by the availability of SPM in the bed, the advection of the salt wedge and the sediment dynamics within the ETM due to erosion and sedimentation and exchange with the basins. de Nijs et al. [2008] found that the main driver of sedimentation towards the basins is the location of the ETM: sediment transport towards the basins is largest when the ETM is located in front of a harbour basin.

3

Sediment plume behaviour

To determine the behaviour of the SURICATES pilot study, the understanding of the system is extended with a literature review on the behaviour of sediment plumes. The understanding of a dredging sediment plume is a combination of hydrodynamics and sediment dynamics and is therefore treated separately. At first the generation of a dredging plume in general is discussed and details on the sediment plume of the pilot study are given. Subsequently a hypothesis is derived to describe the SURICATES plume behaviour on three different length scales: near field, mid field and far field.

3.1. Introduction

When a sediment plume is released in ambient flow, a complex interaction between the plume and flow takes place, driven by density and momentum differences between the flow and the plume. This interaction determines whether the plume acts like a density current or whether it is mixed over the flow, see fig. 3.3. Moreover, the dredging vessel itself can induce additional effects such as propeller mixing and flow widening around the hull of the vessel [de Wit, 2010].

To derive an hypothesis for the behaviour of SURICATES sediment plumes, an analogy is used between the SURICATES sediment plumes and overflow sediment plumes. Overflow plumes are a by-product of dredging operations using a Trailing Suction Hopper Dredger (TSHD). When sediment is dredged excess water (with suspended sediment) is released through an overflow to increase the amount of dredged material in the barge, as shown in fig. 3.1. In appendix C.2 the SURICATES sediment plumes are compared to the overflow plumes to advocate this assumption.

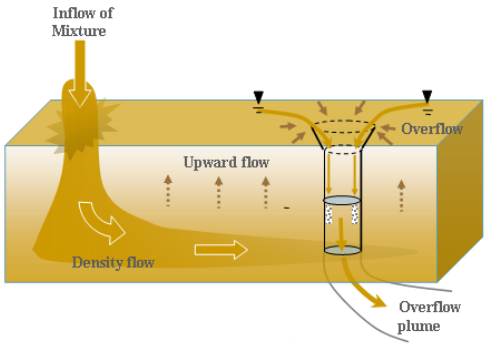

Figure 3.1: Generation of an overflow plume inside the barge of a TSHD. At the left side the dredged sediment water mixture enters the barge. Inside the barge coarser particles settle, while water is pushed upward by the fresh incoming mixture. This mixture containing (little) suspended sediment is released through the overflow [Spearman et al., 2011].

In general the behaviour of a dredging sediment plume can be distinguished on different scales, these scales are subject to different definitions by different authors. In Winterwerp [2002] the following three distinct scales are used:

- **Near field**: $(\mathcal{O}(0.1-1km),\mathcal{O}(hours))$: The sediment plume dynamics are mainly determined by the initial momentum to buoyancy ratio and characteristics of the dredger. The sediment plume is said to be dynamic.
- **Mid field**: $(\mathcal{O}(1-10km),\mathcal{O}(days))$: The sediment plume dynamics are mainly determined by local hydrodynamics and properties of the sediment in the plume. The sediment plume is said to be passive.
- **Far field**: $(\mathcal{O}(10-100km),\mathcal{O}(month-years))$: The sediment plume dynamics are determined by the hydrodynamics and interaction with the bed.

The interaction between near field, mid field and far field is best described by de Wit [2015], stressing the importance of the initial or near field behaviour to understand the behaviour in the mid field and far field. Moreover, the near field behaviour is evident to derive an accurate source term for the far field modelling of the plume in as described in chapter 5 [Becker et al., 2015].

> *The focus of this study is plume mixing in the near field because near field mixing determines the amount and distribution of suspended sediment available in the far field.*

In the following thesis the distinction near field and mid field is set at the area of influence of the dredging vessel and the initial momentum and buoyancy of the plume. This is approximately at a of 0.1 to 1 kilometre or after 15 minutes, see fig. 3.8. In this phase the plume is said to be dynamic and subject to several processes. In this phase general plume theory is applicable. In the subsequent phase, the mid field, the plume exhibits passive behaviour; local hydrodynamics and settling behaviour of individual particles dominates. The distinction between mid field and far field behaviour is drawn at the harbour mouth (located 10 kilometres from the disposal site) or after the particles have settled in the Rotterdam Waterway, as the far field governs the interaction with the bed. In the following paragraphs some background information on the sediment plumes during the pilot study is given and the analogy with the overflow plumes is discussed. Subsequently, an hypothesis is drawn for the expected behaviour of the plume on the near field, mid field and far field scale.

3.1.1. SURICATES sediment plumes

During the execution of the pilot study dredged sediment has been disposed at an allocated location in the *'Bend of Maassluis'*, indicated with *'Disposal'* in fig. 1.1. In section 1.3.1 has been discussed that the disposal boundary conditions are the timing of disposal, type of sediment disposed, execution method and location of disposal. Over the course of the pilot study there has been a variation in the first three mentioned.

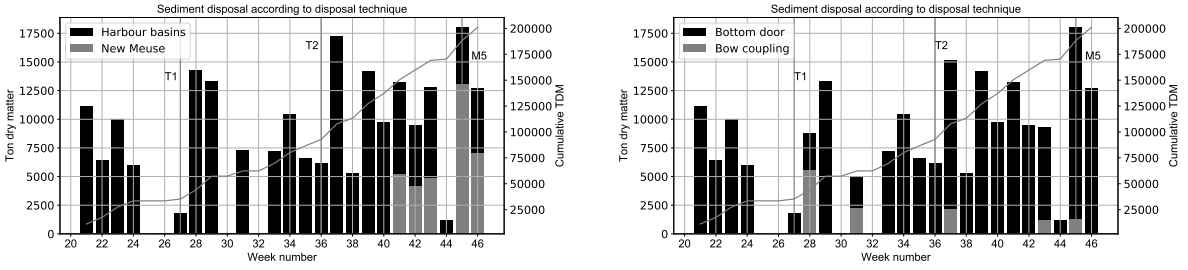

(a) The amount of disposed sediment during the SURICATES pilot study per week according to sediment source

(b) The amount of disposed sediment during the SURICATES pilot study per week according to disposal technique

Figure 3.2: An overview of the disposals of the SURICATES pilot study per week and cumulative over the period. A distinction is made between and the sediment source a) the method of release b).

Sediment source

The first distinction is made between the sediment source: sediment dredged in the New Meuse and sediment dredged in the harbour basins lining the New Meuse, see fig. 3.2a. From this graph it can be deduced that

17% of the sediment is dredged from the New Meuse and the remainder from the basins, predominantly from the Waalhaven and Eemhaven. As there is no large difference in the sediment composition between the Eemhaven or Waalhaven, this is not further scrutinized. The sediment from the New Meuse however has a higher sand fraction than the harbour basins. In chapter 1 and chapter 2 it is already stated that hardly any mud is dredged in the fairway, whereas the sediment dredged from the basins is almost exclusively silt [de Nijs et al., 2008]. This is confirmed by the grab samples taken in the basins, see appendix G.3.1. (Eemhaven (*Vak22 - Vak25*), Waalhaven (*Vak31*) and the fairway (*NMS9,1* and *NMS9,2*)) From these grab samples can be derived that the fairway contains 35 % fines ($< 63\ \mu m$), whereas the basins contain 80% fines. Stutterheim [2002] found similar percentages, with 86 % of the sediment dredged from the basins being smaller than 63 μm and 49 % for the fairway. Apart from the different settling and erosion characteristics, the particle size also has a significant influence on the sensitivity of the measuring techniques, as is explained in appendix D.2.3.

Execution method

Another distinction can be made based on the method of execution. Over the course of time, a few disposals have been executed using bow coupling (making up 7 % of the total amount of disposals) instead of by drawing the bottom doors, see fig. 3.2b. In the first method the sediment is disposed within 4 to 5 minutes resulting in a high average disposal rate of 7.9 TDM/s (22 m^3/s). This plume has an initial downward velocity of $\approx 22 m/s$, resulting in an impact crater in the river bed. Moreover, the sediment is released at the draught of the ship, whereas during bow coupling the sediment is disposed through a pipeline into the surface layer of the water, see fig. 3.4. As such a disposal takes approximately 50 minutes a much lower flow rate is established; 0.47 TDM/s (1.3 m^3/s). The different methods of disposal have a large influence on the expected near field behaviour. Drawing the bottom door results in a plume with behaviour as shown in fig. 3.3a, whereas using bow coupling results in a plume as shown in fig. 3.3b. This difference is further discussed in section 3.2.

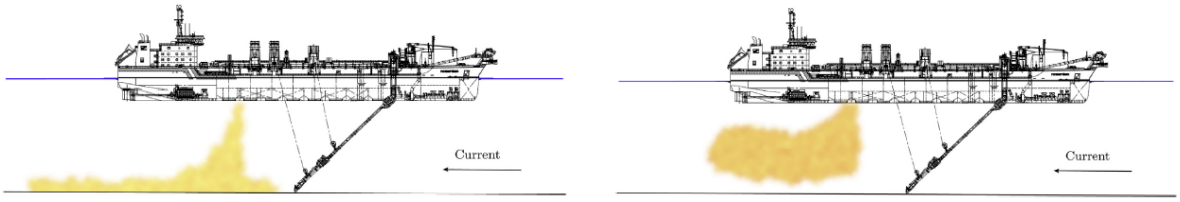

(a) Initial plume behaviour for a momentum dominant plume

(b) Initial plume behaviour for a mixing dominant plume

Figure 3.3: The difference in initial plume behaviour in ambient water for a density dominant plume and a plume for which mixing of the ambient current is dominant [Becker et al., 2015].

Timing of disposal

The timing of the disposals has been related to the predicted depth-averaged high water slack (HWS) times at Maassluis. In the execution plan of the project is stated that disposals preferably take place around predicted HWS. In table 3.1 it can be seen that the majority (78 %) of the disposals has taken place between half an hour prior to HWS to an hour after HWS.

Bin	**-1.5h - -1h**	**-1h - -0.5h**	**-0.5h - HWS**	**HWS - 0.5h**	**0.5h - 1h**	**1h - 1.5h**	**>1.5h**
Percentage	5 %	7 %	15 %	35 %	28 %	7 %	2 %

Table 3.1: Timing of the disposals with respect to the predicted HWS at Hook of Holland. There are 2 disposals more than 2 hours after HWS.

3.2. Near field behaviour

The near field behaviour of a sediment plume is limited to the processes determined by the initial momentum and buoyancy of the plume, as well as vessel induced effects [de Wit, 2015]. In this thesis, the analysis of the near field behaviour is limited to the attributions of initial momentum, buoyancy and interaction with the

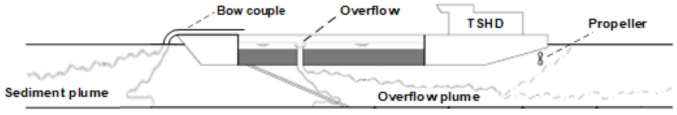

(a) Schematisation of a bow coupling disposal and plume generation

(b) Photo of a bow coupling disposal

Figure 3.4: a) A schematization of the generation of a sediment plume using bow coupling and an overflow plume used as reference. After de Wit et al. [2014]. b) A photo of the bow couple disposal at November 5.

Cross flow. In this phase the plume is said to be dynamic and general plume theory is applicable. As sediment plumes are good examples of buoyant Jet in Cross Flow (JICF), (containing both momentum and buoyancy) general theory on buoyant jets is applicable. It is stressed that the bulk behaviour of the water-sediment mixture (JICF behaviour) is more important to describe the near field behaviour of the JICF, rather than the characteristics of the individual particles within the JICF. For general plume theory the reader is referred to appendix C.1. In the following section emphasis is put on sediment plume behaviour.

3.2.1. Sediment plume behaviour

Winterwerp [2002] proposed two governing parameters to describe the expected initial behaviour of a sediment (overflow) plume in ambient flow: the velocity ratio (ζ) and Richardson number (Ri_p). The Richardson number (Ri_p) is used to describe the initial buoyancy of the plume, see eq. (3.1), in which, ρ_{of} equals the overflow density, ρ_w the density of the ambient water, D the diameter of the outflow pipe which equals the initial diameter of the plume and W_{j0} equals the initial downward velocity of the plume. The velocity ratio, see eq. (3.2), is the ratio between the initial velocity of the sediment plume and the cross flow velocity u_{cf}.

$$Ri_p = \frac{\frac{\rho_{of}-\rho_w}{\rho_w} g D_{j0}}{W_{j0}^2} \tag{3.1}$$

$$\zeta = \frac{u_{cf}}{W_{j0}} \tag{3.2}$$

Based upon these two parameters, Winterwerp [2002], defined three distinct processes to describe the dispersion of a sediment plume in the ambient waters, see fig. 3.5a. These three distinct states are defined as following;

- **Density current:** As the initial plume has negative buoyancy it spreads close to the bed as a density current. This is shown in fig. 3.3a.
- **Mixing:** The plume is caught by the flow and mixed over the depth, due to the low momentum to buoyancy ratio, see fig. 3.3b.
- **Transitional:** A state in which both processes occur simultaneously.

It should be noted however that the state of a plume is not fixed over time and space. As a plume is advected in time and space its initial momentum decreases and given enough distance from the source, every plume is subject to mixing. Plumes with a high Ri to ζ ratio will remain density driven over a longer time / distance than plumes with low Ri to ζ ratio's, in which the ambient current is dominant over the initial momentum of the plume [Winterwerp, 2002]. In fig. 3.5b the transition depths are shown, based on the initial diameter (D) of the plume.

In table 3.2 three different sets of values are shown: *Overflow*, *Bow couple* and *Bottom door*. The first row contains a range of values found for possible overflow (sediment) plumes by Van Eekelen [2007]. These values are based on typical ranges for ρ_0, ρ_a, D and u_{cf}. Since the flow velocity varies significantly over depth in the Rotterdam Waterway the cross flow velocity is not constant. de Wit [2015] validated its theory and model for a range of $0.33 < \zeta < 4$ and $0.01 < Ri < 22$, overflow densities varied between 1035 and 1330 kg/m^3 ($\Delta\rho_0 = 35 - 330\ kg/m^3$). As can be seen, bow coupling releases lie within this range of validation. de Wit

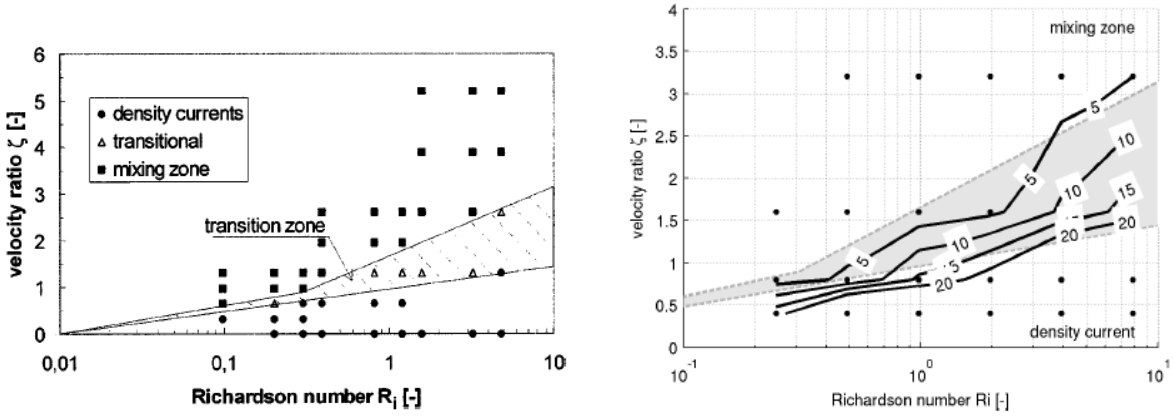

(a) The different state classifications for a dredging plume depending on the Richardson number and velocity ratio.[Winterwerp et al., 2002]

(b) The different transition depths for dredging plumes depending on the initial diameter (D), Richardson number and velocity ratio. [de Wit, 2010]

Figure 3.5: The different classifications of an overflow plume in ambient water

	$\Delta\rho_0$ $[kg/m^3]$	D_{j0} $[m]$	u_{cf} $[m/s]$	W_{j0} $[m/s]$	Ri_p $[-]$	ζ $[-]$
Overflow	40 - 90	1.5 - 4.0	0 - 4.0	0.5 - 1.5	0.1 - 10	0 - 8.0
Bow couple	300	0.6	0.5 - 2.1	4.1	0.1	0.1 - 0.5
Bottom door	300	0.9	0.5 - 2.1	23.0	0.0	0.03

Table 3.2: The different values for the velocity ratio (ζ) and Richardson number (Ri) for an average overflow plume and the sediment plumes using the two different execution methods in this pilot study, assuming two different cross flow velocities (U).

[2015] found that the effect of the cross flow velocity, plume density and disposal rate to have the largest effect on the near field behaviour.

- **Cross flow velocity**
  The larger the cross flow velocity ($u_{cf} = u_a + u_{TSHD}$) the larger the amount of sediment still in suspension. A smaller cross flow velocity promotes the settling of particles.
- **Overflow density and velocity**
  The larger the overflow density and velocity, the larger the sediment flux towards the bed in the near field.

3.2.2. SURICATES sediment plumes

In appendix C.1 and section 3.2.1 the theory on JICF and sediment plumes is discussed in the near field. In this subsection this theory is applied to predict the behaviour of the disposals in the Rotterdam Waterway in the context of the SURICATES pilot study. At first the disposals by bow coupling are discussed, followed by discussing its difference to the bottom door disposals.

Bow coupling

In the following section a hypothesis is drawn for the bow coupling disposals, such as the release on September 11 and November 5, 2019. In the third row of table 3.2, one can see the values for the plume parameters for such a disposal. The density of the plume disposed on November 5 is significantly larger than for ordinary overflow plumes, however the overall density still falls within the range for overflow plumes as by Van Eekelen [2007].

Based on the velocity ratio and Richardson number, initially jet like / density current behaviour is expected,

where no mixing with the ambient flow takes place. In de Wit [2010] a transition depth is defined, expressing the depth from which a transition can be expected from density to mixing dominated flow. For the bow coupling plumes this depth is >> $20D$. With a diameter of $0.6m$, it is expected that mixing happens approximately halfway (>> $12m$) the water column. However, based on general plume theory, see appendix C.1.1, plume behaviour and thus mixing with the ambient flow is initiated after a depth of 4m. Hence mixing is expected to occur at a depth of 4 to 12 m. This is in line with the observations on September 11 and November 5.

Bottom door release

In the case for a plume released through the bottom doors only jet / density current behaviour is expected, since the transition depth (18 m) is larger than the water depth. Therefore, no transition from density current behaviour towards mixing behaviour is expected, see fig. 3.5b. However, strictly speaking this assumption can not be validated with the theory used on overflow plumes as this theory is not validated for the values occurring for bottom door releases. For the bottom door releases disposal takes place at 6 m below the water surface at a high plume flow velocity (23 m/s), which leads to both a velocity factor ≈ 0 and Richardson number ≈ 0. In fig. 3.5a, it can be observed that density current like behaviour is expected. As

In de Wit [2015] is described that, using results by Boot [2000], that a radial spread of a sediment plume is expected as it touches the bed. Subsequently, the sediment plume is expected to spreads like a density current along the bed as shown in fig. 3.6 and fig. 3.3a. This theory is also supported by observations made in the Rotterdam Waterway. During the execution of the SURICATES pilot study a large pit has arisen under the impact of the released sediment plumes. This observation confirms that sediment plumes released through the bottom doors touch the river bed. This has lead to unexpected results from the bathymetry analysis; after a release the amount of sediment in the area of disposal had decreased, see fig. 3.7.

Figure 3.6: Radial spreading and advection as density current. [Winterwerp, 2002]

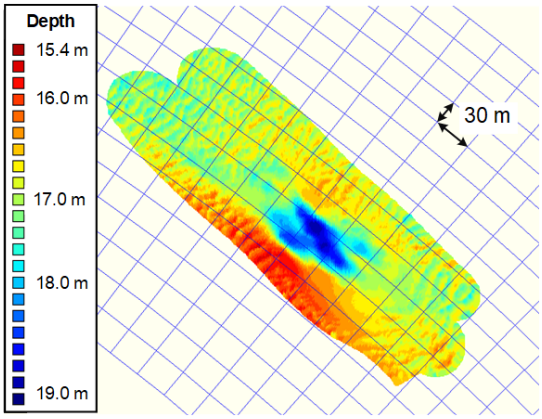

Figure 3.7: The pit at the disposal site probably caused by the impact of the sediment plume.

3.3. Mid field behaviour

The fate of the dredging plume in the mid field is determined by the outcome of the near field behaviour of the plume, the individual (settling) characteristics of the particles within the plume and the governing hydrodynamics [de Wit, 2015]. In this thesis the distinction between near field and mid field is drawn where the sediment plume has lost its initial momentum and buoyancy. This is at 1 kilometer from the disposal site, as indicated in fig. 3.8. The transition between mid field and far field is drawn after the sediment particles of the plume have settled or when the particles are outside the spatial limit of the mid field: the mouth (Maasmond) of the port of Rotterdam. In the following section, first sediment plume behaviour in the mid field in general is discussed, followed by a distinction based on execution method and time of disposal.

To understand the expected behaviour of the sediment plume in the mid field, an analogy is drawn with the fate of fluvial sediment in the Rotterdam Waterway, allowing the application of work by de Nijs [2012]. In de Nijs et al. [2010] is found that at Hook of Holland the net flux of sediment, averaged over a tidal cycle, is

seaward directed. However, near the bed this flux is landward directed, stressing the important where the sediment transport of the plume takes place. If transported above the pycnocline a net seaward transport of the sediment plume is expected. If transported below the pycnocline it is expected to follow the fate of the trapped fluvial sediment.

Moreover, due to differential advection (see appendix B.2), particles higher in the water column are advected further downstream during ebb, whereas particles closer to the bed are advected slower or landward. This is illustrated in fig. 3.8 where a prediction is made on the expected displacement of a sediment plume disposal depending on its water depth. To predict the advection of the plume, the predicted flow velocity at different depths is averaged in time. The predicted advection of the SURICATES plume 1 hour and 2 hours after disposal is shown for various depths in fig. 3.8. In fig. 3.8 it can be seen, that differential advection is significant; if the sediment plume is advected in the top layer it reaches the mouth of the port before LWS, whereas for advection lower in the water column this is very unlikely.

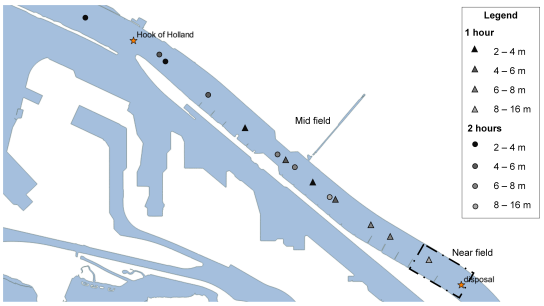

Figure 3.8: The expected displacement of a sediment plume, 1 and 2 hours after release depending on the depth of advection. The expected location of the plume is indicated with two symbols, the plume extends between these two locations.

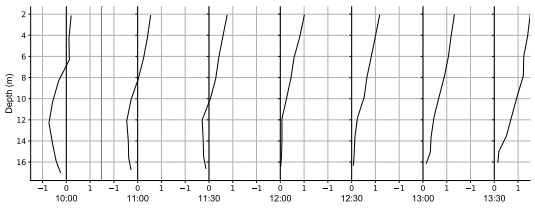

Figure 3.9: Predicted horizontal flow velocity at Maassluis from one hour prior to HWS (at 11:10) until 2.5 hours after HWS at November 5, 2019.

3.3.1. Bow couple

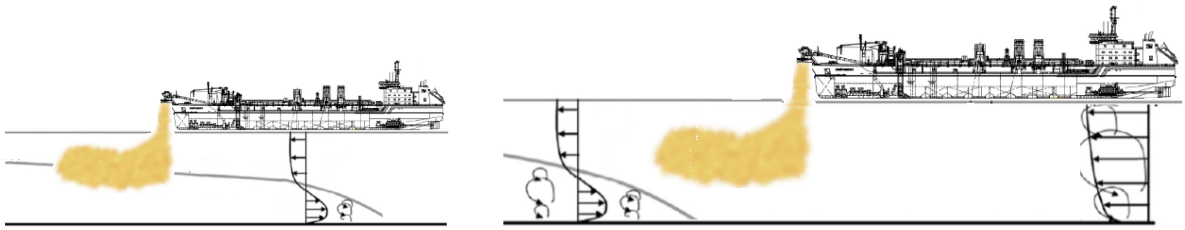

(a) (b)

Figure 3.10: The difference in initial plume behaviour for a sediment plume disposed by bow couple release inside a) and outside b) the salt wedge.

For a sediment plume brought in the system using the bow couple it is expected that the plume is mixed over the water column in the near field, between 4 to 12 meters. It is expected that particles above the pycnocline, which will be limited according to the near field analysis, will slowly rain out as the sediment plume is advected downstream. In fig. 3.10 the spread of sediment by bow coupling is shown outside the salt wedge and on the interface between fresh and salt water. For the particles located disposed outside the salt wedge, a trapping efficiency of 50 % is expected. Since the trapping mechanism of fluvial sediment, as explained in section 2.2.3 and has an efficiency of approximately 50 % [de Nijs et al., 2010]. Moreover, as shown by de Nijs et al. [2010], the amount of SPM above the pycnocline decreases in the downstream direction. However, the raining out of sediment can be disturbed as velocity shearing may induce turbulence and hence increase the local carrying capacity for SPM, as shown in section 2.2.2. Therefore, it is expected, that some advection may take place around the pycnocline due to local induced turbulence inhibiting the raining out of fluvial sediment. For particles disposed directly inside the salt wedge permanent entrapment is expected, as turbulence

damping inhibits upward movement.

As sediment plumes are disposed during ebb, downstream transport is expected initially. However, the displacement of the sediment plume depends strongly on the depth of the sediment plume. During flow reversal from ebb to flood (LWS), the flow velocity decreases and the turbulence field collapses, allowing sediment to settle [de Nijs et al., 2008]. Therefore, it is expected that the majority of the sediment will settle within the Rotterdam Waterway, unless it has reached the Maasmond prior to LWS.

3.3.2. Bottom door

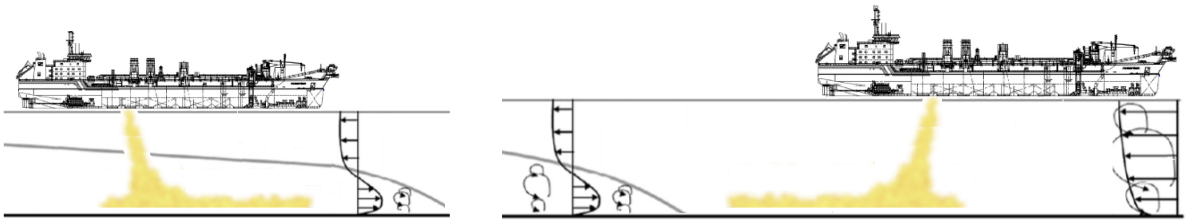

(a) Initial behaviour inside salt wedge

(b) Initial behaviour outside salt wedge

Figure 3.11: The difference in initial plume behaviour for a sediment plume disposed by bottom door release inside a) and outside b) the salt wedge.

For a disposal by bottom door it is expected that the sediment plume is transported close to the bed, as is shown in fig. 3.11. Despite its orientation with respect to the advection of the salt wedge. During a bottom door disposal, local sediment concentrations increase rapidly. From Winterwerp and Van Kessel [2003] is known that for high concentrations of SPM significant sediment induced turbulence damping can arise. The high concentration gradient upon release damps local turbulence and therefore limits vertical mixing. This effect is highly non-linear, for a concentration of 0.01 - 0.05 g/l the sediment flux increases with 10 %, whereas for high background concentrations +/- 0.5 g/l the vertical sediment flux increases with 100 %. This is a positive feedback system which may decrease the carrying capacity of the flow inducing a lutocline. This may lead to the establishment of a fluid mud layer, if concentrations surpass the gelling concentration [Winterwerp and Van Kessel, 2003].

If the sediment by bottom door disposal is disposed outside the salt wedge, as is shown in fig. 3.11a, it is expected that a large amount remains close to the bed. On subsequent flood, sediment can be entrapped underneath the salt wedge or if it has settled be resuspended and entrapped as explained in section 2.2.3. If the sediment is released by bottom door disposal inside the salt wedge, the sediment is initially confined below the pycnocline as shown in fig. 3.11b. Due to turbulence damping the sediment is expected to undergo the repetitive behaviour of entrapped sediment below the pycnocline: settling, resuspension until it is allowed to settle in the harbour basins lining the Rotterdam Waterway. Due to settling lag and the tidal asymmetry net landward transport is further promoted, as is explained in section 2.2.3.

Close to the bed the flow velocity in downstream direction is lower than higher in the water column. As shown in fig. 3.8, a small displacement of a plume at a large depth is expected. Therefore it is expected that only a minor amount of sediment reaches the Maasmond prior to LWS.

3.3.3. Timing of disposal

Based on model studies done prior to the SURICATES pilot study it has been estimated that a disposal at predicted depth-averaged HWS at Maassluis is the most efficient timing of the disposal. As shown in table 3.1 the majority of the disposals has been executed half an hour to one hour after depth-averaged HWS.

During depth averaged HWS, the flow, averaged over the total depth, changes sign from net up estuary directed to net down estuary directed. However, immediately after depth averaged HWS the flow below the pycnocline is still up estuary directed, due to differential advection of the dense water close to the bed, as can be seen in fig. 3.9. The earlier the disposal after HWS the higher the up estuary flow velocity below the pycnocline. In other words the later the disposal is executed the larger the probability that the initial displacement

of the plume is down estuary directed. However, for the total displacement of the plume the net advection is important, not only the initial direction.

The pycnocline height is an important parameter defining the entrapping efficiency of a sediment disposal. Due to turbulence damping it is assumed that sediment reallocated initially below the pycnocline, can not escape the salt wedge. Therefore, the time dependency with respect to HWS is discussed. The later the disposal after HWS, the lower the pycnocline over the vertical. In fig. 3.12a, it can be observed that a small shift of the pycnocline occurs around HWS (11:00) at Maassluis on November 5. Due to the retreating salt wedge, the pycnocline is found significantly lower for later times (fig. 3.12b), therefore it is assumed that less sediment is entrapped initially for a later disposal.

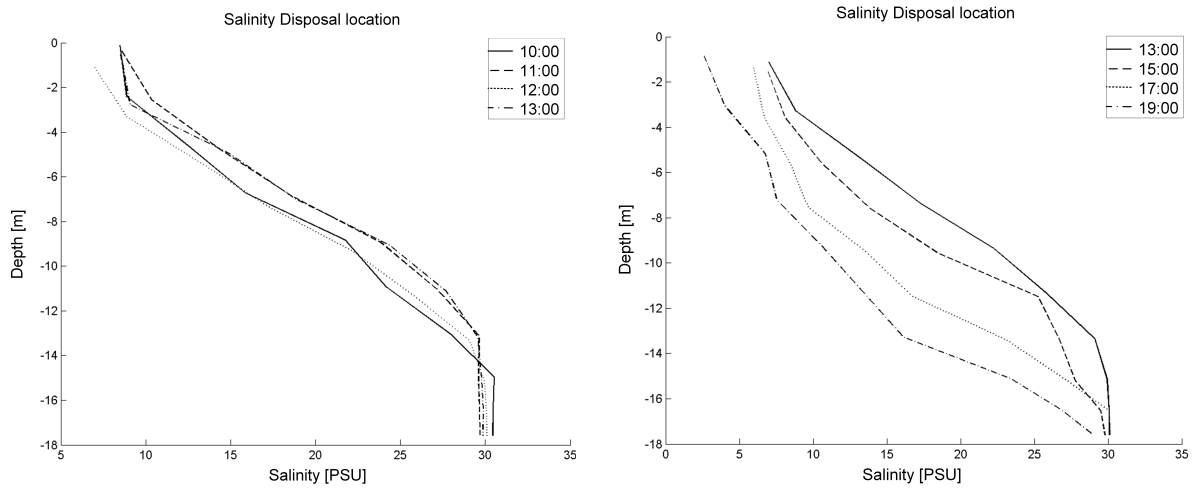

(a) (b)

Figure 3.12: The salinity distribution at the location of disposal at November 5, 2019 according to the model.

Moreover, the amount of diffusion over the water column determines the carrying capacity of the flow. e.g. at 11:00 and 11:30 the amount of shear over the vertical ($\frac{\partial u}{\partial z}$) is largest. From de Nijs et al. [2008] is known that around LWS most carrying capacity is expected around the pycnocline, while at HWS transport takes place over the entire vertical. Moreover, it can be derived that most transport occurs between 0:30 and 2:30 hours after slack water. de Nijs et al. [2008] Therefore, it is expected that when sediment is disposed during low transport conditions, the disposal is more likely to settle faster. And hence remain confined below the pycnocline.

Summarized, shortly after (depth-averaged) slack water there are significant velocity differences over the vertical with up estuary flows below the pycnocline. Moreover, transport capacity is low as the driving forces for turbulence are absent.

3.4. Far field behaviour

The distinction between mid field and far field behaviour is drawn at the Maasmond or after particles have settled inside the Rotterdam Waterway. After settling of the particles, resuspension properties and the hydrodynamics determine the further fate of the plume. To assess the far field behaviour, a distinction is made between particles settled inside the Rotterdam Waterway and which have passed the mouth of the estuary at the Maasmond.

3.4.1. Settling in the Rotterdam Waterway

It is expected that particles which settle inside the Rotterdam Waterway will, after resuspension, be transported upstream and settle inside the harbour basins lining the Rotterdam Waterway. From de Nijs et al.

[2008] is known that the Rotterdam Waterway is too dynamic for the settling of fine particles. This is attributed to the advection of the salt wedge and supported with the lack of mud encountered in dredging records from the Rotterdam Waterway. Moreover, tidal asymmetry increases this net upstream directed sediment transport. In section 2.1.3 is explained that flow velocities are higher during ebb in the upper part of the water column, while moving closer towards the bed the flow velocities are larger during flood.

In general the majority of the sediment will end up in the harbour basins lining the Rotterdam Waterway. However, after significant wind set-up or very low discharge conditions, settling of sediment inside the salt wedge can be promoted in the Maasmond, due to local widening and deepening of the fairway, settling is locally enhanced.

An additional complication, which has arisen after de Nijs [2012], is the disclosure of the sill underneath the Maeslantkering. This disclosure is caused by the deepening of the Rotterdam Waterway, finished in 2019, see appendix A.1. In fig. 3.13 it can be seen that the sill has a height of $\approx 1.5\ m$. This construction can therefore block fluid mud layers or create areas with very low flow velocities allowing sediment to settle. However, the exact effect of the sill construction on sediment transport should be further investigated.

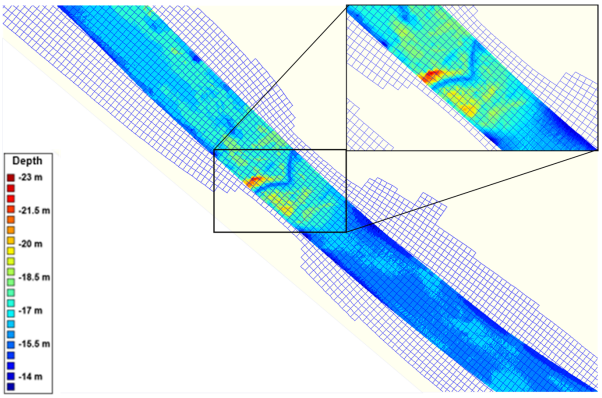

Figure 3.13: Local bathymetry around the Maeslantkering from a bathymetry survey at May 27, 2019 prior to the start of the SURICATES pilot study.

3.4.2. Settling North Sea

If particles pass the Maasmond, the mouth of the harbour, they enter the North Sea. At the outflow of the Rhine into the North Sea a so-called Region Of Freshwater Influence (ROFI) is established, see appendix B.1.1. Due to the dynamics of the Rhine ROFI, the freshwater bulge is deflected towards the north-wast under the influence of the Coriolis force. The depth-averaged flow in the Rhine ROFI is concentrated in a narrow stretch (approximately 20 km wide) along the coast, as this flow transports a significant amount of sediment it is called the 'coast river' [de Boer et al., 2006].

Due to the complexity of the dynamics within the Rhine ROFI, it is hard to predict the sediment pathway to the full extent. One can predict the trajectory of the sediment plume since SPM transport follows the current, however one can not predict where the particles might settle. The location where the particles might settle is important to assess the efficiency of the SURICATES pilot study, as the settling location is inversely proportional to the sediment flux towards the Maasmond. In other words the further away particles settle from the Maasmond the less will return to the Maasmond as shown by Hendriks and Schuurman [2017]. From this study is concluded that a more or less exponential relationship holds between the settling location (i.e. the distance to the Maasmond) and the amount of sediment returned to the Maasmond. For a location located 35 kilometers away from the Maasmond the return flow is only 5%, whereas for the nearest locations this holds 30 - 35 % located at 10 kilometers from the Maasmond. For the dynamics of settled sediment in the Rhine ROFI the reader is referred to appendix B.3.7.

3.5. Summary

In this chapter a hypothesis is drawn on the behaviour of the SURICATES sediment plumes in the Rotterdam Waterway and Rhine ROFI. At first some execution details of the pilot study are given such as sediment source, disposal method and time of disposal. Subsequently, a hypothesis is drawn for the SURICATES sediment plumes. This hypothesis is drawn for both execution methods on three different time and spatial scales: near, mid and far field. For the hypothesis, theory derived by de Wit [2015] and Winterwerp [2002] for overflow sediment plumes is used for the near field behaviour. This analogy is therefore justified at first. To unravel the expected behaviour in the mid and far field behaviour, the analysis of sedimentation mechanisms in the Rotterdam Waterway by de Nijs [2012] is used. This is done to answer the following (sub) research question:

What is the expected behaviour of sediment plumes in the system?

The behaviour of SURICATES sediment plumes is expected to be mainly governed by its location with respect to the pycnocline. As indicated by de Nijs et al. [2008] sediment reallocated above the pycnocline will slowly rain out, due to turbulence damping. However, velocity shearing may induce local transport capacity. Sediment which ends up below the pycnocline remains confined below the pycnocline and is therefore expected to remain within the Rotterdam Waterway.

Bottom door disposals remain close to the bed and are therefore only limited seaward transport can take place. Moreover, the majority of the disposals will be located within the salt wedge where the sediment remains confined. For bow coupling plumes some part of the transport takes place above and around the pycnocline, where velocity is ebb dominant. Nevertheless, for the sediment reallocated above the pycnocline a trapping efficiency of 50 % is estimated.

To answer this question a distinction has to be made between the two different execution methods: disposal by bow coupling and drawing the bottom doors. The latter method is used for 90% of the disposals, however for the near field and mid field behaviour only measurements from disposals by bow coupling are available.

Strictly speaking the disposal by bottom door release is not covered by neither Winterwerp [2002] nor by de Wit [2015]. However, based on the observations and by extrapolating the theory drawn by de Wit [2015] an expectation on the behaviour is drawn. As the bottom doors are drawn, the barge is emptied within minutes, creating a large momentum dominated bulge with a high fall velocity exceeding the individual particle's settling velocity. It is expected that little dispersion takes place over depth due to the high disposal velocity. This theory is supported by the impact crater that has arisen over the course of the execution of the SURICATES pilot study, see fig. 3.7. As the entire amount of sediment sinks underneath the pycnocline it is entrapped here. Local flow velocities determine the fate of the sediment plume. It is expected that the majority of the plume remains within the Rotterdam Waterway during the first tidal cycle, due to the low flow velocities close the bed. Moreover, as local sedimentation rates can surpass the consolidation rate, fluid mud layers may be established under these conditions.

The disposal by bow coupling is used for only 10 % of the disposals, but is subject of the measurement campaign in chapter 6. For a plume released by bow coupling, for the first 4 m jet behaviour is expected, where no dispersion of the plume is expected. Between a depth of 4 m to 12 m dispersion over the depth and width is expected as the plume becomes velocity dominated. Hence it is expected that the majority of the transport of the plume takes place around and below mid depth at depth of $\pm$ 9 to 10 m, around the transition depth. Due to the large velocity differences over the depth, the plume will be subject to significant differential advection; the deeper the fraction of the plume, the slower it is advected downstream. In section 2.2.2 is explained that the carrying capacity is governed by a balance of turbulence damping around the pycnocline and velocity shearing, which is most significant around the pycnocline. In fig. 2.7 it can be seen that this carrying capacity changes over time depending on the governing hydrodynamics. Therefore some transport may take place around the pycnocline. Nevertheless it is expected that before LWS, most particles have not reached the Maasmond and will settle around LWS as the turbulence field collapses during slack water. Also it is expected that at least 50 % of the sediment is rained out in the salt wedge, which is line with the fluvial trapping effiency of de Nijs [2012].

The far field in this study is defined as particles outside the Maasmond or particles which have settled inside the Rotterdam Waterway. For the settled particles, it is estimated to behave in the same manner as fluvial sediment provided from upstream. As stated in de Nijs et al. [2010] this sediment is entrained during subsequent flood and transported upstream. It is expected that the entrapped sediment undergoes the following pattern: advection, settling, resuspension and accumulation in the tip of the salt wedge (ETM) until it flows into less dynamic areas where the sediment is allowed to settle. The fate of the particles at sea is more difficult to predict as it is unknown where these particles will settle. From Hendriks and Schuurman [2017] it is known that the settling location of the particles and the sediment flux towards the Maasmond are inversely proportional.

II

Method & Materials

4

Measurement set-up

In the following chapter the set-up of the measurement campaign is discussed. The main goal of the measurements is to analyse and quantify the spread of the sediment plumes in time and space. In order to do so, a measurement campaign is drawn up by Deltares. [1] *The measurement campaign can be split into two: 1) one campaign, consisting of four measurement surveys, focuses on the near and mid field behaviour of a single disposal, discussed in section 4.2, and 2) a campaign which is set up to examine the cumulative behaviour of all sediment plume disposals over the course of the execution of the SURICATES pilot study, discussed in section 4.3. The results of the measurement campaign are discussed in the subsequent chapter, chapter 6.*

4.1. Introduction

To quantify the spread of the sediment plumes disposed in the context of the SURICATES pilot study an extensive measurement campaign has been set up by *Deltares*. This measurement campaign consists of different surveys, executed prior, during and after the SURICATES pilot study. A distinction is made between the measurement campaign set-up to determine the initial or short term behaviour of an individual sediment plume and the campaign set-up to determine long term behaviour of the SURICATES pilot study, see appendix D.1 for an overview of the full measurement campaign.

In section 4.2, the set-up of two different surveys to examine the initial behaviour of a sediment plume disposed using bow coupling, is described. The first survey is executed on September 11, 2019 for two hours, while the other survey, executed on November 5, 2019 lasted a full tidal cycle, from HWS until HWS. In this section the set-up of the surveys and the equipment used is discussed.

In the second section, section 4.3, the set-up of the long term measurement campaign is discussed.

In section 4.4 a summary is given on the set-up of the measurement campaign.

4.2. Short term measurements

In order to understand the short term behaviour of the SURICATES pilot study the near field and mid field behaviour of the plume dynamics are investigated at first, to align approach with chapter 3.

On September 11, a three hour survey is executed between 18:11 and 20:11, shortly after HWS. As can be seen in appendix G.2.1, 14807 TDM (7.5 % of the total amount) has been disposed in the week prior to September 11. Two disposals have taken place on September 11, one in the morning by drawing the bottom doors and a second one between 17:58 and 19:16 in the evening, subject of the measurement survey. On November 5, 2019 a 13 hour survey campaign executed between 8:00 - 21:00 from flood until flood, covering a tidal cycle. 6187 TDM (3.0 % of the total amount) has been disposed in the week prior to November 5. 8 hours before the start of the measurements, 1080 TDM from the Waalhaven sediment trap has been disposed using the bottom

[1] The writer has only analysed the results of the measurement campaign and has not been involved in this set-up.

door. Between 11:00 and 11:50, 1256 TDM from the New Meuse has been disposed by using bow coupling, which is analysed in the survey.

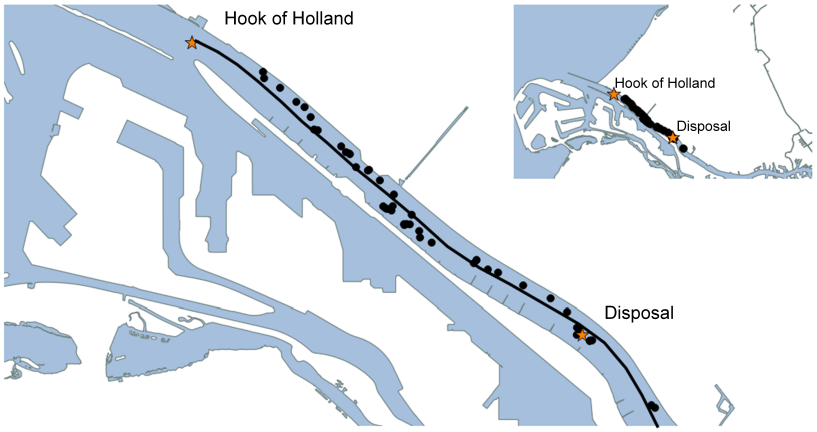

Figure 4.1: The trajectory of the survey vessel and the locations of the 50 silt profiler measurements on November 5, 2019

Measurement set-up

For both surveys a single vessel mounted with an Acoustic Doppler Current Profiler and a silt profiler is used. The ADCP is used to obtain the flow velocity and direction, while the ADCP backscatter measures the absolute backscatter. During this survey the goal is to map the propagation of the sediment plume using a Lagrangian frame of reference. On September 11, this is done by sailing downstream from the reallocation site once. On November 5, this is done by sailing various times up and downstream with the survey vessel between the disposal location at *"The bend of Maassluis"* and Hook of Holland, located 9 kilometres downstream. ADCP backscatter provides an online [2] qualitative view on the amount of SPM over the vertical to the survey vessel as shown in fig. 4.2a. Subsequently, to obtain a profile of SPM and salinity over depth, the surveyors execute a measurement with the silt profiler based on the online results of the ADCP backscatter. In other words, when the ADCP backscatter shows indication of plume advection, the silt profiler is lower to obtain a silt profiler measurement. In total, 11 silt profiler measurements have been taken on September 11 and 50 silt profiler measurements on November 5.

Measurement equipment

As stated above, the survey vessel is mounted with an ADCP backscatter device to obtain online backscatter values while sailing. The ADCP backscatter provides a qualitative view on the amount of SPM over the vertical, i.e. the exact amount of SPM can not be measured, unless the device is thoroughly calibrated. The ADCP measures the absolute backscatter which becomes larger (i.e. less negative) for larger amounts of turbidity. The turbidity is related to the amount of SPM [Sassi et al., 2012].

Moreover, ADCPs have a blanking distance ranging 2 m from the water level and 1.5 m from the bed. Hence the surveyors are lacking information inside this range. Also, the ADCP backscatter used in the survey uses a frequency of 600 Hz, which is more sensitive for coarser fractions than for smaller fractions. Higher frequencies have a smaller range, but are more sensitive to smaller fractions. This may lead to a bias in the results as small concentrations of coarse fraction create the same signal as large concentrations of small fractions [Sassi et al., 2012].

The silt profiler is deployed by the surveyors when the results of the silt profiler gave rise to do so. The silt profiler is a measurement device containing multiple sensors mounted on a frame, developed by Deltares. This frame is connected to a winch allowing the device to be sunk under water and be retrieved when finished. The device contains sensors for the temperature, conductivity and pressure to determine the practical salinity. The SPM concentration can be determined using two different Optical Backscatter (OBS) sensors

[2] The surveyor receives the signal directly on a screen on board

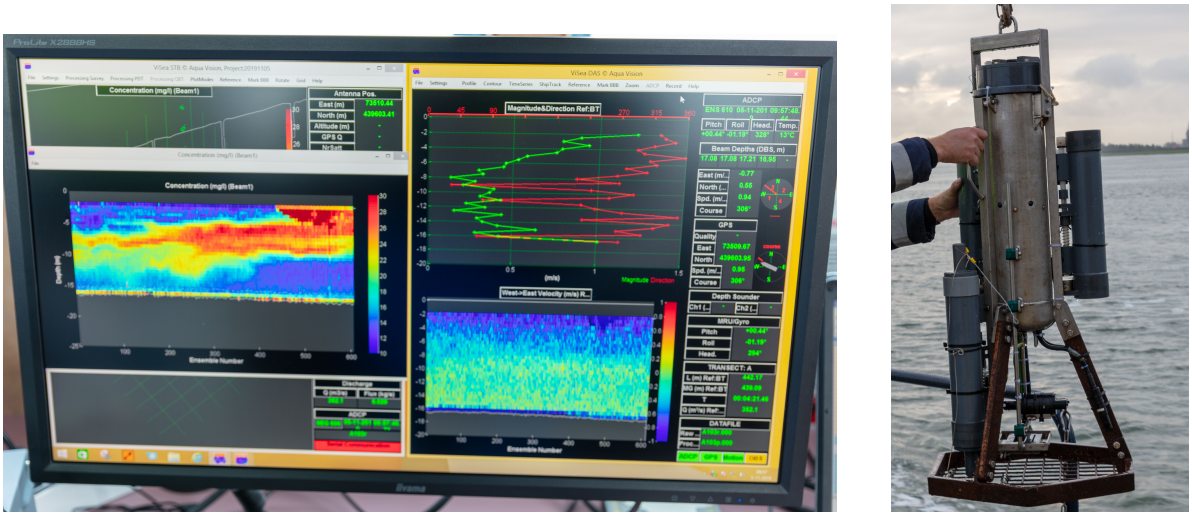

(a) (b)

Figure 4.2: **Overview of the measurement equipment**. a) Overview of the online measurement results on-board of the survey vessel. In clockwise direction: flow direction and magnitude, velocity magnitude, ADCP backscatter (not calibrated) and ADCP backscatter (not calibrated). b) photo of the silt profiler.

with different SPM concentration reaches 0 - 0.04 g/l and 0 - 0.15 g/l , an additional transmission probe (0 - 10 g/l) for the highest SPM concentrations and three bottle samplers [Borst et al., 2013]. In contrast to the ADCP backscatter, the silt profiler provides a calibrated amount of SPM and salinity over the vertical. de Wit [2015] stressed the difficulty of measuring a sediment plume in the vicinity of a dredger, i.e. within 300 m of the dredger, as a large extent of the sediment plume is found in the blanking distance of the ADCP. It is stated that stationary measurements at 1 kilometre from the vessel are more reliable as these are outside the near field effects.

In appendix D.2 the working principles of the silt profiler and ADCP backscatter are discussed more in depth.

Measurement uncertainties

The set-up of the measurement surveys and the equipment used introduces uncertainties.

- **The frame of reference**
  Since the survey vessel moves in time, only parts of the sediment plume can be captures which are advected at the velocity of the survey vessel. This introduces significant bias in the measurements.
- **ADCP backscatter bias**
  Since the ADCP backscatter is not calibrated, the backscatter only provides a qualitative view of SPM over the vertical. Since these are always higher near the bed, plume advection near the bed can be missed as the signal is as expected. Therefore the silt profiler is not lowered when potentially relevant, see fig. 6.20.
- **ADCP backscatter blanking distance**
  The ADCP backscatter has a blanking distance close to the bed, where the largest concentrations of SPM are found. Therefore, plume advection near the bed cannot be measured.

4.3. Long term measurements

To assess the spread of the SURICATES over the long term a different measurement campaign is set up. In this measurement campaign bed samples are taken at three distinct times, to assess the change in bed composition, see appendix D.1.

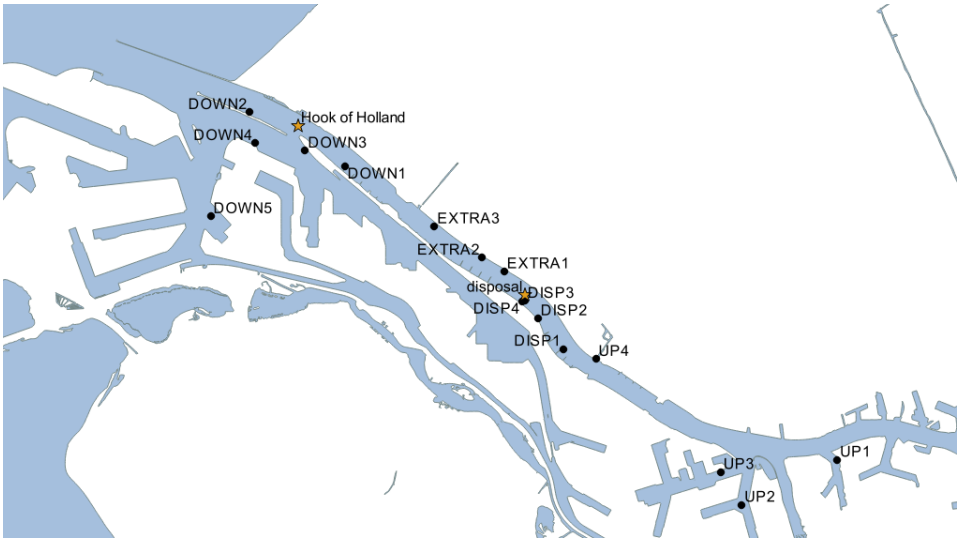

Figure 4.3: The locations of the bed sampling, differentiated according to their location with respect to the disposal area.

- T_0: Sampling executed on February 7 and 8 2019 (3.5 months prior to start). Sampling done by grabbers and columns.

- T_1: Sampling executed on July 2 and 3 2019 (1.5 months after start). Sampling done by Grabber.

- T_2: Sampling executed on September 4 2019 (3.5 months after start). Sampling done by Column.

These samples are taken of the top 30 cm of the bed layer. It is assumed that by taking bed samples, the change in composition of the bed can be determined. A change in silt content in the bed can be an indication of additional sedimentation, since the sediment disposed during the pilot study contains almost exclusively fine material. Therefore, an increase in the bed composition of particles finer than ($< 63\ \mu m$, silt and clay) can be an indication of sedimentation caused by the execution of SURICATES.

The locations of the sediment samples are differentiated with respect to the disposal area. With eight locations (*Down 1 - 5*) and (*Extra 1 - 3*) downstream of the disposal site and four locations upstream (*UP 1 - 4*) and four around the disposal site (*DISP 1 - 4*), as shown in fig. 4.3. All the sample locations are subject to fluvial sedimentation, except for the downstream locations 3, 4 and 5 (*Down 3 - 5*).

Mohan [2019] characterized the sediment samples to derive the grain size distribution. The results in the context of the pilot study are discussed in section 6.3. By measuring the change in bed composition, the measurements are subject to the settling of background sediment or by human interventions such as dredging.

4.4. Summary

For the short term measurement surveys it is chosen by Deltares to use an ADCP backscatter in combination with the silt profiler. Since little was known beforehand on the expected dynamics of a sediment plume and to obtain as many observations of the plume as possible, a Lagrangian Frame Of Reference (FOR) is used. By using ADCP backscatter only a qualitative view on the sediment distribution can be derived and due to its blanking distance the sediment fluxes near the bed cannot be measured. Using a Lagrangian FOR introduces a significant bias, which is explained further in chapter 6.

For the long term measurement campaign is decided by Deltares to determine the change in bed composition. It is assumed that an increase in silt content can be related to the SURICATES pilot study. However, since the pilot study is executed in the natural environment, no distinction can be made between sedimentation introduced by the SURICATES pilot study or due to background sedimentation.

5

Model set-up

In the following chapter the model set-up is described for the different model runs to hindcast the SURICATES pilot study. Two distinctive models are set up, one to model the behaviour of a single plume over half a tidal cycle (short term model) and another model for the behaviour over the full period of the pilot study (long term model). This chapter describes current model practises first, which is similar for both model set-ups, subsequently the set-up for the short and long models are described. The chapter is concluded with a summary on the limitations of the current model practise. The results of the model hindcast are discussed in chapter 7.

5.1. Introduction

To model the SURICATES pilot study on different time and spatial scales in the Port of Rotterdam operational hydrodynamic models and sediment models are used. Hydrodynamic models in general are models solving the Reynolds Averaged Navier-Stokes equation (RANS) equations; a system of equations obeying the conservation of momentum and mass in time and space. The sediment model computes the transport of sediment using the convection-diffusion equation, see appendix E.

Currently the Port of Rotterdam has a model train to forecast and hindcast the hydrodynamics (velocity, water level, salinity) for various locations within the port. This model train is known as the Operationeel Stromings Model (OSR).

Next to this, the port has a calibrated sediment model to predict and hindcast sediment behaviour. This model is based on the DelWAQ (WaterQuality) software. In the first section an overview of the current models is given. Subsequently, the set-up of the two different model runs (short term and long term) is described.

5.2. Overview of the models

In the following section the current modelling practise is described. The current model train, OSR, consists of a larger model and a smaller model, nested inside the larger model. This larger model is the *'Harbourmodel'*, which is a 2Dh (depth-averaged) SIMONA model with a spatial domain ranging 50 km north to 40km south and 25 km offshore in the west, as is shown in fig. 5.1. This Harbourmodel obeys the boundary conditions as shown in table 5.1, such as the astronomical tide at the sea boundaries, and the river discharge and salinity at the river boundaries. These model results are updated using Kalman filtering based on the water level values at the measuring stations (see *'Water level'* in table 5.1). This Hydrometeo information is provided by the *KNMI* and *Rijkswaterstaat*.

The Harbourmodel is run at first, supplying boundary conditions for a 3D SIMONA FLOW NSC model, with a smaller spatial domain but with the same resolution. This 3D model has two versions; NSC coarse and NSC fine, of which the latter grid is three times as fine. The boundary conditions are the previously mentioned environmental parameters and the salinity at the rivers. Currently the combination of the Harbourmodel and the 3D SIMONA is the operational OSR model, which is updated four times a day with the most recent

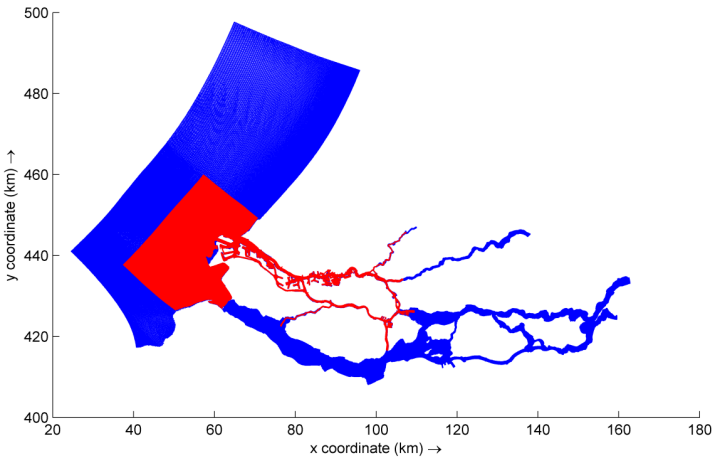

Figure 5.1: A map of the domain of the Harbour model (blue) and NSC model (red) [Kranenburg, 2015].

Parameter	Locations:
Water level:	Brouwershavense Gat, Haringvliet, Hook of Holland, Lichteiland Goeree, Scheveningen
River discharge:	Hagestein (Lek), Tiel (Waal), Megen (Meuse)
Salinity:	Hagestein (Lek), Tiel (Waal), Lith (Meuse)
Wind:	Noorderpier (Hook of Holland)

Table 5.1: The environmental conditions used as reference or boundary conditions supplied to the model. The measuring locations are shown on fig. A.1.

forecast regarding flow velocity and water levels. Moreover, wind data is included using wind data from the measuring station at Noorderpier (Scheveningen) [Kranenburg, 2015]. For the short term model set-up, the NSC-fine model is used. While for the long term model set-up the NSC-coarse model is used. An overview of the difference in the short and long term model set-up is shown in table 5.2. Geraeds [2020] compared the model predictions with measurements to investigate the performance of the hydrodynamic model in the context of SURICATES pilot study. This is further elaborated in section 7.2.

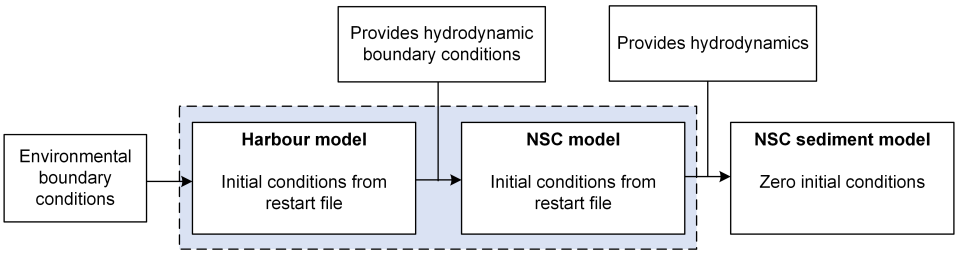

Figure 5.2: The current modelling train to model hydrodynamics for the OSR (blue box) and subsequently sediment dynamics. The flow model and sediment model are non-coupled. After [de Groot, 2018]

From the hydrodynamics the sediment behaviour is modelled using the DelWAQ module. The coupling between the flow model and the sediment modeling is non-coupled, i.e. the hydrodynamics are not affected by the sediment behaviour. The set-up of the sediment model further elaborated in section 5.5.1.

5.3. Grid and bathymetry

The grid used for the Harbourmodel stretches 50 km in northern direction up to Zandvoort and 40 km in southern direction towards Schouwen Duiveland. The western boundaries lie approximately 30 km offshore.

	Short term	Long term
Model used:	NSC-Fine	NSC-Coarse
Hydrodynamics:	FLOW[a]	FLOW
Hydro. / sed. dyn.	Non - coupled	Non - coupled
Grid size:	70 - 35 m	200 - 100 m
Vertical resolution:	10 layers	10 layers
Model period:	Nov. 5	Aug. 30 - Sep. 12
Repeated:	No	22 x[b]
Background concentration:	No	No
Time step DelWAQ	10 s	60 s
Initial conditions DelWAQ:	No sediment	No sediment
Boundary conditions DelWAQ:	No incoming sediment flux	No incoming sediment flux

Table 5.2: Overview of the settings for the model set-up.

[a] Waves are not included
[b] To obtain 9 months of forcing

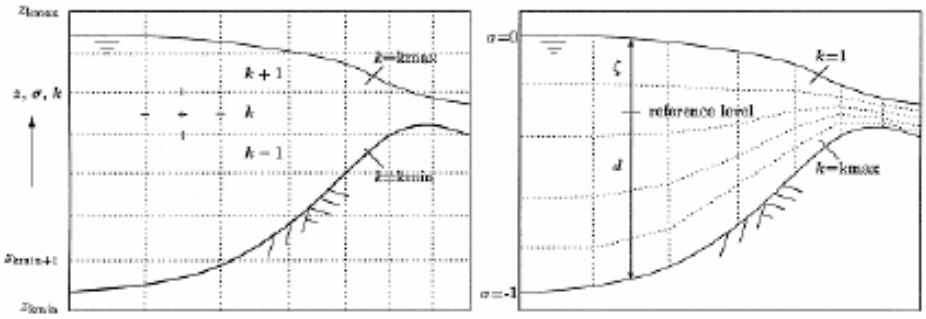

Figure 5.3: Difference in Z-layer (left) and σ-layer distribution (right). [DWA, 2019]

In the east the boundaries are defined at the measuring stations in the Lek (Hagestein), Waal (Tiel) and Meuse (Lith). The size of the computational grid is not equidistant; cell sizes range from 200 x 200 m at sea to +/- 100 m inside the port. The 3D-NSC coarse grid is nested inside this larger computational domain. The 3D-NSC grid stretches 25 kilometers in southern direction to Goeree-Overflakkee and 10 kilometers in the northern direction to Monster, with the same grid size as the harbour model, but extended with 10 depth layers. In the west the boundaries are defined at sea approximately 15 kilometers offshore and provided by the harbour model. The NSC-fine grid spans the same domain with the same vertical resolution, however with a grid 3 times finer in the horizontal plane. Hence one grid cell in the coarse model equals (3x3) 9 grid cells in the fine model, spanning the same domain.

The two different grids are shown in fig. 5.1. For hydrodynamic models in general, different types of layer distribution can be chosen; Z-layers or σ-layers: Z-layers always cover a predefined part of the water depth; e.g. -16m to -18m, regardless of the local bathymetry. σ-layers adapt to the local bathymetry and represent a fixed percentage of the local water depth, see fig. 5.3. The 3D-NSC models (fine and coarse) use a σ-layer decomposition with 10 layers, each representing a percentage of the total depth, which is decreasing towards the bed, see table F.3. This increases the computational accuracy towards the bed. The bathymetry used in the NSC models is updated in August 2019, after the deepening of the Rotterdam Waterway. For further details on the hydrodynamic model used the reader is referred to Geraeds [2020] or Kranenburg [2015].

5.4. Sediment dynamics

To model the sediment dynamics of the SURICATES pilot study, DelWAQ is used for both the short and long term model runs. DelWAQ is a computational program which solves the advection-diffusion equation (eq. (E.16)) for any constituent being transported, using the hydrodynamic forcing provided by a separate

hydrodynamic model. This advection-diffusion equation includes advection, diffusion, (re-) suspension and settling of sediment. Due to the resolution of the grid, DelWAQ is considered to be most efficient for sediment processes on a large scale rather than small scale processes. Therefore these models can not be applied to model near field processes. In models such as DelWAQ, in contrast to Computational Fluid Dynamics models, the Navier Stokes equations are Reynolds averaged, such that flow is stationary on the turbulent time scale. Hence it is an approximation of turbulent processes on a size smaller than the grid cells.

For both the long term modelling and short term modelling a non-coupled hydrodynamic and sediment model is used. This simplification is required to limit the computational costs: a coupled model is deemed at least twice as computationally expensive. As a non-coupled model is used, the effects of hindered settling, buoyancy destruction and sediment-induced baroclinic pressure gradients are not included. This typically introduces errors at locations where high SPM concentrations might occur, as high concentrations of SPM induce density differences over the vertical. In the modelling of the SURICATES pilot study, large SPM concentrations are expected to occur twice: at the time of disposal and during fluid mud processes. After disposal by bottom door, a large amount of SPM is released in a short time. Therefore, high concentrations of SPM can arise, see fig. 3.11. Fluid mud processes may occur during mid field and far field processes. In the far field, fluid mud processes occur during the rapid resuspension of settled SPM on the sea bed, as explained by Spanhoff and Verlaan [2000]. As the hydrodynamics and sediment dynamics are uncoupled, resuspension at sea will be altered. In reality, hindered settling and turbulence damping occurs. Due to the inclusion of sediment induced density differences the sediment concentration is stratified in the coupled model, whereas for the uncoupled model a more homogeneous distribution of SPM is found. It is found in measurements that the resuspended sediment at sea will remain close to the bed [Winterwerp and Van Kessel, 2003]. As the residual current for the near bed flow is different than for depth averaged residual flow, the sediment flow towards the Maasmond is underestimated. Winterwerp and Van Kessel [2003] found that the sediment flux towards the Maasmond is underestimated by a factor 3 to 5 for non-coupled models.

5.4.1. Initial and boundary conditions

In order to exclusively investigate the behaviour of the SURICATES pilot study, the initial conditions are all set to zero, so no sediment is present in the system other than the disposals. For the same reason the sediment fluxes at the boundaries are set to zero: to inhibit inflow of sediment from the model boundaries. This is done for both model set-ups.

5.4.2. Disposal implementation

The disposal of a dredging plume is included in far field models such as DelWAQ by including a local source term in one or more grid cells. In this source term a flow rate and depth (i.e. the $\sigma-$layer) of the disposal and concentration of sediment are prescribed. The estimation of an accurate local source term is rather complicated as it has to circumvent the near field processes of a sediment plume which can not be solved by the model itself. This dynamic phase includes the processes described in section 3.2, buoyancy and momentum of the sediment plume and the interaction of the plume with the crossflow [Becker et al., 2015, de Wit, 2015]. The source term has to be as much representative as possible to include most of these processes. In the model set-up used, the near field processes by altering the depth of disposal. To find an accurate source term, de Wit [2015] advises to use mid field results obtained within 15 minutes or 1 kilometre of the disposal, this complies with silt profiler measurement 9 (Sep. 11). In silt profiler 9, a double peak of SPM can be found between 8 - 10 m depth, see fig. 6.7a. For the disposals by bow coupling the disposal is included in layer 5 (mid-depth), see fig. 5.4 for a comparison between a surface disposal (layer 1) or mid layer disposal (layer 5), which complies with a depth of 8 - 10 m. While, the disposals by drawing the bottom door are included in layer 10 (bed-layer), this is in line with the approach used by Vijverberg et al. [2015].

5.4.3. Substances

The sediment in the model consists of 3 x 3 sediment fractions in total. These are, three fractions of Inorganic Matter in suspension (IM_i) and three fractions for each of the two Inorganic Matters in the bed layers ((IM_iS_1) and (IM_iS_2). The characteristics of these different fractions of Inorganic Matter in suspension are defined by its settling velocity (w_s), critical shear stress for sedimentation (τ_{cr}) and critical shear stress for resuspension (τ_{cr}).

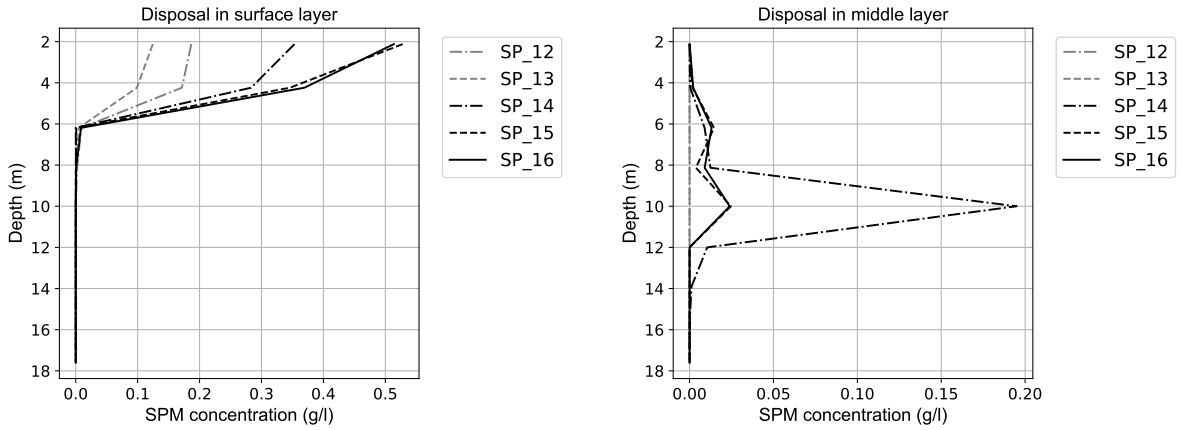

(a) Model result if disposed in top layer

(b) Model result if disposed in layer 5

Figure 5.4: Total amount of suspended sediment at the time and location of the silt profiler measurements 12 - 16. In a) this is compared for the sediment disposed in the surface layer and in b) when it is disposed in the fifth layer, with a depth of 10m.

The sediment fractions used for both the short and long term model runs are in line with previous models studies on SPM behaviour in the Port of Rotterdam, such as de Groot [2018], Hendriks and Schuurman [2017], Vijverberg et al. [2015]. The grain sizes used in these studies are 1, 12 and 34 μm. (w_s = 0.1, 10.8, 86.4 m/d). These grain sizes are representative for the sediment in suspension. In appendix F.1 the full settings of the sediment model are given.

As stated in section 3.1.1 the source of sediment of a disposal can be derived from the hoppers registration: harbour basins or New Meuse. In section 3.1.1 is shown that the source locations along the New Meuse contains a much larger fraction of coarse material than the harbour basins lining the New Meuse. This is also confirmed by the grab samples taken during the measurement campaign, see appendix G.3.1. From Stutterheim [2002],Hendriks and Schuurman [2017], it is known that the percentage of silt (i.e. all fractions $< 63 \mu m$) for the basins equals 86% and for the fairway 49%. This percentage is also applied for the disposals. Based on this the barge composition is assumed as shown in table 5.3.

	Harbour basin		**New Meuse**	
	Size	Amount	Size	Amount
IM1	1 μm	4%	1 μm	5%
IM2	12 μm	31%	12 μm	22%
IM3	34 μm	51%	34 μm	22%
Coarse	n.a. μm	14 %	n.a. μm	51 %

Table 5.3: Composition of the plume for different model runs, varying in grain size distribution.

5.5. Short term model set-up

For the short term model set-up the measurement survey of November 5, 2019 is hindcasted. To do so, the disposal between 11:00 and 11:50 is included, using the model approach as described in fig. 5.2. The Harbourmodel and NSC-flow are started using a restart file from October 20. This provides sufficient time for the model to spin-up. The hydrodynamic results are validated to the measured values in section 7.2.

The hydrodynamic conditions prior to November 5 are described in section 6.2.1 and are characterized by low discharge conditions, 1 day after neap-tide and two days after a high wave period at sea.

In chapter 7 the short term model results are used for a sensitivity analysis and compared to the measurement

results of November 5.

5.5.1. Sediment Dynamics

In order to set up the DelWAQ sediment model time step has to be determined.

Time step

The determination of the time step is a balance between the computational costs and accuracy. The goal of the time step determination is to obtain results which are independent of the time step chosen. For the modelling of the disposal an arbitrary amount of sediment is brought in the system. The initial concentration and boundary concentrations are set to zero everywhere in the system. Subsequently, the results of the time step are verified by trying $\Delta t, 1/2\Delta t, 1/4\Delta t$, etc. until two consecutive time steps converge, i.e give consistent results. In appendix F the convergence of the simulation of $\Delta t = 15, 10, 5 s$ is shown. The time step used is $\Delta t = 10\ s$.

5.6. Long term model set-up

In order to model the long term behaviour, i.e. the whole duration of the SURICATES pilot study a slightly different model train has to be set-up. As the duration of the pilot study is 179 days (from May 20 until November 15, 2019, see appendix D.1), different simplifications have to be made, especially in the forcing of the hydrodynamics. Due to file size it is not possible to force the hydrodynamics one-on-one; a simplification has to be made. This is done by choosing a 14 day period, which represents the hydrodynamics during the pilot study, which can be repeated to obtain the full hydrodynamic forcing of 9 months[1]. A minimum of 14 days is required to include variations in water level and velocity due to spring/neap cycle in the model.

5.6.1. Hydrodynamics

In contrast to the model set-up used for November 5, the hydrodynamics can not be forced one-on-one into the sediment model due to size of the files. A standard approach in such cases is to choose a representative hydrodynamic forcing of 14-days or 30-days to represent the hydrodynamics over the entire period over interest. In de Groot [2018] four different conditions have been chosen, based on two parameters; wave height and river discharge to define different periods of forcing. In de Groot [2018], the mildest conditions have been used for spin-up, leading to a relative large amount of sediment in the system. This stresses the importance of choosing representative hydrodynamics over the full forcing period. In addition, continuity has to be met between the starting point and end of the simulation period, as the hydrodynamic period is repeated. The representative hydrodynamic forcing period chosen is August 30 to September 12. Based on the wave height conditions.

In the following two paragraphs the wave conditions and river discharge during the forcing period are discussed.

Wave height

To obtain a representative period with respect to the wave height, a peak over threshold method is applied. For the wave conditions, high waves are relatively important as they induce large bed shear stresses and hence resuspend sediment. In table F.4 the period of interest: May 20 until November 16 is divided into bins with a length of 14 days. Subsequently the amount of waves above certain threshold values are divided into bins and the two week period which matches the average bin division best, is chosen. The most representative period of the analysed periods is August 26 until September 8, this is a fairly mild period with a few waves above the 2 and 2.5 m threshold. Due to continuity requirements this period is shifted to August 30 until September 13.

However, this simplification overestimates the wave conditions for 6 periods of 2 weeks and underestimates the wave conditions for the other 6 weeks. From de Groot [2018] it is known that choosing a mild forcing condition leads to a substantial amount of sediment storage at the North Sea.

[1] This includes three additional months to obtain an equilibrium.

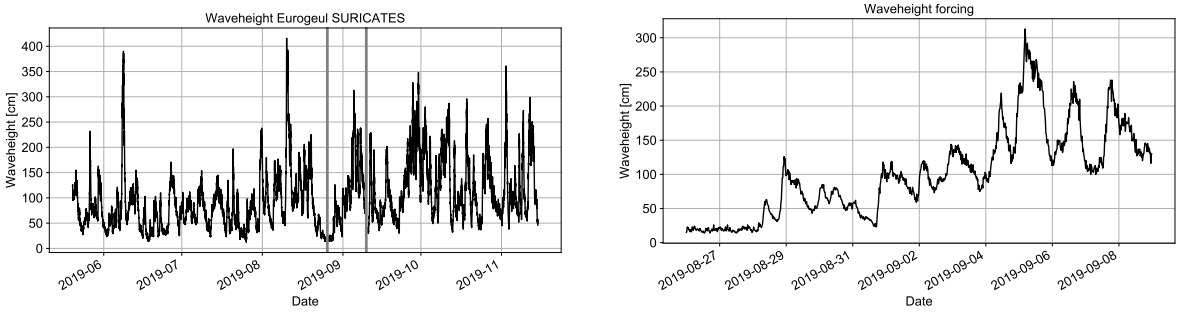

(a) Wave height at Eurogeul during the pilot study

(b) Wave height at Eurogeul repeated in the model set-up

Figure 5.5: The wave conditions as measured close to the Maasmond during the SURICATES pilot study and the waveheight of the model input used for the long term measurements.

River discharge

Average discharge conditions are assumed to be representative discharge conditions. The discharge conditions for the hydrodynamic forcing, underestimates the average discharge with $200 m^3/s$. The average discharge during August 30 to September 13 equals $1500 m^3/s$ compared to an average discharge of $1700 m^3/s$ for the SURICATES pilot study. It should be noted these are still very low compared to the yearly-average discharge conditions of $2300 m^3/s$.

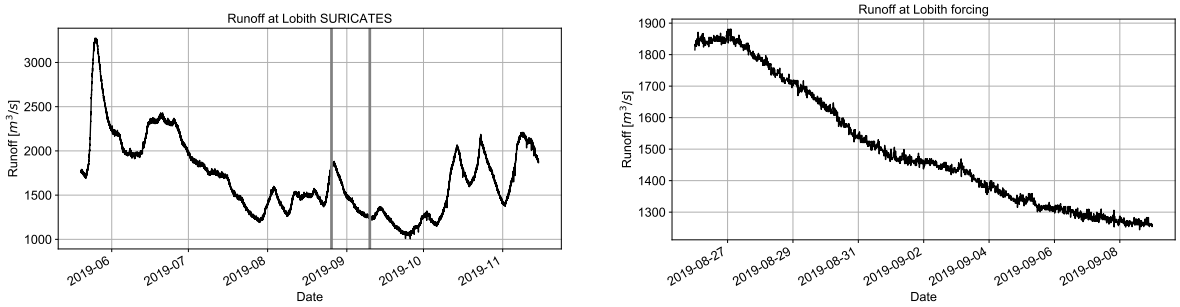

(a) Fresh water discharge during the entire SURICATES pilot study

(b) Fresh water discharge as repeated in the model

Figure 5.6: The fresh water discharge at Lobith for the entire SURICATES pilot study and the fresh water discharge repeated in the long term study.

Although, the relation between discharge conditions and siltation events in general for the Rotterdam Waterway are unknown, the consequence of a smaller assumed average river discharge are expected to be two-fold in case of modelling the SURICATES pilot study. As stated previously, for low discharge conditions the salt wedge may extend further landward and may lead to lower ebb velocities. The salt wedge and the ETM are considered to be the main drivers of siltation of the port basins, hence for high discharge conditions sedimentation of the basins is expected to be limited. The second effect is related to the reduced lock exchange mechanism, reducing peak flood velocities. While in general more SPM can be transported towards the sea for high discharge conditions, the lock-exchange mechanism is increased, raising near-bed flood flow velocities, which enlarges the return flow of sediment upstream from the Maasmond.

5.6.2. Sediment dynamics

This section describes the implementation of the 127 sediment disposals, which have been executed over the course of the SURICATES pilot study. For the sediment plume a distinction is made based on the origin of the sediment being disposed, see table 5.3.

However, as not the 'real' hydrodynamics are imposed, each of the disposals has to be shifted to match the timing with respect to the tidal period.

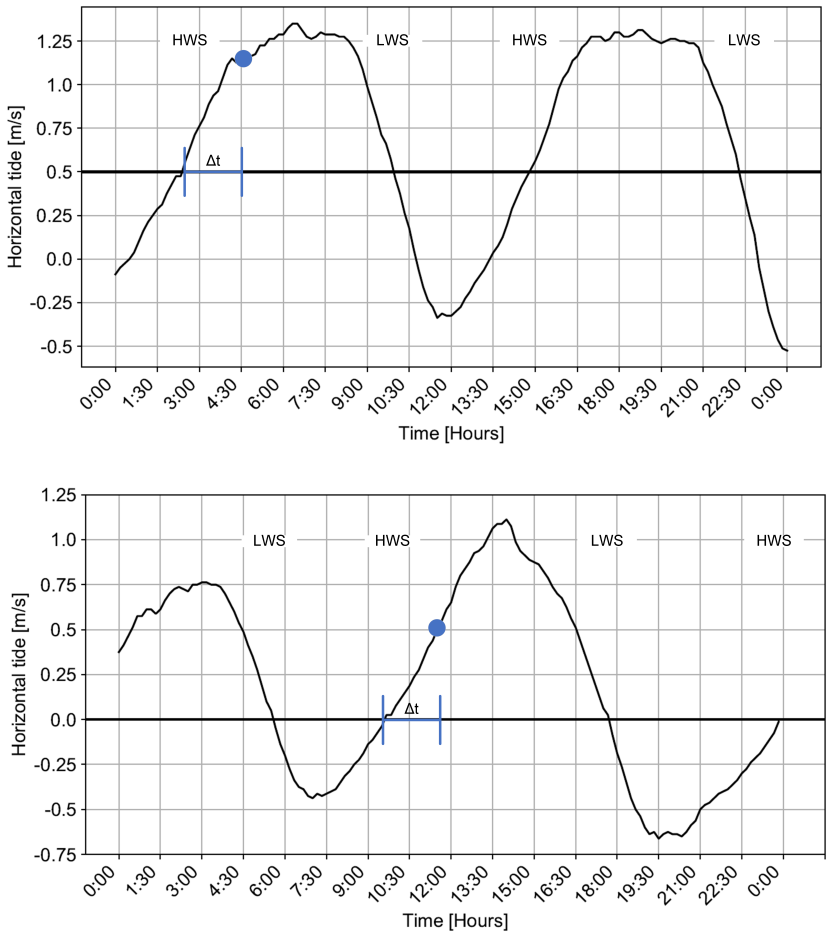

Figure 5.7: The shift of the disposal (blue dot) from November 5 to the repeated time series of Aug. 30 - Sep. 13 with respect to HWS. In this case the disposal at 4:30 Nov. 5 (upper figure) (2 hours after High Water Slack (HWS)) is shifted to August 30. 11:30, also 2 hours after HWS (lower figure).

Sediment disposals

For the long term modelling the hydrodynamic conditions from August 30 to September 13 are repeated. Therefore the disposals, from May 27 until November 20 have to be fitted into this hydrodynamic forcing. This is done based on the timing of the predicted depth-averaged HWS at Maassluis according to OSR. In PortofRotterdam [2018] is stated that the disposals should occur shortly after HWS at Maassluis.

In fig. 5.7 the principle of the shift with respect to HWS at Maassluis is shown. Based on the original time, the difference in time (Δt) between depth-averaged HWS and the time of disposal is determined. Subsequently, the disposal is shifted towards the hydrodynamic period of August 30 to September 13, obeying the same time difference (Δt) between HWS and the disposal.

Time step

For the long term model runs a larger time step has to be chosen as the resolution is smaller. In appendix F the convergence of the simulation of $\Delta t = 30s, 60s, 150smin$ is shown. The time step used is $\Delta t = 60s$.

5.7. Summary

In the past chapter is described how a model is set up to model the hydrodynamics and sediment dynamics of the SURICATES pilot study on different time scales. In the following section will be reflected on the following (sub-)research question:

Which assumptions and simplifications must be made to model SURICATES on different time and spatial scales?

To model SURICATES on different time and spatial scales two different model set-ups are used. In the models, the hydrodynamics and sediment behaviour are non-coupled, therefore the hydrodynamics are not influenced by the sediment concentration. This has the largest effect when high concentrations of SPM are expected, e.g. after bottom door disposals and during resuspension at sea. Due to the coarseness of the model, near field effects can not be resolved. Therefore, near field effects are circumvented by altering the depth of disposal in the model.

For the long term model set-up the hydrodynamics during the six month pilot study cannot be included into the model. To obtain nine months of hydrodynamic forcing, a representative two week hydrodynamic period is repeated. This fourteen day period included the variation in hydrodynamics induced by the neap/spring-cycle, but does not include variations in wind, wind set-up or discharge occurring during these nine months.

At first the simplifications made are discussed, followed by the model assumptions.

5.7.1. Model simplifications

For both the long term modelling and short term modelling, the implementation of the sediment disposals is simplified. In the model, the near field effects as described in section 3.2 cannot be included, due to the coarseness of the model used. This near field behaviour is simplified by placing the sediment disposals halfway the water column and close to bed to account for the near field effects. However, the amount of mixing with the ambient flow cannot be included adequately.

For both the long term and short term model hindcast a non-coupled hydrodynamic and sediment model is used. This simplification is required to limit the computational costs; a coupled model is deemed at least twice as computationally expensive. As a non-coupled model is used, the effects of hindered settling, buoyancy destruction and sediment-induced baroclinic pressure gradients are not included. This typically introduces errors at locations where high SPM concentrations might occur, as high concentrations of SPM induce density differences over the vertical. In the modelling of the SURICATES pilot study, large SPM concentrations are expected to occur twice: at the time of disposal and during fluid mud processes. After disposal by bottom door, a large amount of SPM is released, in a short time. Therefore, high concentrations of SPM can arise. From Winterwerp and Van Kessel [2003] is known that for high concentrations of SPM significant sediment induced turbulence damping can arise. The high concentration gradient upon release damp the local turbulence and therefore limits vertical mixing. This effect is highly non-linear, for a background concentration of 0.01 - 0.05 g/l the sediment flux increases with 10 %, whereas for high background concentrations +/- 0.5 g/l the vertical sediment flux increases with 100 %. Therefore, vertical sediment fluxes around the disposal might be underestimated in the model.

Fluid mud processes may occur during mid field and far field processes. In the far field, fluid mud processes occur during the rapid resuspension of settled SPM on the sea bed, as explained by Spanhoff and Verlaan [2000]. As the hydrodynamics and sediment dynamics are uncoupled, resuspension at sea will be altered. Due to the inclusion of sediment induced density differences the sediment concentration is stratified in the coupled model, whereas for the uncoupled model a more homogeneous distribution of SPM is found. Winterwerp and Van Kessel [2003] found that the sediment flux towards the Maasmond is underestimated by a factor 3 to 5 for non-coupled models.

Small variations in the bathymetry are not included in the model. Therefore, the sill at the Maeslantkering (fig. 3.13) and the pit (fig. 3.7, created by the impact of the disposals, are not included in the model. It is hypothesized in section 3.4 that the sill at the Maeslantkering may function as a barrier for sediment fluxes at the bed. Moreover, the pit may act as a sediment trap in which sediment can be (temporarily) deposited.

For the long term modelling a large simplification is made in the forcing of the hydrodynamics. To model the entire period of interest, a two week hydrodynamic forcing is repeated. This hydrodynamic forcing period

is not an one-on-one representation of the actual hydrodynamics during the SURICATES pilot study. The freshwater discharge during the forcing period is lower than the average discharge during the nine months considered. This lower discharge is assumed to promote the sedimentation of the harbour basins lining the Rotterdam Waterway.

5.7.2. Model assumptions

Apart from the above mentioned simplifications a few assumptions have been made. As discussed in the sensitivity analysis, the exact compositions of the barge is unknown. Currently the composition of the barge is based on grab samples executed prior to the start of the experiment and from previous studies done in the area, such as de Groot [2018], Vijverberg et al. [2015]. The sediment distribution used in both studies is assumed to be relatively fine when compared to grab samples taken at the source location. By using relatively fine material, the amount of settling is reduced.

At last, since a FLOW model is used, the effects of waves are not included. This assumption is assumed to be valid for the short term model hindcasts, as the waves generated at sea are significantly damped at the entrance. The effects of waves on the sediment flux inside the Rotterdam Waterway is assumed to be limited. However, for the long term model hindcast, sediment resuspension at sea is underestimated.

III

Results

6

Measurement results

In the following chapter the data obtained throughout the execution of the SURICATES project is analysed and discussed. The main goal of the data analysis is to quantify the spread of the sediment in time and space, based on different measurement surveys which have been executed over time. The spread of the sediment in time and space is investigated on two different scales; on the near field and mid field scale to understand the short term behaviour of the sediment plume after release, this is discussed in section 6.2. Ohter surveys have been executed to examine the cumulative behaviour of all sediment plume disposals over the course of the execution of the SURICATES pilot study, this is discussed in section 6.3. This chapter is concluded with a summary and reflection on the research sub-question.

6.1. Introduction

In section 6.2, two different surveys are used to examine the behaviour of a sediment plume disposed using bow coupling. The first survey is executed on September 11, 2019 for two hours, while the other survey lasted a full tidal cycle, from HWS until HWS on November 5, 2019. In this chapter at first the governing hydrodynamics (wind, wave and river discharge) on both days are discussed, followed by a description of the set-up for the measurement survey.

In the second section, section 6.3, the long term measurement results are discussed. To do so, the hydrodynamics during the full extent of the pilot study, May - November 2019 are discussed as these define both the behaviour of the background concentration as the cumulative behaviour of the sediment plumes. Subsequently, the results of the grab samples are discussed, while keeping the variability of the background concentration induced by the hydrodynamics in mind.

In section 6.4 a summary of this chapter is given, in which is reflected on the third research question; *How is the reallocated sediment distributed in time and space on different time- and spatial scales?* Subsequently, in chapter 7 the results of the measurement campaign are compared with the output of the model study.

6.2. Short term behaviour

To understand the near field to mid field behaviour of the sediment plume multiple surveys have been conducted, of which two will be discussed in this thesis. The surveys are set up to measure the concentration of SPM, salinity and flow velocities in the region of interest. The first survey (Sep. 11) is executed with a survey vessel sailing around the disposal location and sailing downstream once. While, the longer survey (Nov. 5) started prior to a disposal measuring the incoming concentration of SPM. During the survey the vessel has been sailing between Hook of Holland and Maassluis multiple times.

At first the hydrodynamics on September 11 and November 5 are described, based on data from measurement stations. The second part, section 6.2.2 and section 6.2.3, shows the results of measurement surveys. The September 11 survey has been relatively short and only consists of measurement taken with the silt profiler,

while for the November 5 survey, both the results of the ADCP backscatter and the silt profiler are discussed. These values are compared with values the expected background concentration as discussed in section 2.2.3, to distinguish background concentration of SPM and concentration induced by the sediment plume.

6.2.1. Hydrodynamics

As the hydrodynamics are the main forcing of suspended sediment behaviour and plume behaviour, the hydrodynamics on September 11, November 5 and the preceding days is analysed.

River discharge

As stated in section 1.1 the discharge through the Rotterdam Waterway is for 80 % determined by the Rhine discharge. Therefore, the Rhine discharge at Lobith[1] is used to determine the freshwater discharge in the Rotterdam Waterway. On September 11, the discharge conditions are very low, with a discharge on the preceding days at 1300 m^3/s. On November 5, the Rhine discharge equals 1740 m^3/s, which is significantly below the yearly average of 2200 m^3/s, but equal to the average Rhine discharge during the duration of the pilot study of 1700 m^3/s. Low discharge conditions in general lead to a smaller supply of fluvial sediment from upstream and allows the salt wedge to extend further landward.

Tide

September 11 is three days prior to full moon and thus spring tide, while November 5 is one day after the last quarter hence neap tide. During neap tide the salt intrusion length is shorter than for average conditions, while for spring tide the salt intrusion length in general extends further than for average conditions. In fig. 6.1 the horizontal tide at Hook of Holland (HvH) and predicted horizontal tide at HvH and at the upstream end of our area of interest are shown first petroleum harbour (*1e PETH*), see fig. 1.1. Due to internal tidal asymmetry the propagation velocity of the horizontal tide reduces strongly along the Rotterdam Waterway. Also, ebb periods last significantly larger than flood periods, which is typical for the Rotterdam Waterway as discussed in section 2.1.3.

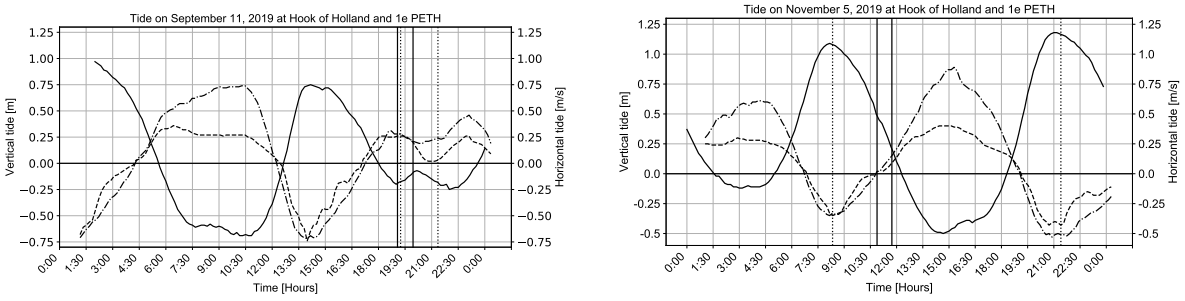

(a) (b)

Figure 6.1: Tide at September 11 (a) and November 5 (b), 2019 at Hook of Holland and 1e Petroleumhaven (1e PETH). The straight lines indicate the vertical tide, the dashed lines with dots the horizontal tide at the 1e PETH and the dashed lines the horizontal tide at Hook of Holland. The velocities are positive in the downstream direction The vertical lines indicate the duration of the sediment disposals, the dashed vertical lines indicate the duration of the measurement surveys. The vertical tide is obtained from the station at Hook of Holland, whereas the horizontal tide are hindcasted data from Operationeel Stromings Model (OSR). On September 11, LWS occurred at 5:30 and 17:40, HWS at 3:45 and 23:50. LW at 10:00 and 21:00, HW at 0:10 and 12:45. On November 5, HWS occurred at 11:00 and 23:30, LWS at 4:10 and 16:25. LW at 3:00 and 14:45, HW at 8:00 and 21:00.

Wind and wind set-up

The wind speed is important for resuspended sediment at sea and for the amount of mixing in the Rhine ROFI and Rotterdam Waterway. As stated in appendix B.1.1 the Rotterdam Waterway and Rhine ROFI can be considered to be well-mixed over the vertical.

[1] Lobith is located at the Dutch-German border, leading to a two day delay between the value at Lobith and in the Port of Rotterdam [Spanhoff and Verlaan, 2000]

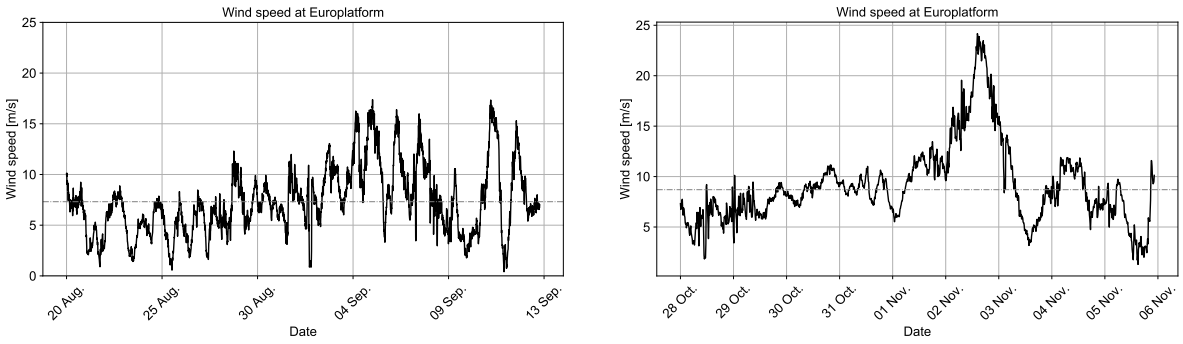

(a) (b)

Figure 6.2: Wind speed at Europlatform prior to September 11 (a) and November 5 (b). The dashed grey line indicates the average wind speed of the time series being 7.8 m/s and 9 m/s.

Due to strong winds, the water level in front of the port is increased (wind set-up), as the water is pushed against the coast. Wind set-up is calculated by taking the difference between the calculated astronomical tide and measured water level. As the water level is increased, the barotropic pressure gradient is increased as well, pushing the salt wedge further landward. Prior to September 11, some set-up is noticeable at Hook of Holland. Due to combined effect of low discharge conditions, set-up at sea (and spring tide to a smaller extent) it is expected that the salt wedge is noticeable throughout the domain of interest over the full period of time. Prior to November 5, a decline in the set-up is noticeable, however the system is expected to be still in recovery from the set-up induced by the storm on November 3, as described in section 2.1.3 de Nijs et al. [2010]. This explains the relatively high salinity on November 5.

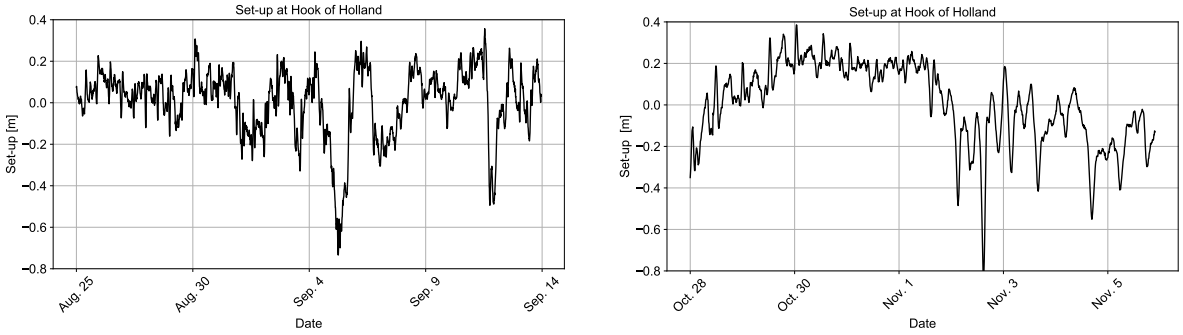

(a) (b)

Figure 6.3: Wind set-up prior to September 11 (a) and November 5 (b) at Hook of Holland.

6.2.2. September 11

The survey executed on September 11 lasts 3 hours from 18:00 - 21:00 and is therefore useful to verify the hypothesis on near and mid field behaviour as described in chapter 6.

The silt profiler measurement 1 - 11 can be split in two. The measurements 1 - 8 are taken in the vicinity of the ship, during the disposal, suitable for an analysis of the near field behaviour of the sediment plume. The measurements 9 - 11 are taken after the disposal approximately 1, 2 and 3 kilometers downstream from the reallocation site, useful for a mid field analysis.

In measurement 1 and 2 it can be seen that initially the majority of the sediment is dispersed over the first 7 meters. The lack of a clear SPM peak in measurement 3 and measurement 4 is probably simply caused by the distance from the ship. From Measurement 5 - 8 can be derived that the sediment plume has the tendency to

Silt profiler	Time	Distance (km)
1	18:11	7.75
2	18:03	7.92
3	18:19	7.48
4	18:30	7.25
5	18:43	7.79
6	18:49	7.59
7	18:56	7.72
8	19:04	7.51
9	19:46	6.42
10	19:56	5.63
11	20:10	4.21

(a) Time and location of the silt profiler measurements 1 - 11

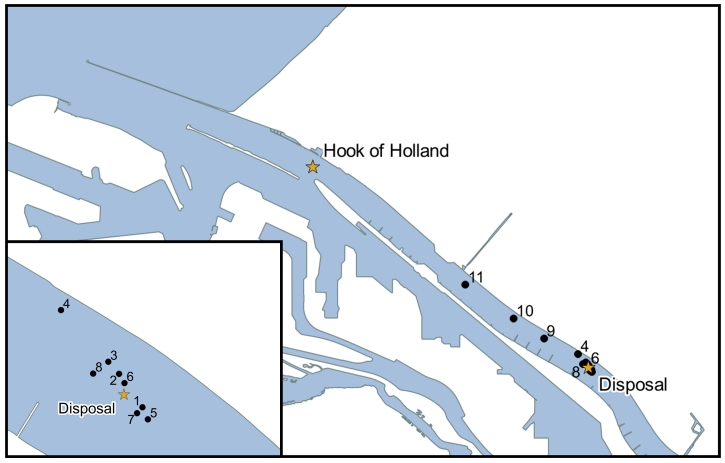

(b) Location of the silt profiler 1 - 11

Figure 6.4: The location of the silt profiler measurements 1 to 11 on September 11, 2019 between 18:00 and 20:10. The distance refers to the distance from Hook of Holland.

disperse over depth. Moreover, it can be seen that the water column is clear from SPM above the pycnocline. As indicated in section 3.3, SPM confined below the pycnocline is most likely entrapped below the pycnocline and follow the fate of entrapped fluvial sediment as described by de Nijs [2012]. The interpretation of the measurement results are shown in fig. 6.6.

Measurement 9, can be regarded as mid field as it is taken 40 minutes after the disposal and 1 kilometre downstream of the disposal. The measurement shows a similar pattern as the measurement 5 - 8; part of the SPM is confined below the pycnocline and some transport takes place around the pycnocline. However, the lack of SPM found below a depth of 10 m is explained by the displacement of the survey vessel. According to fig. 6.8, parts of the plume can only be noticed between 2 to 10 m depth. This artefact or measurement bias is introduced by the advection of the survey vessel and differential advection and is further explained in section 6.2.3.

Measurement 10 lacks a clear signal of the sediment plume, as the SPM concentrations lie within the range of expected SPM concentrations. According to fig. 6.8, parts of the plume should be noticeable at a depth of 2 to 8 m. Since no signal of the plume is found at this depth, it is assumed that the plume has rained out below the pycnocline. The peak values between 10 to 12.5 m for measurement 10 can be an indication of parts of the plume which have been advected higher up in the water column and settled initially. However, as seen in section 2.2.2, this larger concentration of SPM is not necessarily linked to a larger availability of SPM, but can be caused by a larger carrying capacity as well.

In short, the September 11 measurements seem in line with the near field hypothesis drawn in section 3.2. In this hypothesis it is expected that the sediment plume remains a jet between the first $\approx 4m$ and the transition depth at $\approx 12m$, after which it disperses over depth. Especially measurement 5 - 8 and 9 are clear in the sediment plume being advected around and below the pycnocline, which is in line with the hypothesis.

6.2.3. November 5

The location and the transects sailed by the vessel during the November 5 survey are shown in fig. 4.1. The measurement campaign is split in four distinct time periods:

- **Period I (8:00 - 11:00):** These measurements are taken prior to the 11:00 disposal to measure incoming SPM during flood.
- **Period II (11:00 - 13:00):** These measurements are taken around the vessel and while sailing towards Hook of Holland following the plume.
- **Period III (13:00 - 16:00):** These measurements are taken after the signal of the plume is lost until Low

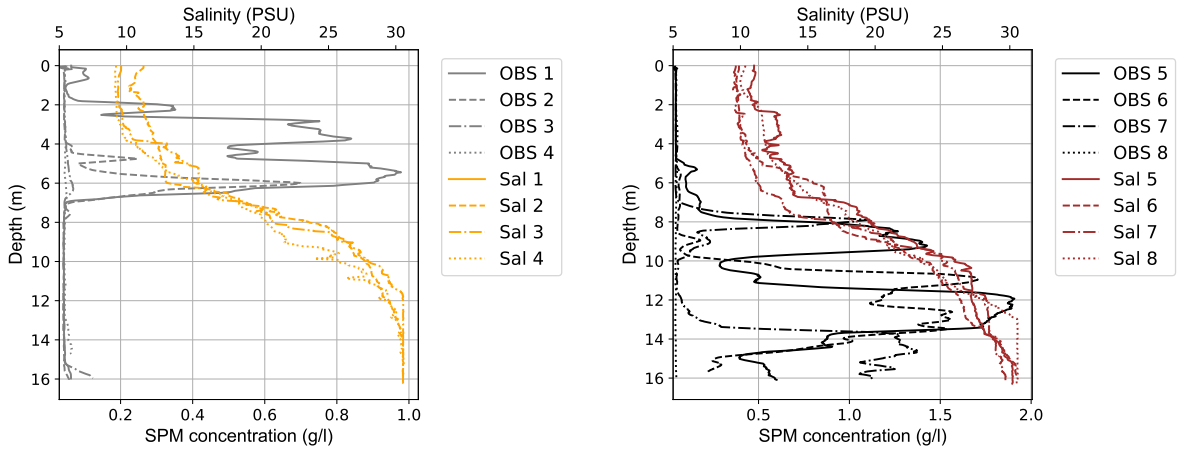

(a) Silt profiler 1 - 4

(b) Silt profiler 5 - 8

Figure 6.5: The results of the silt profiler measurements 1 - 8 taken in the vicinity of the dredging vessel during disposal on September 11.

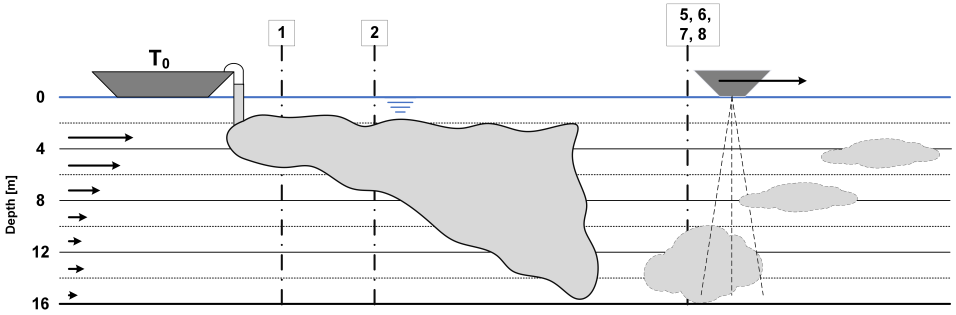

Figure 6.6: Current interpretation of the plume behaviour. The numbers and dashed lines indicate the location of the silt profiler measurements 1, 2, 5, 6, and 7. The arrows indicate the flow velocity and velocity of the survey vessel.

Water Slack.

- **Period IV (16:00 - 21:00):** The last measurements are taken during rising tide to measure the amount of incoming SPM after flow reversal.

In the following paragraphs the SURICATES sediment plume dynamics are discussed during each of these four different periods. The results are obtained with both the ADCP backscatter and silt profiler using a Lagrangian frame of reference.

Period I: 8:00 - 11:00 Prior to disposal during flood

The first period consists of three different trajectories, all sailed during flood prior to the main disposal, to measure the background concentration and amount of incoming SPM.

All seven measurements, fig. G.6, show sediment concentrations in the range of the expected background concentration as derived in section 2.2.3 for flood conditions. Overall, it can be concluded that the distribution of SPM over the vertical is not higher during flood than can be expected from previous measurement campaigns. However, this can not reject the hypothesis of the non-existence of a return flow of sediment. First of all, if the return flow takes place close to the bed, this is not measured with the ADCP backscatter, due to the blanking distance. Next to this, the 7 vertical profiles from the silt profiler only provide a very local view in time and space.

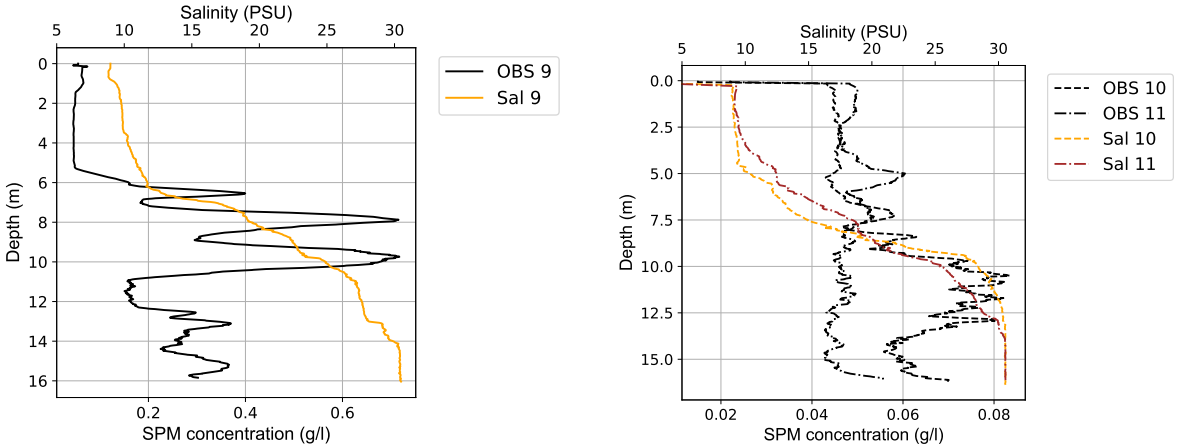

(a) Silt profiler 9

(b) Silt profiler 10 - 11

Figure 6.7: The results of the silt profiler measurements 9 - 11 taken at 1, 2 and 3 kilometres from the reallocation site after the disposal on September 11.

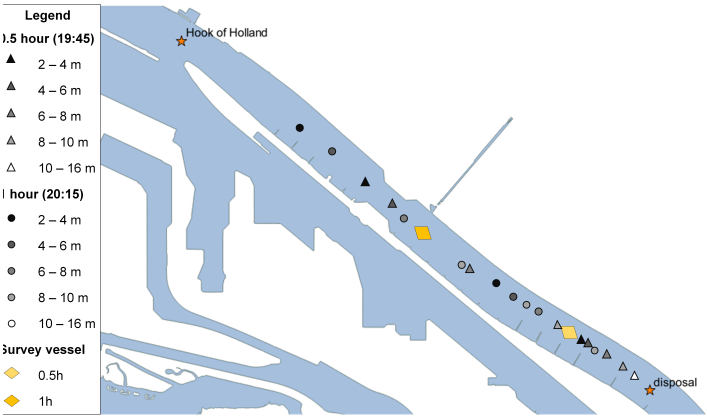

Figure 6.8: The predicted displacement of the sediment plume based on measured average velocities at the respective depths, illustrating the effect of differential advection. The coloured diamonds indicate the location of the survey vessel at time of the measurements.

Period II: 11:00 - 13:00 Disposal

The second period consists of two different sets of measurements: 1) the first set is taken close to the vessel during the disposal (11:00 - 11:50) to analyse the near field behaviour and 2) the second set of measurements is taken while following the sediment plume in downstream direction (11:50 - 13:00), for a near field to mid field analysis. From the backscatter and silt profiler data an Lagrangian perspective on the initial cloud dynamics is discussed.

Measurement 8 to 11 are taken close to the vessel during disposal at 7.9 km from Hook of Holland (HvH), between 11:09 and 11:38 during disposal. From the silt profiler measurement 8, fig. 6.12 a high and narrow peak in SPM concentration can be observed at a depth of 2.5m; which is an indication of little mixing and typical for jet behaviour. Measurement 9, shows a wider SPM distribution peak; which is an indication of some mixing between 2.5 m to 7.5 m depth in the vertical direction. Measurement 10 shows a more dispersed pattern, indicating that the plume is dispersed below a depth of 10m. Measurement 11 shows a double peak in concentration, with a peak larger than found at measurement 9. This can be an indication of the centre line of the plume; where the concentration is largest. The lack of SPM higher in the water column can be explained with differential advection or by settling of the sediment. If the silt profiler measurements are compared with the qualitative view provided by the ADCP backscatter in the same transect (fig. 6.11), a net downward movement of the sediment plume is confirmed. For all measurements, including the ADCP backscatter, either a high SPM concentration is noticeable high in the water column; between -2.5m and -5.0m or between

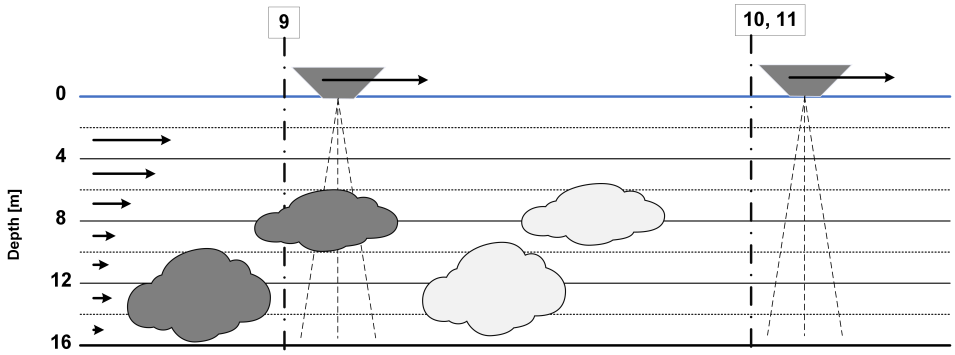

Figure 6.9: Current interpretation of the sediment plume behaviour in the mid field. The numbers and dashed lines indicate the location of the silt profiler measurements 9, 2, 5, 6, and 7. The arrows indicate the flow velocity and velocity of the survey vessel.

Silt profiler	Time	Distance (km)
11:00 - 11:50		
8	11:09	7.84
9	11:15	7.82
10	11:29	7.89
11	11:38	8.14
11:45 - 12:10		
12	11:46	7.54
13	11:52	7.2
14	11:57	6.71
15	12:02	6.25
16	12:08	5.85
17	12:08	5.85
12:45 - 13:00		
18	12:44	2.12
19	12:49	1.62
20	12:55	1.25

(a) Time and location of the silt profiler measurements 8 - 20

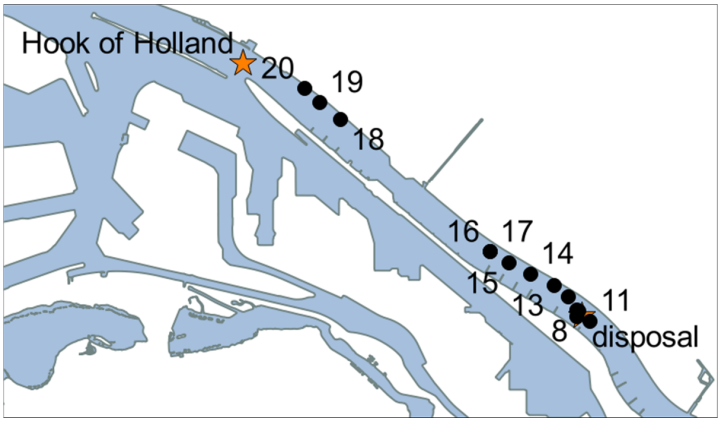

(b) Location of the silt profiler 8 - 20

Figure 6.10: The location of the silt profiler measurements 8 to 20, the distance is measured from Hook of Holland.

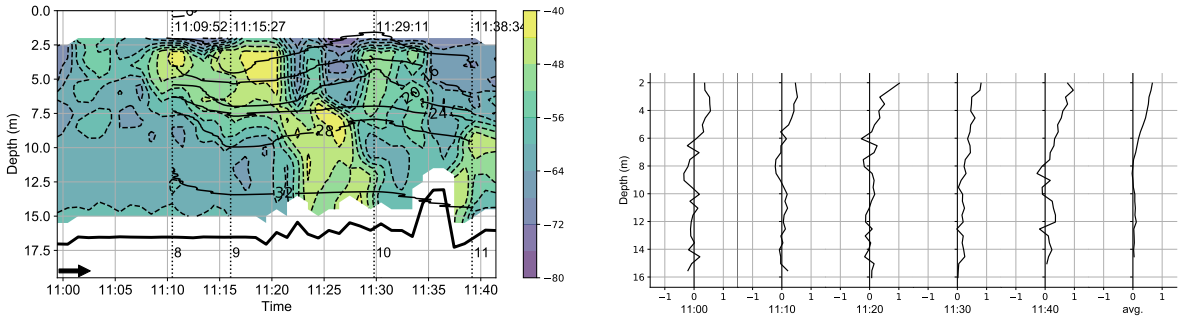

(a) (b)

Figure 6.11: Results from the ADCP and ADCP backcatter between 11:00-11:50 during disposal. a) The dashed lines indicate the contours of the amount of absolute backscatter, the straight lines indicate the isohalines with constant salinity in PSU. The vertical dashed lines indicate the location of the silt profiler measurements with its according time and number. b) The total measured horizontal flow velocity.

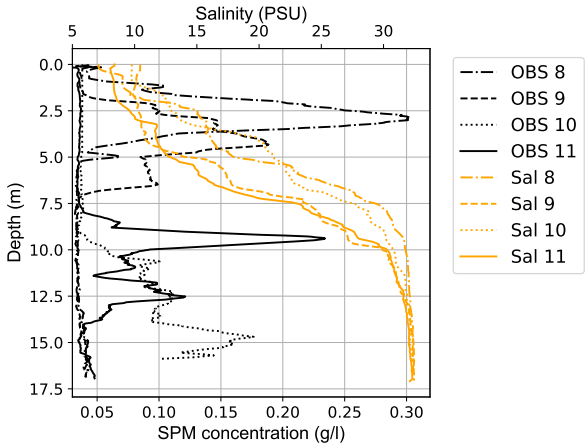

Figure 6.12: Silt profiler measurement 8-11 taken in period 2, between 12:45 and 13:00. The black lines indicate the concentration of SPM in g/l. The orange lines indicate the salinity over the vertical in PSU.

-7.5m and -10.0m, which complicates the interpretation of the measurements. As the measurements 8 - 11 are taken around the vessel during disposal, but at a different time and location, part of the plume could have been dispersed over time. It is assumed that most sediment is dispersed over the depth around and below the pycnocline and that little sediment is advected above the pycnocline. This current interpretation is shown in fig. 6.13. Moreover, most sediment above the pycnocline is expected to be absent in subsequent measurements due to the raining out of sediment.

Measurement 12 to 17 are taken while following the plume in downstream direction from 11:50 to 13:00. The picture that arises from the ADCP backscatter and silt profiler measurement 11, 12 and 13, is a clear plume of sediment at a depth of 7.5 to 10 m. Between 11:52 and 12:10, while sailing downstream the location of the SPM peak over the vertical seems to rise: measurement 15 shows a single peak of SPM at a depth of -5 m. This rise in SPM concentration is explained using the concept of differential advection, see fig. 6.13 and fig. 6.16. Between 11:46 and 12:10 the survey vessel reached an average velocity of 1.29 m/s, reaching 1.7 km in 22 minutes from the disposal site. From the flow velocity measurements (see fig. 6.14 and table G.4) it is known that the average flow velocity between 11:45 and 12:10 equals 1 m/s at the surface and < 0.30 m/s below -8m NAP. Hence, the vessel has most likely overtaken the sediment plume. Therefore the survey vessel only shows the parts of the plume advected at the velocity of the survey vessel. If differential advection is kept in mind, the following observations from fig. 6.15 can be made.

- The largest amount of SPM can be found between a depth of 7.5 to 10m. (based on OBS 11 - 13). And sinks over time, see measurement 10 and 11.

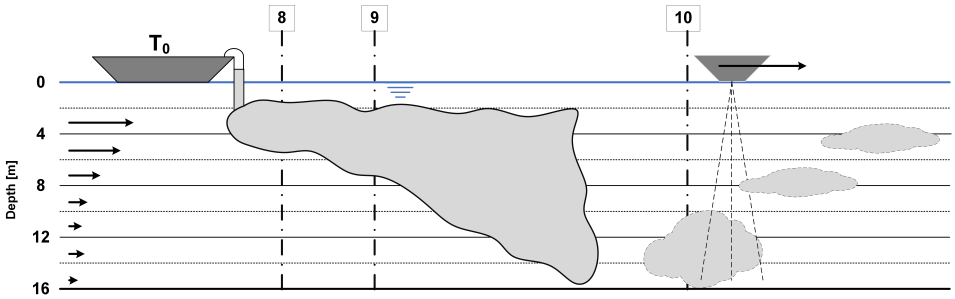

Figure 6.13: Current interpretation of the plume behaviour. The numbers and dashed lines indicate the location of the silt profiler measurements 8 to 10. The arrows on the left indicate the flow velocity and the arrow at the survey vessel the velocity of the survey vessel on scale.

- The concentration above the pycnocline is subject to significant dilution. This can be biased, caused by the propagation velocity of the survey vessel or by SPM raining out.

These observations are in line with the observations made on September 11.

From fig. 6.14 it can be derived that the signal of the plume is lost shortly after 2 kilometers. As stated previously, most likely the survey has been sailing too fast to track the sediment plume in the mid field, hence in fig. 6.17b SPM values are in range if normal conditions. Only a small peak above the pycnocline can be observed for all three measurements. Based on fig. 6.16 it can be concluded that this peak is not caused by the advection of the sediment plume.

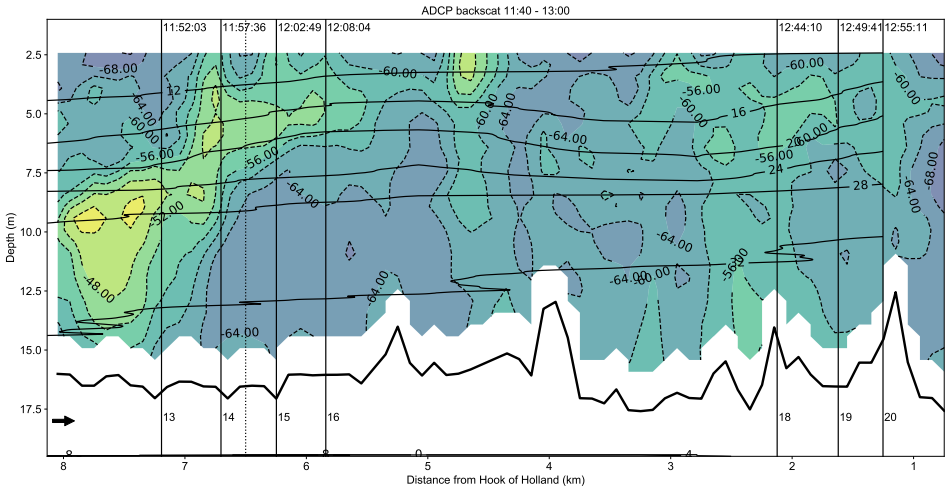

(a) ADCP backscatter

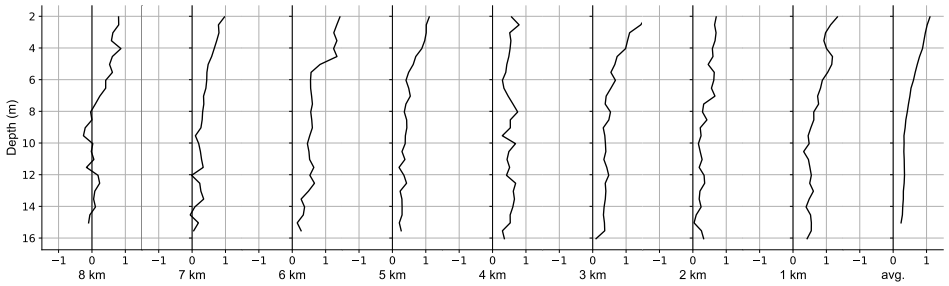

(b) Total horizontal flow velocities

Figure 6.14: Results from the ADCP and ADCP backcatter between 11:45 - 13:00 after disposal. a) The dashed lines indicate the contours of the amount of absolute backscatter, the straight lines indicate the isohalines with constant salinity in PSU. The vertical dashed lines indicate the location of the silt profiler measurements with its according time and number. b) The total measured horizontal flow velocity.

Period III: 13:00 - 18:00

The third period lasts from 13:00 - 18:00 in order to find the initial plume or its remains, still during ebb. Here we consider a single transect sailed between 13:00 - 15:15 from Hook of Holland in upstream direction. This is in the opposite direction of the assumed direction of the plume advection. This shrinks the relative size of the plume, making it more difficult to detect the plume. These measurements are taken at least two hours after disposal, therefore it is expected that the plume is difficult to detect as the sediment concentration due to the plume advection is in the same order as the background concentration.

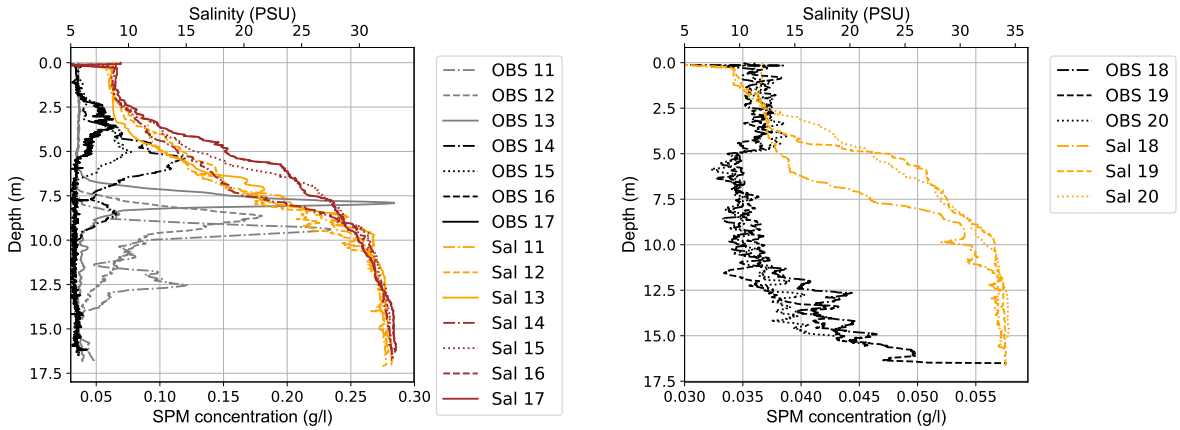

(a) Silt profiler measurements 11-17

(b) Silt profiler measurements 18-20

Figure 6.15: Silt profiler measurement taken in period 2, between 11:45 and 12:10 (measurement 12 - 17) while sailing downstream from the disposal site. Measurement 18 to 20 are taken close to Hook of Holland, 1 hour after disposal (12:45 - 13:00). The black and gray lines indicate the concentration of SPM in g/l. The orange and red lines indicate the salinity over the vertical in PSU.

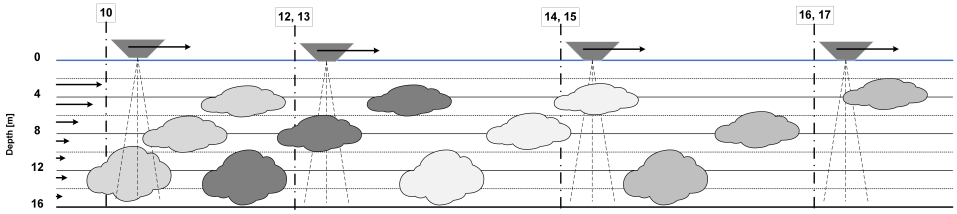

Figure 6.16: Current interpretation of the plume behaviour. The numbers and dashed lines indicate the location of the silt profiler measurements 10 to 17. The arrows indicate the flow velocity and velocity of the survey vessel. The colours of the plume indicate the time; a matching color.

Silt profiler	Time	Distance (km)
13:00 - 13:30		
22	13:09	1.31
23	13:24	1.96
24	13:34	2.29
13:45 - 14:15		
25	13:50	3.16
26	13:55	3.14
27	14:11	3.55
28	14:16	3.56
14:30 - 14:50		
30	14:33	4.26
31	14:38	4.22
32	14:38	4.22
33	14:43	4.18
34	14:47	4.11
14:50 - 15:15		
35	14:58	4.63
36	15:03	4.59
37	15:07	4.56
38	15:12	4.57

(a) Time and location of the silt profiler measurements 22 - 38

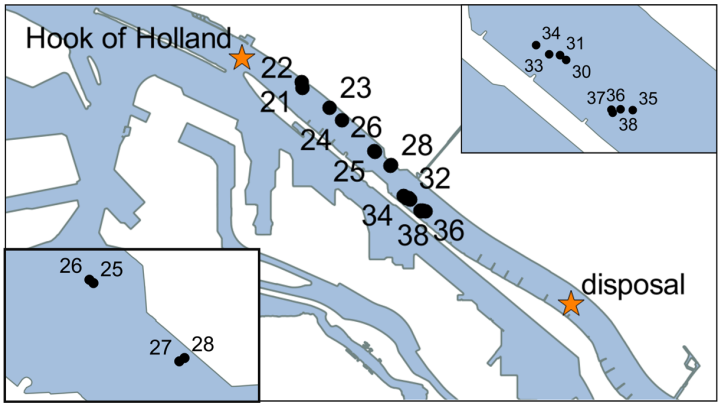

(b) Location of the silt profiler 22 - 38

Figure 6.18: The location of the silt profiler measurements 22 to 38 and the trajectories sailed by the ADCP backscatter between 13:00 - 15:15.

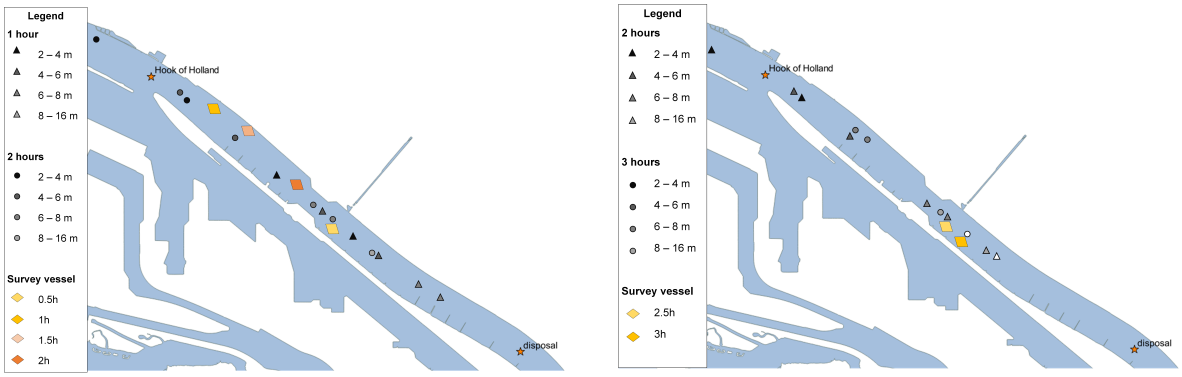

(a) Predicted displacement 11:50 - 13:50

(b) Predicted displacement 11:50 - 14:50

Figure 6.17: The predicted displacement of the sediment plume based on measured average velocities at the respective depths, illustrating the effect of differential advection. The coloured diamonds indicate the location of the survey vessel 0.5h, 1h, 1.5h, 2h, 2.5h and 3 hours after 11:50. The displacement after 1 hour coincides with the measurements 18 - 20, after 2 hours with measurement 24 - 26 and after 3 hours with measurements 32 - 37.

In fig. 6.19a local peaks in backscatter are noticeable just below the pycnocline, e.g. around 13:50 and 14:45. The first small and short peak can possibly be attributed to the plume fraction being advected at this depth, using the estimation of the sediment plume location; table G.4 and fig. 6.17b. However, in measurement 25 and 26, fig. G.8a, this peak is not noticeable.

The measurements 30 to 38 are all taken upstream of the Maeslantkering while sailing back and forth between 14:30 and 15:15. Measurement 30 - 34 are taken in the proximity of measurements 4 and 5, with half a tidal phase difference (ebb vs. flood). When these measurements are compared the measured sediment concentration is the same.

The measurement 35 - 38 are taken slightly further downstream of measurements 30 - 34. These measurements show very interesting results, with SPM concentrations ranging from 0.08 g/l to 0.16 g/l in the 3 meters closest to the bed. To explain the local maxima, very local spatial differences may play a role. Although the measurements are not taken in locations with strongly varying bathymetry or behind a obstacles, in fig. 2.11 one can observe that peaks in SPM near the bed can be very local.

Another explanation can be seeked in the advection of the sediment plume. Measurement 35 - 38 are taken between 14:50 - 15:15 at 4.5 kilometres from Hook of Holland, according to fig. 6.17a and table G.4, the fraction of the sediment plume at 10 - 16m depth, is approximated to be there at the same time, hence the peaks in sediment concentration can be attributed to the advection of the sediment plume.

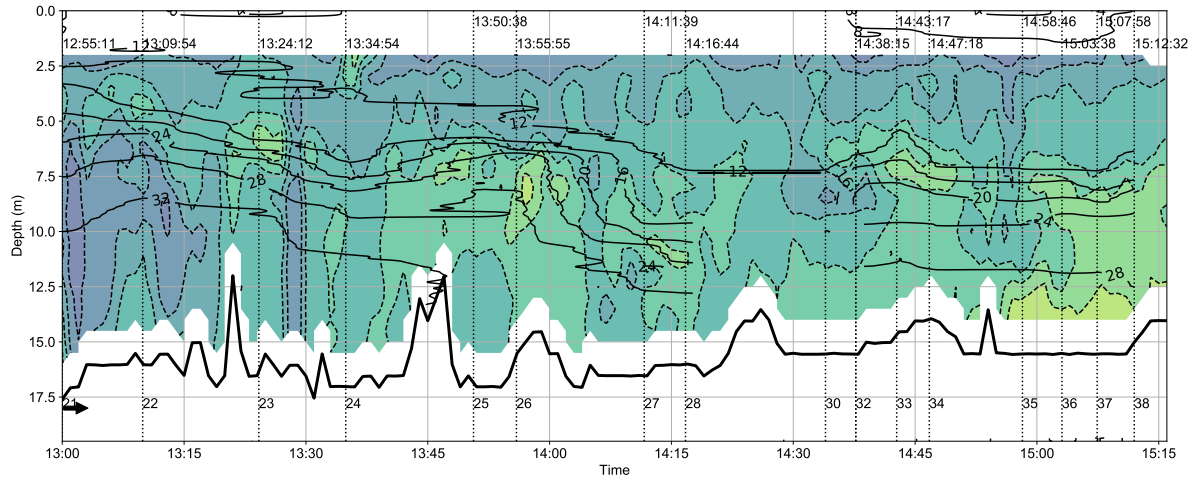

(a) ADCP backscatter

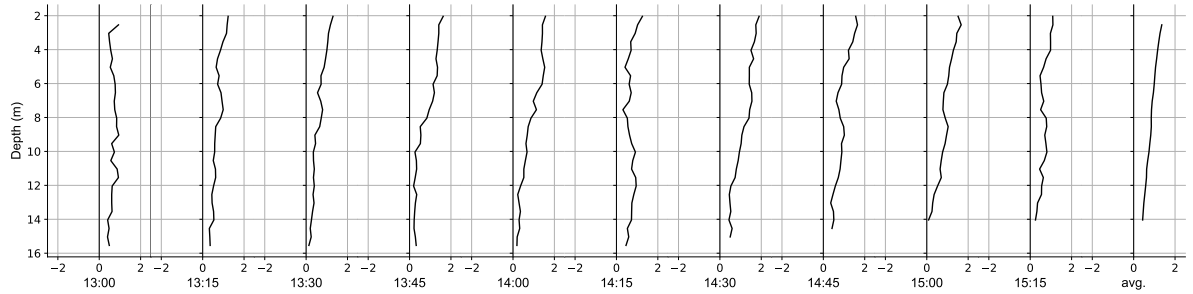

(b) Horizontal flow velocity

Figure 6.19: Results from the ADCP and ADCP backcatter between 13:00 - 15:00. a) The dashed lines indicate the contours of the amount of absolute backscatter, the straight lines indicate the isohalines with constant salinity in PSU. The vertical dashed lines indicate the location of the silt profiler measurements with its according time and number. b) The total measured horizontal flow velocity.

Period IV: 16:00 - 21:00

Measurement 39 - 42, fig. G.11 are taken slightly upstream of, and two hours after measurements 30 - 38. However, these measurements do not show the same peak in SPM concentrations as found in the measurements 39 - 42. The values found for measurement 39 - 42 are comparable to the results found for measurements 4 and 5. Hence, no trace of a remainder of the plume is found. Moreover, above the pycnocline, the measurements 30-34, 35-38 and 39,42 all show the same concentrations, which are in line with the expected sediment concentration. It can therefore be concluded that no remainder of the sediment plumes can be detected above the pycnocline. Measurement 43 - 44 are taken further downstream, but also downstream no increase related to the sediment plume dynamics can be detected.

The last measurements (45 - 50) are taken after depth-averaged LWS and subsequent flood, again to measure the amount of SPM that is returned, after flow reversal. Between 18:00 - 18:50 the survey vessel sailed from Hook of Holland towards the reallocation area; where no irregularities in the distribution of SPM over the vertical can be detected, see fig. G.13.

Subsequently the vessel has been sailing around the disposal area. During this trajectory measurement 45 and 46 are taken at the disposal area. Measurement 45 shows a peak of 0.10 g/l at the bed and measurement 46 a peak concentration of 0.29 g/l. Apart from previously mentioned salt wedge dynamics or plume dynamics a third option can lead to this peak concentration at the bed: during the disposals a pit has formed at the disposal area. These measurements are taken inside this pit, see (fig. 6.23). This pit can function as a temporary storage of sediment, e.g. as a sediment trap as it is deeper than it surroundings, explaining the high measured SPM concentrations.

The last trajectory is taken from 20:00 to 21:00 while sailing from Hook of Holland towards Maassluis, see

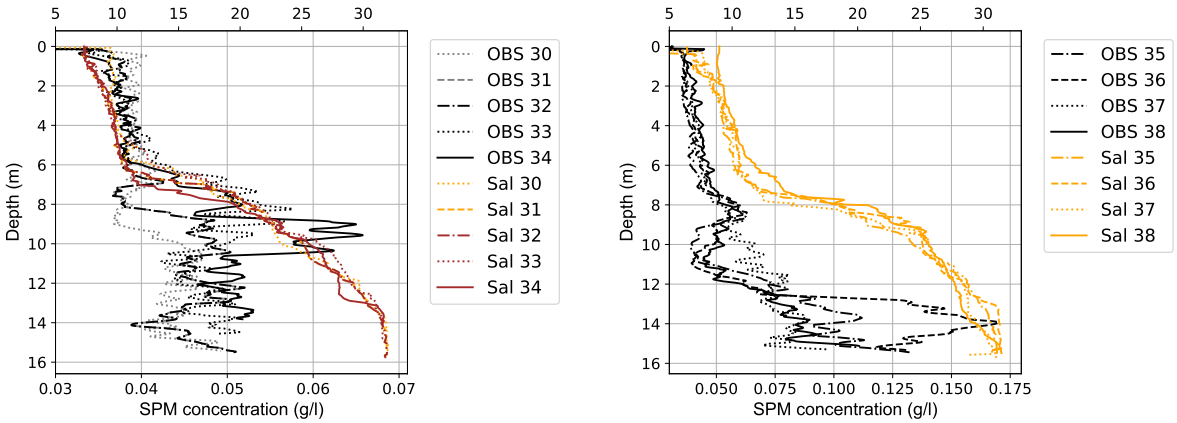

(a) Silt profiler 30 - 34

(b) Silt profiler 35 - 38

Figure 6.20: Silt profiler measurement 30-38 taken in period III, between 14:30 and 15:15, while sailing upstream. The black and gray lines indicate the concentration of SPM in g/l. The orange and red lines indicate the salinity over the vertical in PSU

Silt profiler	Time	Distance (km)
18:45 - 19:15		
45	18:56	8.12
46	19:17	8.11
20:00 - 20:15		
47	19:59	2.45
48	20:05	2.5
20:30 - 20:45		
49	20:35	5.85
50	20:41	6

(a) Time and location of the silt profiler measurements 45 - 50

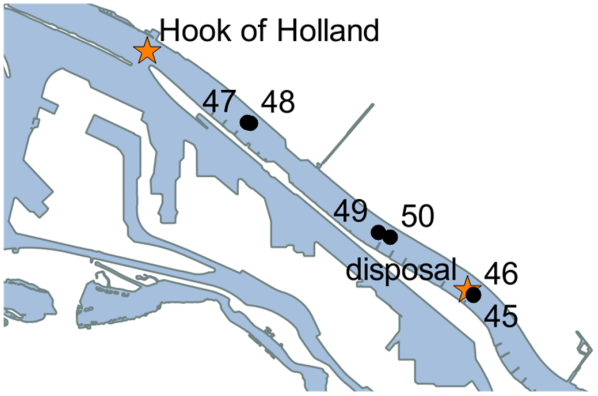

(b) Location of the silt profiler 45 - 50

Figure 6.21: The location of the silt profiler measurements 45 to 50 and the trajectories sailed by the ADCP backscatter between 18:45 - 19:15, 20:00 - 20:15 and 20:30 - 20:45

fig. G.16. The ADCP backscatter measurements are supported by 4 silt profiler measurements; 47 - 50. These measurements are taken 3.5 kilometres apart from each other, with the Maeslantkering in between. The SPM concentrations found are in line with the expected background concentration, hence no signal of the sediment plume is detected.

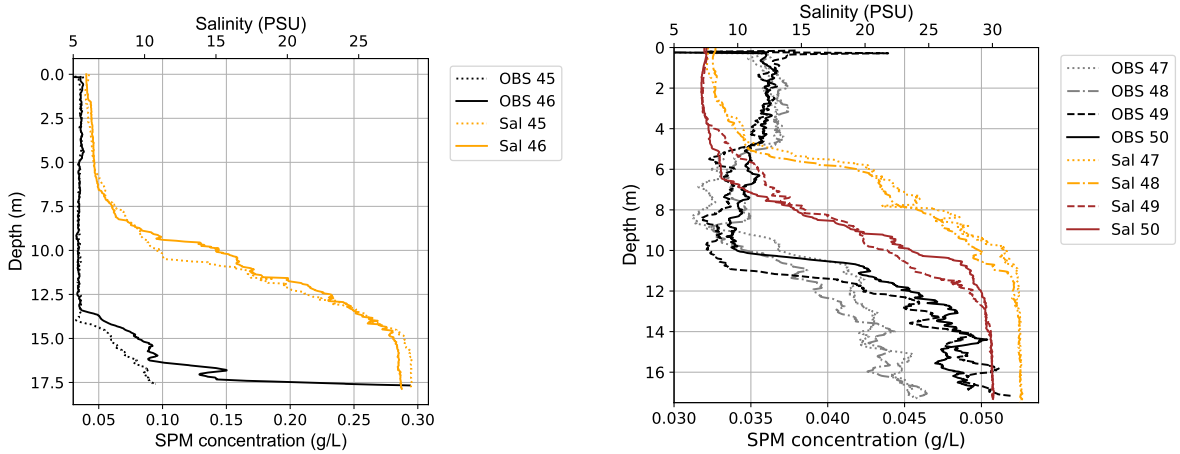

(a) Silt profiler measurement 45 and 46

(b) Silt profiler measurement 47 to 50

Figure 6.22: Silt profiler measurement 45-50 taken in period IV, between 19:00 and 20:45, while sailing upstream. The black and gray lines indicate the concentration of SPM in g/l. The orange and red lines indicate the salinity over the vertical in PSU.

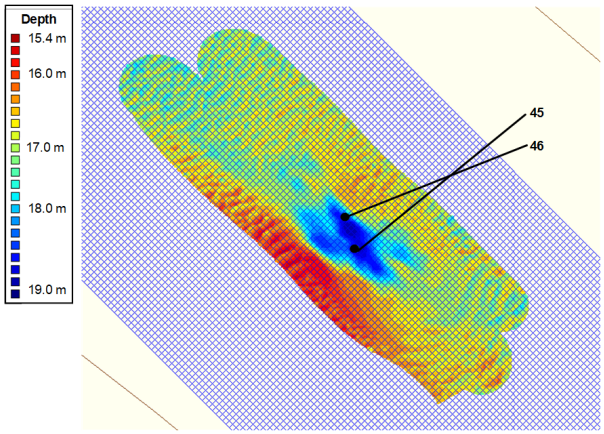

Figure 6.23: The silt profiler measurements 45 and 46 inside the erosion pit.

6.3. Long term behaviour

In chapter 4 the set-up of the long term measurement campaign is discussed. In this section, the results of the change in bed composition is discussed. At first the hydrodynamics, the wave height and river discharge, of the system over the entire span of the experiment are discussed. The subsequent section will discuss the grain size distribution of the system in equilibrium conditions. Concluded with the measurement results.

6.3.1. Hydrodynamics

The following section will discuss the hydrodynamics from January 1, 2019 up to December 2019. This is one month prior to T_0 until the end of the pilot study. For the wave height data from the Eurogeul is used whereas for the river discharge is measured at Lobith.

Wave height

The wave height at sea and at the mouth of the port is an important parameter as sedimentation in the Maasmond and southern basins is strongly correlated to high wave conditions at sea, this is explained in appendix B.3.7 [Spanhoff and Verlaan, 2000].

The wave height data is obtained from the Eurogeul platform located offshore of the harbour mouth. From

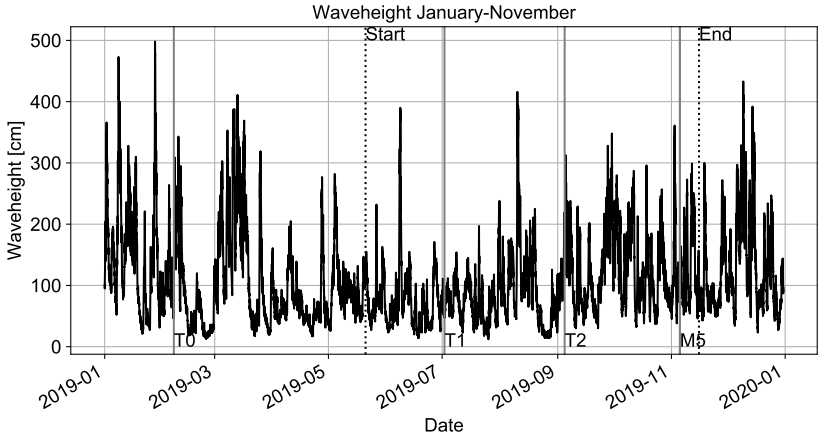

Figure 6.24: The wave height from January 2019 until December 2019, with the lines indicating T_0, T_1 ,T_2 and M_5.

Measurement	Discharge	Wave height
T_0	Avg.	High
T_1	Avg.	Low
T_2	Low	High

Table 6.1: Hydrodynamic conditions prior to long term the measurements

the wave height, it can be observed that the zero measurement, T_0 is taken after relative high wave conditions. Therefore, it is expected that the samples taken close to the mouth of the port (*Down 2 - 5*) contain a relative high amount of silt and clay.

Based on fig. 6.24 the wave climate prior to T_1 and T_2 is very similar. 2 weeks prior to both measurements, high waves have been registered followed by a mild period. Although, from Spanhoff and Verlaan [2000] the exact lag between a high wave event and the observed sedimentation event is unknown, wave induced sedimentation at the downstream sampling locations 2 - 5 is expected.

River discharge

The discharge in the Rotterdam Waterway is for 80 % determined by the discharge in the Rhine. Historically the discharge at the Rhine is related to the discharge measured at Lobith. The average Rhine discharge during the duration of the pilot study is 1700 m^3/s; whereas the yearly averaged runoff equals 2200 m^3/s. Low discharge conditions in general lead to a smaller supply of fluvial sediment and the salt wedge extends further landward.

From literature no conclusion can be drawn on the effect of river discharge variability on the amount of SPM in concentration. de Kok [2002] investigated the effect of the freshwater discharge distribution between the Haringvliet and the Maasmond on the SPM distribution. In this study, although based on model results, a weak correlation ($r^2 = 0.59$) between Rhine discharge and sedimentation in the Maasmond and Calandkanaal is found. Moreover, during high discharge conditions near-bed residual currents towards the Maasmond are stronger due to increased stratification.

In general for high fresh water discharge conditions more fluvial SPM is provided from upstream. It should be noted however, that for low discharge conditions the salt wedge stretches further landward, while entrapping more fluvial sediment. For very high discharges the salt wedge is suppressed up to the mouth of the harbour. For such conditions SPM from the ETM is allowed to settle in the Maasmond [de Nijs et al., 2008, de Nijs and Pietrzak, 2012]. Therefore, no closing conclusion can be drawn on the relation between freshwater discharge and sedimentation in the harbour basins lining the Rotterdam Waterway.

The combined effect of wave conditions and discharge is summarized in table 6.1.

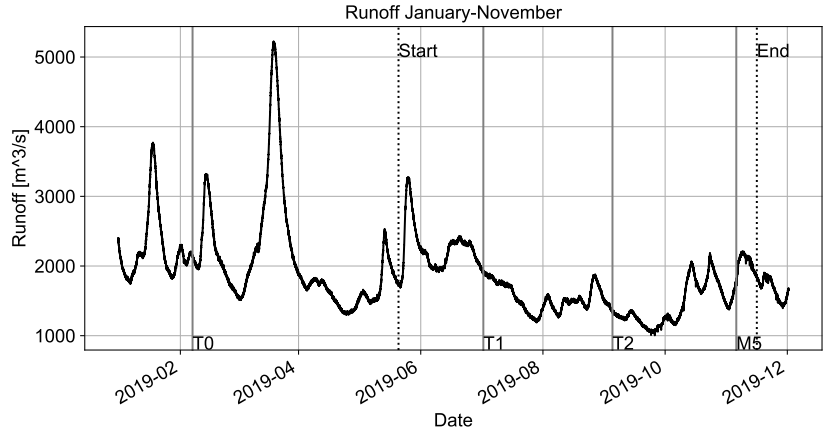

Figure 6.25: The Rhine discharge at Lobith from January 2019 until December 2019, with the lines indicating T_0, T_1 ,T_2 and M_5.

6.3.2. Equilibrium grain size distribution

In this section the grain size distribution found in literature is discussed. From de Nijs [2012], Spanhoff and Verlaan [2000] it is known that the fairway of the Maasmond - Calandkanaal exclusively consists of fine mud particle. The Rotterdam Waterway mainly consists of sand, however with an alternating pattern of silt ranging between 10 to 40 %. This is explained by the dynamics of the salt wedge and ETM, see section 2.2.3.

From Huismans et al. [2013] it is known that D_{50} increases in downstream direction due to a larger portion of sand in the Rotterdam Waterway. When moving downstream sand ($64 - 2000\mu m$) percentages increases from 30 to > 60 %. The amount of silt decreases from 40 % to less than 5 % moving downstream. This is based on grab samples taken in the Rotterdam Waterway and New Meuse in 2004 and 2014, see fig. 6.26. Moreover, one can notice a large range in the distribution of the sediment at the same location. This complicates the definition of an expected amount of silt in the bed compositions.

6.3.3. Sampling grain size distribution

As described earlier, various grab sampling campaigns have been executed prior, during and after the SURICATES pilot study: T_0, T_1 and T_2, see appendix D.1. These samples are taken of the top 30 cm of the bed layer. It is assumed that a change in bed composition can be an indication of additional sedimentation, the sediment disposed in general is fine material.

- T_0: Sampling executed on February 7 and 8 2019 (3.5 months prior to start). Sampling done by grabbers and columns.
- T_1: Sampling executed on July 2 and 3 2019 (1.5 months after start). Sampling done by Grabber.
- T_2: Sampling executed on September 4 2019 (3.5 months after start). Sampling done by Column.

Mohan [2019] characterized the sediment samples to derive the grain size distribution. The locations of the sediment samples are differentiated with respect to the disposal area. With eight locations (*Down 1 - 5*) and (*Extra 1 - 3*) downstream of the disposal site and four locations upstream (*UP 1 - 4*) and four around the disposal site (*DISP 1 - 4*), as shown in fig. 4.3.

Background sediment fluxes

Between T_0 and T_1, 39.000 TDM has been reallocated while the gross sediment flux in the same time is estimated at 1.4 million TDM, see fig. 1.2. Between T_1 and TT_2, 57.000 TDM have been disposed while background fluxes is estimated at 0.57 million TDM. The SURICATES sediment therefore has a significance of 2.8 % and 10 %. It is therefore questionable whether changes in bed sample composition can be related to the execution of the SURICATES pilot study.

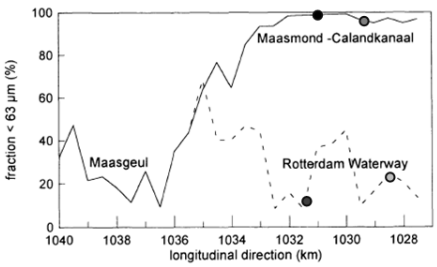

(a) Amount of silt (< 63 μm) in the bed sediment taken in the Maasmond-Calandkanaal and Rotterdam Waterway in June 1992 [Spanhoff and Verlaan, 2000]. Moving right is upstream direction.

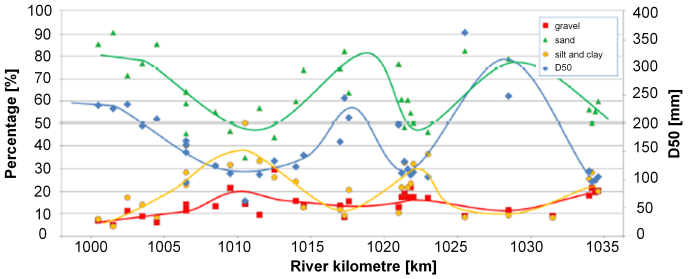

(b) Grain size distribution of bed samples along the Rotterdam Waterway and New Meuse [Huismans et al., 2013]. Moving right is downstream direction.

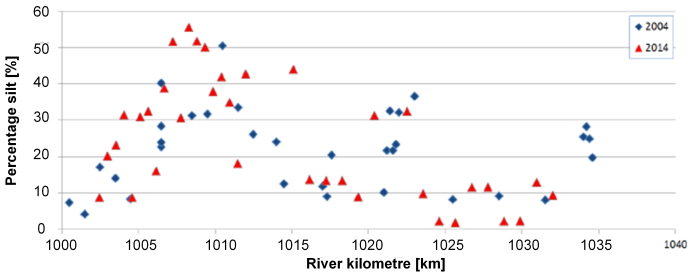

(c) Grain size distribution of bed samples along the Rotterdam Waterway and New Meuse in 2004 and 2014 [Huismans et al., 2013]. Moving right is downstream direction.

Figure 6.26: The grain size distribution of the bed in the Maasmond according to Spanhoff and Verlaan [2000] and in the Rotterdam Waterway according to Huismans et al. [2013]. The dots indicate the locations of the downstream samples. For the river kilometres see fig. A.2.

Downstream of the disposal area

For the downstream locations a distinction is made between the samples taken inside the Rotterdam Waterway; *Down1* and *Down2* and the locations in the Maasmond-Calandkanaal; *Down3* and *Down4*. Both Down1 and Down2 (black and grey dot in fig. 6.26a) are located at the south bank of the Waterway. Down3 is located at the north bank of the Maasmond-Calandkanaal and Down4 at the south bank ((black and grey dot in fig. 6.26a). Down5 is taken in a basin lining the Beerkanaal at the east bank.

	T_0-T_1	T_1-T_2	T_0-T_2
Down1	+++	-	++
Down2	++	- - -	-
Down3	+	-	
Down4	+	+	++
Down5			

Table 6.2: The change in silt content in the different bed samples taken downstream of the disposal location between T_0, T_1 and T_2. A + or - sign is the equivalent of 15 % increase or decrease.

When the results at T_0 are analyzed one would expect results to align with the pattern shown in fig. 6.26a. From fig. 6.26a it is expected that Down3 and Down4 contain exclusively silt fractions. For Down1 and Down2 the opposite is expected. In fig. 6.28 and fig. G.17 one observes comparable silt concentrations at T_0 between Down3 and Down4, however being significantly smaller than > 90%, which is expected according to fig. 6.26a. At Down1 and Down2 results differ significantly between the two locations. In fig. 6.26a a similar pattern is observed, with silt concentrations ranging between 15 % and 40 %.

From the grab samples a change in bed composition can be derived. For *Down1* and *Down2* the silt con-

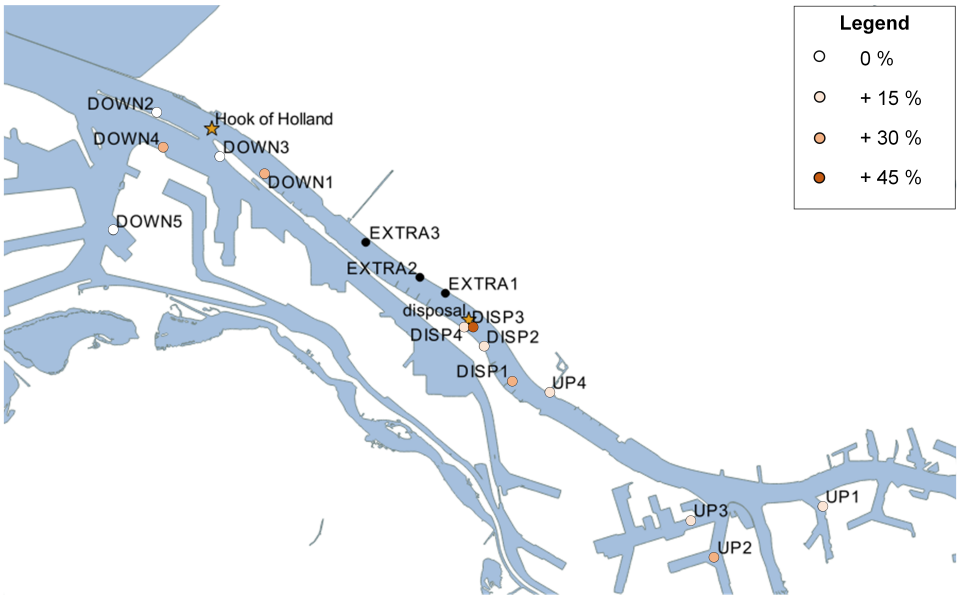

Figure 6.27: The results of the bed sampling campaign, differentiated according to their location with respect to the disposal area. The percentages indicate the change in fine content ($< 63\ \mu m$) between between T_0 and T_2.

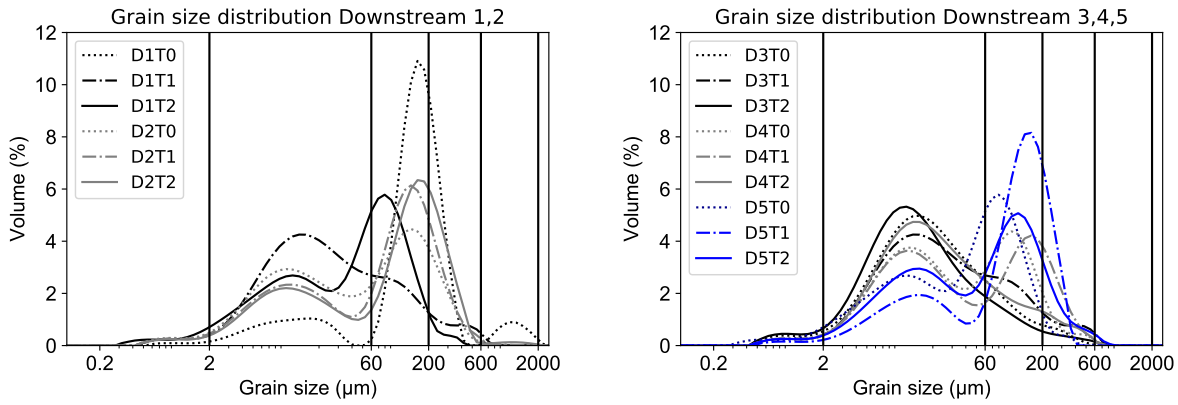

(a) Grain size distribution of bed sample at *'Down1'* and *'Down2'*

(b) Grain size distribution of bed sample at *'Down3'* to *'Down5'*

Figure 6.28: The grain size distributions of the bed samples taken at the downstream locations at T_0, T_1 and T_2.

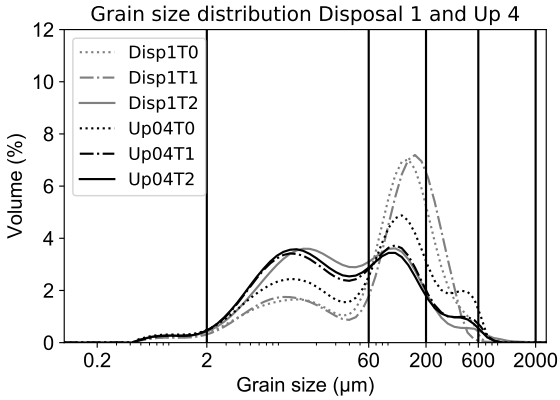

(a) Grain size distribution of bed sample at *'Disp1'* and *'Up04'*

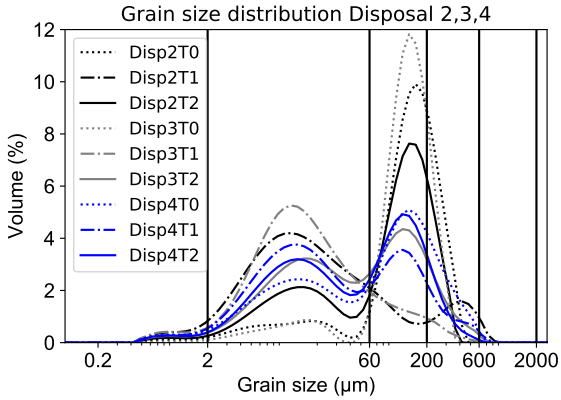

(b) Grain size distribution of bed sample at *'Disp2'* to *'Disp4'*

Figure 6.29: The grain size distributions of the bed samples taken at the locations close to the reallocation area at T_0, T_1 and T_2.

centration in the bed increases between T_0 and T_1 and decreases between T_1 and T_2. However, the effect between T_0 and T_2 is different; for Down1 the total amount of silt has increased whereas for Down2 this has decreased, see table 6.2. Since the initial concentrations for silt differ a lot a part of the explanation may be herein. At T_1 the amount of silt for both Down1 and Down2 is significantly larger than one would expect when compared to fig. 6.26a. This can be attributed to a distortion of the equilibrium due to SURICATES. At T_2 the amount of silt at 'Down1' is still significantly larger than expected. Again this can be an indication of induced sedimentation due to SURICATES. Down3 and Down4 show very similar results with equal concentrations at T_0 and T_1. Only at T_2 the amount of sediment shows the same pattern; an increase in silt between T_0 and T_1 and decreases between T_1 and T_2, Down4, in contrast shows a slightly different pattern with a continuous increase in silt concentration. At last, the concentrations at Down5 remained more or less the same. From de Bruijn [2018] it is known that flow velocities are low to very low at this location. Hence, little sedimentation is expected at this location over time. Therefore, the measurement seem a confirmation of this hypothesis.

In general one can notice a sharp increase in the silt content between T_0 and T_1 and a decrease in the fine and medium sand content. For locations down1 to down4 this change is close to exact. This increase in silt content between T_0 and T_1 ranges between 20% for location 3 to 55% for location 1. Subsequently, between T_1 and T_2 for downstream 1-4 the silt content decreases; 10% to 50%; hence the net effect between T_0 and T_2 is for Down 1, 3 and 4 an increase in the silt content ranging between 10% to 40% is noticeable.

Disposal area

Around the disposal site 4 different samples have been taken; *Disp1 - Disp4.* All these locations are located on the south bank of the Rotterdam Waterway between Rhine kilometer 1020 - 1023.

	T_0-T_1	T_1-T_2	T_0-T_2
Disp1		++	++
Disp2	++++	- - -	+
Disp3	++++	–	+++
Disp4	+	-	+

Table 6.3: The change in silt content for the bed samples taken around the disposal location between T_0, T_1 and T_2. A + or - sign is the equivalent of 15 % increase or decrease.

At T_0 the amount of silt ranges between +- 10 % for *'Disp2'* and *'Disp3'* to 30 and 40 % for *'Disp1'* and *'Disp4'*. In fig. 6.26 one can observe that the amount of silt ranges between 10 to 40 %. Hence all the samples fall within the expected ranges at T_0.

At *'Disp2'* and *'Disp3'* the change in bed composition over time is very similar, with a sharp increase between T_0 and T_1 and a subsequent decrease between T_1 and T_2, see table 6.3. At *'Disp4'* a similar pattern is ob-

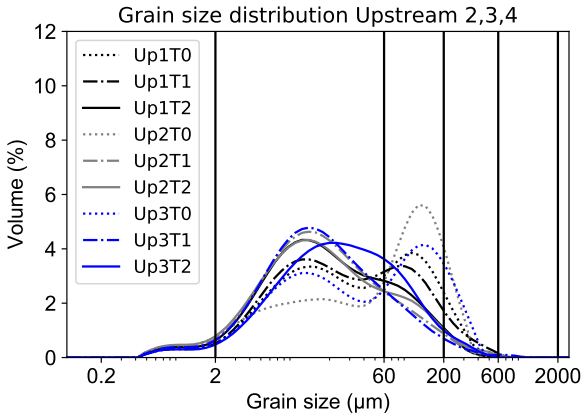

Figure 6.30: The grain size distributions of the bed samples taken at the locations upstream of the reallocation area at T_0, T_1 and T_2.

served, however to a smaller extent. Overall; all samples show a decrease in sand fractions and increase in silt between T_0 and T_2. This increase in silt is strongest at location *'Disp3'*. At T_2 all locations contain a larger amount of silt than one would expect based on the samples shown in fig. 6.26c. This could be an indication of induced sedimentation at the south bank of the disposal site.

Upstream of the disposal area

	T_0-T_1	T_1-T_2	T_0-T_2
Up1		+	+
Up2	++		++
Up3	++		+
Up4	+		+

Table 6.4: The change in silt content for the bed samples taken upstream of the disposal location between T_0, T_1 and T_2. A + or - sign is the equivalent of 15 % increase or decrease.

The four upstream locations; *'UP1'* to *'UP4'* are located inside the harbour basins lining the Rotterdam Waterway; the first Petroleum harbour (*'UP1'*), the Botlek (*'UP2'* and *'UP3'*) and the last one in Maassluis *'UP4'*.

At T_0 the amount of silt between the basins ranges between +- 40 % for *'UP2'* and *'UP4'* to +- 60 % for *'UP1'* and 50 % for *'UP3'*. These samples are all slightly coarser than the samples collected from the dredging locations more upstream, which is in line with fig. 6.26c and also slightly coarser than the samples taken from the Waalhaven and Eemhaven, see appendix G.3.1.

All locations show an increase of silt between T_0 and T_1 and between T_0 and T_2, see table 6.4. Which can be a clear indication for increased sedimentation in the upstream basins. However, it should be taken into account that the samples taken inside the basins can be largely influenced by the dredging activities executed inside the basin or the settling of other sediment.

Conclusion

The majority of the grab samples show an increase in the fraction silt. The samples taken outside the harbour basins are assumed to be in equilibrium as no human interference takes place at these locations. Therefore the increase of silt can be related to either the hydrodynamic forcing or due to SURICATES disposal.

As can be seen in fig. 6.26a and fig. 6.26c the amount of silt is subject to significant ranges under the same circumstances in the Rotterdam Waterway. Therefore a certain change in composition of the bed is within the expected range which limits the applicability of using the grab samples as evidence for increased sedimentation.

6.4. Summary

In this chapter the results of the measurement campaigns, focusing on the short and long term behaviour of the SURICATES sediment plumes, are discussed to answer the following research question:

How is the reallocated sediment distributed in time and space on different time and spatial scales?

When the short term measurement surveys are considered it appears that most sediment is spread around and below the pycnocline after disposal by bow coupling. This is in line with the expected near field behaviour as discussed in section 3.2. In the mid field, no sediment peaks are found above the pycnocline, advocating the assumption of SPM raining out above the pycnocline. However, measuring the mid field behaviour has been complicated by the dilution of the sediment plume signal with respect to the background concentration and due to measurement bias caused by the frame of reference.

From the long term measurements, indications for increased sedimentation around the disposal location and upstream of the disposal can be found. However, it is stressed that these observations are indications. First of all, the composition of the bed in the Rotterdam Waterway varies strongly in time and space. Next to this, the largest changes in bed composition are found between T_0 and T_1, while the SURICATES pilot study only has a contribution of 3 % to the total sediment fluxes between these two sampling dates. Therefore, variations in bed composition are likely to be driven by other processes than the execution of the pilot study.

At first, the short term behaviour of the sediment plume behaviour is discussed, based on two measurement surveys: September 11 and November 5. The governing hydrodynamics differ slightly between the two days, affecting the mid field and far field behaviour. September 11 is during average tidal conditions, while November 5 is one day after neap tide. River discharges for September 11 are considered to be very low (1300 m^3/s) and low for November 5 (1700 m^3/s), since the yearly average discharge equals 2200 m^3/s. A low discharge is related to a reduced lock exchange mechanism, a smaller supply of fluvial sediment from upstream and with a larger intrusion length of the salt wedge. November 5 is preceded by a very stormy day (10 Beaufort), mixing the Rhine-ROFI and Rotterdam Waterway, whereas September 11 is preceded by days with average wind conditions (5 Beaufort).

Since the surveys are executed over a limited range of time and space, the applicability is limited to the understanding of near and mid field behaviour. From the measurement 1 - 8 (Sep 11.) the same near field behaviour as in section 3.2 is found. Initially the plume spreads over a depth of 2 to 6 meters. The same is found for the measurements 8 - 12 taken on November 5, in the vicinity of the vessel. Subsequently, the plume sinks further, with increasing concentrations towards the bed. In the measurement 9, the peak of SPM is found at a depth of 8 to 10 m, which approves the hypothesis of sediment plume advection at mid depth. As the this measurement lack SPM above the pycnocline, it is assumed that the water column above the pycnocline is cleared from SPM, which is confirmed using the predicted advection based on the flow velocities. In contrast, for measurements 13 - 16 at November 5 very small concentrations of SPM are found above the pycnocline. However, as these measurements are taken at a certain distance and time from the disposal site, differential advection has introduced bias in this measurement.

As time passes it is likely that the plume has dispersed significantly in space. Therefore, the signal of the plume can not be distinguished from the background sediment. However, in subsequent measurements, peak values are found close to the bed, e.g. measurement 35 - 38 and 46. Based on the measured flow velocities, see table G.4, it is hypothesised where the sediment plume might be located at different times. From this estimation, it is found that the measurement 35 - 38 and 46 can be caused by the advection of the sediment plume close to the bed. But from fig. 2.11, it is known that the concentration of SPM, due to the advection of the salt wedge can vary significantly in time and space close to the bed.

The largest challenge while processing the measurements is the lack of data from an Eulerian frame of reference. It is therefore strongly recommended to include fixed measurement stations for the following cam-

paign. A fixed measurement station is excluded from bias in the measurements induced by the travelling velocity of the vessel. Moreover, at approximately 1 km from the dredging vessel most near field effects have worked out. Therefore an accurate estimation for the source term can be made [de Wit, 2015].

At last, the long term measurement campaign, using two different surveys is assessed. Throughout the measurement campaign bed samples are taken at three distinct times, T_0 three months prior to the start of the experiment, and two during the pilot study T_1 and T_2. As mainly fine material is disposed, an increase in silt content in the bed samples can be caused by the SURICATES pilot study. The majority of the grab samples show an increase in the amount of fine particles ($< 63\mu m$). However, the amount of silt in the Rotterdam Waterway varies strongly in time and space. Next to this, the SURICATES sediment pilot study has a small significance of 2.8 % and 10 % between the sampling dates, in comparison to the background sediment fluxes. It is therefore questionable whether changes in the composition of the bed can be related to the execution of the SURICATES pilot study.

7

Model results

In the following chapter the results of short term and long term model hindcast are shown and discussed. At first the hydrodynamic validation is discussed. This is done based on literature, measurements from the fixed stations and the measurements done at November 5. Subsequently the results of the short term and long term sediment model hindcast are discussed. These results are interpreted and validated based on the expected plume behaviour. Next to this, the short term and long term results are compared with the results from the measurement campaigns. At last it is discussed to what extent the models are capable to reproduce the expected and measured sediment distribution.

7.1. Introduction

In the following chapter the results of the short term and long term model hindcasts are shown, validated and discussed. The short model runs are based on the disposal executed on November 5 to understand the initial behaviour of a sediment plume during a single tidal cycle. The long term hindcast is done to model the behaviour over the complete course of the pilot study. The set-up of these models is discussed in the chapter 5, as well as the underlying assumptions and simplifications. In this chapter at first the hydrodynamic validation is discussed. Several studies have been carried out to assess the performance of the operational hydrodynamic models. These results and the implication for the modelling of SPM is determined. Next to this, the hydrodynamics of the model input are verified by comparing the model output to the measurement stations in the port of Rottedam. For November 5, a comparison between the salinity measurements obtained with the silt profiler measurements and model output is included as well.

In the short term modelling results, section 7.3, the measurement survey of November 5 is hindcasted. Moreover, a sensitivity analysis is carried out to derive the influence of a variation in disposal method, time of disposal and material disposed. This sensitivity analysis reflects on uncertainties in the model set-up, such as the coarseness of the material, but also on parameters that have been varied over the course of the pilot study. Next to the sensitivity analysis a comparison between the model and silt profiler measurements is made.

In section 7.6, the results of the long term model hindcast are presented. This chapter is closed with a discussion on the last (sub-)research question; *To what extent can current models reproduce the sediment distribution as found in the data analysis?*.

7.2. Hydrodynamic validation

As the hydrodynamics are the main forcing for sediment behaviour, it is important to understand and acknowledge the limitations of the hydrodynamic modelling. Over time, various studies have been performed to determine the accuracy of the operational hydrodynamic models. The hydrodynamics in the area of interest are governed by the following parameters; river discharge, tide, wind (direction and strength), wind

set-up and offshore wave height. The hydrodynamic model might perform differently under different hydrodynamic conditions. Therefore, the effects of different hydrodynamic conditions on the model accuracy are discussed. The effect of the hydrodynamic parameters is summarized below;

- **Wind**: Wind increases mixing over the vertical and set-up on the North Sea. Storms may lead to a well-mixed state in Rhine ROFI.
- **Tide**: During spring tide the Rotterdam Waterway is well-mixed, while during neap tide, conditions can be stratified. Moreover, the salt wedge extends further landward during spring tide than neap tide.
- **Discharge**: Low discharge events lead to a larger intrusion length of the salt wedge. Moreover, residual bed currents are reduced due to weaker lock-exchange mechanism.

The hydrodynamic model is validated by Kranenburg [2015], Rotsaert [2010] for the hydrodynamic conditions mentioned in table 7.1. Both the short term model set-up (neap tide, low discharge, large set-up) as the long term hydrodynamics (neap, average and spring tide, average discharge conditions and little set-up) are validated.

Discharge	**Tide**		
	Neap	Average	Spring
Low	Large set-up [a]	-	-
Average [b]	Little set-up	Both	Little set-up
High	Little set-up	Both	Large set-up

Table 7.1: The hydrodynamic conditions for the validation of the OSR model

[a] Nov 5.
[b] Aug. 30 - Sep. 13

7.2.1. Salinity

Kranenburg [2015] compared the performance of the OSR-model with measuring stations and mobile measurements. From this study is concluded that in general salinity time series for measurement stations upstream and high in the water column perform best. Moreover, from vertical distributions of salinity, is concluded that stratification and salinity in general are underestimated. As stratification is underestimated, turbulence damping is underestimated as well. As effect, sediment distribution close to the bed is underestimated and above the pycnocline overestimated.

As part of the SURICATES study, the hydrodynamics of the Rotterdam Waterway and performance of the models are investigated by Geraeds [2020] based on a measurement campaign on August 13, 2019. In this thesis, the overestimation of the pycnocline height and underestimation of the intrusion length of the salt wedge are observed as well.

de Nijs and Pietrzak [2012] also observed the aforementioned deficiencies in the salinity reproduction. This overprediction leads to an inaccuracy in the reproduction of the baroclinic pressure gradient and hence the local shear. Nevertheless, the governing trapping mechanism of fluvial sediment raining out above the pycnocline is well represented in the model.

7.2.2. Water level and flow velocity

In Rotsaert and Collard [2009] the predictive capabilities of the OSR model for the water levels and flow velocities are investigated. It must be noted that this validation is written prior to the construction of Maasvlakte 2 and the deepening of the Rotterdam Waterway, (see appendix A.1). Also the model uses a smaller vertical resolution (8 σ-layers instead of 10).

The water level is validated using four measuring stations along the Rotterdam Waterway and New Meuse, being Hook of Holland, Maassluis, Vlaardingen and Rotterdam (from West to East), see fig. 7.1. The water level is validated under a wide range of variable parameters (tide, set-up and run-off), as sown in table 7.1.

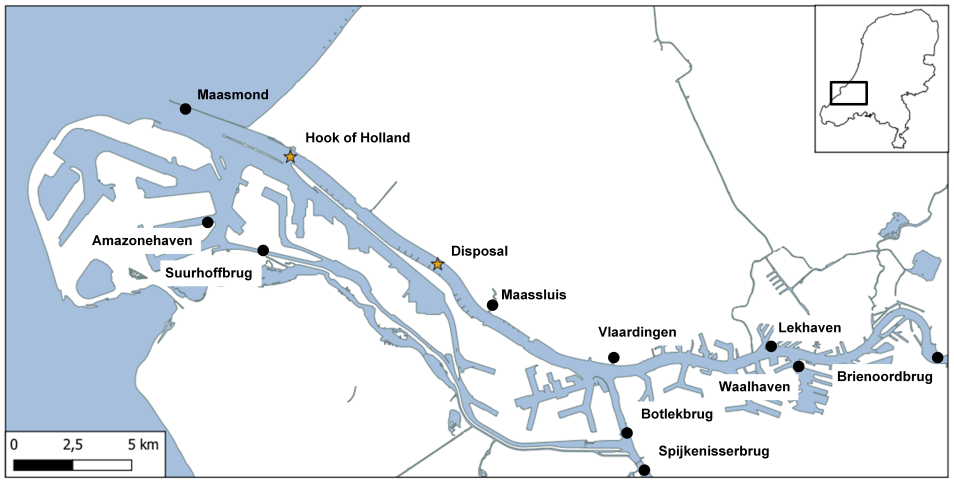

Figure 7.1: A map with the location of the fixed measurement stations

It is concluded that water levels are a little under predicted. The largest differences arise during neap-tide, for low and average discharge conditions during calm weather and stormy weather. Moreover, for all storm conditions the water level is underpredicted. In general, the accuracy of the predicted water level decreases moving eastwards.

The flow velocity is validated at the Maasmond, Amazonehaven, Suurhoffbrug, Botlekbrug, Spijkenisserbrug and Waalhaven, see fig. 7.1. In general, differences are largest under storm conditions. However, for all stations the average difference is only 0 - 3 cm/s (3 %). The standard deviation is approximately 15 cm/s for all stations but can increase to 37 cm/s for some stations under storm conditions.

7.3. Short term hydrodynamic validation

In the following section the hydrodynamic model results from November 5, 2019 are compared with the mobile measurements taken on the same day and the fixed measurement stations.

Based on the comparison of the moving measurements to the silt profiler measurements a consistent underprediction of the salinity is observed. In the model, the pycnocline seems to be located deeper in the water column than for the measurements. This might place the sediment release by bow coupling artificially above the pycnocline instead of below.

7.3.1. Fixed measurement stations

In the following section the hydrodynamics are validated based on the fixed measuring stations at Hook of Holland (-2.5 m NAP), Lekhaven (-2.5 m, -5 m, -7.0 m NAP) and Spijkenisserbrug (-2.5 m, -4.5 m, -9.0 m NAP). To do so, time series of water level and salinity are compared. In fig. 7.1 the location of the measurement stations within the port is shown.

Salinity

From the model-measurement comparison on November 5 in general a very good agreement can be noticed. Moreover, it is observed that only for the Spijkenisserbrug, fig. H.6 a consistent overestimation of the salinity can be observed. The accuracy in the salinity distribution decreases moving further from the North Sea. For the other measurement stations, Hook of Holland, fig. H.1 and Lekhaven, fig. H.2 a minor underestimation of the salinity seems to appear during ebb and an overestimation during flood.

Water level

In appendix H.1.2 the modelled water level is compared with the measured water level at the three measuring stations along the Rotterdam Waterway (Hook of Holland, Maassluis and Vlaardingen). In general it can be

concluded that the water level prediction is very good and consistent in time. Only around HW and LW small discrepancies occur, especially at Vlaardingen. Moreover, the tidal asymmetry is evident with HW at 8:10, 8:30 and 9:00 and LW at 14:40, 14:50 and 15:20, at Hook of Holland, Maassluis and Vlaardingen. This is in line with the conclusions drawn by Rotsaert and Collard [2009].

7.3.2. Moving measurements

Apart from the fixed measurements stations, the vertical distribution of the salinity is compared to the silt profiler measurements, 1 - 50. In general the model underestimates the salinity and pycnocline height based on the moving measurements. Only around LWS, (measurement 39 - 44, see appendix H.1.3) the salinity is overestimated by the model. In this section only the salinity reproduction during the disposal is discussed, for the other results the reader is referred to appendix H.1.3.

Period II: 11:00 - 13:00 Ebb

The second period covers all the measurements taken while following the plume, and are therefore taken during ebb. Again the height of the pycnocline is overestimated in the model, i.e. the pycnocline stretches 2.5 m deeper than the measurements. This also causes large differences in the measured and modelled value. Due to this difference in height of the pycnocline, the sediment disposal placed halfway the water column may be placed artificially above the pycnocline, instead of below. The accuracy increases with the tide; measurements 12 to 16 show smaller differences between the measured and modelled value. At the surface and around the bed the difference is limited to 2 PSU.

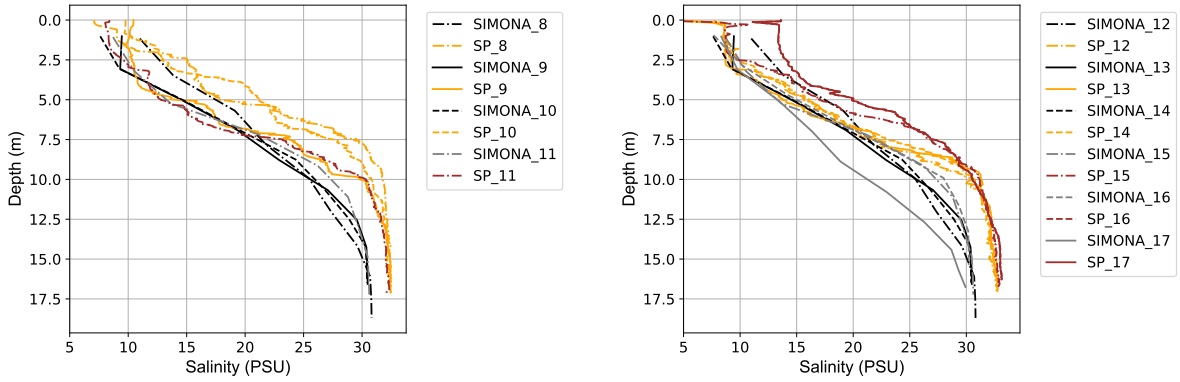

(a) (b)

Figure 7.2: Comparison of SIMONA output and Silt profiler measurement 8 - 17, taken during disposal. *'SP'* refers to the measured salinity by the silt profiler which is an average value of upcast and downcast.

7.4. Short term model results

In the following section the sediment model results of the November 5 hindcast are discussed. This is done to understand how a single disposal behaves in the model, which is also compared with the measurements done on November 5. Over the execution of the SURICATES pilot study there has been a variation in the execution of the disposals. As mentioned in section 3.1.1, there has been a variation in time of disposal (with respect to HWS), sediment source and disposal method. To understand the effect of the variation in these parameters on the initial to mid field behaviour of the plume a sensitivity analysis is carried out at first.

7.4.1. Sensitivity analysis

In the following sensitivity analysis the variation in time of disposal, sediment source and disposal method is investigated. A variation in the execution method is circumvented in the model simulation by altering the rate and depth of disposal. The sediment source is varied by the changing the distribution of the grain sizes and the time of disposal with respect to HWS has also been varied. From the sensitivity analysis the effect

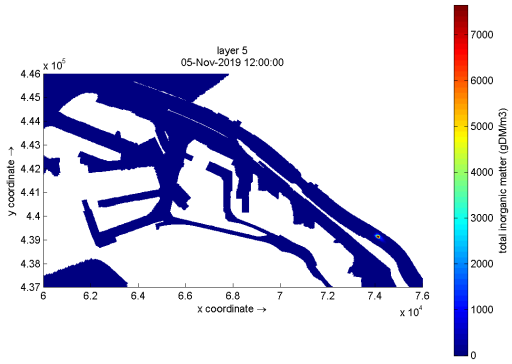

(a) Sediment plume at 12:00

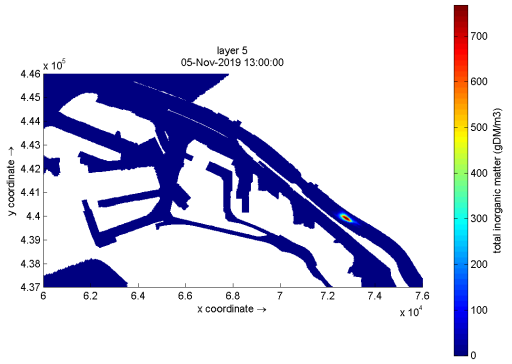

(b) Sediment plume at 13:00

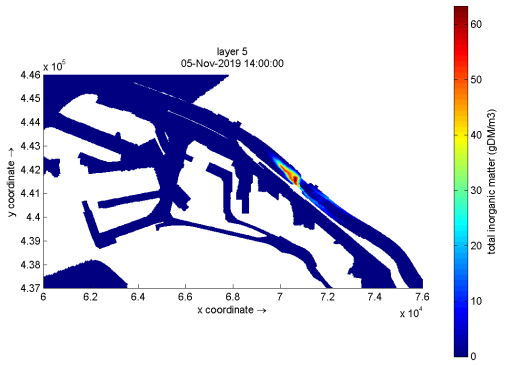

(c) Sediment plume at 14:00

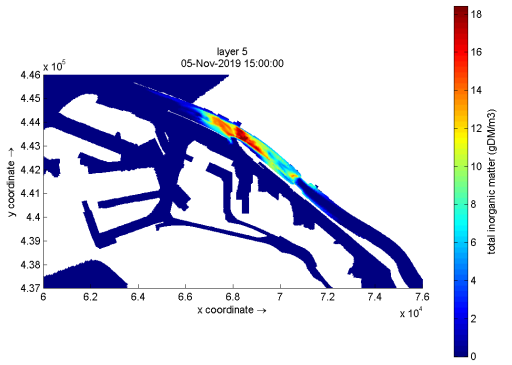

(d) Sediment plume at 15:00

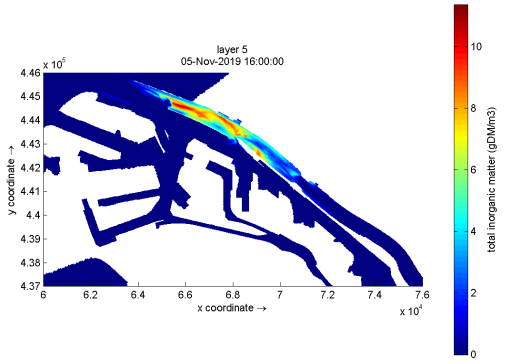

(e) Sediment plume at 16:00

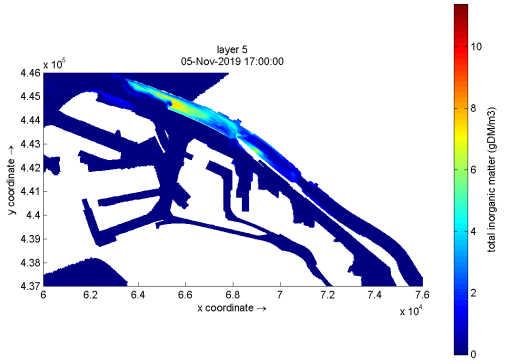

(f) Sediment plume at 17:00

Figure 7.3: The initial behaviour of the sediment plume in the fifth layer when it is disposed in the fifth layer according to the model, during the first five hours after release. The unit for the concentration gDM/m^3 is equivalent to $10^-3 g/l$.

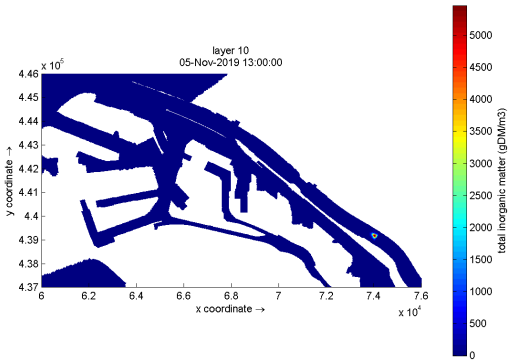

(a) Sediment plume at 13:00

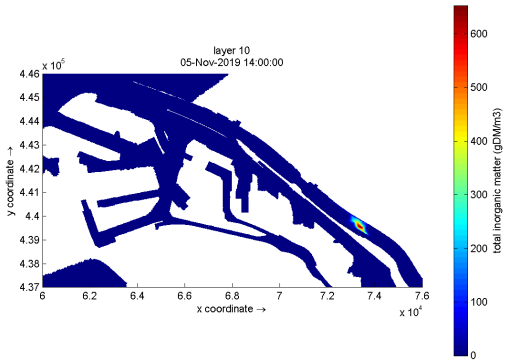

(b) Sediment plume at 14:00

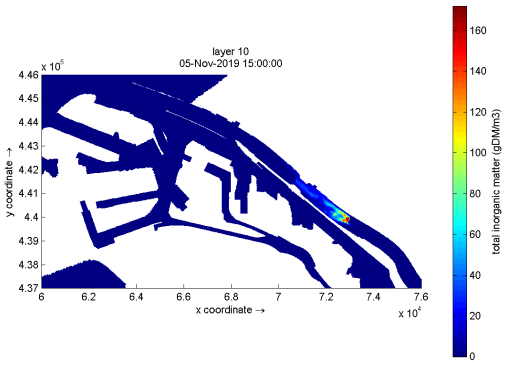

(c) Sediment plume at 15:00

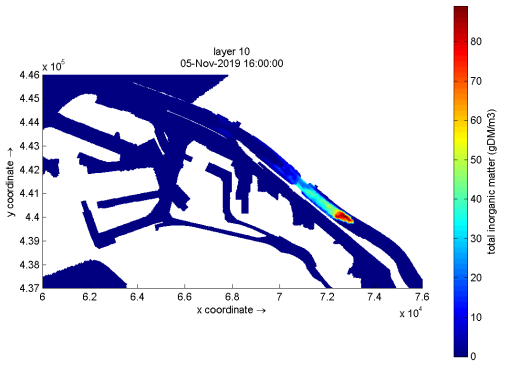

(d) Sediment plume at 16:00

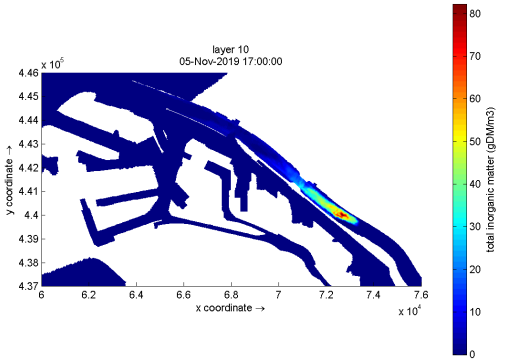

(e) Sediment plume at 17:00

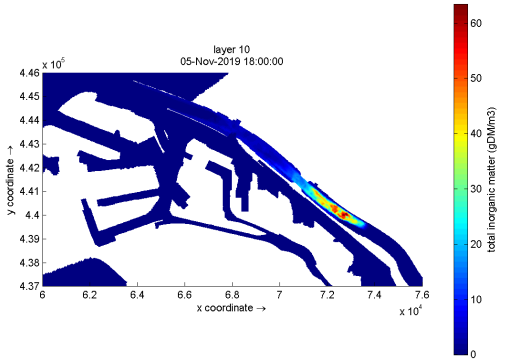

(f) Sediment plume at 18:00

Figure 7.4: The initial behaviour of the sediment plume in the tenth layer when it is disposed in the tenth layer according to the model, during the first five hours after release. The unit for the concentration gDM/m^3 is equivalent to $10^-3 g/l$.

of each of these parameters can be derived, to quantify an uncertainty or quantify a variation in the pilot execution. The sensitivity to each of the parameters is derived by changing them with respect to a base case.

In this research the base case is defined to represent the most common disposal, which is a disposal by bottom door release, with sediment from the harbour basins and disposed 0.5h after HWS. *November 5*, is the set of parameters most representative for the disposal carried out at November 5 and subject of the data analysis carried out at section 7.3. In fig. 7.3 and fig. 7.4 the short term behaviour, according to the model is shown for the *November 5* disposal and the *base case* disposal. This difference is further quantified in table 7.2. It can be observed that the behaviour of the two disposals is different, stressing the importance of this sensitivity analysis to derive the parameters driving this difference in behaviour.

	Maasmond				**Disposal Area**			
	RWW in & out	RWW - Beer	NS net.	NS flux	Ups.	Down.	Susp.	Settle
Base case	11%	7%	13%	13%	18%	41%	5%	39%
Base Nov. 5	13%	10%	23%	14%	9%	57%	4%	20%

Table 7.2: The sediment fluxes for the base case disposal and the November 5 disposal at the borders of interest, in correspondence with the behaviour shown in fig. 7.3 and fig. 7.4.

In table 7.3 the different models runs are defined. As can be seen, three parameters differ between the *Base case* and *November 5*, therefore the effect of each parameter is investigated by isolating them. '*Grain size*' represents a variation in the grain size, '*Layer*' represents the effect of a disposal in a different part of the water column, *Timing* represents the effect of an earlier or later disposal, with respect to depth averaged HWS. At last, the effect of the duration, *'Duration*' of the disposal is investigated.

The sensitivity to the parameters is quantified using mass balances of two areas shown in fig. 7.5. A mass balance of the Maasmond is used to determine the outgoing gross and net flux to the North Sea and a mass balance of the disposal area is used to determine the initial efficiency of the disposal.

'RWW in & out' is the amount of sediment returned into the Rotterdam Waterway after it has flown into the Maasmond, *'RWW - Beer'* is the total amount of sediment flowing out the Rotterdam Waterway into the Beerkanaal, *'NS net.'* is the percentage of the total amount of disposed sediment that flows into the North Sea and *'NS flux'* is the percentage of sediment returned into the Maasmond after it has flown into the North Sea.

'Ups.' is the percentage of the total amount of sediment disposed flowing upstream from the disposal area and *'Down.'* is the percentage of the total amount of sediment disposed flowing downstream of the disposal area. *'Susp.'* is the amount of sediment that remains in suspension inside the area of disposal and *'Settle'* is the amount of sediment that has settled on the bed inside the disposal area.

	Base case		**Grain size**	**Layer**		**Timing**		**Duration**
	Base	05 Nov.	Coarse	Surface	Mid	Earlier	Later	
Time	0.5 h	0.5 h	0.5 h	0.5 h	0.5 h	*-0.5 h*	*1.5 h*	0.5h
Duration	4 min	50 min	4 min	4 min	4 min	4 min	4 min	*50 min*
Layer	lay 10	lay 5	lay 10	*lay 1*	*lay 5*	lay 10	lay 10	lay 10
Grain size								
IM1	1 μm	1 μm	*15* μm	1 μm	1 μm	1 μm	1 μm	1 μm
IM2	15 μm	15 μm	*34* μm	15 μm	15 μm	15 μm	15 μm	15 μm
IM3	34 μm	34μm	*63* μm	34 μm	34 μm	34 μm	34 μm	34 μm

Table 7.3: An overview of the parameter variation in the sensitivity analysis. *'Grain Size'* refers to the compisition of the sediment disposal, *'Layer'* refers to the layer of disposal implementation, *'Timing'* refers to the amount of time after HWS at Maassluis and *'Duration'* refers to the duration of the disposal. The parameter changed with respect to the base case is printer in *italics*.

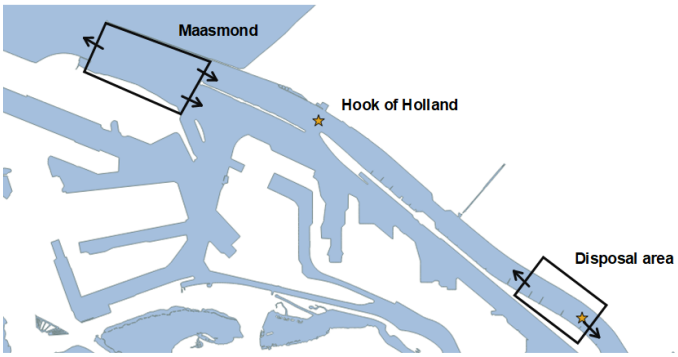

Figure 7.5: An overview of the two balance areas with its fluxes. The Maasmond has a sediment flux with the Rotterdam Waterway (north east) and Beerkanaal (south-east) and the North Sea (west). The disposal area has sediment fluxes dowstream (west) and upstream (east)

Grain size sensitivity

As discussed in section 5.4.2 the exact composition of the different disposals is not measured and hence unknown. Currently the composition of the barge is based on Stutterheim [2002], grab samples taken prior to the start of the SURICATES pilot study and previous studies. It is chosen to be consistent with previous studies and use the same grain sizes as used by e.g. de Groot [2018], Vijverberg et al. [2015].

In table 7.4 a mass balance of the grain sizes ranging from 1 μm to 63 μm is shown. It is found that particles with a grain size of 1μm do not settle. Only 2% of the particles with a grain size of 15 μm settles in the disposal area. For coarser particles this increases, for 34 μm 86 % settles and for 63 μm this equals 98 %. Hence, particles larger than 34 μm are barely in suspension. This is in contrast to the silt profiler measurements, where is observed that initially particles remain in suspension.

Therefore, it can be concluded that the difference in size for IM3 (63 μm or 34 μm) is not that significant, but rather the size of IM1 (1 μm or 15 μm) and IM2 (15 μm or 34 μm). This explains the large difference between the results for the *'Base case'* and *'Coarse'*.

	Maasmond				**Disposal Area**			
	RWW in & out	RWW - Beer	NS net.	NS flux	Ups.	Down.	Susp.	Settle
1 μm	8%	6%	33%	11%	26%	67%	7%	0%
15 μm	12%	7%	25%	13%	30%	60%	8%	2%
34 μm	28%	16%	0%	37%	4%	16%	1%	79%
63 μm	17%	4%	0%	70%	3%	0%	0%	97%

Table 7.4: The sediment fluxes for a varying grain size.

Sensitivity layer of disposal

As explained in section 3.1.1 two different methods of disposal have been applied over the course of the SURICATES pilot study: bow coupling and bottom door release. A bottom door release and bow coupling release have a different depth of disposal and rate of disposal. The effect of the layer of disposal is discussed in this paragraph, the disposal rate has no influence on the sediment fluxes, see appendix H.1.4.

A bottom door release is interpreted as a density dominated sediment plume sinking immediately to the bed / close to the bed. Therefore, the base case has a disposal in the lowest layer close to the bed. This is in line with the modelling assumption done by Vijverberg et al. [2015], who allocated bottom door disposals in the layer closest to the bed as well.

The disposal by bow coupling is surrounded by more uncertainties and near field effects and is therefore harder to accurately include in the model. From de Wit [2015] and the measurements it is interpreted that the sediment plume disperses quickly over the depth. In section 5.4.2 is shown that a disposal halfway the

water column (σ-layer 5) is more in line with measurement observations than a disposal in the surface layer (σ-layer 1).

In line with the previous analyses two balances are established; a mass balance of the Maasmond and a mass balance of the disposal area. For the Maasmond it is clear and as expected that for a sediment plume placed higher in the water column, the net flux towards the North Sea is larger. The reason for this is twofold, flow velocities are larger in the upper part of the water column. This second reason is more evident when considering the balance of the disposal area. As 39 % of the amount of sediment disposed settles in the 10 hours after disposal when placed in the bed layer. When *'Surface'* and *'Halfway'* are compared, the difference in flux towards the North Sea is interesting, especially considering the small difference in downstream flowing sediment from the disposal area. In other words, when the sediment is placed halfway the water column, a larger portion of the sediment is located between the Maasmond and the disposal area. Whereas for a surface disposal the majority flows into the North Sea. For the base case, the majority of the sediment settles in the disposal area or flows upstream.

	Maasmond				**Disposal Area**			
	RWW in & out	RWW - Beer	NS net.	NS flux	Ups.	Down.	Susp.	Settle
Surface	8%	8%	59%	13%	1%	98%	1%	0%
Halfway	14%	12%	25%	15%	5%	88%	4%	3%
Base case	11%	7%	13%	13%	18%	41%	5%	39%

Table 7.5: The sediment fluxes for a disposal in the surface layer (layer 1), halfway the water column (layer 5) and the base case disposal (layer 10).

The effect in the mass balances can be explained when the plume advection is compared from an Eulerian perspective. In fig. H.30c the total amount of SPM passing Hook of Holland is observed for a disposal halfway the water column. From this figure the amount of differential advection is significant. The plume advected close to the bed is delayed with one hour compared to the plume advected halfway the water column.

Sensitivity time of disposal

According to model simulations done prior to the execution the most efficient time for disposal is approximately 0.5 hours to 1 hours after predicted depth-averaged High Water Slack (HWS) at Maassluis (PortofRotterdam [2018]). However, as shown in table 3.1 there has been a wide variety in the time of disposal with respect to HWS. As discussed in chapter 3, down estuary flow velocities are larger and the pycnocline lower during a later disposal and therefore it is expected that less particles settle inside the disposal area or flow upstream for a later disposal.

	Maasmond				**Disposal Area**			
	RWW in & out	RWW - Beer	NS net.	NS flux	Ups.	Down.	Susp.	Settle
-1 h	7%	10%	15%	12%	17%	37%	4%	45%
Base case	11%	7%	13%	15%	18%	41%	5%	39%
+ 1 h	7%	12%	9%	13%	20%	47%	5%	30%

Table 7.6: The sediment fluxes for a disposal 1.5 hour prior to HWS (- 1 h), half an hour after HWS (base case) and 1.5 hour after HWS (+ 1 h).

From table 7.5 a few interesting observations can be made. A later disposal leads to less settling inside the disposal area and a larger flux in the downstream and upstream direction, explained by higher flow velocities during disposal. However, when the flux towards the North Sea is considered, an early disposal is advantageous.

In short, for a later disposal more sediment settles or remains in suspension in an area between the Maasmond and the disposal area. When the outgoing flux of the disposal area is considered, an early disposal is advantageous. In section 3.4 it is hypothesised that the majority of the settled sediment remains in the system. Therefore, late disposals are considered to be most advantageous.

	Maasmond				Disposal Area			
	RWW in & out	RWW - Beer	NS net.	NS flux	Ups.	Down.	Susp.	Settle
Early-bed	7%	10%	15%	12%	17%	37%	4%	45%
Base case	7%	11%	13%	13%	18%	41%	5%	39%
Late-bed	7%	12%	9%	16%	20%	47%	5%	30%
Middle-early	11%	13%	24%	14%	7%	71%	4%	18%
Middle-base	14%	12%	25%	15%	5%	88%	4%	3%
Middle-late	15%	12%	22%	14%	3%	92 %	3%	2%

Table 7.7: The sediment fluxes for a combination of a variation in 1) layer of disposal: *bed* is layer 10 and *middle* is layer 5, and 2) time of disposal *early* is 1.5 hour prior to HWS, *base* is half an hour after HWS and *late* is 1.5 hour after HWS.

However, there is the possibility of a correlation between time of disposal and depth of disposal, i.e. an late disposal can be disadvantageous when combined with bow coupling, due to the location of the salt wedge.

As can be seen in table 7.7 the effect of the time of disposal is larger for disposals executed halfway (bow-coupling) the water column than for disposals close to the bed.

Conclusion sensitivity analysis

From the sensitivity analysis it is concluded that the layer of disposal has the largest influence. The other observations are summarized as following:

- The layer of disposal and thus the method of disposal, has the largest influence on the sediment fluxes, both the up and downstream fluxes at the disposal area as well as the outgoing flux towards the North Sea. Both these fluxes are twice as large for a disposal halfway the water column than in the bed layer.
- The assumed composition or grain sizes used also has a large influence. However, the correct implementation is subject to calibration.
- The timing of disposal has quite a significant in influence on the net fluxes, an early disposal has 50 % more outgoing flux at the North Sea than a late disposal. However, the amount of settled particles is also 50 % larger for an early disposal. Therefore, the time of disposal mainly determines where particles settle.
- The combined effect of a late disposal and using the bow coupling technique has the largest influence on reducing the amount of settling in the disposal area. This is explained using the advection of the salt wedge and the development of the ebb flow.

7.4.2. Short term model - measurement comparison

In the following section some modelling results are compared with the silt profiler measurements of November 5. The values of *November 5*, shown in table 7.3 are used as model settings.

In both the measurements taken at September 11 and November 5 significant dilution of the SPM concentrations is observed. This dilution complicates the distinction between background concentrations and plume induced sediment concentrations. Since the model lacks background concentrations of sediment, one-on-one comparison of the model and measurements cannot be done. Therefore, it is compared whether the signal, a peak in SPM concentration, in the silt profiler measurements and model results is consistent. The analysis will be split in the initial measurements taken during disposal (near field) and the measurements taken while sailing downstream (mid field).

Measurements 8 to 17

The measurements 8 to 12 are taken in the vicinity of the vessel during disposal. It is interesting to notice that the concentrations found in the model are twice as large as these found in the measurements. The largest concentrations measured by the silt profiler reaches 0.28 g/l, which is at least twice as small as the peak values

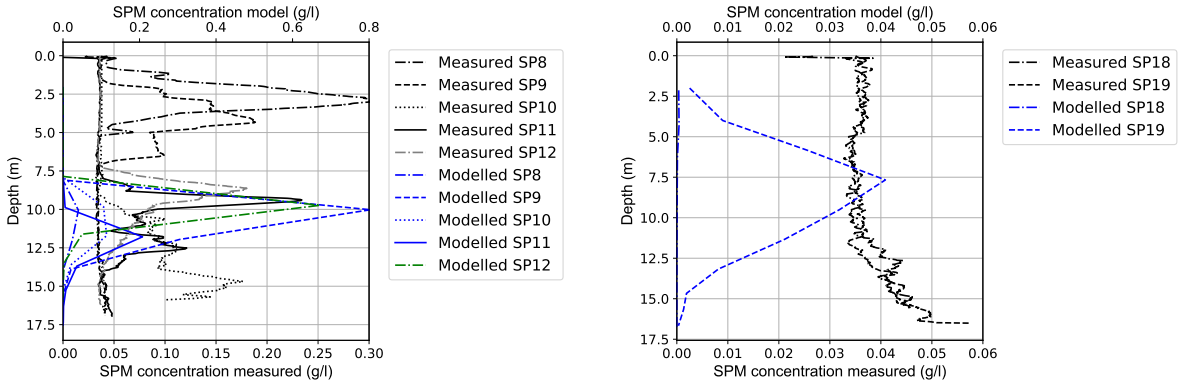

(a) Model - measurement comparison at silt profiler measurement 8 - 12

(b) Model - measurement comparison at silt profiler measurement 18 - 19

Figure 7.6: Model results and measurement results at location and time of silt profiler measurements. The location and time of the vertical profiles agrees with the location and time of the measurement shown in chapter 6.

found during the silt profiler measurements. Moreover, the amount of dispersion in the measurements seems larger than in the model simulations: peak concentrations are 'smeared' over depth instead of returning a single peak value.

The results of the model results 8 - 12 differ a lot. This stresses the importance of the timing of the measurements, an early or late measurements may lead to a misinterpretation of the measurements.

The results of the measurements 13 - 18, see fig. H.28 only contain very limited amounts of sediment ($\mathcal{O} < 0.01 g/l$. This does not agree with the measurements taken by the silt profiler. This is probably caused by the measurements taken too early, as shown in fig. 6.17a.

Measurements 30 - 38

In fig. 6.20 it can be observed, although taken close and after each other, that the peak concentrations vary a factor 2 to 3 between the measurements. In section 6.2.3 it is discussed that this peak may be attributed to the plume being advected close to the bed, as well as to salt wedge dynamics. Although this does not explain the variation between the measurements themselves. In the model runs this variation between the measurements is not encountered, see fig. 7.7. The measurements show consistent results between 0.02 to 0.025 g/l, decreasing in time.

The model supports the hypothesis of the bed plume being advected at a very low speed close to the bed. However, the concentrations of the plume only reach 0.025 g/l, which is within the range of expected variation between measurements. Therefore, no conclusions can be drawn on the performance of the model when compared to the measurements.

At last, the shape of the profiles found in the silt profiler differs significantly when compared to the model results for the silt profiler measurement 30 - 34. The silt profiler measurements all show an increase in sediment around the pycnocline. In the model results this increase is located much closer to the bed. This is also in contrast to observations done by de Nijs and Pietrzak [2012], who observed SPM being more dispersed over the vertical in the model.

Measurements 45 - 46

Apart from the measurements 30 - 38, measurement 45 and 46 (fig. 6.22) also show a peak in the near bed concentration. The peak concentrations can be explained by the advection of the salt wedge, the near bed plume of the disposal or by the re-entrainment of sediment from the pit, see fig. 3.7. The latter effect is not included in the model. Due to the coarseness of the grid, silt profiler 45 and 46 are allocated in the same grid cell. The difference in the two measurements is therefore caused by the difference in time. In the modelling results it can be noticed that this time difference leads to substantial different results. This stresses

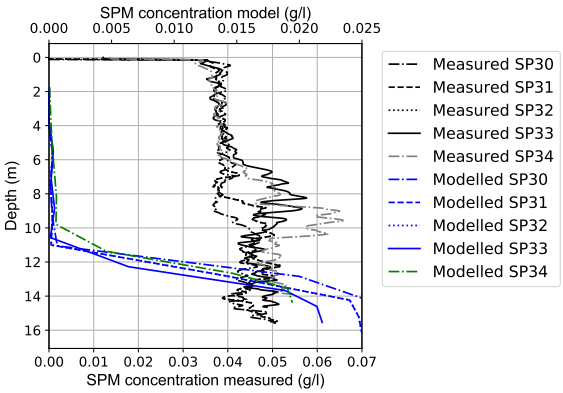

(a) Model - measurement comparison at silt profiler measurement 30 - 34

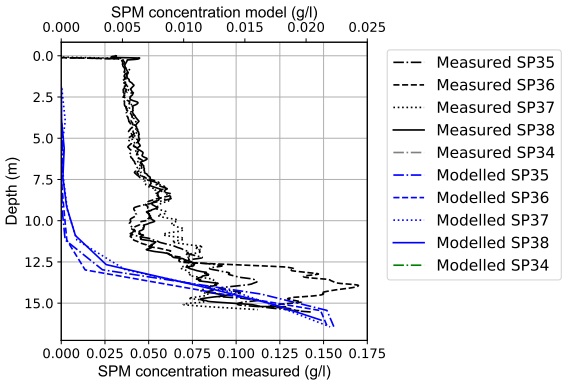

(b) Model - measurement comparison at silt profiler measurement 35 - 38

Figure 7.7: Model results at location and time of silt profiler measurements. The location and time of the vertical profiles agrees with the location and time of the measurement shown in chapter 6.

the importance of the timing of the measurements when taken in the Lagrangian frame of reference. Also the peak in SPM concentration in the model and measurement seem to match.

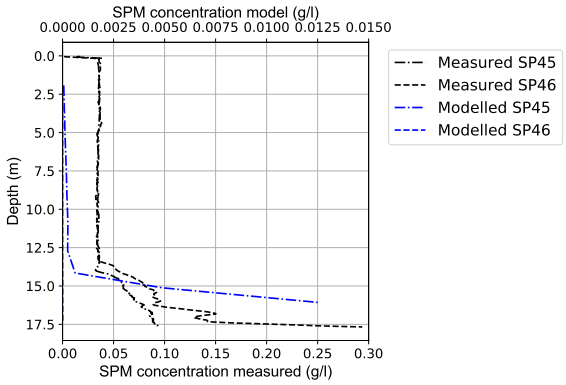

Figure 7.8: Model - measurement comparison at the location and time of silt profiler measurements 45 - 46. The location and time of the vertical profiles agrees with the location and time of the measurement shown in chapter 6.

7.5. Long term hydrodynamic validation

For the long term modelling hindcast, the hydrodynamics from August 30 - September 13 are used and repeated. In the following section the hydrodynamics are validated based on the same fixed measuring stations as used for the short term modelling. These are, Hook of Holland (-2.5 m NAP), Lekhaven (-2.5 m, -5 m, -7.0 m NAP) and Spijkenisserbrug (-2.5 m, -4.5 m, -9.0 m NAP).

From the measurement at Hook of Holland, fig. H.21 the salinity is consistently overpredicted during flood with 5 to 10 PSU. This is also observed for the same measurement station in Geraeds [2020]. For the measurement stations located further inside the port, Lekhaven, fig. H.22 and Spijkenisserbrug, fig. H.25 the accuracy in the salinity reproduction seems to improve. In contrast to Hook of Holland, the modelled salinity is consistently underpredicted by the model at Lekhaven. At Spijkenisserbrug a good agreement is found with only minor underestimations of the salinity.

The effect of the deficiencies in the measured salinity at measurement stations on the behaviour of SPM is complicated to assess. For the behaviour of SPM, the vertical distribution of the salinity, especially the height of the pycnocline is assumed to be most important. This cannot be derived from the time-series comparison

represented here. The time-series presented here, does show that the hydrodynamics used, are consistent with the measurements and are therefore mainly used as validation of the hydrodynamic model input.

7.6. Long term model results

For the long term modelling results the two week hydrodynamic forcing from August 30 to September 13 is repeated while including all 127 disposals. In total nine months are computed, this consists of six months of the SURICATES pilot study (May 20 - November 20) and three additional months to obtain equilibrium. This coincides with the period May 18, 2019 until March 16, 2020.

The most important result is the net flux of the disposal area, which is a good indicator of the efficiency of the pilot study. In table 7.8 it can be seen that only 27 % of the sediment is allocated downstream of the disposal location, as a consequence 73 % of the sediment flows upstream of the disposal location towards the harbour basins. In section 7.6.1 the sediment fluxes are discussed in detail and in section 7.6.2 the long term model results are compared with the long term measurements.

	Disposal Area	
Grain size	Upstream	Downstream
Total	**73%**	**27%**
IM1	6 %	94 %
IM2	21 %	79 %
IM3	78 %	22 %

Table 7.8: The net sediment flux of the disposal area.

7.6.1. Sediment fluxes

In fig. 7.9 the location where the sediment settles is shown. It can be observed that the largest concentration of settled sediment is found in the basins lining the Rotterdam Waterway. This is in line with the hypothesis drawn in section 3.4. It is predicted, that in line with the estimations done by de Nijs [2012], 50 % of the sediment provided is entrapped within the Rotterdam Waterway. As the Rotterdam Waterway is too dynamic, the sediment undergoes the following pattern; advection, settling, resuspension until it flows into the harbour basins, where the sediment is allowed to settle.

In table 7.8 the net flux of the disposal area is shown. It can be observed that 73 % is transported upstream of the disposal location and 27 % downstream. It should be noted that this differs significantly per inorganic fraction considered. As stated in chapter 5, three different fractions of sediment (IM1, IM2, IM3) are included, with grain sizes of 1, 12 and 34 μm. If the fluxes of the disposal area are considered, 94 %, 79 % and 22% (for 1, 12 and 34 μm) of the fractions flows downstream of the disposal area, stressing the importance of an accurate grain size representation. It can be noticed that the approximate sediment fluxes are in line with the sediment flux approximation of de Nijs [2012].

The sediment flowing downstream from the disposal area, barely flow towards the North Sea (14 %).The remaining sediment is transported into the neighbouring Calandkanaal, Hartelkanaal and Beerkanaal, while little sedimentation is observed in the Maasmond. From the sediment transported upstream, 21 % settles in the Calandkanaal. This is in line with a tracer analysis done by de Nijs et al. [2010], where was found that 10 - 25 % of the sediment deposits in the Europoort / Calandkanaal have a fluvial origin.

73 % of the sediment reallocated is assumed to flow upstream from the disposal area. It has been hypothesised that the majority of this sediment settles in the basins lining the Rotterdam Waterway, as described in section 3.4. In table 7.10 it can be seen that the largest amount of sediment is deposited in the Botlek, which is the first (seen from the disposal site) and largest basin lining the Rotterdam Waterway. The Botlek is subject to the largest amount of sedimentation as on flood tide the ETM propagates first along the Botlek and subsequently bifurcates into the New Meuse and Old Meuse [de Nijs and Pietrzak, 2012].

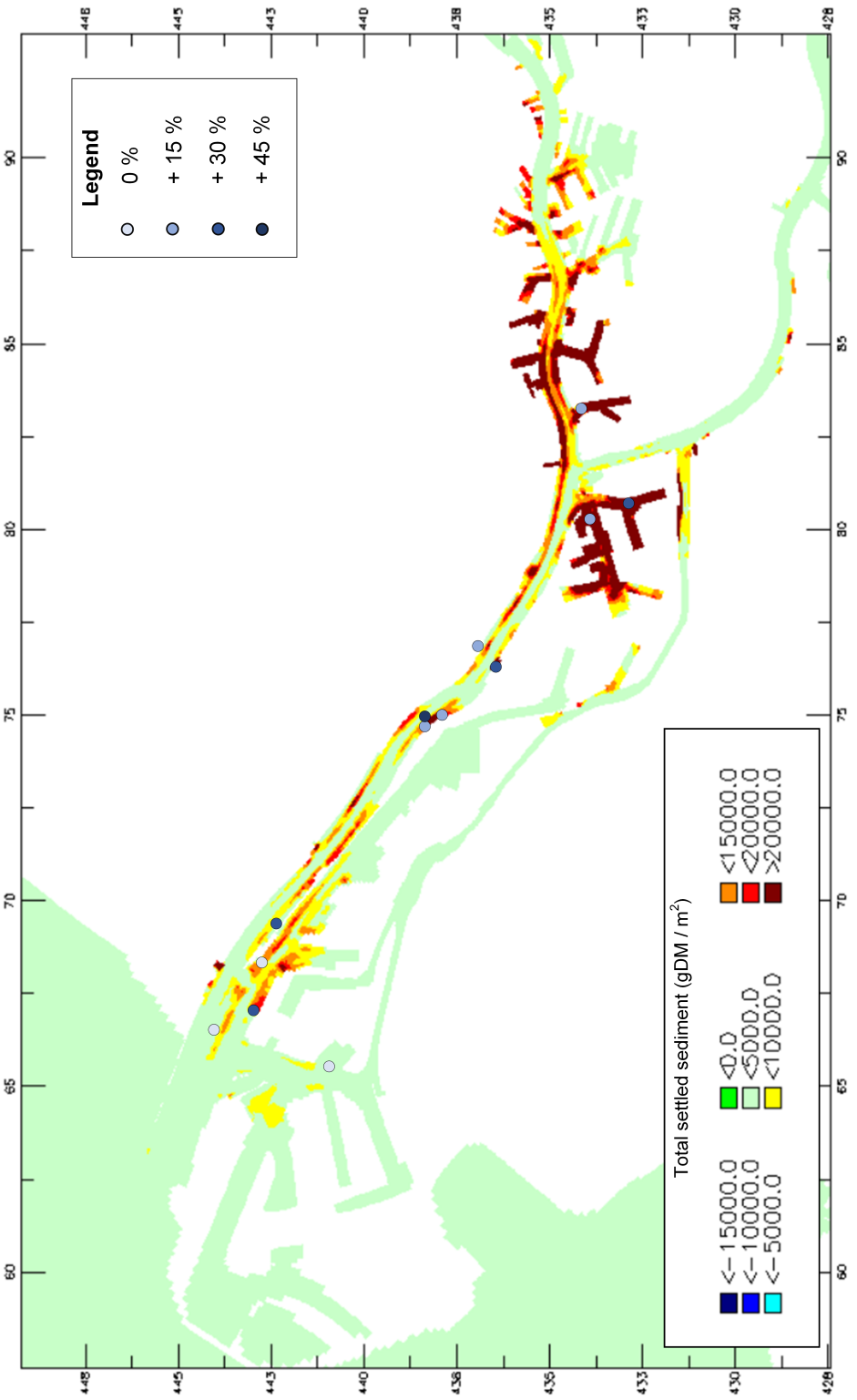

Figure 7.9: An overview of the port of Rotterdam and the amount of settled sediment from the SURICATES pilot study. The dots indicate the long term sample locations and the increase in silt content between T0 and T2 in %.

	D. RWW	MMD	Disp	Clknl.	Brknl.	MV.	MV. 2	Hlknl.	NS_W	NS_E	Total:
Total:	3%	4%	3%	6%	2%	0%	2%	3%	0%	3%	**27 %**
Upstream:	13%	15%	10%	21%	8%	2%	6%	13%	3%	11%	**100 %**

Table 7.9: The downstream sediment fluxes and settling location of the sediment from the SURICATES pilot study. *'D. RWW'* refers to the part of the Rotterdam Waterway downstream of the disposal location up to the Maasmond, *'MMD.'* refers to the Maasmond, *'Disp.'* refers to the disposal location, *'Clknl'* and *'Brknl'* refer to the Calandkanaal and Beerkanaal, *'MV.'* and *'MV. 2'* refer to the Maasvlakte and Maasvlakte 2, *'Hlknl'* refers to the Hartelkanaal, and *'NS_W'* and *'NS_E'* refer to the west and east part of the North Sea. For the locations see fig. A.2.

	BTLK	1ePETH	2ePETH	EEM.	WAAL.	N. Meuse	O. Meuse	Up. RWW	Total:
Total:	30%	5%	6%	2%	2%	18%	2%	7%	**73%**
Upstream:	41%	7%	9%	3%	3%	25%	3%	9%	**100 %**

Table 7.10: The upstream sediment fluxes and settling location of the sediment from the SURICATES pilot study. *'BTLK'* refers to Botlek, *'EEM.'* refers to the Eemhaven, *'WAAL.'* refers to the Waalhaven, *N. Meuse* and *O. Meuse* refer to the New and Old Meuse and *'Up. RWW'* refers to the part of the Rotterdam Waterway upstream of the disposal location up to the Botlek. For the locations see fig. A.2.

7.6.2. Model - measurement comparison

To validate the long term model results generally two different methods can be used: 1) comparing to dredging records and 2) comparison to measurements. The first method, comparison to dredging records is deemed meaningless, as the amount of sediment settled in the harbour basins is relatively small in comparison to background sediment fluxes. 22 % of the SURICATES sediment is expected to end up in the Botlek in nine months. This equals only 10 % of the total dredging budget of the Botlek in the same period. (127,000 vs 1.2 million m^3, [de Bruijn, 2018]). Therefore, one cannot verify the sediment fluxes of the long term model results with the dredging budgets.

In fig. 7.9 the change in silt content based on the long term measurements is included. In this map, an agreement between the measurements and model results is found. However, the locations with the largest sedimentation in the model, e.g. the harbour basins, do not correlate with the locations with the largest sedimentation in the measurements. Next to this, in section 6.3 it is discussed, that the composition of the bed in the Rotterdam Waterway is subject to a large range of possible compositions. Therefore, it is concluded that a change in bed composition can be caused by a difference in natural variation as well.

7.7. Summary

In this chapter the results of the short term and long term model hindcast are presented and compared to the measurement results of chapter 6, in order to answer the following research question:

To what extent can the model reproduce the sediment distribution as found in the SURICATES pilot distribution?

In this chapter the behaviour of the SURICATES sediment plumes is compared to the hypothesis drawn up in chapter 3 and the results of the modelling campaign in chapter 6.

When the short term model hindcast is considered, the behaviour of the disposals seem in line with the predicted behaviour as described in chapter 3. Especially the importance of the method of execution: bow coupling or bottom door disposal is evident. However, a comparison with model results is complicated for three reasons: 1) the model results are most reliable in the mid field and far field, whereas the signal of the plume in the measurements is most clear in the near field, 2) the measurements with the silt profiler are taken at a fixed time and position, in fig. 7.3 one can observe that phase difference and spatial difference are likely to occur, 3) due to dispersion the plume signal weakens quickly after disposal, e.g. in fig. 7.3 from $\mathcal{O}(1-10g/l)$ after release to $\mathcal{O}(0.001-0.01g/l)$ three hours after release. At last, it is observed that the model results are very sensitive to the layer of disposal and grain sizes used.

If the long term results are considered, the cumulative behaviour of all sediment disposals appear to be in line with the hypothesis drawn up in chapter 3 as well. Since most disposals are allocated by bottom door disposals, the sediment is allocated in the salt wedge where it remains confined. This sediment undergoes a repetitive behaviour of settling, resuspension, accumulation at the tip of the salt wedge until it is allowed to settle in the harbour basins lining the Rotterdam Waterway. The long term model results show that 73 % of the sediment flows upstream, hence conforming this hypothesis. In section 6.3, despite the limited applicability, an increased silt content is observed for nearly all locations. The locations of increased silt content corresponds to the locations with deposited SURICATES sediment. It should be noted however that the long term model results are very different for the grain size considered, illustrating the importance of a thorough calibration of the sediment model parameters.

7.7.1. Hydrodynamic validation

As part of the larger SURICATES research project, Geraeds [2020] determined the performance of both hydrodynamic models used in this thesis: the NSC-fine and NSC-coarse model. It is found that generally, both models are able to reproduce water levels and velocity structure well. However, the reproduction of the salinity structure and advection of the salt wedge are less well reproduced by the models. Both Geraeds [2020] and de Nijs and Pietrzak [2012] found that the models overpredict the height of the pycnocline and underpredict the intrusion length of the salt wedge. The pycnocline is associated with turbulence damping and subsequent trapping of sediment. In general, SPM concentrations are more smeared over the vertical, leading to high SPM concentration high in the water column. Due to this smearing peak concentrations are lower than measured in the ETM due to the over prediction of the pycnocline height de Nijs and Pietrzak [2012]. The overprediction of the pycnocline height may place sediment disposals below the pycnocline in the model instead of above. In contrast, in the hydrodynamic validation is found that the pycnocline is located lower in the model hindcast for November 5 than for the measurements during disposal. Therefore, sediment disposals may be artificially be placed on top of the pycnocline instead of below the pycnocline. The intrusion length of the salt wedge is associated with the trapping of fluvial sediment and the trapping efficiency of the Rotterdam Waterway as a whole. For a short salt wedge intrusion length, sediment is deposited in the Maasmond. According to de Nijs and Pietrzak [2012], the inaccuracy of the salinity structure can be caused by artificial vertical velocities, induced by the hydrostatic pressure assumption and artificial diffusion. An underestimation of the salt wedge length may artificially place disposals in fresh water, instead of in the salt wedge. This

might reduce the amount of sediment entrapped within the salt wedge. Despite this deficiency, the major trapping mechanism, the advection of the salt wedge, SPM accumulation and subsequent formation of an Estuarine Turbidity Maximum (ETM) are well reproduced by the models [de Nijs and Pietrzak, 2012].

Moreover, the model has an artificially high and increased background diffusivity to include additional turbulence [Kranenburg, 2015]. This background diffusion is calibrated based on salinity measurements. However, SPM is subject to the same diffusion parameters in the model, while it lacks thorough calibration of this large diffusion parameter. This might overestimate the amount of initial mixing of a sediment disposal.

7.7.2. Short term modelling

Strictly speaking, the exact sediment distribution as found in the silt profiler measurements can not be reproduced with the current model set up, due to the lack of background concentration in the model. The background concentration is not implemented in the model for two reasons: 1) This research focuses on the behaviour of the sediment behaviour of the SURICATES pilot study. By introducing background concentrations it would be more difficult to distinguish sediment plume related concentrations from background concentrations in the model, 2) The sediment dynamics and hydrodynamics are not coupled. Therefore the background concentration does not influence the sediment behaviour of the disposal. However, if the background concentration is ignored from the silt profiler measurements, and one compares the signal of the measurements to the model results, similarities are found. This observation is used to advocate the calibration of the model in the near and mid field.

From the sensitivity analysis it is concluded that the layer of disposal and thus the method of disposal, has the largest influence on the sediment fluxes in the short term modelling. Based on the comparison with the silt profiler measurements, the depth of disposal in the model set-up is calibrated. However, this calibration is very limited, while the sensitivity analysis shows the importance of this parameter setting.

Another parameter with a large influence is the grain size distribution used in the model set-up. In this thesis, the same grain size distribution as de Groot [2018] and Vijverberg et al. [2015] is used. However, from the sensitivity analysis and observations by de Groot [2018] is found that the smallest fraction does not settle inside the port. Also, the grab samples advocate the use of a coarser fraction than 1 μm in the model set-up.

7.7.3. Long term modelling

From the long term model hindcasts it is estimated that 73 % of the reallocated sediment in the Rotterdam Waterway flows upstream from the disposal location. This percentage is in line with the estimation done by de Nijs [2012] and in line with the expected behaviour as described in section 3.4. As the majority of the sediment is reallocated by bottom door disposal it is allocated in the salt wedge. Within the salt wedge sediment behaviour is described as a repetitive pattern of advection, settling, resuspension and accumulation in the tip of the salt wedge (ETM) until it flows into harbour basins where it is allowed to settle. It is stressed that the sediment fluxes depend strongly on the considered sediment fraction, e.g. for the smallest fraction 94 % of the sediment flows downstream in contrast to 22 % for the most coarse fraction. de Groot [2018] found that not only the settling velocity determines the behaviour of the sediment fractions, the resuspension parameters have a large influence as well. It is stressed that a thorough calibration of all sediment parameter settings is therefore required.

When the long term model results are compared with the long term measurement results, an agreement in the location of increased sediment is found. However, a thorough model measurement comparison is complicated due to the limited reliability of the long term measurements. Next to this, the sediment fluxes of the long term model results cannot be verified with the dredging budgets of the basins due to limited size of the pilot study. The lack of in calibration of the measurement results limits the reliability of the long term model results.

IV

Concluding remarks

8

Discussion

In this chapter is reflected on the work as a whole. Emphasis is put on assumptions made and their effect, as well as limitations of the thesis. This discussion is split into three different parts, reflecting on the literature study, the measurement campaign and the modelling hindcasts.

8.1. Literature study

Analogy with fluvial sediment
To derive a hypothesis for the behaviour of the sediment plumes in the mid field and far field, an analogy is drawn between the released sediment and fluvial sediment in the Rotterdam Waterway. This allows the application of work done by de Nijs [2012], who found how fluvial sediment rains out above the pycnocline. Turbulence damping subsequently inhibits upward moving, entrapping the fluvial sediment below the pycnocline. It is expected that the sediment plumes behave similar in the mid field and far field. The measurement and model results are in line with the observations by de Nijs [2012], e.g. the mechanism trapping fluvial sediment within the Rotterdam Waterway acts on the SURICATES sediment plumes in the same way. This assumption assumes that the majority of the sediment settles shortly after disposal, possibly leading to an overestimation of the sediment that remains in the system.

Comparison to overflow plumes
The hypothesis on the expected behaviour of the sediment plumes in the near field is based on the research done by de Wit [2015] and Winterwerp [2002] on overflow plumes. Generally, the momentum of overflow plumes is smaller while the buoyancy is larger. Therefore, the theory on overflow plumes is not validated in the range of the buoyancy and momentum of the SURICATES sediment plumes. This might lead to a wrong prediction of the near field behaviour of the sediment plumes.

Human interventions in the port of Rotterdam
The work by de Nijs [2012] has been executed prior to the construction of Maasvlakte 2, the widening of the Breeddiep, and the deepening of the Rotterdam Waterway and Botlek. Geraeds [2020] nevertheless found that most hydrodynamic processes as found by de Nijs [2012] are still governing, despite the mentioned interventions. Huismans et al. [2013] found that the effect of the construction of Maasvlakte 2 is limited for the hydrodynamics in the Rotterdam Waterway. Huismans et al. [2013] also predicted the possible effects of the deepening of the Rotterdam Waterway on the hydrodynamics and sediment behaviour. Due to the deepening, the tidal volume and tidal asymmetry increases, potentially importing more marine sediment. This is also promoted as the difference in depth between the Maasmond and Rotterdam Waterway is reduced. Moreover, it is expected that the salt wedge extends further landward as salt intrusion is promoted. From de Nijs [2012] is known that the salt intrusion length determines the amount of entrapped fluvial sediment. This might increase the trapping efficiency of the SURICATES sediment plumes.

8.2. Measurement campaign

Plume dispersion with respect to background concentration
The reallocated SURICATES sediment plumes are subject to a lot of mixing as the concentration gradient is largest shortly after release. Therefore the signal, that is a clear peak of sediment concentration caused by the disposal, weakens quickly after disposal, complicating the allocation of the sediment plume. Next to this, differences in the concentration of SPM can also be attributed to an increase in transport capacity or due to an increase of available sediment other than the sediment plume, such as resuspension from the bed. In section 2.2.3 it is observed that there is a large variation in SPM in time and space. Therefore peaks in the SPM concentration, especially near the bed, are not necessarily caused by a sediment disposal.

Difference in execution method
Both measurement surveys of this study (Sep. 11 and Nov. 5, 2019) have been executed for only one disposal technique: bow coupling. Therefore, the measurement surveys only provide an insight in the near field and mid field dynamics of this execution method. Other surveys, e.g. on July 7 and July 11 have been executed during a bottom door disposal, but have not provided useful results and are therefore not included in this thesis. 93 % of the sediment disposals have been executed by drawing the bottom doors, while the remaining 7 % is disposed using bow coupling. The near field and mid field behaviour of a disposal by bottom door is therefore mainly based on literature, observations done by the surveyors and the local change in bathymetry. Based on these observations it is assumed that the sediment disposals, reallocated by drawing the bottom doors are reallocated close to the bed, below the pycnocline. As the sediment is reallocated below the pycnocline, upward movement is inhibited due to turbulence damping and the sediment is assumed to remain within the Rotterdam Waterway until it is allowed to settle in the harbour basins. As shown in section 7.4.1, this assumed initial behaviour has a large effect on the results of the model hindcast, as well as the expected behaviour of the plume in the mid field and far field. Therefore, sedimentation fluxes towards the harbour basins may be overestimated, as the depth of disposal is assumed to be negatively correlated with the downstream flux of sediment.

Short term measurement equipment
The set-up of the measurement survey introduces some inaccuracies as well. To measure the sediment distribution over the vertical two different quantities are measured: absolute backscatter and optical backscatter. The absolute backscatter is obtained using an Acoustic Doppler Current Profiler (ADCP) and provides continuous results to the surveyors. The silt profiler, providing the optical backscatter, has to be deployed for three minutes to obtain a single, but detailed, distribution of SPM over the vertical. As the ADCP backscatter has not been calibrated, it is used for qualitative comparison and detection of the sediment plume only. As a consequence of the working principle, the ADCP backscatter contains a blanking distance. Therefore, no values are obtained from the top 2.5 m and 1.5 m from the bed. This explains the difficulty capturing the sediment plume released by drawing the bottom doors where the majority of the sediment is assumed to be mixed and advected close to the bed. Moreover, not only bottom door releases are affected, as it is hypothesised that a substantial amount of sediment released by bow coupling is advected close to the bed in the mid and far field as well. Since the surveyors miss the possible advection of SPM close to the bed, the silt profiler is barely deployed when potentially relevant to capture sediment advection close to the bed.

Short term measurement set-up
The frame of reference used in the measurements has introduced considerable bias as well. The measurement surveys are set-up in a Lagrangian frame of reference. Since the plume is advected at different velocities due to differential advection and the survey vessel moves with a fixed speed, the survey vessel is only able to measure parts of the sediment plume advected at the same velocity as the velocity of the vessel. Moreover, the sailing velocity of the survey vessel appears to be larger than the expected advection of the sediment plume, explaining the difficulty in capturing the sediment plume in the mid field. Therefore the observations in the near field are used to derive a hypothesis for the mid field behaviour, while this hypothesis can not be confirmed by the measurements. It is assumed that the upper part of the water column is cleared of sediment from the disposal and that the sediment plume is mainly advected around and below the pycnocline, while this is only confirmed by one measurement. This assumption might underestimate the amount of sediment flowing downstream over the long term, as confined sediment is expected to end up in the harbour basins instead of in the North Sea.

Long term measurement set-up

For the long term assessment, i.e. the cumulative behaviour of all sediment disposals, a different measuring campaign has been set-up. In the measurement campaign bed samples are taken at three different times: the first samples (T_0) are taken prior to the pilot study while the other two surveys (T_1 and T_2) are taken during the pilot study. For the bed samples a shift towards finer material might be an indication of increased sedimentation due to the pilot study as mainly fine material is disposed throughout the pilot study. For nearly all locations an increase in silt content between T_0 and T_2 is observed. However, the increase in fine sediment can also be attributed to background sedimentation or natural variation, since the silt content in the Rotterdam Waterway varies strongly in time and space. Also, between T_0 and T_1, the sediment from the SURICATES pilot study only contributes for 2.8 % to the total sediment fluxes in the Rotterdam Waterway. Between T_1 and T_2 this equals 10 %. It is therefore questionable whether changes in bed sample composition can be related to the execution of the SURICATES pilot study. Therefore the hypothesis on the long term behaviour, as well as the long term model hindcasts can not be calibrated.

8.3. Model hindcasts

Reproduction hydrodynamics

In support of the measurement campaign, model hindcasts are executed, using operational hydrodynamic and sediment models. In line with the measurement campaign, two different modelling set-ups are used: (1) one set-up is used to model the short term behaviour of one single release and; (2) the other set-up is used to model the cumulative behaviour of all SURICATES sediment disposals. To model the sediment dynamics, the governing hydrodynamics are modelled first. As part of the larger SURICATES research project, Geraeds [2020] determined the performance of both hydrodynamic models used in this thesis: the NSC-fine and NSC-coarse model. It is found that generally, both models are able to reproduce water levels and velocity structure well. However, the reproduction of the salinity structure and advection of the salt wedge are less well reproduced by the models; both Geraeds [2020] and de Nijs and Pietrzak [2012] found that the models overpredict the height of the pycnocline and underpredict the intrusion length of the salt wedge. The pycnocline is associated with turbulence damping and subsequent trapping of sediment. In general, high SPM concentrations are found higher in the model than in measurements. While peak concentrations are lower than measured in the ETM due to the over prediction of the pycnocline height de Nijs and Pietrzak [2012]. The overprediction of the pycnocline height may place sediment disposals below the pycnocline in the model instead of above. The intrusion length of the salt wedge is associated with the trapping of fluvial sediment and the trapping efficiency of the Rotterdam Waterway as a whole. For a short salt wedge intrusion length, sediment is deposited in the Maasmond. According to de Nijs and Pietrzak [2012], the inaccuracy of the salinity structure can be caused by artificial vertical velocities, induced by the hydrostatic pressure assumption and artificial diffusion. An underestimation of the salt wedge length may artificially place disposals in fresh water, instead of in the salt wedge. This might reduce the amount of sediment entrapped within the salt wedge. Despite this deficiency, the major trapping mechanism, the advection of the salt wedge, SPM accumulation and subsequent formation of an Estuarine Turbidity Maximum (ETM) are well reproduced by the models. Moreover, the model has an artificially high and increased background diffusivity to include additional turbulence [Kranenburg, 2015]. This background diffusion is calibrated based on salinity measurements. However, SPM is subject to the same diffusion parameters in the model, while it lacks thorough calibration of this large diffusion parameter. This might overestimate the amount of initial mixing of a sediment disposal.

Model set-up used

The models used, NSC-fine and NSC-coarse, only include flow processes and lack a coupling between sediment dynamics and hydrodynamics. Since only flow processes are resolved, waves are not included in the model. Waves are considered to be the main driver for resuspension of sediment at sea, while the effect on sediment dynamics within the Rotterdam Waterway are assumed to be negligible. Since only 3 % of the total sediment from the SURICATES reallocations settles permanently within the North Sea, the exclusion of waves is assumed to be justified. As the sediment dynamics and hydrodynamics are non coupled, density effects are not included in the model. This typically introduces errors at locations where high SPM concentrations might occur, as high concentrations of SPM induce density differences over the vertical. In the modelling of the SURICATES pilot study, large SPM concentrations are expected to occur twice: at the time of disposal and during fluid mud processes. After disposal by bottom door, a large amount of SPM is released, in a short time. Therefore, high concentrations of SPM can arise. Due to the non coupling, mixing may be overestimated as in reality the turbulence field is altered for very high concentrations as explained in section 2.2.1. Winterwerp

and Van Kessel [2003] estimated that the sediment flux from the North Sea towards the Maasmond is underestimated by a factor 3 to 5, since the main sediment flux towards the Maasmond consists of wave induced fluid mud layers.

Sediment model calibration
Any model prediction or hindcasting requires verification or calibration to ensure and improve its reliability. In this research a strong paradox arises in the measurement/model comparison. The model used, both the NSC-coarse and NSC-fine model are most suitable to predict hydrodynamics and sediment behaviour on large and long time scales. However, the most reliable and useful measurement results are obtained shorty after disposal and close to the vessel. This complicates the comparison of model results with measurements. In fact, the near field measurement results are rather used to calibrate the sediment settings. Based on the comparison to silt profiler measurements, it is concluded that the model is calibrated sufficiently, however large uncertainties remain. For example, the layer of disposal halfway the water column seems justified based on mid field observations, but the chosen grain sizes can only be calibrated to a small extent. Also, as indicated by de Groot [2018], the settings for the different resuspension parameters have a large influence on the sediment behaviour. The measurement results obtained, do not allow the calibration of these resuspension parameters. As the resuspension of sediment is overpredicted upstream sediment fluxes may be overestimated.

Disposal implementation
The initial or near field behaviour of the sediment disposals cannot be resolved by the sediment models used. Accurately modelling these processes requires a model (e.g. CFD) where the smallest scale of the model coincides with the turbulent scale, hence not requiring parameterisation of turbulence [de Wit, 2015]. In the model used, NSC-fine and NSC-Coarse, turbulence is parametrised on a coarse scale by the k-ϵ closure model. The disposal are implemented into the sediment models as a point source with a fixed depth. These near field effects are taken into account, by allocating the sediment disposals halfway the water column for a bow coupling disposal and close to the bed for a disposal by bottom door. However, the sediment model is not able to reproduce the initial mixing induced by the concentration gradient. By placing the sediment disposal too high in the water column, downstream sediment fluxes are assumed to be overestimated. While sediment disposals placed too close to the bed might overestimate the upstream sediment flux.

Long term hydrodynamic representation
Next to the short term model hindcast, the entire duration of the SURICATES pilot study has been hindcasted. For the long term model set-up, a two week representative hydrodynamic forcing is repeated in the sediment model until nine [1] months are reached. This two week hydrodynamic forcing is chosen in such a way that it is representative for the total duration of the SURICATES pilot study and to include a spring-neap cycle. However, this hydrodynamic forcing is not an one-on-one representation of the entire hydrodynamic forcing. As shown in fig. 5.6 the fresh water discharge being repeated lacks the peak discharge at the end of May, while being below the yearly discharge and average SURICATES discharge. Lower discharge conditions are considered disadvantageous, as sedimentation of the harbour basins is promoted. Another inaccuracy is introduced with the introduction of the timing of the disposals. The different disposals are mapped from their original time of disposal to a time and date from the two week hydrodynamics used. As explained in section 5.6, this shift is done using the timing of predicted depth-averaged high-water slack at Maassluis, since this reference point is used by the dredging company as well. This reference point or any reference point, is not exact, and might place disposals in a different phase of the tide. In section 7.4.1, is shown that the timing of disposal has a large influence on the sediment fluxes. Therefore, the model hindcast might under predict the downstream sediment fluxes as the wrong time of disposal is used.

[1] The duration of the pilot study and three additional months to obtain equilibrium

9

Conclusion and recommendations

In order to reduce dredging costs in the port of Rotterdam, a different sediment reallocation strategy has been examined over five months, named the *SURICATES* pilot study. To verify whether this different reallocation strategy is an efficient measure to reduce dredging costs, a thorough understanding of the pilot study is required. Therefore the main objective of this thesis is formulated as, *Use the results obtained from the measurement campaign and operational sediment models, to hindcast the behaviour of the SURICATES pilot study on different spatial and time scales.* This thesis has focused on the SURICATES pilot study on two scales, using two different methods. At first, the behaviour of a single disposal, focusing on the near and mid field behaviour of a sediment plume has been hypothesised and subsequently tested using the results of two measurement surveys and a model hindcast. To verify whether the SURICATES pilot study is an efficient measure to reduce dredging costs, the cumulative behaviour of all sediment reallocations has been examined as well, using the same methodology: hypothesis, measurement results and a model hindcast.

In this chapter the main conclusions of this work are presented by first elaborating on the different sub-questions, subsequently converging towards the answer of the main research question. The main conclusions are followed by recommendations for future work.

9.1. Conclusion

In order to answer the main research questions, sub-questions have been defined. The answers to the different sub-questions is briefly discussed below, to converge towards the answer on the main research question.

1. **Which processes govern the hydrodynamics and the sediment behaviour in the port of Rotterdam?** From de Nijs [2012] it is known that the governing hydrodynamics in the Rotterdam Waterway are characterised by tidal asymmetry, baroclinic exchange flows, advection of the salt wedge and turbulence damping around the pycnocline. Due to the strong tidal asymmetry imposed at the mouth, ebb periods last longer while peak flood velocities are larger. The advection of the salt wedge and the damping of turbulence at the interface between fresh water and the saltier water below are the main trapping mechanism of fluvial sediment in the Rotterdam Waterway. Fluvial sediment from upstream rains out above the salt wedge while turbulence damping inhibits upward movement. The length of the salt wedge determines the amount of fluvial sediment entrapped. The sediment entrapped below the pycnocline undergoes a vast pattern of advection, settling and resuspension until it flows into low dynamic zones such as the harbour basins lining the Rotterdam Waterway. The lack of settled mud in the Rotterdam Waterway advocates this theory. This leads to a very efficient trapping mechanism, entrapping nearly 50 % of the fluvial sediment. Due to these advective properties, sediment concentrations vary significantly in the Rotterdam Waterway, between $\mathcal{O}(0.01\ g/l)$ above the pycnocline up to $\mathcal{O}(1\ g/l)$ in the ETM. During high discharge conditions, the ETM can be suppressed up to the Maasmond, allowing fluvial sediment to settle here. The harbour basins lining the southern part of the port, e.g. Europoort and Maasvlakte, are subject to a different sedimentation mechanism. During storms at sea, fine sediment is quickly resuspended by wave induced bottom shear stresses. As sediment concentrations are

high, a fluid mud layer is mobilised. This layer follows the near bed residual flow towards the Maasmond. Due to depth differences in the Maasmond, this fluid mud layer flows towards the southern harbour basins and not into the Rotterdam Waterway.

2. **What is the expected behaviour of sediment plumes in the system?**
   From literature, e.g. de Wit [2015], Winterwerp [2002] the governing parameters of sediment plumes in the near field are found. In the near field, plume behaviour is governed by its momentum to buoyancy ratio. These parameters are used to predict the behaviour of the SURICATES sediment plumes. The near field behaviour of the sediment plumes is mainly determined by the method of disposal: bow coupling or bottom door release. For the bow coupling release it is found that, due to the initial momentum to buoyancy ratio, mixing mainly takes place between a depth of 4 to 12 m. In contrast, a bottom door disposal only exhibits jet behaviour, related to its high release velocity. Therefore no mixing over the horizontal can take place. Due to this high release velocity an impact crater is observed at the disposal location (fig. 3.7).

   In the mid field, the hydrodynamics and sediment particle properties determine the behaviour of the sediment plume. For a bow couple release, advection is expected to takes place around the pycnocline while at the same time sediment slowly rains out below the pycnocline. For a bottom door release the sediment is expected to be entrapped below the pycnocline, where upward movement is inhibited due to turbulence damping.

   In the far field, the behaviour is characterised by the properties of the bed and hydrodynamics. It is expected that sediment entrapped below the pycnocline remains entrapped and undergoes the vast pattern of advection, settling, resuspension and accumulation at the tip of the salt wedge (ETM), until it is allowed to settle in a harbour basin. For sediment reaching the North Sea, it is expected to follow the residual flow in the Rhine ROFI, towards the north along the coast.

3. **How is the reallocated sediment distributed in time and space on different spatial and time scales?**
   Based on the short term measurement surveys (September 11 and November 9, 2019), the near field predictions are confirmed, i.e. little mixing occurs in the top layers of the water column. Subsequently, the plume mixes halfway the water column, while being advected around and below the pycnocline. As the survey vessel sails with a fixed velocity, significant bias is introduced in the measurements. In combination with the dilution of the sediment concentration of the sediment plume, application in the mid field and far field of the measurements is limited.

   Based on the long term measurements, an increase of fine sediment is found for nearly all sampling locations, especially in both Botlek locations (*Upstream 2* and *Upstream 3*). This agrees with the mid and far field hypothesis that the majority of the sediment being entrapped is subsequently deposited in the harbour basins. However, it is stressed that the amount of sediment from the SURICATES pilot study is relatively small when compared to the total background sediment fluxes in the Rotterdam Waterway. Therefore, the increase in fine sediment at the sampling locations can also be explained due to differences in hydrodynamic forcing and settled background concentration.

4. **Which assumptions and simplifications have to be made to model the SURICATES pilot study on different time and spatial scales?**
   To hindcast the SURICATES pilot study using hydrodynamic and sediment models, different assumptions and simplifications have been made. The major simplification is the implementation of the disposals. As shown in section 3.2, the behaviour of a sediment plume in ambient water in the near field is governed by its momentum to buoyancy ratio, properties which cannot be included in the model. In the model a disposal is simplified into a point source at a certain location with a fixed depth. Based on the expected behaviour of the sediment plume and measurements in the near field, the depth of the disposal is chosen and justified.

   Apart from the depth of disposal, the composition of the barges (the grain sizes distribution of the material disposed) is unknown. The grain sizes used in the modelling study are based on previous work, [de Groot, 2018, Hendriks and Schuurman, 2017, Vijverberg et al., 2015] but is relatively fine in comparison to the grab samples taken at the source location.

   Next to this, to hindcast a period of 9 months, a simplification in the hydrodynamic forcing has been made. In this study a two week representative forcing is chosen based on wave heights at sea. The hy-

drodynamic forcing contains a low discharge condition, which promotes sedimentation in the basins, while sediment transport towards the Maasmond and North Sea is limited.

5. **To what extent can current models reproduce the sediment distribution as found in the data analysis?**
   From de Nijs and Pietrzak [2012] and Geraeds [2020] it is known in advance that the pycnocline height is overestimated and the salt intrusion length underestimated. Due to the overestimation of the pycnocline height, SPM concentrations are higher in the upper part of the column and SPM concentrations in the ETM are smaller, as the peak concentration is mixed over a larger area. The amount of entrapped sediment might be underestimated, as the length of the salt wedge mainly determines the trapping efficiency within the Rotterdam Waterway. Also disposals may be artificially placed outside the salt wedge or below the pycnocline in the model.

   The model results are in line with the hypothesis formulated in chapter 3. However, comparison with measurements is strongly preferred to increase the reliability of the modelling results. Unfortunately, the comparison of modelling results with measurement results is complicated. Most useful measurement results have been obtained in the near field, in the vicinity of the dredging vessel during disposal. However, the model is not suitable to predict the near field processes due to its coarseness. Unfortunately, mid field measurement results are lacking to evaluate the model in the mid field.

   Long term model versus measurement comparison is strongly complicated due to the limited size of the SURICATES pilot study in comparison to background sediment concentrations. In the long term measurement campaign a (small) increase in fine sediment in the upstream harbours is found, which is in line with the long term model results. However, the significance of the SURICATES sediment flux between the measurements is estimated at 3 and 10 %. Therefore, variations and fluctuations in bed compositions at the measurement locations are most likely to be explained by a variation in hydrodynamic forcing or human interventions such as maintenance dredging. At last the sediment fluxes vary for the different fractions of sediment. This is caused by the difference in settling velocity and resuspension properties of the different fractions.

The answers to the the sub questions are summarised in the answer to the main question;

What governs the behaviour of sediment plumes disposed in the Port of Rotterdam, in the context of the SURICATES pilot study, on different spatial and time scales, based on field measurements and model results?

From the measurements done in the near field, it is found that the sediment plume utilising a bow couple release is subject to significant dispersion and is mostly advected around or below the pycnocline. It is therefore assumed that these sediment plumes exhibit the same behaviour as fluvial SPM, of which most of the sediment rains out above the salt wedge and subsequently remains confined below the pycnocline [de Nijs, 2012]. For disposals executed by drawing the bottom doors, this effect is even stronger, as the entire sediment plume is expected to be confined below the pycnocline immediately. Subsequently, the sediment is expected to undergo the following pattern; advection, settling, resuspension and accumulation at the tip of the salt wedge, until it flows into less dynamic areas such as the harbour basins lining the Rotterdam Waterway where the sediment is allowed to settle. From the sensitivity analysis is found that both the flux towards the North Sea and the downstream flux from the reallocation area, after one tidal cycle, are twice as large for a disposal by bow coupling than for a bottom door release. Since 88 % of the sediment is reallocated by drawing the bottom doors, it is expected that the majority of the sediment remains in the system and settles in the harbour basins lining the Rotterdam Waterway. In the modelling hindcast, covering the entire duration of the SURICATES pilot study, it is found that indeed 73 % of the sediment is advected upstream from the disposal location, of which subsequently 42 % settles in the Botlek harbour and 24 % in the adjacent basins. The measurement survey provides indications to confirm this conclusion, however due to the relatively small size of the pilot study, when compared to the background sediment fluxes, variations in the long term measurements are not necessarily caused by the SURICATES pilot study.

9.2. Recommendations

In this thesis, modelling and measuring of the SURICATES pilot study has been discussed in order to enhance the understanding of the pilot study. From the discussion and conclusion a few recommendations follow. The recommendations are split into recommendations to improve the measurement campaign, the model hindcasting and the execution of the pilot study in general.

9.2.1. Measuring improvements

Good measurements are key to understand experiments, calibrate models and hence increase the performance and reliability of these models and research as a whole. The following recommendations can be used to improve a future measurement campaign.

- **Measurement frame of reference**
  For the short term measurement surveys focusing on the near and mid field behaviour of the sediment plumes, a Lagrangian frame of reference is used, in which the survey vessel moves in time and space. This frame of reference is chosen to obtain measurement results from different locations at different times. However, this frame of reference introduces a significant bias in the measurement results. Since the survey vessel moves in time and space, it is only able to capture fractions of the sediment plume being advected at the same velocity as the survey vessel. Therefore skewed measurement results may be obtained. This bias can be overcome by using an Eulerian frame of reference in which the location of the survey vessel is fixed. The major disadvantage of the latter method is that data can only be obtained from this fixed location rather than from multiple locations. Preferably, this fixed location is located at 1 kilometre from the disposal, where the near field effects are limited [de Wit, 2015]. It is further recommended to use more survey vessels in a following survey. When an extra survey vessel is added, mass balances can be established, preferably between locations upstream and downstream of the disposal location. Such a mass balance can be used to derive the sediment fluxes from the different disposals. Moreover, these mass balances can be used to calibrate and verify the sediment model used.
- **Determine carrying capacity of the flow**
  An increase of SPM concentration can be explained by an increased carrying capacity of the flow or by a larger availability of SPM. A larger availability of sediment can be explained by a disposal, while a larger capacity of the flow is induced by changing hydrodynamics. To attribute an increase of measured SPM to a disposal, one has to reject the possibility to attribute a larger SPM concentration to a larger carrying capacity of the flow. Moreover, it is found by Winterwerp and Van Kessel [2003] that if the amount of available sediment surpasses the carrying capacity, the turbulence field keeping the SPM in suspension collapses; conditions for which fluid mud layers can be formed. de Nijs et al. [2008] determined the carrying capacity of the flow qualitatively, however it is recommended to determine the carrying capacity quantitatively as well in the next measurement survey.
- **Long term measurements**
  The current set-up of the long term measurements is subject to the influence of background sedimentation. As discussed, the size of the SURICATES pilot study is relatively small compared to the background sediment fluxes. Therefore fluctuations in the measurement results can be explained by a difference in hydrodynamic forcing or settled background concentration as well. It is recommended to use a different tracer than Rhine sediment. For example, in the mud motor pilot study executed in 2019, a coloured fluorescent tracer was added to the disposed sediment allowing to track the spread of the sediment [Baptist et al., 2019].

9.2.2. Modelling improvements

Hydrodynamic and sediment models are good instruments to predict the hydrodynamics and sediment dynamics. In this thesis, operational models are used to hindcast the pilot study on two different scales. Apart from general model improvements, a thorough calibration is recommended to increase the reliability of the model.

- **Calibration of the sediment model**
  The current hydrodynamic models have been calibrated and its performance is determined in different

studies, such as de Nijs and Pietrzak [2012], Geraeds [2020], Rotsaert and Collard [2009]. In contrast, the sediment model lacks a comparable calibration, especially for the current application. Moreover, for different sediment studies different sediment parameters have been used. The use of different sediment parameters, especially the settling velocity and resuspension parameters of the different fractions, complicates the comparison of these different modelling studies. Furthermore, it shows the difficulty of finding reliable sediment parameter settings in the area of interest. In the sensitivity analysis and long term model results, the importance of such parameters is shown. It is therefore strongly recommended to calibrate the sediment models and parameters in the near future. It is also recommended to calibrate the source term used to include the sediment disposals. Currently the near field effects are included by changing the layer of disposal, but this can also be included by temporarily increasing the diffusion rate in the sediment model.

- **Model extensions**
  The current model set-up only includes flow processes and an offline coupling between the hydrodynamics and sediment behaviour. Waves are responsible for the stirring of sediment in the North Sea. It is recommended to investigate the possible improvement of the hydrodynamics by including waves. Since the sediment dynamics and hydrodynamics are non coupled, density effects are not included in the model. This typically introduces errors at locations where high SPM concentrations might occur, as high concentrations of SPM induce density differences over the vertical. In the modelling of the SURICATES pilot study, large SPM concentrations are expected to occur twice: at the time of disposal and during fluid mud processes. After disposal by bottom door, a large amount of SPM is released, in a short time. Therefore, high concentrations of SPM can arise. Winterwerp et al. [2002] found that sediment transport towards the Maasmond increases with a factor 3 to 5 when the sediment model is coupled to the hydrodynamics. This motivates the use of a coupled model, in which the effect of high concentrations of SPM on the hydrodynamics are included.

- **Effect of artificial background diffusion**
  In Rotsaert and Collard [2009] and Geraeds [2020] is found that the diffusion settings of the hydrodynamic model are set at artificially high values. This is done to improve the salinity distribution of the NSC-coarse and NSC-fine model. Currently, the same diffusion parameter is used in the sediment model. The effect of this artificial high diffusion parameter is unknown, but might explain the high amount of mixing encountered in the mid field after a sediment disposal. It is recommended to investigate the effect of this higher background diffusion on sediment behaviour in general and on the SURICATES pilot study in particular.

- **Long term sensitivity analysis**
  The current long term model set-up is used to hindcast the pilot study as it is executed. It is recommended to execute a similar sensitivity analysis as is done in the short term model set-up to derive the effect of a different time of disposal, grain size or execution method on the long term results as well.

9.2.3. General recommendations

Apart from specific recommendations for either measuring or modelling, some general recommendations are made as well, reflecting the SURICATES pilot study as a whole.

- **Different conditions**
  It is encouraged to execute this study under different hydrodynamic conditions. From de Nijs [2012] it is known that the distance from the head of the salt wedge to the mouth of the estuary mainly controls the amount of entrapped fluvial sediment. Apart from the tidal forcing, fresh water discharge and wind set-up in preceding days determines this distance. It is therefore recommended to compare the current model study for low discharge conditions with high discharge conditions, which is assumed to be beneficial for the efficiency of the SURICATES pilot study. For example, small amounts of trapping occurs typically after surges on the North Sea (after set-up events, water is temporarily stored in the basins and has to flow out), between spring and neap tide and during (very) high fresh water discharges.

- **Research in near field behaviour**
  The behaviour of the sediment plume in the near field, especially in combination with a stratified and shear flow, is subject to large uncertainties. In this thesis, the complex interaction of a sediment plume

in ambient flow has been hypothesised, mainly using observations done by de Wit [2015], for overflow plumes. However, these observations have been done for a sediment plume in non-stratified and uniform flow conditions. Van Eekelen [2007] found that the effect of stratification on sediment plume behaviour is limited to a reduced density difference between the sediment plume and ambient flow. However, the effect of turbulence damping and shear flow, which are profound in the Rotterdam Waterway, is not mentioned. Moreover, for a disposal by bottom door different near field effects may arise due to the sudden increase in concentration of SPM. As the sedimentation rate can be temporarily larger than the consolidation rate, fluid mud layers may arise. It is therefore recommended to investigate the effect of stratification and shear flow on sediment plumes, and the possible occurrence of fluid mud layers in the near field.

- **Bathymetry effects**
  Throughout the Rotterdam Waterway, local differences in bathymetry are noticed. Two profound differences in bathymetry are the sill construction underneath the Maeslantkering and the impact pit at the disposal location (see fig. 3.13 and fig. 3.7). The sill construction underneath the Maeslantkering has an estimated height of 1 m, possibly blocking a return flow of sediment. Next to the sill construction, a large pit has arisen at the disposal location, with a depth of approximately 2 m. This pit has arisen during the execution of the pilot study and is most likely caused by the impact of the disposals by bottom door. This pit may function as a local sediment trap, (temporarily) storing SPM. However, the exact role of this local sill and pit has to be investigated further.

Bibliography

D-Water Quality Manual. Technical report, Deltares, Delft, 2019.

Martin J. Baptist, T. Gerkema, B. C. van Prooijen, D. S. van Maren, M. van Regteren, K. Schulz, I. Colosimo, J. Vroom, T. van Kessel, B. Grasmeijer, P. Willemsen, K. Elschot, A. V. de Groot, J. Cleveringa, E. M.M. van Eekelen, F. Schuurman, H. J. de Lange, and M. E.B. van Puijenbroek. Beneficial use of dredged sediment to enhance salt marsh development by applying a 'Mud Motor'. *Ecological Engineering*, 127:312–323, feb 2019. ISSN 09258574. doi: 10.1016/j.ecoleng.2018.11.019.

M.J. Baptist, E.E. Van Eekelen, Grasmeijer B. Dankers, P.J.T., T. Van Kessel, and D.S Van Maren. Working with Nature in Wadden Sea Ports. *Coasts & Ports 2017 Conference – Cairns, 21-23 June 2017*, 2017.

Johannes Becker, Erik van Eekelen, Joost van Wiechen, William de Lange, Thijs Damsma, Tijmen Smolders, and Mark van Koningsveld. Estimating source terms for far field dredge plume modelling. *Journal of Environmental Management*, 149:282–293, 2015. ISSN 10958630. doi: 10.1016/j.jenvman.2014.10.022. URL `http://dx.doi.org/10.1016/j.jenvman.2014.10.022`.

M. Boot. *Near-field verspreiding van het overvloeiverlies van een sleephopperzuiger*. PhD thesis, Delft University of Technology, 2000.

W. Borst, T. Vellinga, and O. Van Tongeren. The Monitoring Programme for the Maasvlakte 2 Construction at the Port of Rotterdam - Part II. *Terra et Aqua*, (130):20–32, 2013.

J. Bosboom and M. Stive. *Coastal Dynamics I, Lecture Notes CIE4305*. Delft Academic Press (VSSD), 2015. ISBN 9789065623720.

H. Chanson. Mixing in estuaries, 2004.

G. J. de Boer. *On the interaction between tides and stratification in the Rhine Region of Freshwater Influence*. 2009. ISBN 9789090238487. URL `http://www.narcis.nl/publication/RecordID/oai:tudelft.nl:uuid:c5c07865-be69-4db2-91e6-f675411a4136{%}5Cnhttp://repository.tudelft.nl/view/ir/uuid:c5c07865-be69-4db2-91e6-f675411a4136/`.

G. J. de Boer, J. D. Pietrzak, and J. C. Winterwerp. On the vertical structure of the Rhine region of freshwater influence. *Ocean Dynamics*, 56(3-4):198–216, 2006. ISSN 16167341. doi: 10.1007/s10236-005-0042-1.

L H de Bruijn. Maintenance dredging in the port of rotterdam: A research to the increase in maintenance dredging volume at port of rotterdam, 9 2018.

S. de Groot. Suspended Sediment Modelling in the Port of Rotterdam. 2018.

J. M. de Kok. The influence of fresh water distribution on SPM transport in the Dutch coastal zone. *Proceedings in Marine Science*, 5(C):563–576, 2002. ISSN 15682692. doi: 10.1016/S1568-2692(02)80040-7.

M. A.J. de Nijs, J. C. Winterwerp, and J. D. Pietrzak. Chapter 25 SPM variations in a harbour basin. *Proceedings in Marine Science*, 9:357–378, 2008. ISSN 15682692. doi: 10.1016/S1568-2692(08)80027-7.

M. A.J. de Nijs, J. C. Winterwerp, and J. D. Pietrzak. On harbour siltation in the fresh-salt water mixing region. *Continental Shelf Research*, 29(1):175–193, 2009. ISSN 02784343. doi: 10.1016/j.csr.2008.01.019.

M. A.J. de Nijs, J. C. Winterwerp, and J. D. Pietrzak. The effects of the internal flow structure on SPM entrapment in the Rotterdam Waterway. *Journal of Physical Oceanography*, 40(11):2357–2380, 2010. ISSN 00223670. doi: 10.1175/2010JPO4233.1.

M. A.J. de Nijs, J. C. Winterwerp, and J. D. Pietrzak. Advection of the salt wedge and evolution of the internal flow structure in the rotterdam waterway. *Journal of Physical Oceanography*, 41(1):3–27, 2011a. ISSN 00223670. doi: 10.1175/2010JPO4228.1.

M. A.J. de Nijs, J. C. Winterwerp, and J. D. Pietrzak. An explanation for salinity- and SPM-induced vertical countergradient buoyancy fluxes. *Ocean Dynamics*, 61(4):497–524, 2011b. ISSN 16167341. doi: 10.1007/s10236-011-0375-x.

Michel A J de Nijs. *On sedimentation processes in a stratified estuarine system*. PhD thesis, Delft University of Technology, 2012.

Michel A.J. de Nijs and Julie D. Pietrzak. Saltwater intrusion and ETM dynamics in a tidally-energetic stratified estuary. *Ocean Modelling*, 49-50:60–85, 2012. ISSN 14635003. doi: 10.1016/j.ocemod.2012.03.004. URL `http://dx.doi.org/10.1016/j.ocemod.2012.03.004`.

L de Wit. Near field 3D CFD modelling of overflow plumes. (1989), 2010. URL `http://www.svasek.nl/news/WODCON{_}paper{_}LdeWit.pdf`.

L. de Wit. *3D CFD modelling of overflow dredging plumes*. PhD thesis, Delft University of Technology, 2015.

Lynyrd de Wit, Cees van Rhee, and Arno Talmon. Influence of important near field processes on the source term of suspended sediments from a dredging plume caused by a trailing suction hopper dredger: the effect of dredging speed, propeller, overflow location and pulsing. *Environmental Fluid Mechanics*, 15(1):41–66, 2014. ISSN 15731510. doi: 10.1007/s10652-014-9357-0.

J. Dronkers. Tidal asymmetry and estuarine morphology. *Netherlands Journal of Sea Research*, 20(2-3):117–131, 1986. ISSN 00777579. doi: 10.1016/0077-7579(86)90036-0.

D. Eisma, P. Bernard, G. C. Cadée, V. Ittekkot, J. Kalf, R. Laane, J. M. Martin, W. G. Mook, A. van Put, and T. Schuhmacher. SUSPENDED-MATTER PARTICLE SIZE IN SOME WEST-EUROPEAN ESTUARIES; PART I: PARTICLE-SIZE DISTRIBUTION. *Netherlands Journal of Sea Research*, 28(3):193–214, 1991a. ISSN 00777579. doi: 10.1016/0077-7579(91)90018-V.

D. Eisma, P. Bernard, G. C. Cadée, V. Ittekkot, J. Kalf, R. Laane, J. M. Martin, W. G. Mook, A. van Put, and T. Schuhmacher. Suspended-matter particle size in some West-European estuaries; part II: A review on floc formation and break-up. *Netherlands Journal of Sea Research*, 28(3):215–220, 1991b. ISSN 00777579. doi: 10.1016/0077-7579(91)90018-V.

V. M. Gatto, B. C. van Prooijen, and Z. B. Wang. Net sediment transport in tidal basins: quantifying the tidal barotropic mechanisms in a unified framework. *Ocean Dynamics*, 67(11):1385–1406, 2017. ISSN 16167228. doi: 10.1007/s10236-017-1099-3.

M E G Geraeds. *Modelling the hydrodynamics of an eco-innovative sediment reuse project in the Rotterdam Waterway*. PhD thesis, Delft Universtiy of Technology, 2020.

W Rockwell Geyer. The Importance of Suppression of Turbulence by Stratification on the Estuarine Turbidity Maximum. Technical Report 1, 1993.

H.C.M. Hendriks and F.P. Schuurman. Modellering alternatieve loswal locaties. page 54, 2017.

K. Huhn, A. Paul, and M. Seyferth. Modeling sediment transport patterns during an upwelling event. *Journal of Geophysical Research: Oceans*, 112(C10), 2007. doi: 10.1029/2005JC003107. URL `https://agupubs.onlinelibrary.wiley.com/doi/abs/10.1029/2005JC003107`.

Y. Huismans, C.F. van der Mark, J.J. van der Werf, and T. van Kessel. Effect verdieping Nieuwe Waterweg op vaargeulonderhoud. Technical report, 2013.

IOC SCOR. IAPSO: The international thermodynamic equation of seawater–2010: Calculation and use of thermodynamic properties, Intergovernmental Oceanographic Commission, Manuals and Guides No. 56. *UNESCO, Manuals and Guides*, 56:1–196, 2010.

D. A. Jay and J. D. Musiak. Particle trapping in estuarine tidal flows. *Journal of Geophysical Research*, 99:445–461, 10 1994.

W.M. Kranenburg. *Evaluatie van het OSR-model voor zoutindringing in de Rijn- Maasmonding (I), Onderdeel KPP B&O Waterkwaliteitsmodelschematisaties 2014*. Number Ii. 2015. ISBN 1209459000.

R.B. Krone. he significance of aggregate properties to transport processes. *Estuarine Cohesive Sediment Dynamics. Lecture Notes on Coastal and Estuarine Studies*, 14, 1986.

P. MacCready and W. R. Geyer. Advances in Estuarine Physics. *Annual Review of Marine Science*, 2(1):35–58, 2010. ISSN 1941-1405. doi: 10.1146/annurev-marine-120308-081015.

L.M. Merckelbach. A model for high-frequency acoustic doppler current profiler backscatter from suspended sediment in strong currents. *Continental Shelf Research*, 26(11):1316 – 1335, 2006. ISSN 0278-4343. doi: https://doi.org/10.1016/j.csr.2006.04.009. URL `http://www.sciencedirect.com/science/article/pii/S027843430600135X`.

K. Mohan. *Characterization of sediment from the Port of Rotterdam*. PhD thesis, Delft University of Technology, 2019.

H. B. Park and G. Hong Lee. Evaluation of ADCP backscatter inversion to suspended sediment concentration in estuarine environments. *Ocean Science Journal*, 51(1):109–125, 2016. ISSN 17385261. doi: 10.1007/s12601-016-0010-3.

L. Perk, R. Steijn, and J. Adema. Mer verdieping nieuwe waterweg en botlek achtergrondstudie morfologie. Technical report, 2015.

J.D. Pietrzak. Class Notes for CIE5302: An Introduction to Stratified Flows for Civil and Offshore Engineering. *Delft University of Technology*, pages 1–155, 2015.

PortofRotterdam. Workplan: Interreg project sediment uses as resources in circular and in territorial economies. (suricates), 2018.

W. Rodi. *Turbulent Buoyant Jets and Plumes*. Pergamon, 1982. ISBN 9781483189871.

M. Rotsaert. Afregeling OSR systeem Verificatie Zout. Technical report, Svasek, Rotterdam, 2010.

M. Rotsaert and E.A. Collard. Kwaliteitsbeoordeling OSR systeem Havenbedrijf Rotterdam Definitief Rapport. Technical Report april, Svasek Hydraulics, 2009.

M. G. Sassi, A. J.F. Hoitink, and B. Vermeulen. Impact of sound attenuation by suspended sediment on ADCP backscatter calibrations. *Water Resources Research*, 48(9):1–14, 2012. ISSN 00431397. doi: 10.1029/2012WR012008.

J. H. Simpson, J. Brown, J. Matthews, and G. Allen. Tidal straining, density currents, and stirring in the control of estuarine stratification. *Estuaries*, 13(2):125–132, 1990. ISSN 01608347. doi: 10.2307/1351581.

R. Spanhoff and P. A.J. Verlaan. Massive sedimentation events at the mouth of the Rotterdam Waterway. *Journal of Coastal Research*, 16(2):458–469, 2000. ISSN 0749-0208.

Jeremy Spearman, Arjan de Heer, Stefan Aarninkhof, and Mark van Koningsveld. Validation of the TASS system for predicting the environmental effects of trailing suction hopper dredgers. *Terra et Aqua*, 2016(125):14–22, 2011. URL `http://repository.tudelft.nl/view/ir/uuid:6f32ee7a-a54c-4286-995d-53126e5e2323/`.

Keith D Stolzenbach and Menachem Elimelech. The effect of particle density on collisions between sinking particles: implications for particle aggregation in the ocean. *Deep-Sea Research l,*, 41, 1994.

Stutterheim. van Noord tot Noordwest, Een studie naar de berging van baggerspecie op loswallen. Technical Report november, Rijksinstituut voor Kust en Zee/RIKZ, 2002.

Auke H. Tempel. Sediment traps for reducing maintenance dredging costs in the Port of Rotterdam. 2019.

W. Uijttewaal. Lecture notes turbulence in hydraulics cie5312, 2015.

Robert van Bruchem. Monstercampagne rotterdam 2019, 2019.

P.F. van Dreume. Slib- en zandbeweging in het noordelijk deltabekken : in de periode 1982-1992, 1995.

E. E. Van Eekelen. Experimental research on dynamic dredge overflow plumes. *Repository.Tudelft.Nl*, 2007. URL http://repository.tudelft.nl/assets/uuid:54829c36-b70d-48e1-a47f-cd8be008ca6c/ceg{_}vaneekelen{_}2007.pdf.

E.E. Van Eekelen, P.J.T. Grasmeijer B. Baptist, M.J. Dankers, T. Van Kessel, and D.S Van Maren. Muddy Waters and the Wadden Sea Harbour. *WODCON XXI Proceedings of the Twenty-First World Dredging Congress, June 13–17, 2016*, 2016.

T.hijs Van Kessel and doi = 10.1016/j.csr.2010.04.008 file = :C\:/Users/Daan/Documents/Afstuderen/Literatuur_Daan/Artike ed/VanKessel_2010_Modelling theseasonaldynamicsofSPMwithasimplealgorithm.pdf:pdf issn = 02784343 journal = Continental Shelf Research keywords = 3D model Seasonal,Bed algorithm,Dynamics,North sea,Suspended sediment number = 10 SUPPL. pages = S124–S134 publisher = Elsevier title = Modelling the seasonal dynamics of SPM with a simple algorithm for the buffering of fines in a sandy seabed url = http://dx.doi.org/10.1016/j.csr.2010.04.008 volume = 31 year = 2011 Winterwerp, J C.

L. C. Van Rijn. *Manual sediment transport measurements in rivers, estuaries and coastal areas*. Aqua publications, the Netherlands, 2006. ISBN 9080035688.

S.ubhas K. Venayagamoorthy. On the flux Richardson number in stably stratified turbulence. *Journal of Fluid Mechanics*, 798(July):R1, 2016. ISSN 14697645. doi: 10.1017/jfm.2016.340.

T. Vijverberg, P. Dankers, and T. van Kessel. Grootschalige slibverspreiding uit loswallen. (december), 2015.

J. C. Winterwerp. Near-field behavior of dredging spill in shallow water. *Journal of Waterway, Port, Coastal and Ocean Engineering*, 128(2):96–98, 2002. ISSN 0733950X. doi: 10.1061/(ASCE)0733-950X(2002)128:2(96).

J. C. Winterwerp. Stratification effects by fine suspended sediment at low, medium, and very high concentrations. *Journal of Geophysical Research: Oceans*, 111(5):1–11, 2006. ISSN 21699291. doi: 10.1029/2005JC003019.

J. C Winterwerp and W. G. M. Kesteren. Introduction to the physics of cohesive sediment in the marine environment, 2004. URL http://site.ebrary.com/id/10169872.

J. C. Winterwerp and T. Van Kessel. Siltation by sediment-induced density currents. *Ocean Dynamics*, 53(3):186–196, 2003. ISSN 16167341. doi: 10.1007/s10236-003-0038-7.

J. C. Winterwerp, A. W. Bmens, N. Gratiot, C. Kranenburg, M. Mory, and E. A. Toorman. Dynamics of Concentrated Benthic suspension layers. *Proceedings in Marine Science*, 5(C):41–55, 2002. ISSN 15682692. doi: 10.1016/S1568-2692(02)80007-9.

J.C. Winterwerp and B.C. van Prooijen. Lecture notes sediment dynamics, 2015.

M Zijlema. Class Notes for CIE4340: Computational modelling of flow and transport. *Delft University of Technology*, pages 1–178, 2019.

V

Appendix

A

Introduction

A.1. Human interventions in the port of Rotterdam

Over the course of time several changes have been made in the port of Rotterdam. Below a timeline with the most important events since 2008 is given.

- 2008: Start construction of Maasvlakte 2
- 2011: Start construction of Sand Engine
- 2011: Connection of Maasvlakte 2 with Maasvlakte 1
- 2016: Widening of the Breeddiep
- 2019: Deepening of the Rotterdam Waterway and Botlek

For the SURICATES project the deepening of the Rotterdam Waterway has the largest impact. Between the Maasmond and the Botlek, up to the Beneluxtunnel the Rotterdam Waterway has been deepened with 1.5 meters increasing the accessibility of the port. Increasing the Nautical guaranteed depth from -15.0 m to -16.3 m NAP. In Perk et al. [2015] the expected effects are investigated in the context of an EIA for the deepening of the Rotterdam Waterway and Botlek. In this report is concluded that the amount of water flowing in increases and fresh water runoff decreases. It is expected that the amount of sediment to be dredged will increase with 10 % to 20% in the Rotterdam Waterway and New Meuse. This is in agreement with the assessment performed in 2013, Huismans et al. [2013]. In this latter assessment an increased tidal asymmetry is found in combination with a small increase in salinity. Moreover, an increase in siltation of 10 % for the Botlek is predicted as the exchange volume increases in the same order. However, as the ETM moves further upstream due to increased tidal asymmetry the amount of available silt may decrease for the Botlek.

From de Bruijn [2018] it is known that the increased amount of dredged sediment may be contributed to a redistribution of sediment rates within the CaBe-system (CallandBeerkanaal-system). This redistribution is related to the increase horizontal flow velocities after the construction of the Maasvlakte 2.

A.2. Previous pilot studies

The reallocation of sediment within the port has been executed before. In 2008 a small-scale experiment with $80.000 m^3$ (current pilot study aims at $500.000 m^3$) has been executed, however due to the small amounts no conclusions have been drawn from this experiment. In 2009 another pilot study has been executed, in this case with $500.000 m^3$. During 4 weeks (current pilot study has a duration of 16 weeks), the silt has been reallocated in a predetermined site close to Maassluis, which is in accordance to the new pilot study [PortofRotterdam, 2018].

From the 2009 pilot study a few conclusions and recommendations have been drawn;

- **Conclusions**
  - The nautical depth has been guaranteed throughout the reallocation, despite its high disposal rate.
  - Additional dredging is limited to 20 % of the reallocated sediment.
  - The sediment has spread over a relative large area which is in accordance with the model results
- **Recommendations**
  - More theoretical background is required to consider different/better reallocation locations
  - Repeating the pilot can enhance theoretical knowledge and improve long term understanding.

In the research proposal these recommendations and conclusions have been taken into account.

A.2.1. Port of Rotterdam

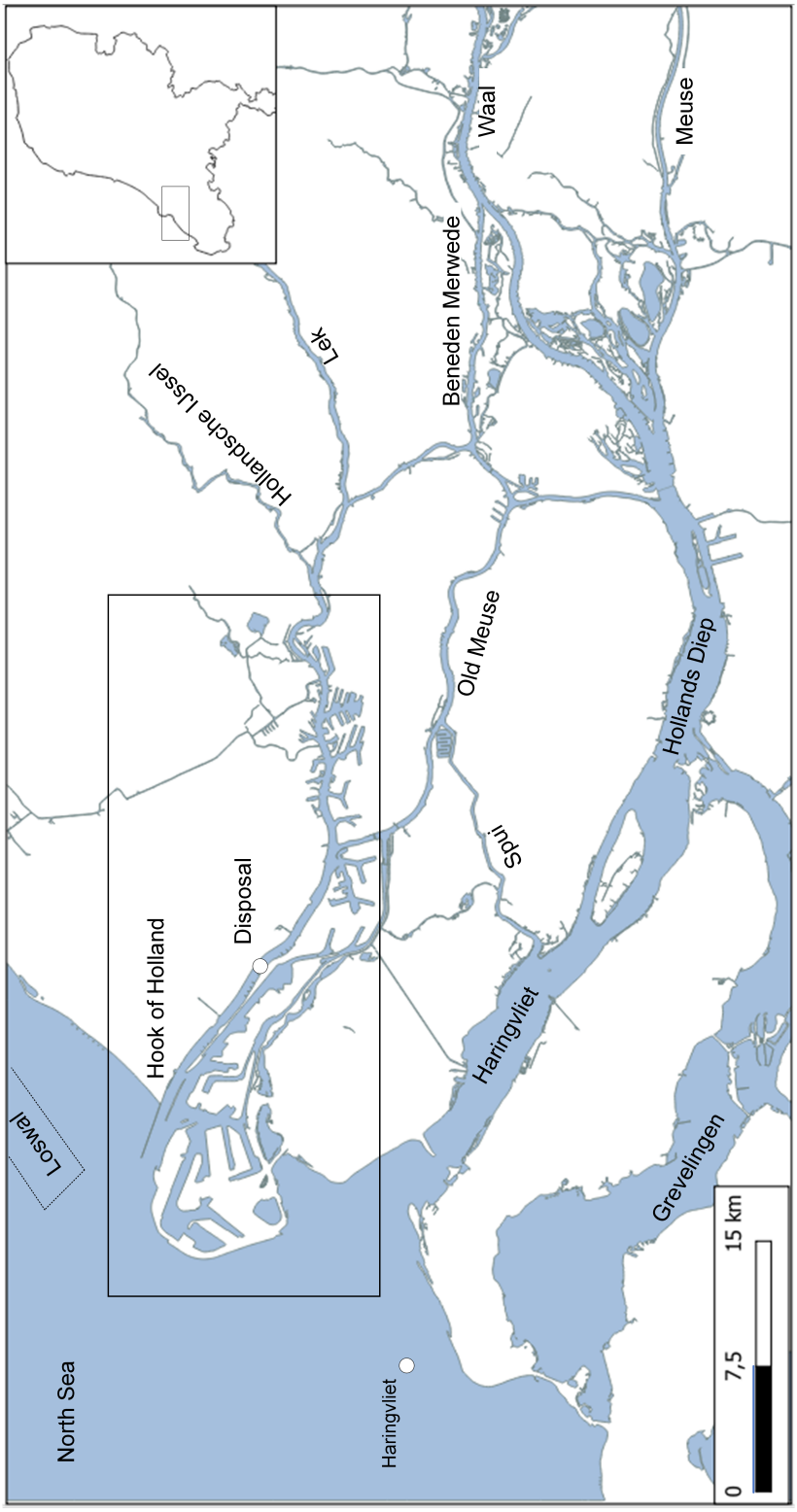

Figure A.1: Map of the region around the Port of Rotterdam including its surrounding rivers.

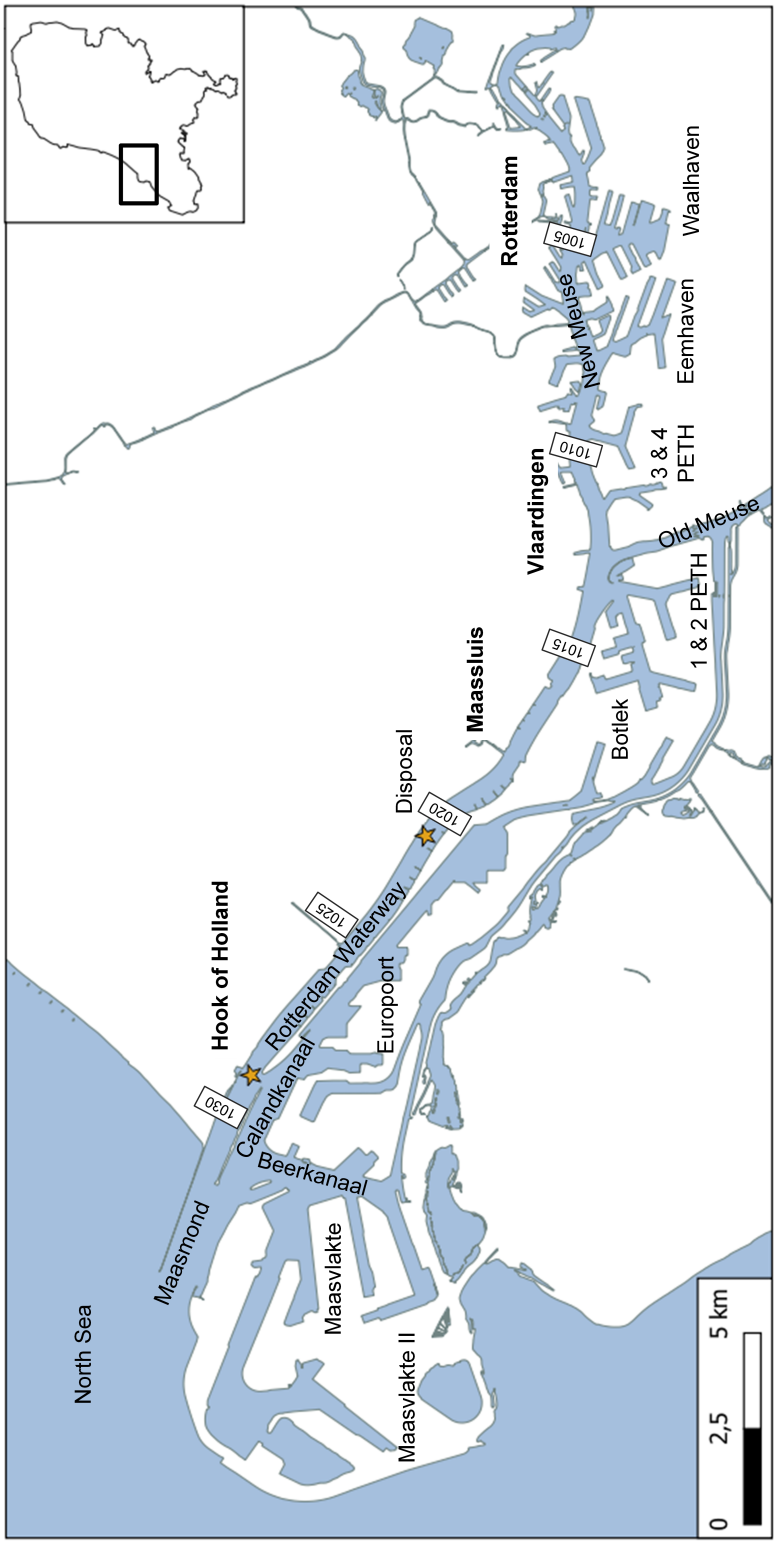

Figure A.2: Map of the Port of Rotterdam including points of interest and the river kilometres.

B

Literature

B.1. Hydrodynamics

B.1.1. Dynamics of the Rhine ROFI

At locations where fresh water is discharged into coastal waters, a Region Of Freshwater Influence (ROFI) arises. Such areas are characterized by fresh water bulges floating on top of the saltier water due to density differences.

de Boer [2009] found cold water at the surface in the coastal zone of the Rhine-ROFI during summer conditions which he attributed to *upwelling* taking place in ROFI due to a combination of thermal wind and tidal straining. The occurrence of upwelling and downwelling is explained as following; for stratified conditions during neap tide the tidal currents exhibit strong cross-shore components; with a velocity difference up to 0.7 m/s. The tidal current during stratified periods is described by ellipses at the surface in the anti-cyclonic direction (= clockwise) and at the bottom layer ellipses in the cyclonic direction (=anti-clockwise). The consequence is a strong exchange flow over the vertical as shown in fig. B.2. However, during well-mixed conditions the tidal currents alongshore are rectilinear, hence the schematizing shown in fig. B.2 is only valid for stratified conditions as no cross-shore currents arise during mixed conditions. Or as stated by de Boer [2009], during well-mixed conditions there is no interaction between the alongshore Kelvin wave velocities and the dominant cross-shore density gradient. In the paper two different explanations for the ellipses over the vertical are given. Due to Coriolis all flows are directed towards the right on the Northern Hemisphere, however the magnitude of the Coriolis force is proportionate to the flow velocity, leading to different deflection angles of the velocity vectors over the vertical (as the flow velocity varies with depth). Combined with continuity requirements at the coastal wall, this leads to opposing directions for the current at the surface and at the bottom. For well-mixed conditions this effect is inhibited as the velocity gradient diminishes under the influence of turbulence, see fig. B.1.

Apart from the periodic behaviour on the tidal time scale (semi-diurnal and spring-neap cycle) stratification and well-mixed conditions may arise due to events of increased river run-off (leading to stronger stratification) or due to storm events (leading to stronger mixing). As tidal upwelling is a current from the lower layers to the surface, its significance is a net flux of SPM towards the coast and towards the Rotterdam Waterway. (Winterwerp and van Prooijen [2015]).

Mixing vs. stratification

In ROFI's and estuaries, a continuous process of competition between stratification and mixing takes place. In general stratification is driven by estuarine circulation and tidal straining, whereas mixing is caused by wind, waves, river discharge and tidal stirring. Due to the aforementioned processes the Rhine ROFI and Rotterdam Waterway continuously changes between a well-mixed and stratified state. [Pietrzak, 2015]. In general the Rhine ROFI is well-mixed during spring tides and storm conditions.[de Boer, 2009]

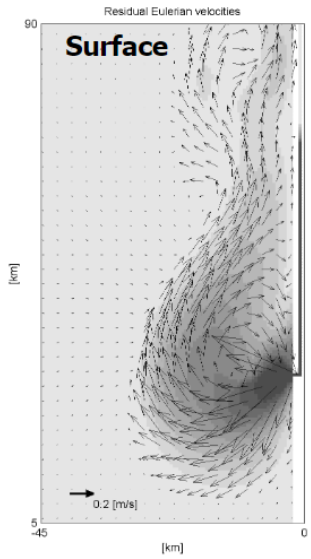

(a) Residual current in the surface layer of the Rhine-ROFI

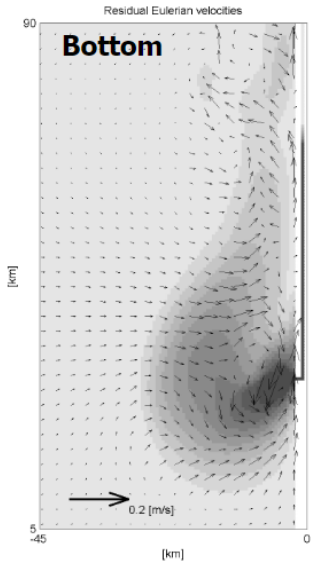

(b) Residual current in the bed layer of the Rhine-ROFI

Figure B.1: The flow patterns as found in the Rhine ROFI. While sediment remains in suspension it is likely to follow the pathway of the surface currents, while resuspended sediment is more likely to follow the pathway of the bed currents.[de Boer et al., 2006]

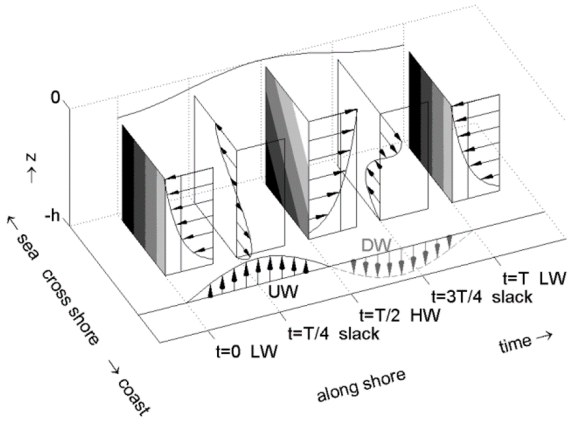

Figure B.2: Schematization of up- and downwelling due to tidal straining for stratified conditions. [de Boer, 2009]

B.1.2. Baroclinic effects

Reduced gravity

In stratified flow conditions a particle experiences less gravity compared to homogeneous flow conditions. The reduced gravity (g') is used to determine the internal wave speed and internal buoyancy. The reduced gravity can be calculated as following [Pietrzak, 2015]:

$$g' = \frac{\rho_2 - \rho_1}{\rho_2} g \tag{B.1}$$

In which ρ_1 is the smaller density and ρ_2 the larger density.

Buoyancy frequency

The buoyancy frequency is defined as the frequency of the movement of a disturbed particle in the vertical driven by density differences. In other words, the frequency of the motion of a 'heavy' particle moving towards the lower layer (due to gravity) and movement upwards as part of its oscillation. The frequency is given in eq. (B.2) and depends on the reference density (ρ_0) and the density gradient over the vertical. [Pietrzak, 2015]

$$N^2 = -\frac{g}{\rho_0} \frac{\partial \rho}{\partial z} \tag{B.2}$$

Richardson number

The *Richardson number* is used in various formulations to indicate relations between density differences and the stability of the flow under these circumstances. The following types of Richardson number are explained below:

- Richardson number or gradient Richardson number
- Flux Richardson number

Gradient Richardson number The Richardson number is an indication for the stability of stratified flows. The formulation depends on the amount of kinetic energy and potential energy and is depth dependent. And can be seen as the amount of stratification (nominator) divided by the amount of turbulence (denominator), using mixing length theory. When the amount of generated turbulence is larger than the damping of turbulence, the turbulent mixing layer grows. In stable conditions the amount of generated turbulence equals the damping of turbulence.

The formulation is given as following;

$$Ri = \frac{-g \frac{\partial \rho}{\partial z}}{\rho (\frac{\partial u}{\partial z})^2} = \frac{N^2}{(\frac{\partial u}{\partial z})^2} \tag{B.3}$$

In which;

- $Ri < 0$: Statically unstable
- $Ri = 0$: Homogeneous substance; no stratification
- $0 < Ri < 1/4$: Unstable stratification
- $Ri > 1/4$: Stable stratification

In which stable stratification is defined as the condition in which the lower layer is the heaviest layer and any heavy particle in the upper layer is transported back to this lower layer.

In unstable stratification the vertical shear in the flow is large enough to cause Kelvin-Helmholtz instabilities. At first the shear at the interface between the two layers causes waves to form, as the velocity shear may

overcome the tendency of the fluid to remain stratified. These waves become asymmetric and skewed due to non-linear effects and eventually break. Leading to a lot of mixing [Pietrzak, 2015].

Flux Richardson number *The flux Richardson number (Ri_f)* is mostly used to define the mixing efficiency for a stably stratified fluid. It is a measure of the amount of kinetic energy that has been irreversibly converted, mostly from Available Potential Energy to Background Potential Energy by turbulent mixing. And is hence defined as the ratio of the buoyancy flux (B) which is driven by APE and the production rate of turbulent kinetic energy (P) [Venayagamoorthy, 2016].

$$Ri_f = \frac{B}{P} = -\frac{g\overline{w'\rho'}}{\rho\overline{u'w'}\partial u/\partial z} \tag{B.4}$$

B.2. Differential advection

When the velocity varies in a plane of reference e.g width or depth, this is referred to as shear flow conditions. In such cases, the distribution of the concentration of a solvent (e.g. the distribution of SPM) can be altered by the difference in velocity. In fig. B.3 it can be seen that the distribution of an concentration of a solvent is distorted; the initial concentration at the top is advected further in the x-direction than at the bottom due to the larger flow velocity. This is called shear dispersion, caused by differential advection. Additionally diffusion takes place, shown in fig. B.3 as third step.

In formula, the the shear dispersion equation reads as following;

$$\underbrace{\frac{\partial c}{\partial t}}_{\text{Concentration change in time}} + \underbrace{u(y)\frac{\partial c}{\partial x}}_{\text{Differential advection}} = \underbrace{D\frac{\partial^2 c}{\partial y^2}}_{\text{Transverse diffusion}} \tag{B.5}$$

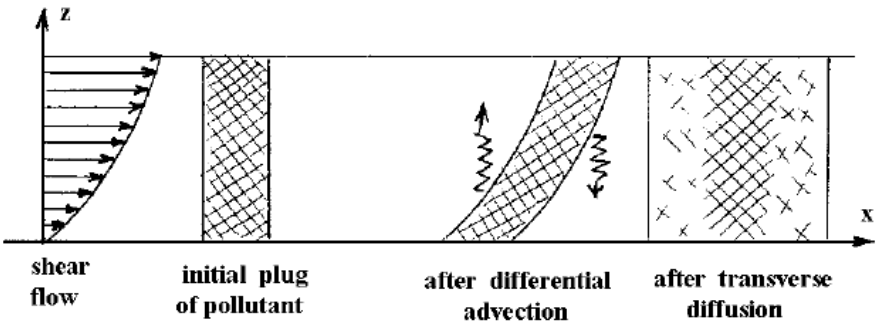

Figure B.3: Schematization of Shear-dispersion equation, separating the processes of differential advection and transverse diffusion [Chanson, 2004].

B.2.1. Coriolis parameter

The Coriolis parameter is an approximation of the Coriolis force on a particle induced by the rotation of the earth in which the force is assumed to be constant with latitude. Therefore the force depends on the latitude (φ) and the Earth's angular velocity (Ω) [Pietrzak, 2015].

$$f = 2\Omega sin(\varphi) \tag{B.6}$$

B.3. Sediment dynamics

B.3.1. Material and transport properties

As indicated in fig. B.4 for sediment transport a distinction can be made according to either the origin of the material or the way it is transported. For this distinction often the following terms are used; *wash load, bed material load, bed-load transport* and *suspended load transport.*

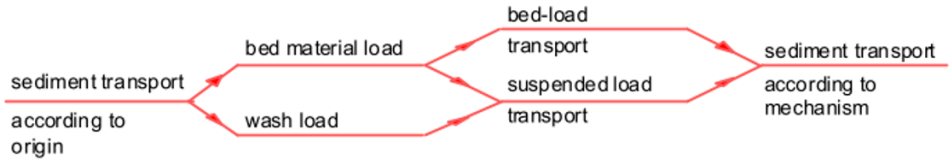

Figure B.4: The classification of different transport modes based on origin or mechanism [Winterwerp and van Prooijen, 2015]

According to origin of the sediment a distinction can be made between bed material load and wash load. Wash load is very fine sediment supplied from upstream with very low settling velocities kept in suspension by local turbulence. As this material is not encountered in the bed the distinction in name is made based hereon. Equilibrium in the water column is found when the amount of particles go upwards as fall downwards (Turbulent flux = falling) Moreover no exchange with the bed occurs. Bed material load is the sediment found in the bed and can be transported close to the bed as bed-load transport due to rolling, sliding and saltation or as suspended load transport. In contrast, Wash load can only be transported as suspended transport [Winterwerp and van Prooijen, 2015].

B.3.2. Sediment classification

Sediment is classified using the classification as stated in the NEN-5104.

Particle	Size	Settling Velocity	Settling Velocity
Clay	$< 2.0\,\mu m$	$< 0.003\,mm/s$	$< 0.26\,m/d$
Silt	$2.0 - 60\,\mu m$	$0.003 - 3.1\,mm/s$	$0.26 - 270\,m/d$
Fine sand	$60 - 200\,\mu m$	$3.1 - 34.2\,mm/s$	$270 - 3,000\,m/d$
Medium sand	$200 - 600\,\mu m$	$34.2 - 300\,mm/s$	$3,000 - 26,000\,m/d$
Coarse sand	$600 - 2,000\,\mu m$	$300 - 3,420\,mm/s$	$26,000 - 300,000\,m/d$
Gravel	$> 2,000\,\mu m$	$> 3,420\,mm/s$	$> 300,000\,m/d$

Table B.1: Sediment classification based on grain-size, according to NEN-5104 ([Winterwerp and Kesteren, 2004])

B.3.3. Particle Reynolds number

Particle Reynolds number (Re_p) is a measure of the settling velocity (W_s) of the particle and its diameter (D) related to the viscosity (μ) of the surrounding fluid.

$$Re_p = \frac{DW_s}{\mu} \tag{B.7}$$

B.3.4. Flocculation

As suspended fine particles, or wash load, from the rivers mix with seawater in estuaries it becomes mutually cohesive. As particles become cohesive, particles may bound together under forcing to form larger particles in a process called aggregation. In Krone [1986] a distinction between different aggregation processes is made in which irreversible (under marine conditions) aggregation is called coagulation; these first mud particles are the smallest aggregates in nature. Flocculation is a reversible process and is the process of aggregating particles into flocs and floc break-down at the same time. Flocculation is governed by the

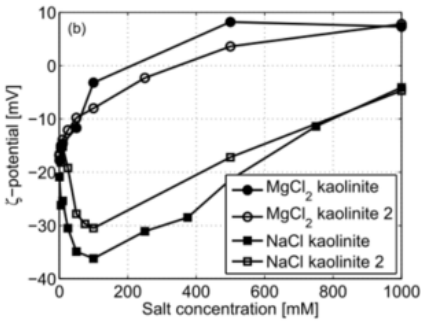

(a) ζ-potential for different salt-mineral combinations in different salt concentrations. In general the zeta potential is closest to 0 for increasing salt concentrations. [Winterwerp and van Prooijen, 2015]

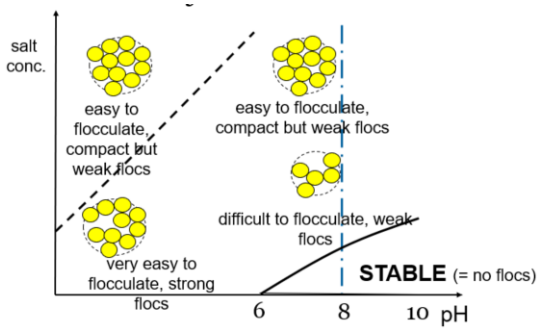

(b) Floc formation for different salinity and acidity. In marine environments the pH is constant:8. (Blue line)

Figure B.5: ζ-potential and type of flocs for different salinity and acidity. [Winterwerp and van Prooijen, 2015]

following three processes; Brownian motion, differential settling and velocity gradients. Brownian motions (random small fluctuations of a particle) causes particles to collide to form aggregates and is closely linked to turbulence inducing these random motions. As these first aggregates have a larger settling velocity these particles will overtake the smaller particles (differential settling) causing more collisions. Turbulence (or velocity gradients) will enhance the random motion of the particles and enhance further collisions. However due to turbulent shear, turbulence may cause floc break-up as well. In Stolzenbach and Elimelech [1994] it is concluded however, that in marine environments such as estuaries, the effect of Brownian motions and differential settling is much smaller than of turbulence and therefore negligible. [Winterwerp and Kesteren, 2004]

The rate of formation of these floc particles depends on, a.o. the concentration of suspended particles, the strength of the interparticle cohesion, the salinity, the acidity (pH) and the hydraulic stresses applied on the aggregates. For small shear rates, the mean particle size increases at first (since it enhances collision), but decreases for larger values (as it causes floc break down), whereas the floc size increases with an increasing amount of suspended particles.

These particles are bound together by Van Der Waals forces. Originally clay particles are negatively charged at the surface and hence repulsing one another. However in an estuarine environment these particles are neutralized, i.e. the anions at the surface of the clay particle bind with the cations (e.g. sodium ions in seawater). Therefore, if the amount of cations is too little, the suspension is stable; the particles disperse due to Brownian motion and do not settle. [Winterwerp and Kesteren, 2004]

To measure the repulsion or attraction between different particles the $\zeta - potential$ parameter can be used. In general floc formation, and floc strenght depends on acidity (pH), the salinity, the valence and the distance between the particles. The $\zeta - potential$, is a function of the first three aforementioned . For zero $\zeta - potential$, the net repulsion is zero and particles aggregate easy and quickly. For negative $\zeta - potential$ a very open floc structure arises as the particle-particle contact is edge-to-face.

Although not a very common method nowadays, the $\zeta - potential$ is a very useful parameter to determine the capability or floculation conditions of suspended sediment to form flocs.

These formed flocs, which can be ten to thousands bounded clay particles have large open structures due to the large water content of flocs (80 to 98 % of the total volume). Therefore floc behaviour is very different from the behaviour of the individual particles it is made of.

As can be seen in fig. 2.5, a floc can either settle or break-up. In general it is assumed that the maximum floc size is related to the Kolmogorov length scale (λ_k). For particles larger than the Kolmogorov length scale, (see section 2.1.2), turbulent stresses increases rapidly leading to break-up of the particle. Typical values for the Kolmogorov length scale in estuaries range from 0.1 to 1.0 mm. [Winterwerp and Kesteren, 2004] [Winterwerp and van Prooijen, 2015]

In the Rotterdam Waterway the effect of flocculation is negligible. This is shown by Eisma et al. [1991b],

but can also be derived from appendix G.3.2 in which the ζ-potential for various samples in the Rotterdam Waterway is analysed.

B.3.5. Hindered settling

In general, for increasing SPM concentrations settling velocities increase due to increased flocculation. However for higher concentrations of SPM, also Hindered settling occurs, reducing the effective settling velocity. Over the vertical in general a lutocline occurs; above the lutocline small SPM concentrations are found and hence large fall velocities. Below the lutocline the high SPM concentrations are encountered with low settling velocities due to hindered settling. Due to the high SPM concentrations below the lutocline, vertical mixing is limited due to turbulence damping; decreasing the settling velocity even further. Due to the combined effect of hindered settling, turbulence and flocculation it is very difficult to determine the settling velocity for fine cohesive sediments. Typical median velocities range from $0.001 mm/s$ for non flocculated sediment to $10 mm/s$ from in-situ measurements. [Winterwerp and van Prooijen, 2015]. In Winterwerp [2006] eq. (B.8) is derived to account for hindered settling, with w_{s0} being the non-hindered settling velocity, ϕ the ratio between the concentration and the gelling concentration ($\phi = c/c_{gel}$). c_{gel} equals $\approx 60 g/l$ in the Rotterdam Waterway. The significance of the gelling concentration is further explained in section 2.2.1. [Winterwerp and Van Kessel, 2003]

$$w_s = (1-\phi)^5 w_{s0} \tag{B.8}$$

The gelling point is the sediment concentration where the mixture of water and sediment flocs form a supportive network in which the flocs supports each other. The gelling concentration is derived by Winterwerp and Kesteren [2004] by using a flocculation model, see eq. (B.9).

$$c_{gel} = \rho_s \left(\frac{D}{D_p} \right)^{(3-n_f)} \tag{B.9}$$

In which ρ_s equals the density of sand, D_p the individual particle size, D_f the floc size size and n_f the fractial dimension.

B.3.6. Rouse-profile

The *Rouse profile* describes the distribution of SPM over the vertical in equilibrium conditions ($\frac{dc}{dt} = 0$) and therefore is a balance of the amount of turbulent mixing (keeping the SPM in suspension) and settling. In general mixing tries to homogenize a suspension to obtain equal concentration distribution whereas settling causes the particles to fall. Hence an equilibrium concentration profile over the vertical can be derived by the following balance, in which ϵ equals the turbulent diffusivity (see section 2.1.2).

$$\underbrace{w_s c}_{\text{Settling flux}} = \underbrace{\epsilon_{T,z} \frac{dc}{dz}}_{\text{Turbulence flux}} \tag{B.10}$$

However the following assumptions have to be valid to apply the Rouse profile.

- Steady flow in a uniform channel
- Constant and uniform density
- Parabolic eddy viscosity profile
- Constant and uniform settling velocity
- Constant and uniform Schmidt number

In general, none of these assumptions are valid in case of stratified flows, such as the Rhine-Meuse estuary.

B.3.7. Marine sedimentation in the port

In Spanhoff and Verlaan [2000] massive sedimentation events at the Maasmond, the mouth of the port, are investigated. In this paper a correlation is found between storm events at sea and increased sediment concentrations in the Maasmond. This is explained as following; during storm conditions, high waves lead to strong wave induced bed shear stresses within the wave boundary layer. The amount of shearing within this boundary layer is extremely high and able to induce a homogenous distribution of resuspended mud and fine sand within the boundary layer. This layer is named the Wave-Induced High Concentration Suspension Layer (WI-HCSL). Above the boundary layer the amount of turbulence is limited; hence the carrying capacity of the flow limited. This results in a sediment stratification with high SPM concentrations close to the bed. After a storm event (when the Rhine ROFI is well-mixed) a fluid mud layer arises with densities up to $1.200 kg/m^3$, with concentrations ranging between 10 to 300 g/l. This fluid mud layer can reach a thickness of 2m shortly after a storm event floating over the sandy bed, but under average conditions has a thickness of a few decimeters. The movement of this boundary layer follows the tide, with a residual direction towards the Maasmond, as is discussed in appendix B.1.1. It is assumed that the mobilization of the fluid mud layer is not caused by the fluidization of mud layers in the seabed as the amount of mud in the North Sea is deemed to be insufficient. With increasing river discharge, stratification is increased and thus the strength of the residual flow and size with net landward directed flow increases. Spanhoff and Verlaan [2000] also concludes that turbulence induced by current shearing is not sufficient in the area of interest, relating the import of sediment to the high waves.

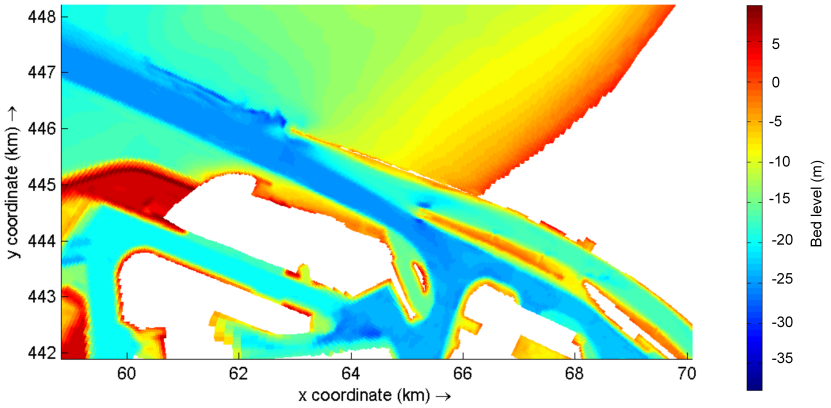

Figure B.6: Bathymetry differences in the Maasmond. The entrance to the Rotterdam Waterway is shallower than the entrance to the Calandkanaal and Beerkanaal.

When this layer enters the Maasmond, the amount of turbulence is limited due to reduced wave activity, forming a fluid mud layer as the sediment starts to settle. Within the Maasmond two distinct channels can be observed, the mouth of the Rotterdam Waterway in the north bank and the mouth of the Beerkanaal/Calandkanaal at the south bank, see fig. 2.12. Due to the freshwater discharge in the northern branch depth-averaged ebb velocities reach $1.0-1.2\ m/s$ (seaward directed) and $0.35-0.45\ m/s$ during flood (landward directed). In the southern part of the Maasmond the depth-averaged tidal currents equal $0.5\ m/s$ on both flood and ebb tide, but decreases more landward to $0.2-0.4\ m/s$. The peak flood and ebb velocities in the northern branch are 2 hours delayed allowing little exchange between the northern and southern branch. This large difference in tidal peak velocities explains the difference in settling behaviour in the northern and southern branch of the mouth. Moreover, due to difference in bathymetry, see fig. B.6, the fluid mud layer will not enter the Rotterdam Waterway. Explaining the fluvial origin of the sediment found in the harbour basins lining the Rotterdam Waterway. [de Nijs et al., 2010][Spanhoff and Verlaan, 2000]

If particles settle within the Rhine ROFI, two mechanisms may entrain them from the bed; upwelling and wave induced bed shear stresses. In appendix B.1.1 is described that up and downwelling events occur in the Rhine ROFI. In Huhn et al. [2007] is shown that upwelling events in general, not specific in the Rhine ROFI, may lift the fine material to the surface. As the residual flow in the surface flow is directed towards the north, upwelling events are beneficial to limit return flows towards the Maasmond. In section 2.2.3 the roles on the sedimentation of the port of Rotterdam is discussed. The combined effect of wave induced bottom shear stresses and the direction of the near-bed residual flow, drives the large fluxes of (fluvial) SPM towards

the Maasmond, in the form of fluid mud layers. In Hendriks and Schuurman [2017] the importance of the wave conditions is distressed; it is concluded that 62.4 % of the SPM transport at sea occurred in 6 % of time. The reason is twofold; under mild conditions SPM settles, increasing the SPM stored in the bed. During a subsequent storm the majority is eroded and resuspended.

From the same study and from de Kok [2002] is known that the return flow from the Loswal locations is limited during low freshwater discharge conditions, which is explained with a reduced lock exchange mechanism; low freshwater discharges reduce the bed current towards the Maasmond.

The amount of SPM being resuspended is, apart from the wave conditions, determined by the consolidation rate of the sediment in the bed. An abundance in unconsolidated silt leads to much larger SPM peak during a storm than well consolidated silt for a comparable wave condition. The amount of consolidation is based on the type of sediment and the 'history' of the sediment; erosion and sedimentation conditions over the past. From Hendriks and Schuurman [2017] it is also known that the sediment stays can be stored in the system up to 10 years.

Upon arrival at the Maasmond, the sediment, in the form of fluid mud layers mostly settles in the Maasmond or is diverted into the Calandkanaal and Beerkanaal. This concept is supported with the lack of marine sediment found inside the harbour basins lining the Rotterdam Waterway.

In Hendriks and Schuurman [2017] is found in model studies that siltation towards the Maasmond can be split into equal portions of a consistent baseload and peak loads with a sedimentation rate up to 10x the baseload; 62.4 % of the SPM transport at sea occurred during 6 % of time. In this study is also concluded that the correlation between siltation rates and wave induced bottom shear stresses are the largest. In this study is hypothesized that difference in siltation rates can be caused by variations in available sediment rather than hydrodynamic conditions.

For the influence of the freshwater discharge a strong correlation between high freshwater discharges and siltation rates in the Maasmond is found. This is explained by two driving mechanisms; an increased discharge means a higher supply of fluvial sediment from upstream. The other mechanism is explained using the phenomena of the increased lock exchange mechanism; for high river discharges the flow towards the Maasmond and in the Rotterdam Waterway close to the bed is increased. The latter mechanism is found to be dominant. [Hendriks and Schuurman, 2017]

C

Sediment plume behaviour

C.1. Buoyant jet behaviour

Because the settling velocity of the sediment within a dredging plume is significantly smaller than the initial vertical velocity of a dredging plume (W_{j0}) a dredging plume initially behaves like a turbulent negative buoyant jet in cross flow (*JICF*). At least in the initial phase. Other examples of a JICF are chimney plumes and wastewater outlets.

In the near field a distinction is made between plume behaviour and jet behaviour to describe JICF behaviour. Upon release the buoyant JICF contains vertical velocity only. However, moving downstream with the plume the buoyant jet will bend in the direction of the cross flow: i.e. the horizontal velocity increases due to the cross flow. Initially the behaviour is mainly governed by the initial momentum of the JICF, but moving downstream buoyancy governs the main behaviour of the plume. This ratio: initial momentum vs. momentum generated by buoyancy is used to define a difference in expected behaviour of a JICF: jet like behaviour or plume behaviour. This ratio is based on the ratio of initial momentum (eq. (C.5)) and momentum created by buoyancy effects, (eq. (C.6)) [Rodi, 1982].

- **Jet:** The initial momentum of the plume is larger than the generated momentum by buoyancy effects.
- **Plume:** The momentum created by buoyancy effects is larger than its initial momentum; buoyancy dominates.

Over time and space all buoyant jets turn into plumes, as more buoyancy will be transferred into momentum. Rodi [1982] defined several lengths scales to indicate this transition, see (eq. (C.1) until eq. (C.6)).

$$l_m = \frac{(Q_{j0}W_{j0})^{3/4}}{B_{j0}^{1/2}} \tag{C.1}$$

$$z_M = \frac{(Q_{j0}W_{j0})^{1/2}}{u_{cf}} \tag{C.2}$$

$$z_B = \frac{B_{j0}}{u_{cf}^3} \tag{C.3}$$

$$z_C = z_M \left(\frac{z_M}{z_B}\right)^{1/3} \tag{C.4}$$

$$Q_{j0} = \frac{1}{4}\pi D_{j0}^2 W_{j0} \tag{C.5}$$

$$B_{j0} = \frac{\Delta\rho_0}{\rho_{cf}} g Q_{j0} \tag{C.6}$$

In which, Q_{j0} is the initial volume flux, B_{j0} the initial buoyancy flux, $\Delta\rho_0 = (\frac{\rho_{of}-\rho_w}{\rho_w})$, the density difference between the ambient water (ρ_{cf}) and overflow density (ρ_{of}), W_{j0} the initial velocity of the sediment plume and u_{cf} the cross flow velocity which is the superposition of the vessel velocity and flow velocity; $u_{cf} = u_a + u_{TSHD}$.

With these length scales (l_m, z_M, z_B and z_C) a distinction can be made between jet, plume, bent over jet

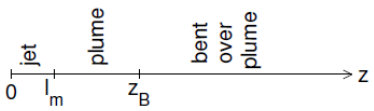

(a) The different length scales if $z_B > z_M$

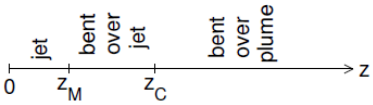

(b) The different length scales if $z_M > z_B$

Figure C.1: The different length scales and flow regimes defining the sediment plume behaviour of a JICF [de Wit, 2015].

	$\Delta\rho_0$ $[kg/m^3]$	D_{j0} $[m]$	u_{cf} $[m/s]$	W_{j0} $[m/s]$	Ri_p $[-]$	ζ $[-]$	l_m $[m]$	z_M $[m]$	z_B $[m]$
Overflow	40 - 90	1.5 - 4.0	0 - 4.0	0.5 - 1.5	0.1 - 10	0 - 8.0	0.7 - 7.5	0.2 - 5.3	0 - 11.7
Experiment	200	2	1.5	2	1.0	0.8	-	-	-
Bow couple	300	0.6	0.5 - 2.1	4.1	0.1	0.1 - 0.5	1.6	1.1 - 4.4	0.4 - 32
Bottom door	300	0.9	0.5 - 2.1	23.0	0.0	0.03	0.3	26.2	∞

Table C.1: The different values for the velocity ratio (ζ) and Richardson number (Ri) for an average overflow plume, the plume considered in the CFD simulation and the sediment plumes using the two different execution methods in this pilot study, assuming two different cross flow velocities (U).

and bent over plume behaviour, see fig. C.1. It should be noted that all JICFs start as a jet and end as a bent over plume in the direction of the ambient current. The length scales are used to describe what happens in between.

If $z_B > z_M$, (fig. C.1a) the JICF will bend in the direction of the cross flow and act like a bent-over jet, when $z > z_M$. This behaviour continues until a depth of $z > z_C$ is reached; the behaviour changes to a bent-over plume.

If $z_M > z_B$, (fig. C.1b), due to the small amount of initial momentum, the JCIF will act like a plume if $z > l_m$, this implies that the JCIF is buoyancy dominated. At $z > z_B$, the JICF acts as a bent over plume. In the bent over plume phase the combined effect of the cross flow and buoyancy dominates the influence of initial momentum.

C.1.1. SURICATES sediment plumes

Since both $z_B > z_M$ and $z_M > z_B$, a combined behaviour of fig. C.1b and fig. C.1a is expected. As the cross flow velocity decreases with depth, the highest and lowest cross flow velocities are shown in table 3.2.

Hence, the expected behaviour is as following; over the first 1.6 m the sediment plume acts as a jet, containing its initial momentum only. Subsequently, the jet is bend over and the sediment plume ends as a plume containing buoyancy only. In this last phase the plume is caught by the cross flow and is bend over, which is the final state of all buoyancy JICF, independent of its initial momentum to buoyancy ratio.

For bottom door disposals the jet length scale (z_M) is larger than the local depth, see table C.1. Therefore, only jet / density current behaviour is expected over the vertical.

C.2. Overflow plumes

The understanding of the behaviour of the sediment plume dynamics is based on current research on overflow plumes. Overflow plumes are by-products of dredging operations using TSHDs. To increase the volume of solids inside the barge of a TSHD, excess water is released through an overflow, after initial settling has taken place, see fig. 3.1. Since these overflow plumes are associated with turbidity in the ambient water they are topic of much of the research on sediment plume behaviour in the context of environmental impact assessments. However, there are small differences between overflow plumes and the sediment plume investigated in this research, possibly violating this analogy. These differences and their implications will be discussed hereafter.

The depth of disposal for an overflow plume is often at the draught of the vessel, which coincides with the

disposal location of a bottom door disposal. But, bow coupling plumes are released at the water surface. Also the location of the overflow is most often located 1/4 to 1/2 of a boat length from the hull of the vessel, this coincides with the location of the bottom doors, whereas the bow couple is located at the hull, see fig. 3.4a. For the bottom door release the effect of initial momentum will dominate the behaviour of the plume, therefore, most vessel induced effects, such as hull induced effects and propeller induced effects can be neglected. For the bow coupling release, these effects can only be neglected if the vessel is aligned with the flow [de Wit, 2015].

During to the generation of an overflow plume, small amounts of air can be entrapped in the overflow plume, possibly leading to lifting of the particles. Due to the difference in production process, it is assumed that the SURICATES sediment plumes lack air entrainment. Also, fluctuation of the outflow discharge of the overflow plume may lead to pulsing. As not all processes are monitored during the pilot study, all above mentioned effects are not further investigated [de Wit, 2015].

Moreover, the concentration of suspended solids of an overflow plume is approximately 20 % ($200 g/l$) and contains predominantly fines ($< 63 \mu m$) as the coarser particles settle inside the barge. [Spearman et al., 2011] [de Wit et al., 2014]. This concentration is more or less equal to the concentration SPM inside the barges for the SURICATES pilot study (see appendix G.1 and fig. 1.2). However, the composition of the barges with a sediment source from the New Meuse (making up 10 % of the total disposals) contain a slight fraction of course material in contrast to the overflow plumes.

In Van Eekelen [2007] the effect of stratification on near field behaviour is found to be limited to a smaller density difference between the plume and denser water instead of freshwater. Therefore, the effect of stratification is assumed to be limited.

D

Measurement set-up

D.1. Measurement campaign timeline

For clarification the different events related to the SURICATES pilot are summarized in a clear timeline. In total sediment has been disposed from May 20 until November 15 with small interruptions for various reasons. The letters refer to the different measurements taken, T_i refer to the sediment sampling measurements and M_i refers to measurements done with the survey vessel as shown in table D.1.

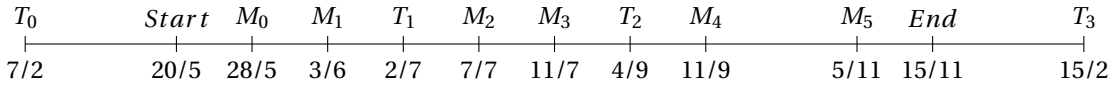

Measurement	Date	Week	Quantities	Instruments
T0	7 Feb.	6	Particle size distribution	Grab sampling and column
T1	2 Jul.	27	Particle size distribution	Grab sampling
T2	4 Sep.	36	Particle size distribution	Column
M0	28 May	22	Bathymetry	ADCP, multibeam
M1	3 Jun.	23	Bathymetry	ADCP, multibeam
M2	7 Jul.	28	Flow velocity, salinity, SSC	ADCP, silt profiler, multibeam, bathymetry
M3	11 Jul.	28	Flow velocity, salinity, SSC	ADCP, silt profiler, multibeam, bathymetry
M4	11 Sep.	37	Flow velocity, salinity, SSC	ADCP, silt profiler, multibeam, bathymetry
M5	5 Nov.	45	Flow velocity, salinity, SSC	ADCP, silt profiler, multibeam, bathymetry

Table D.1: An explanation and clarification of the different measurements done throughout the SURICATES pilot study

D.2. Short term measurements

D.2.1. Silt profiler

Working principle

The silt profiler is a measuring device containing various measuring equipment to determine the concentration of suspended matter (SPM), water temperature, pressure and conductivity all mounted to a frame. To measure the concentration of SPM, the silt profiler is equipped with two different Optical Backscatter Sensors (OBS) and an transmission probe each with different ranges; $0.1-1 g/l$, $1-10 g/l$ and $10-35 g/l$. Moreover, bottled samples can be taken at various depths to obtain grain size distributions and to verify SPM concentrations. When used, the Silt Profiler is deployed freefalling with an average falling speed of $1 m/s$. [de Nijs et al.,

2010] On average an upcast and downcast measurement together last 3 minutes. To obtain the full range of silt concentration the transmission probe, with the third range is used.

An OBS measures turbidity and SSC by detecting the amount of scattered infrared light between the transmitter (an infrared emitting diode) and detector (four photod iodes). The amount of scattering is determined by the size, composition and shape of a particle; therefore it is evident to calibrate the OBS sensors with in-situ samples. The silt-profiler data for the SURICATES measuring campaign is calibrated using four samples from the Eemhaven [Van Rijn, 2006].

Data processing

In order to use the data obtained from the Silt profiler some adjustments to the data has to be done in order to use them.

- At first the dataset is split into the upcast and downcast measurement. It is assumed that the the maximum pressure equals the bottom. And hence marks the split in downcast and upcast.
- As the silt profiler is deployed, the moment of impact with the water may cause local turbulence and bubbles inducing artificial turbidity and thus SSC. As the silt profiler hits the bottom, the impact with the bottom may cause local resuspension of silt at the bottom. Therefore, it is most reliable to measure the concentration in the first 3 meters of the water column with the upcast measurements and the remainder with the average and the last meter with the downcast measurements to measure the layers close to the bottom.
- Subsequently these datasets are interpolated on the same grid with a length of 1950 grid cells over the depth for which 1 cell equals 1cm.
- At last these values are smoothed with a uniform filter, which uses a moving average with a window of 25 cells over the vertical.
- The salinity and depth are calculated from the given pressure, temperature and conductivity using TEOS-10 [IOC SCOR, 2010] and averaged for upcast and downcast. The salinity is subsequently smoothed using a uniform filter.

D.2.2. ADCP velocity

Working principle

Acoustic Doppler Current Profilers (ADCP) can be used to measure the flow velocity and amount of absolute backscatter. This can be done by stationary measurements with fixed instruments at the bed or by ADCP's fixed to a vessel to execute moving measurements. The ADCP can be used to obtain a value for the backscatter and for the velocity using the same emitted signal. However, the velocity measurements are based on a shift of frequency between the emitted and received signal, whereas the ADCP backscatter' working principle is based on the change in strength of this signal, as the strength of the backscatter signal is related to the amount of scattering caused by the particles. [Merckelbach, 2006] In the following paragraph the processing of the ADCP velocity results and more details on the working principle are given. In appendix D.2.3, the same is done for ADCP backscatter.

The working principal of the ADCP is as following; When a particle suspended in the water moves away from the emitted signal, its frequency is decreased and when a particle moves towards the emitted signal its frequency increases with respect to the emitted signal. This phenomena is known as the Doppler' shift. The signal is emitted by a transmit transducer and subsequently the signal is received by three transducers, mounted under an angle of 30 deg. The amount of Doppler shift is then related to the trajectory of a particle in these three directions from which the velocity can be derived [Van Rijn, 2006].

Data processing

To process the ADCP data the following steps are undertaken;

- The total dataset of ADCP results is split in separate trajectories.

- The velocities are interpolated on an along channel equidistant grid, with a grid size of 0.1m in the along channel direction and 0.5m over the height, to match the height with the bin width of the ADCP.
- Most ensembles last 2.12 seconds containing 50 bins over the depth with a bin width of 50 cm. Each ensemble is an average of 5 pings.
- The blanking distance is 2 or 2.5 m from the water surface and 1.5 m from the bed.

The velocity vector of the ADCP is computed in two directions in the north and east direction based on the Rijksdriehoek Frame of Reference. This direction of the main axes does not align with the main axes of the channel, and the shift between the channel alignment and the axes is not constant. Since the river is relatively straight, lateral velocities are expected to be small. Therefore it is assumed that the along channel vector is equal to the total velocity vector.

D.2.3. ADCP backscatter

Working principle

Apart from measuring velocities ADCP have gained popularity to determine Suspended Sediment Concentration based on acoustic backscatting. The main working principle is based on the change in energy of the particles as they are reflected back towards the receiver.

As the ADCP emits a sound pulse, this pulse detects any suspended material and hence scatters the amount of energy of the sound pulse. As the emitters also contains the receptor, the amount of received acoustic energy can be related to the amount of scattering. The amount of scattering is then scaled using the speed of sound in water, the sound propagation characteristics and the scattering strength of the suspended material. This allows the use of an relationship between the amount of backscatter and the characteristics of the suspended matter [Van Rijn, 2006].

In different studies positive results were found for ADCPs using frequencies between $0.3 - 2.4 MHz$ for particles with sizes between $1 - 100 \mu m$. The backscatter strength (S_v (dB)) is determined by the sensor and determined by a.o. the attenuation coefficient. Subsequently, the SSC can be determined using a logarithmic relation between the backscatter strength and the SSC. (scaled using a calibration concentration) However, this attenuation coefficient (α) consists of two distinct attenuation coefficients; attenuation due to seawater (α_w) and attenuation due to scatters in suspension (α_s). The attenuation in seawater is primarily determined by the frequency of the ADCP and partially on temperature, salinity, pressure, pH and speed of sound. Where in general the attenuation due to seawater increases for higher frequencies. For the ADCP used, a correction is made using a constant salinity of 35 PSU, zero turbidity ($0.0 mg/l$) and a non-constant water temperature. Also, when SSC is expected to be smaller than $0.2 g/l$, the attenuation due to seawater has a larger influence than the attenuation due to sediment. Whereas the attenuation due to suspended sediment is apart from SSC also influenced by the size, shape and density of the particles. In general an ADCP backscatter with higher frequency has a higher spatial resolution, detects finer particles, but has a smaller range. In general, best results are obtained for environments with a small difference in grain sizes, concentration and density [Park and Hong Lee, 2016].

Data processing

For the processing of the ADCP backscatter data the following steps are taken:

- Most ensembles last 2.12 seconds containing 50 bins over the depth with a binwidth of 50 cm. Each ensemble is an average of 5 pings.
- The first 2 or 2.5 m are not measured and the last 1.5m close to the bed is left blank as well.
- The values measured are interpolated to a grid of 0.5m over the depth and 0.1m in space or 1 minute in time.
- At last the values are smoothed using a 3 by 3 uniform block filter.

E

Model Equations

In chapter 5 the models used to model the hydrodynamics and sediment dynamics are described. These models are build to solve equations describing the hydrodynamics and sediment behaviour. In the following chapter these underlying equations are shown and explained. Starting with the hydrodynamics.

E.1. Hydrodynamics

Most flow processes in shallow water, i.e. most rivers, coasts and estuaries can be described using the Reynolds averaged Navier-Stokes (RANS) equations. The RANS equations are based on conservation of mass and energy and Newton's second law.

The following approximations are applied:

- **Compressibility**
  A fluid is assumed incompressible. Therefore the density is constant and can be left out of the continuity equation.
- **Turbulence**
  The turbulent fluctuations of the velocity (which occur at a scale much smaller than the computational domain) are related to average flow velocity characteristics by Reynolds decomposition. While the relation between turbulence, velocity, temperature, pressure and concentrations are included using a turbulence closure model, based on empirical relationships between turbulence and the mean flow [Zijlema, 2019].
- **Boussinesq approximation**
  A particle is assumed to be such small that horizontal variation in the density can be neglected.
- **Hydrostatic assumption**
  The pressure is assumed to be hydrostatic over the vertical, reducing the vertical momentum balance to the hydrostatic balance equation.
- **F-plane approximation**
  The Coriolis parameter is constant for a given latitude, see eq. (E.7).

Continuity equation

The continuity equation is based on the conservation of mass of an incompressible fluid (hence density is constant) and reads as following;

$$\frac{\partial u}{\partial x} + \frac{\partial v}{\partial y} + \frac{\partial w}{\partial z} = 0 \tag{E.1}$$

With u being the stream wise velocity, v the lateral velocity and w the vertical velocity. x, y and z are the relative positions in the same plane.

Momentum balance

The momentum equations are based on Newton's second law of motion which states, *"the rate of increase of momentum in fluid element = sum of forces on fluid element."*

The forces acting on a fluid are pressure forces, viscous forces and gravity.

$$\frac{\partial u}{\partial t}+\frac{\partial uu}{\partial x}+\frac{\partial uv}{\partial y}+\frac{\partial uw}{\partial z}-fv+\frac{1}{\rho_0}\frac{\partial p}{\partial x}-F_x-\frac{\partial}{\partial z}\left(v_t\frac{\partial u}{\partial z}\right)=0 \tag{E.2}$$

$$\frac{\partial v}{\partial t}+\frac{\partial uv}{\partial x}+\frac{\partial vv}{\partial y}+\frac{\partial vw}{\partial z}+fu+\frac{1}{\rho_0}\frac{\partial p}{\partial y}-F_y-\frac{\partial}{\partial z}\left(v_t\frac{\partial v}{\partial z}\right)=0 \tag{E.3}$$

$$\frac{\partial w}{\partial t}+\frac{\partial uw}{\partial x}+\frac{\partial wv}{\partial y}+\frac{\partial ww}{\partial z}+\frac{1}{\rho}\frac{\partial p}{\partial z}+g-F_y-\frac{\partial}{\partial z}\left(v_t\frac{\partial w}{\partial z}\right)=0 \tag{E.4}$$

In which v_t represent the vertical eddy viscosity, f the Coriolis Term (see eq. (E.7)) and F_x , F_y represent the unbalance of horizontal Reynolds stresses, which are computed as following;

$$F_x=\frac{\partial}{\partial x}\left(2v_H\frac{\partial u}{\partial x}\right)+\frac{\partial}{\partial y}\left(v_H\left(\frac{\partial u}{\partial y}+\frac{\partial v}{\partial x}\right)\right) \tag{E.5}$$

$$F_y=\frac{\partial}{\partial x}\left(2v_H\frac{\partial v}{\partial y}\right)+\frac{\partial}{\partial x}\left(v_H\left(\frac{\partial u}{\partial y}+\frac{\partial v}{\partial x}\right)\right) \tag{E.6}$$

$$f=2\Omega sin(\phi) \tag{E.7}$$

Shallow water equation

From the continuity equation and momentum balance the water depth and water level can be computed according to the shallow water equation (by integrating the Navier-Stokes equations over the depth):

$$\frac{\partial \eta}{\partial t}+\frac{\partial uh}{\partial x}+\frac{vh}{\partial y}=0 \tag{E.8}$$

Energy and salinity transport

Energy, in the form of heat and salinity are advective processes determining the local density through the equation of state [Pietrzak, 2015]. The advection and transport of these two phenomena are required to determine the density in the momentum balance. The heat and salinity are calculated using the convection diffusion equation:

$$\frac{\partial S}{\partial t}+\frac{\partial uS}{\partial x}+\frac{\partial vS}{\partial y}+\frac{\partial wS}{\partial z}-2D_h\left(\frac{\partial^2 S}{\partial x^2}+\frac{\partial^2 S}{\partial y^2}\right)-\frac{\partial}{\partial z}\left(D_T\frac{\partial S}{\partial z}\right)=S_{ss} \tag{E.9}$$

$$\frac{\partial T}{\partial t}+\frac{\partial uT}{\partial x}+\frac{\partial vT}{\partial y}+\frac{\partial wT}{\partial z}-2D_h\left(\frac{\partial^2 T}{\partial x^2}+\frac{\partial^2 T}{\partial y^2}\right)-\frac{\partial}{\partial z}\left(D_T\frac{\partial T}{\partial z}\right)=T_{ss}+\frac{1}{\rho}Q_H \tag{E.10}$$

In which, S equals the salinity, T the temperature, D_h the horizontal eddy diffusivity and D_t the vertical eddy diffusivity, S_{ss} and T_{ss} the source terms for salinity and temperature and Q_H the heating flux source term [Pietrzak, 2015].

Turbulence modelling

Since the smallest scales of turbulence are much smaller than the model scale applied, not all turbulent fluctuations can be included in the model. In RANS equations, a time filter much larger than the turbulent time scale is applied. This creates a stationary flow on the turbulent time scale and leaves it non-stationary on the often much larger time scale of the problem at hand. This is called Reynolds decomposition, in which u the total flow velocity is decomposed into a large scale constant flow velocity ($\overline{u}$) and a smaller scale representing the turbulent fluctuations (u').

$$u = \overline{u} + u' \tag{E.11}$$

However, still a correlation between turbulence, velocity, temperature, pressure and concentrations is required. These are based on empirical relationships between turbulent transport and the mean flow. This is done by computing the eddy diffusivity (D_T) and eddy viscosity (υ_T), from the kinetic energy and turbulent dissipation rate.

$$\upsilon_T = c_\mu \frac{k^2}{\epsilon} \tag{E.12}$$

$$D_T = \frac{\upsilon_T}{\sigma_T} \tag{E.13}$$

In which k, equals the turbulent kinetic energy (appendix E.1), ϵ (appendix E.1) the turbulent dissipation rate, σ_T the Prandtl-Schmidt number and c_μ the buoyancy term.

$$k = \frac{1}{2}\overline{u'u'} \tag{E.14}$$

$$\epsilon = \frac{1}{2}\upsilon\left(\overline{\frac{\partial u'}{\partial x} + \frac{\partial v'}{\partial y}}\right)^2 \tag{E.15}$$

E.2. Sediment dynamics

The mass balance of suspended sediment is governed by the convection diffusion equation describing the advection or displacement of sediment and its spread over the vertical. To do so, it is assumed that suspended cohesive sediment can be treated as a single phase fluid. For small concentrations of suspended sediment, i.e. concentrations below the gelling point, inter-particle stresses are negligible. Therefore particles are forced by a combined effect of turbulence and settling velocity. The convection diffusion equation for sediment transport reads as following:

$$\frac{\partial c}{\partial t} + \frac{\partial uc}{\partial x} + \frac{\partial vc}{\partial y} + \frac{\partial (w - w_s)c}{\partial z} - 2D_h\left(\frac{\partial^2 c}{\partial x^2} + \frac{\partial^2 c}{\partial y^2}\right) - \frac{\partial}{\partial z}\left(D_T\frac{\partial c}{\partial z}\right) = S_c \tag{E.16}$$

In which, c equals the sediment concentration, w_c the sediment settling velocity, D_h the horizontal eddy diffusivity and D_t the vertical eddy diffusivity, assuming that molecular diffusion coefficient and the eddy diffusivity are the are the same for all sediment fractions. Which is true for small fractions ($w_s << w$) and small concentrations.

F

Model set-up

F.1. Model settings

In table F.2 the settings of the sediment model for the short term simulation and long term simulation are shown.

Parameter	Name	Unit	IM1	IM2	IM3
Grain size:	Particle size	μm	1	15	34
VSedIMx	Sedimentation velocity	m/d	0.1	10.8	86.4
TaucSIMx	Critical shear stress for sedimentation	n/m^2	0.0	0.0	0.0
FrIMxSedS2	Fraction sedimentation IMx to layer S2	-	0.2	0.2	0.2
FrTIMS2Max	Maximum fraction total IM in layer S2	-	1	1	1
SWResIMx	Switch resuspension IMx	-	1	1	1
ZResIMx	Zeroth order resuspension rate	-	8640	8640	8640
VResIMx	First order resuspension rate	d^{-1}	0.1	0.3	0.1
TaucRS1IMx	Critical shear stress for resuspension of IMx from S1	n/m^2	0.2	0.2	0.2
TaucRS2IMx	Critical shear stress for resuspension of IMx from S2	n/m^2	1000	1000	1000
PsedminIMx	Probability for sedimentation	-	1.0	0.1	0.1

Table F.1: Paramater settings per sediment fraction IM_x

Layer	Thickness
1	12 %
2	12 %
3	11 %
4	11 %
5	11 %
6	11 %
7	11 %
8	9 %
9	6 %
10	6 %

Table F.3: Distribution of the layer thickness with layer 1 at the top of the water column and layer 10 near the bed.

Parameter	Name	Unit	Value
TauShields	Shield stress for resuspension	n/m^2	1
GRAIN50	Median grain size	m	0.00
GRAV	Gravititational acceleration	m/s^2	9.81
KinViscos	Kinematic viscosity	m^2/s	0.00
RHOSAND	Density sediment particle	kg/m^3	2.60E+06
RhoWater	Density water	kg/m^3	1020.00
PORS2	Porosity layer S2	m^3_{pores}/m^3_{bulk}	0
ThickS2	Thickness layer S2	m	0.05
MinDepth	Minimum depth for sedimentation	m	0.01
MaxResPup	Max resuspension flux from layer S2	$g/m^2/d$	3600
FactResPup	van Rijn pickup factor layer S2	-	0.00
TaucRS1DM	Shield stress for resuspension	n/m^2	1000
Rough	Nikuradse roughness length scale	-	0.00
WindDir	Wind direction	deg	225
FETCH	Fetch length	m	5.00E+04
Manncoef	Manning coefficient	m	0.02

Table F.2: Parameter settings for all sediment fractions

F.1.1. Two layer bed model

For a sandy bed with some fines, such as the Rotterdam Waterway and North-Sea [de Nijs et al., 2008], the mobilization of the fines is governed by the hydrodynamic conditions whereas the entrainment of the fines is determined by the entrainment of sand. This is explained by Van Kessel and Winterwerp; as the sand is coarser than the fines, the fines are 'locked-up' between the sand particles. Therefore the mud particles can only be set to motion if the sand particles surrounding the fines are set to motion. Therefore Van Kessel and Winterwerp, developed a two layer model as displayed in fig. 2.6 which contains a fine top layer, a sand layer underneath with some locked-up finer particles and the interaction between them. The top-layer mainly consists of a thin fluff layer of fine sediment depositions, which is highly dynamic; the particles settle during Slack water and can be resuspended (or entrained) by the tidal currents. In contrast, the second layer has limited dynamics and is only brought in suspension by highly dynamic conditions such as storms or spring tide, while it is capable to store large amounts of fines in the bed. [Winterwerp and van Prooijen, 2015]

Van Kessel and Winterwerp, transformed the Partheniades-Krone relation (eq. (2.2)) into eq. (F.1), by introducing several additional parameters to describe the interaction between the two layers, also it should be noted that eq. (F.5) uses eq. (2.4) with $n = 1.5$ As layer 2 contains sand.

$$h\frac{dC}{dt} = E_1 + E_2 - D_1 - D_2 \tag{F.1}$$

$$D_1 = (1-\alpha)w_s C \tag{F.2}$$

$$D_2 = \alpha w_s C \tag{F.3}$$

$$E_1 = min(M_0; m_1 M_1)\left(\frac{\tau_b}{\tau_{cr,1}} - 1\right) \tag{F.4}$$

$$E_2 = p_2 M_2 \left(\frac{\tau_b}{\tau_{cr,2}} - 1\right)^{1.5} \tag{F.5}$$

In which $\frac{dc}{dt}$ is the change in SPM concentration in the water column, h the local water depth, D_i, the deposition of layer *i*, E_i the entrainment of layer *i*, M_i represents the resuspension parameter for layer *i*, which is mainly used as calibration parameter, m_1 the sediment mass per unit area in the bed, C the near bed concentration of SPM, p_2 the fraction of fines in layer 2 and α the fraction of total deposited fine sediments which are buried in the second layer ($\alpha << 1$). For now it is known that α depends, a.o. on the bed form migration, pore water underpressures and bioturbation, however exact values are unknown. Pore water flows are generated by pressure differences over the bed, bedform migration is the erosion of a bed crest into a through of the same bed; mixing the sediment in the bed and bioturbation may enhance the burying of fine particles deeper into the sandy bed. The top-layer mainly consists of a thin fluff layer of fine sediment depositions, which is highly dynamic; the particles settle during Slack water and can be resuspended (or entrained) by the tidal currents. In contrast, the second layer has limited dynamics and is only brought in suspension by highly dynamic conditions such as storms or spring tide, while it is capable to store large amounts of fines in the bed. [Winterwerp and van Prooijen, 2015]

F.2. Short term model set-up

The determination of the time step is to find a balance between the computational costs and the accuracy of the results. The goal is to obtain results which are as much independent of the time step chosen. For the modelling of the disposal an arbitrary amount of sediment is brought in the system. The initial concentration and boundary concentrations are set to zero everywhere in the system. In the figures the following time steps are compared; $\Delta t = 5, 10, 15\ s$.

Over the following figures, the concentration of the different sediment fractions (IM_1, IM_2, IM_3) and its concentration in each of the bed layers (IM_iS_1, IM_iS_2) are compared at Hook of Holland, the Maeslantkering, km 1028 and at Maassluis, slightly downstream of the disposal area.

The largest difference occurs in the first concentration peak at the Maeslant Barrier. Where the difference in concentration between $\Delta t = 5, 10, 15s$ equals $0.001 gDM/m^3$ (7%) per time-step. Therefore one can conclude that no convergence has occured.

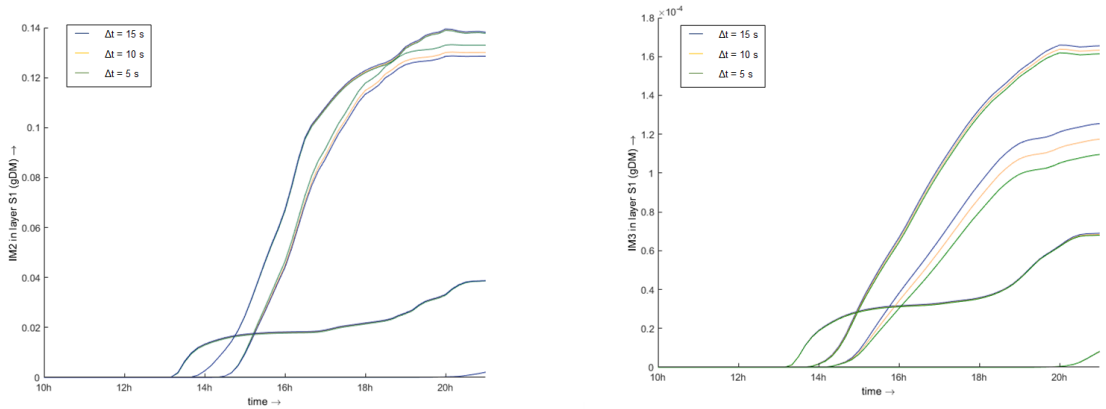

(a) IM_2S_1 for various time steps

(b) IM_3S_1 for various time steps

Figure F.1: Timestep comparison for different sediment fractions

F.2.1. Modelling challenges

To catch a physical process in a numerical model different simplifications and assumptions have to be made. The initial behaviour of the plume is best described in de Wit [2015] in which it is considered as a CFD problem. The major limitation of D3D-WAQ is the lack of coupling between hydrodynamics and sediment behaviour. In WAQ the sediment release is a point source instead of a plume, neglecting near-field effects.

One of the challenges is the grain-size distribution of the plume. In total .. disposal have been executed over a period of five months. No sampling of the barge of the dredgers has been executed. Therefore the composition of the sediment released is unknown, it is therefore assumed that the composition of the plume is equal to the composition of the bed where the sediment is dredged.

Moreover, the total range in sediment size has to be represented by only three fractions; IM1 - IM3. The selection of the most representative grain size and concentration of these samples is arbitrary.

Initial behaviour of the plume, as described in de Wit [2015] and Winterwerp [2002] is signified by a sinking density plume and a subsequent spread over the vertical, with a surface and bed plume. In the model however, sediment can not exhibit this behaviour; when sediment is released in a layer below the surface a particle will not move upward due to the definition of the settling velocity.

Another challenge is the calibration of the model. In the model there is no background concentration, so in comparing the model results with the measurements the background concentration has to be taken into account. Moreover, the measurements only provide the value of SSC over the vertical for a very specific time and location. In verification of the results, the measurements are not taken during the highest concentrations of the plume, but too early or too late. Without knowing the amount of background concentration the exact value of the peak remains unknown. As the size of the peak values is unknown, it is unknown if the values found for the silt profiler measurements are the peak concentrations of the plume or smaller.

In the vessel the concentration and flow velocity are measured. Moreover, the amount of TDM is calculated based on the depth of the vessel and volume inside the barge.

Another challenge lies in the amount of sediment compared to the background concentrations. The background concentrations of SPM are $\mathcal{O}0.05 g/l$. After disposal the peak concentrations found in the measurements equal $+-0.30 g/l$. However, in the subsequent measurements it can be seen that the concentration of the plume in the measurements decreases quickly to 0.10 in measurement 16.

F.2.2. Long-term model set-up

Time step

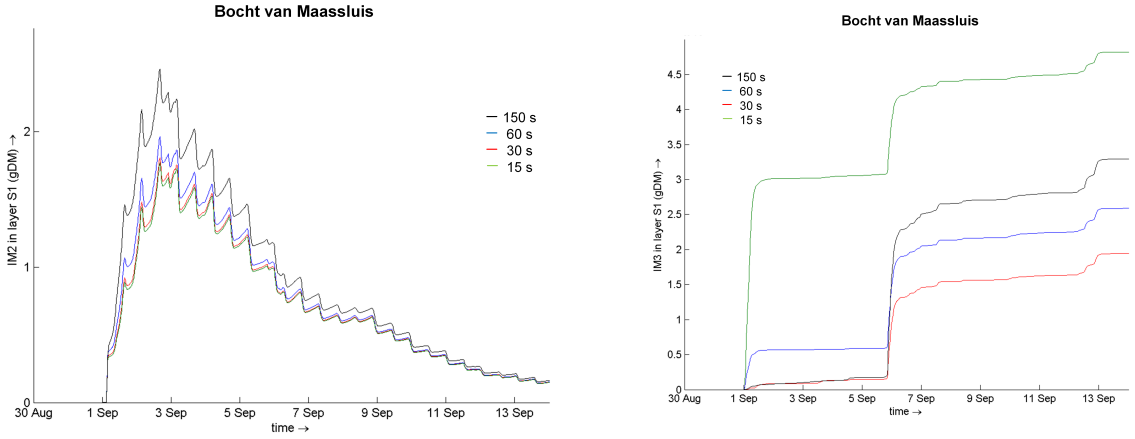

(a) IM_2S_1 for various time steps at Maassluis

(b) IM_3S_1 for various time steps at Maasvlakte 2

Figure F.2: Timestep comparison, between Δt = 300s, 60s, 30s and 15s at Maassluis and at Maasvlakte 2.

Wave conditions

From	Until	Avg.	>4 m	>3.5 m	>3 m	>2.5 m	>2 m	>1.5 m	Discharge
22-Apr	05-May	0.85	0	0	0	0	28	20	1433.7
06-May	19-May	0.90	0	0	0	26	64	53	1819.1
20-May	02-Jun	0.76	0	0	0	0	8	28	2415.7
03-Jun	16-Jun	0.89	0	11	24	17	12	13	2067.7
17-Jun	30-Jun	0.60	0	0	0	0	0	9	2265.4
01-Jul	14-Jul	0.78	0	0	0	0	0	2	1800.6
15-Jul	28-Jul	0.64	0	0	0	0	0	12	1428.6
29-Jul	11-Aug	1.20	1	21	23	18	66	135	1396.1
12-Aug	25-Aug	0.90	0	0	0	0	11	139	1501
26-Aug	08-Sep	1.01	0	0	1	24	68	92	1497.8
09-Sep	22-Sep	0.84	0	0	0	0	25	83	1229.1
23-Sep	06-Oct	1.57	0	0	14	53	180	265	1162.1
07-Oct	20-Oct	1.28	0	0	0	36	127	184	1665.8
21-Oct	03-Nov	1.14	0	2	13	12	75	142	1717
04-Nov	16-Nov	1.24	0	2	28	125	475	771	1522.9
Entire period									
	Total	0.98	1	34	75	185	664	1219	1699.3
	Avg. / week		0.00	2.64	5.83	14.39	51.64	94.81	

Table F.4: Wave conditions prior to and during the SURICATES study.

G

Measurement results

G.1. Barge density and concentration

The sediment disposed in the Waterway is suspended and therefore released as a sediment water mixture. Unfortunately the amount of information from the dredger' registration is limited to the amount of sediment disposed (in m^3), sediment source and the time of disposal. The concentration of suspended solids inside the barge is not fixed and depends on the efficiency of the dredging operation. From internal memo's the following factors are applied for the ratio between TDM and total m^3's. This factor depends on the vessel used; but on average this ratio yields 2.79 $m^3 : TDM$. This ratio is slightly larger than the ratio used in Hendriks and Schuurman [2017] using a ratio of 2.49$m^3 : TDM$ for the fairway and 2.46$m^3 : TDM$ for the basins.

The concentration of solids is calculated as following;

$$TDM = \frac{\rho_{barge} - \rho_{water}}{\rho_{solid} - \rho_{water}} V_{barge}\, \rho_{solid} \tag{G.1}$$

$$Concentration = \frac{M_{sediment}}{V_{barge}} \tag{G.2}$$

G.2. Short term measurements

G.2.1. Sediment disposals

Date	Time	TDM	Sediment source
Sep. 3	09:49 - 09:52	1663	Waalhaven
Sep. 3	21:37 - 21:41	1151	Waalhaven
Sep. 5	12:15 - 12:18	1710	Waalhaven
Sep. 5	23:22 - 23:25	1600	Waalhaven
Sep. 10	05:20 - 05:24	2340	Eemhaven
Sep. 10	17:29 - 17:31	2101	Eemhaven
Sep. 11	06:03 - 06:06	2146	Eemhaven
Sep. 11	*17:58 - 19:16*	*2096*	*Eemhaven*
Total:		**14807**	

(a) Amount of sediment disposed prior to September 11, 2019

Date	Time	TDM	Sediment source
Oct. 28	05:25-05:35	1202	Waalhaven
Nov. 4	10:24-10:30	1455	New Meuse
Nov. 4	00:14-00:19	1186	Waalhaven
Nov. 5	01:00-01:07	1079	Waalhaven
Nov. 5	*11:00-11:50*	*1256*	*New Meuse*
Total:		**6178**	

(b) Amount of sediment disposed prior to November 5, 2019

Figure G.1: Amount of sediment disposed prior to both measurement surveys

G.2.2. September 11

	18:00-20:15			20:15-21:00		
	avg. vel.	dist.	dist.	avg. vel.	dist.	dist.
2 - 4m	0.78	4.56	3.44	0.72	8.94	0.59
4 - 6m	0.69	4.04	3.96	0.69	8.23	2.26
6 - 8m	0.51	2.99	5.01	0.51	6.1	4.06
8 - 10m	0.27	1.57	6.43	0.23	2.97	5.21
10 - 12m	0.05	0.29	7.71	0.01	0.35	5.65
12 - 14m	0.0	0.0	8.0	0.01	-0.6	5.66
14 - 16m	0.02	0.12	7.88	-	2.34	5.66

Table G.1: The average flow velocity taken measured obtained from ADCP flow measurements in m/s. The first distance is from the disposal site. The other distance mentioned is the distance from Hook of Holland, used as reference point throughout this thesis.

G.2.3. November 5

In the following sections the results of the ADCP backscatter and velocity are shown for different trajectories. The measurements are separated according to their period.

Period I: 8:00 - 11:00

Silt profiler	Time	Distance (km)
8:15 - 9:00		
1	08:23	3.36
2	08:34	3.8
3	08:42	4.13
4	08:48	4.23
5	08:54	4.16
9:00 - 9:30		
6	09:27	9.55
7	09:33	9.63

(a) Time and location of the silt profiler measurements 1 - 7

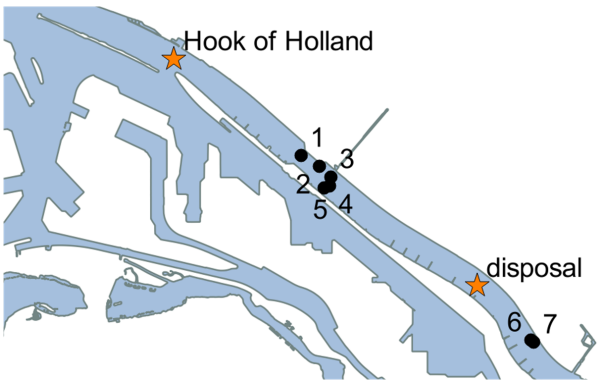

(b) Location of the silt profiler 1 - 7

Figure G.2: The location of the silt profiler measurements 1 to 7 and the trajectories sailed by the ADCP backscatter between 8:30-9:00 (1) and 9:10 - 9:35 (2).

Silt profiler	Time	Distance	Depth	Clay	Silt	Fine	Medium	Coarse
8:15 - 9:00								
1	08:23	3.36 km	3.0 m	0.92	99.07	0.01	0	0
2	08:34	3.8 km						
3	08:42	4.13 km	3.0 m	0.57	97.47	1.96	0	0
4	08:48	4.23 km						
5	08:54	4.16 km	14.0 m	1.74	84.01	14.25	0	0
			14.0 m	2.6	88.97	8.43	0	0
9:00 - 9:30								
6	09:27	9.55 km	14.0 m	2.13	88.56	9.32	0	0
			14.0 m	2.04	89.11	8.85	0	0
7	09:33	9.63 km						

Table G.2: The silt profiler measurements, including the grain-size distributions of the relevant samples. Fine, medium and coarse refer to fine-sand, medium-sand and coarse-sand fractions. The distance refers to the distance from Hook of Holland.

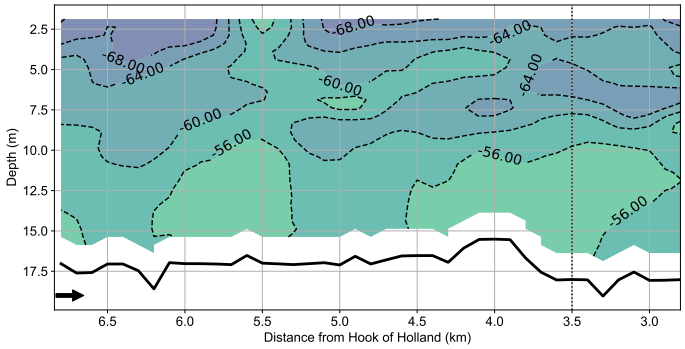

(a) ADCP backscatter from 7:54 to 8:15

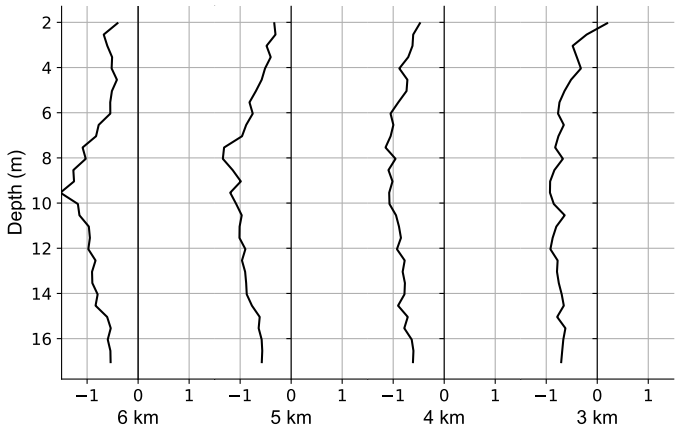

(b) Flow velocity between 7:54 and 8:15

Figure G.3: The results of the ADCP backscatter and the total horizontal flow velocity between 7:54 and 8:15. The contours indicate the amount of backscatter, the smaller the backscatter the larger the amount of SSC.

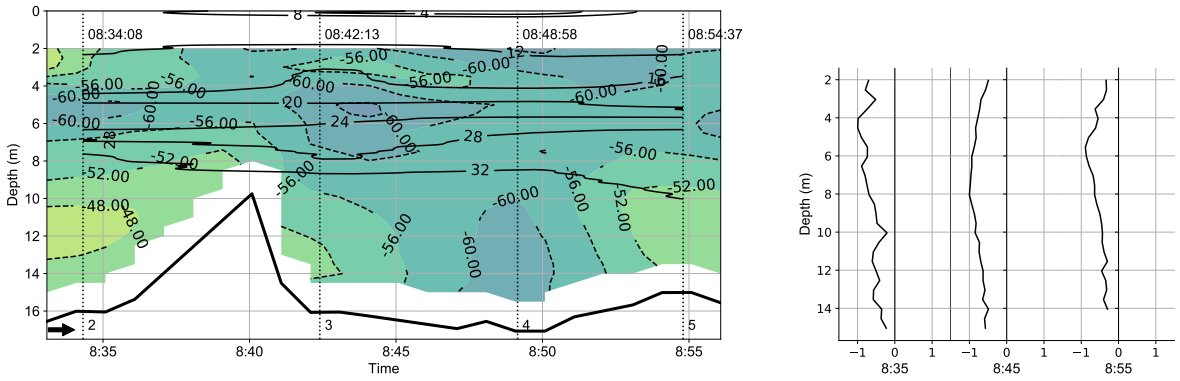

(a) ADCP backscatter

(b) Total horizontal flow velocity

Figure G.4: The results of the ADCP backscatter and velocity between 8:30 and 8:55. The contours indicate the amount of backscatter, the smaller the backscatter the larger the amount of SSC. The straight black lines indicate the salinity over the vertical in PSU. The dashed vertical lines indicate the location and time of the silt profiler measurements 1 to 5.

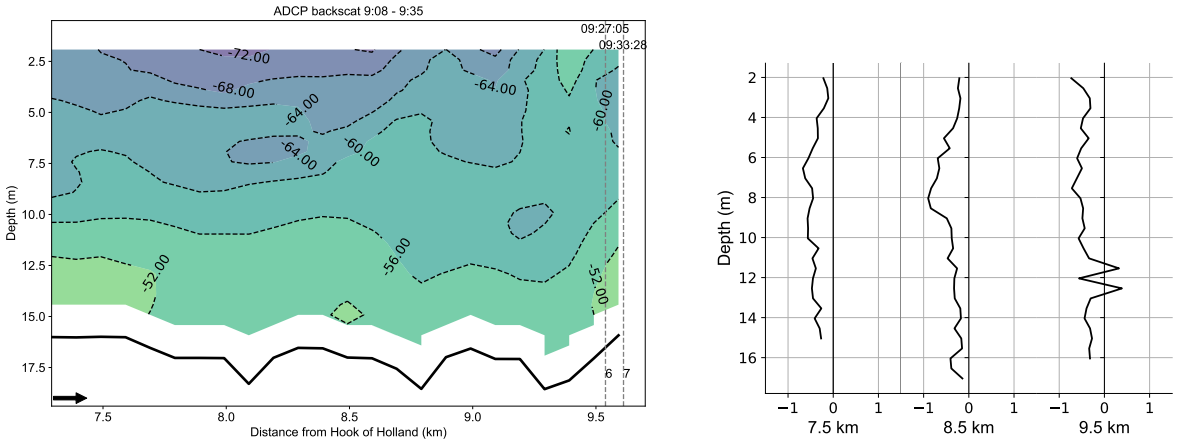

(a) ADCP backscatter

(b) Total horizontal flow velocity

Figure G.5: The amount of ADCP backscatter and the total horizontal flow velocity between 9:08 and 9:35, while sailing upstream. The dashed lines indicate the location and time of silt profiler measurements 6 and 7.

The trajectories are classified as following; during the first one the survey vessel sailed downstream from Maassluis towards the Maeslantkering, during the second trajectory several measurement are taken around the Maeslantkering and during the third trajectory the vessel has been sailing upstream from the disposal site towards Maassluis. The measurements are just after high water, with negative velocities [1] over the vertical only. In fig. G.2 the time and location of the silt profiler measurements 1 - 7 are shown.

[1] In the upstream direction

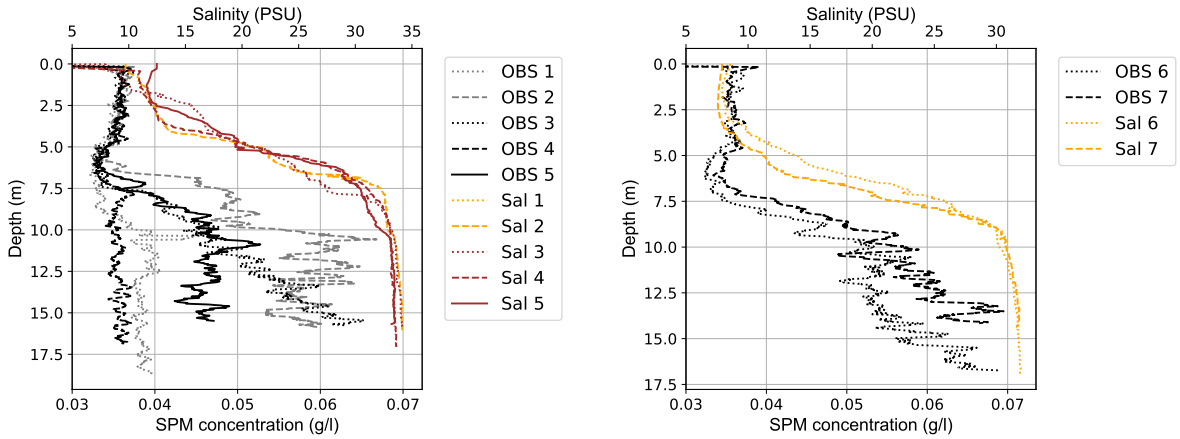

(a) Silt profiler measurements 1-5

(b) Silt profiler measurements 6-7

Figure G.6: Silt profiler measurement 1-7 taken in period I, between 8:00 and 9:30, while sailing upstream. The black and gray lines indicate the concentration of SPM in g/l. The orange and red lines indicate the salinity over the vertical in Practical Salinity Unit (PSU)

The first transect between 7:54 and 8:15 is taken while sailing towards the Maeslantkering during flood. The results of the ADCP backscatter, and flow velocity over the vertical are shown in fig. G.3. From previous studies, e.g. de Nijs et al. [2010] and Eisma et al. [1991b] it is known that in the Rotterdam Waterway sediment concentrations increase towards the bed. In the ADCP backscatter this should result in increasing values over the depth. From the ADCP backscatter no irregularities are found; hence it is assumed that no remains of the previous disposal is detected.

In de Nijs et al. [2010] the SPM concentrations at Hook of Holland range from 0.015 above the pycnocline to 0.03 g/L close to the bed during HW; which is comparable to measurement 1. However, in Eulerian measurements sailing towards HvH during flood SPM concentrations range from 0.03 g/l above the pycnocline to 0.08 g/L close to the bed, with peak values around 0.1 - 0.2 g/l in de Nijs et al. [2010]. Apart from the peak values, these are values found in the same order as measurement 2,3 and 5.

What is interesting to notice is the increase in SPM below the pycnocline for the measurements taken upstream of the Maeslantkering, in the November 5 survey. Although the values fall within expected ranges, the peak concentration SPM in measurement 3 is almost double the concentration of SPM in measurement 1 and 4. The difference between measurement 2,3 and measurement 4,5 can be explained by the location of the measurement with respect to the main channel. Therefore it is assumed that differences in SPM for measurement 2 - 5 are predominantly caused by local spatial differences, rather than the exhibition of a previous disposal. From the flow velocities it can be derived that the velocity for each of the transects is negative [2] over the vertical.

Almost 6 kilometers upstream, measurement 6 and 7 are taken (fig. G.6b), which affirm the pattern found for measurement 2,3 and 5; with concentrations of 0.035 g/l above the pycnocline increasing to 0.07 g/L. As expected, SPM concentrations increase moving upstream, which can also be observed in de Nijs et al. [2010]. Measurement 6 and 7 are taken at 9:27 and 9:33 (flood) upstream of the reallocation area, before the disposal. The profile that arises, is very comparable to the results obtained for measurement 1 to 4. With low SPM concentrations above the pycnocline and increasing SPM concentrations towards the bed. Overall the SPM concentrations in measurement 6 and 7 are slightly larger than for 1-5. This increase, however can not be linked to the behaviour of a previous disposal, but simply by the SPM distribution pattern found for ordinary conditions.

Overall, it can be concluded that the distribution of SPM over the vertical is not higher during flood than can be expected from previous measurement campaigns. However, this can not reject the hypothesis of the non-existence of a return flow of sediment. First of all, if the return flow takes place in the upper part or of the water column or close to the bed, this is not measured with the ADCP backscatter, due to the blanking distance. Next to this, the 7 vertical profiles from the silt profiler only provide a very local view in time and

[2] Upstream velocities are negative, downstream velocities are positive

space. At last, the values are compared to a measurement campaign executed under different hydrodynamic forcing and for a different port layout, see appendix A.1.

Moreover, from the bottle samples taken between 8:23 and 9:29, shown in table G.2, one can observe a clear difference in the distribution of the grain size over the vertical. The samples 1 and 2 taken close to the water are nearly exclusive silt; whereas as the samples closer to the bed also contain more silt and fine sand. However, this is in line with expectations. Eisma et al. [1991a] concluded that in the Waterway the grain-sizes in suspension increase towards the bed.

Period II: 11:00 - 13:00

Silt profiler	Time	Distance (km)
13:00 - 13:30		
22	13:09	1.31
23	13:24	1.96
24	13:34	2.29
13:45 - 14:15		
25	13:50	3.16
26	13:55	3.14
27	14:11	3.55
28	14:16	3.56

(a) Time and location of the silt profiler measurements 1 - 7

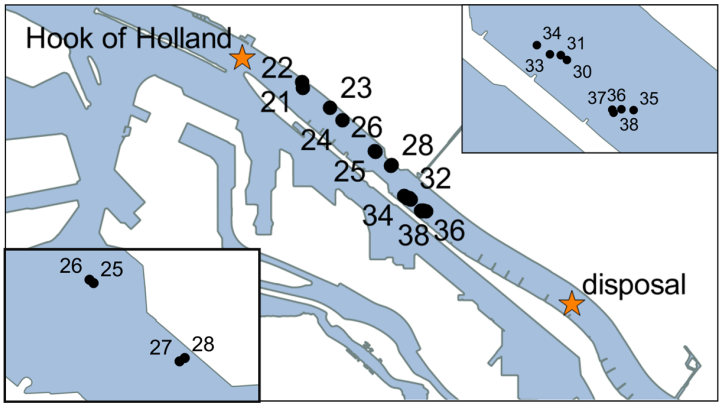

(b) Location of the silt profiler 1 - 7

Figure G.7: The location of the silt profiler measurements 22 to 28.

In fig. 6.19, the measured velocity and backscatter from the ADCP are shown. The first three measurements (22-24) are taken while sailing from Hook of Holland towards the Maeslantkering. Measurement 22 and 23, fig. G.8a show a more or less homogeneous SPM distribution over the vertical, with only a minor increase towards the bed. Measurement 24 shows a distribution which seems in line with the measurements 6 and 7; a double 'peak' in the SPM concentration and a small decrease around the pycnocline due to reduced carrying capacity. Measurement 21 also shows this pattern of a limited carrying capacity around the pycnocline.

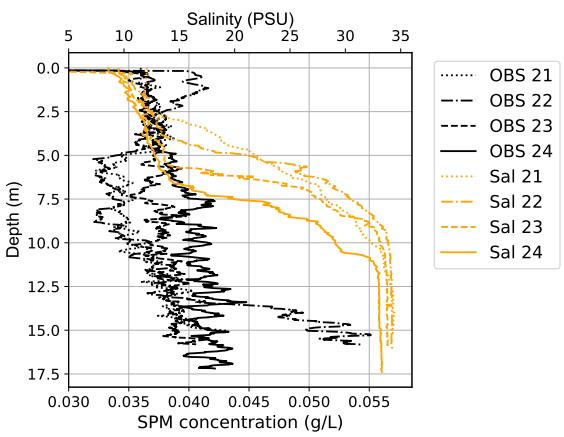

(a) Silt profiler measurements 21 to 24

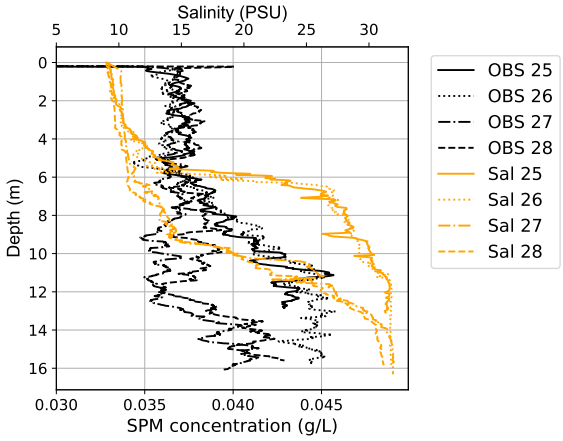

(b) Silt profiler measurements 25 to 28

Figure G.8: Silt profiler measurement 21-28 taken in period III, between 13:00 and 14:15, while sailing towards upstream. The black and gray lines indicate the concentration of SPM in g/l. The orange and red lines indicate the salinity over the vertical in PSU.

	11:50-12:50			11:50-13:50			11:50-14:50		
	avg. vel.	dist.	dist.	avg. vel.	dist.	dist	avg. vel.	dist.	dist.
2 - 4m	1.01	3.64	4.36	1.02	7.41	0.59	1.32	11.1	-3.1
4 - 6m	0.77	2.79	5.21	0.8	5.74	2.26	1.1	8.61	-0.61
6 - 8m	0.45	1.62	6.38	0.55	3.94	4.06	0.94	5.91	2.09
8 - 10m	0.24	0.85	7.15	0.39	2.79	5.21	0.84	4.18	3.82
10 - 12m	0.17	0.61	7.39	0.33	2.35	5.65	0.68	3.52	4.48
12 - 14m	0.21	0.78	7.22	0.32	2.34	5.66	0.54	3.51	4.49
14 - 16m	0.13	0.48	7.52	0.27	1.9	6.1	0.4	2.88	5.12

Table G.4: The average flow velocity taken measured obtained from ADCP flow measurements in m/s. The first distance is from the disposal site. The other distance mentioned the distance from Hook of Holland.

Period IV: 16:00 - 21:00

Between 15:40 - 16:45 the survey vessel sailed back to Maassluis, as shown in fig. G.10. During this trip no silt profiler measurements have been executed. From the ADCP backscatter one can observe a slight difference in absolute backscatter over the vertical. Moreover, close to the bed the LWS has taken place; hence little transport of sediment is expected due to a reduced flow velocity.

Between 16:45 and 18:00 the vessel sailed from the reallocation area downstream towards Hook of Holland, in the direction of the (depth-averaged) tide, but in opposite direction of the flow direction close to the bed. Again no irregularities are found from the ADCP backscatter or from the silt profiler measurements taken; measurements 39 - 42.

Silt profiler	Time	Distance (km)
17:00 - 18:00		
39	17:16	5.1
40	17:21	4.9
41	17:28	4.82
42	17:34	4.56
43	17:53	3.08
44	17:59	2.97

(a) Time and location of the silt profiler measurements 39 - 44

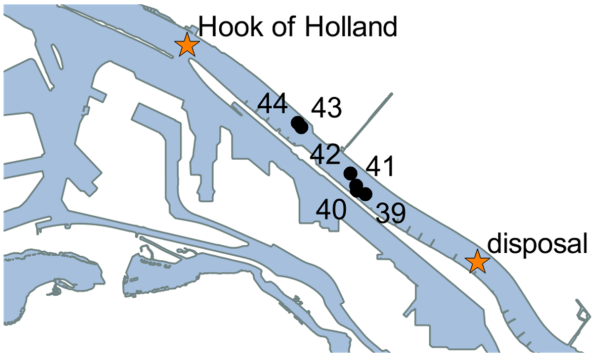

(b) Location of the silt profiler 39 - 44

Figure G.9: The location of the silt profiler measurements 39 to 44 taken while sailing towards Hook of Holland between 17:00 and 18:00, still during depth-averaged ebb.

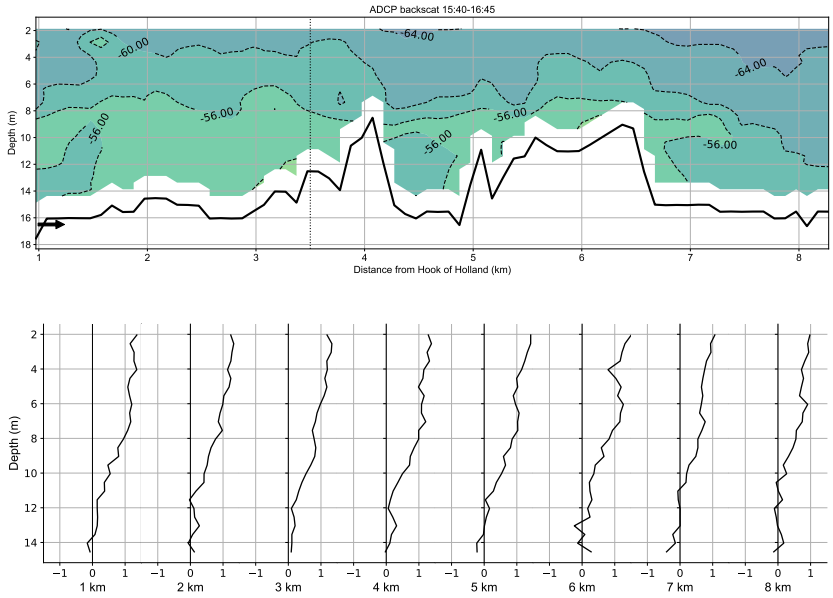

Figure G.10: ADCP backscatter (a) and velocities while sailing towards Hook of Holland between 15:40 and 16:45 just after disposal.

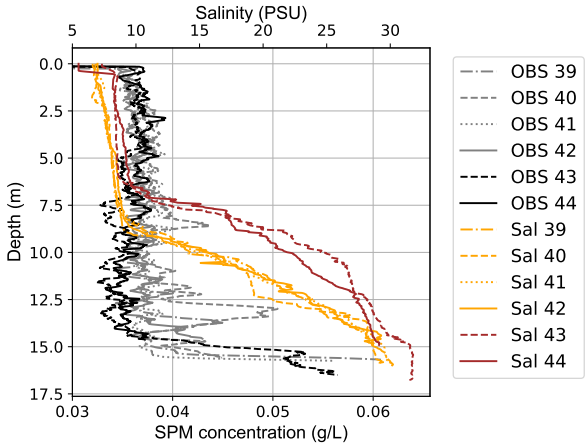

Figure G.11: Silt profiler measurement 39 to 44. The values 39 - 42 (downstream Maeslantkering) are shown in gray and the values upstream in black.

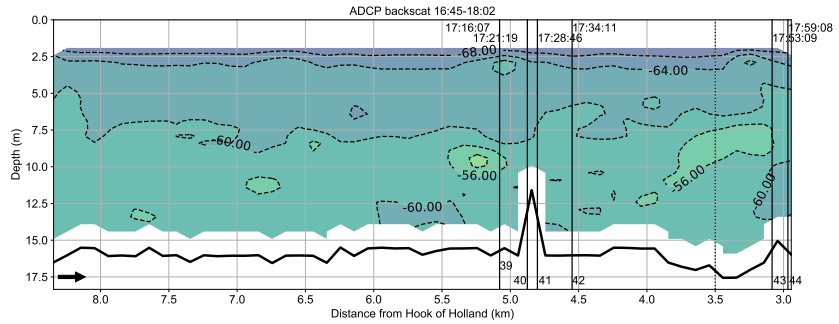

(a)

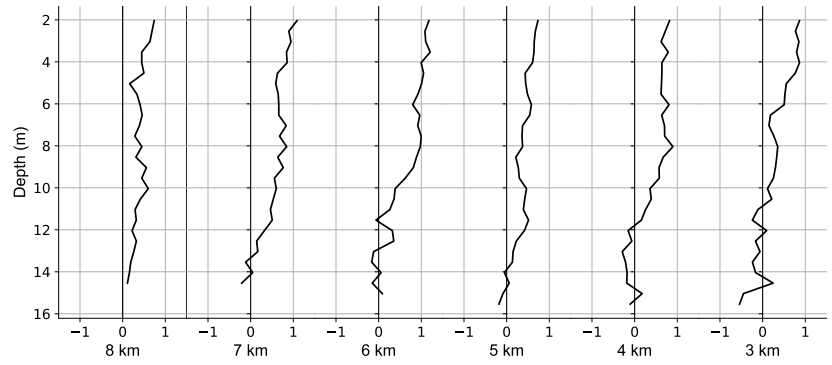

(b)

Figure G.12: ADCP backscatter (a) and velocities while sailing towards Hook of Holland between 16:45 and 18:00 just after disposal.

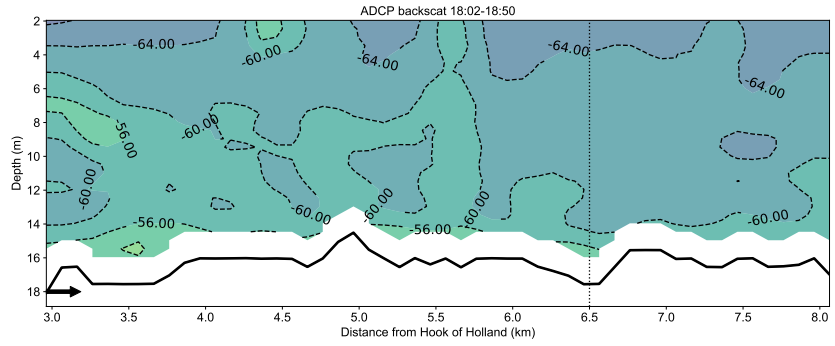

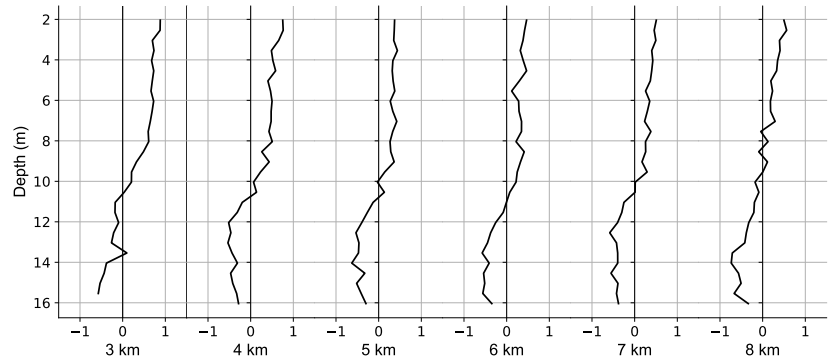

Figure G.13: ADCP backscatter (a) and velocities while sailing towards Hook of Holland between 18:00 and 18:50 just after disposal.

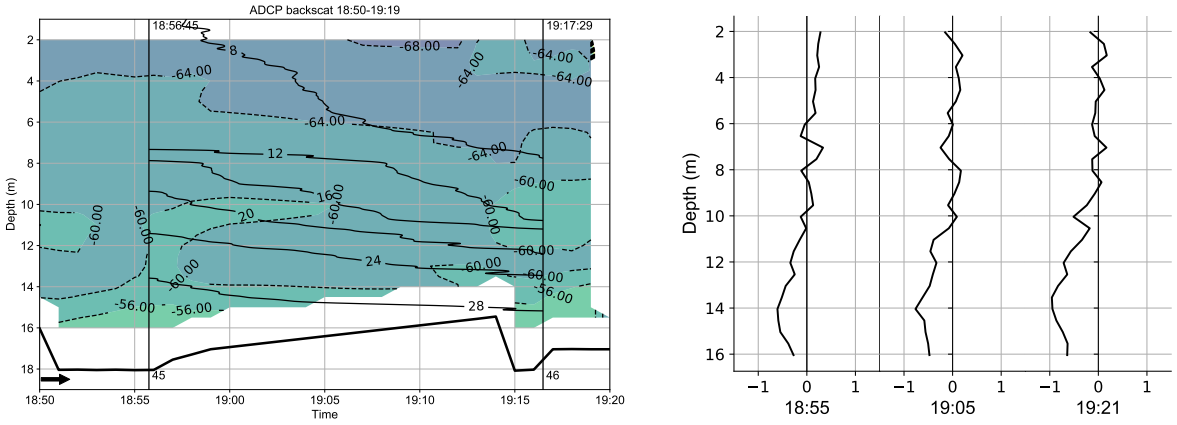

Figure G.14: ADCP backscatter and flow velocity between 18:50 and 19:20

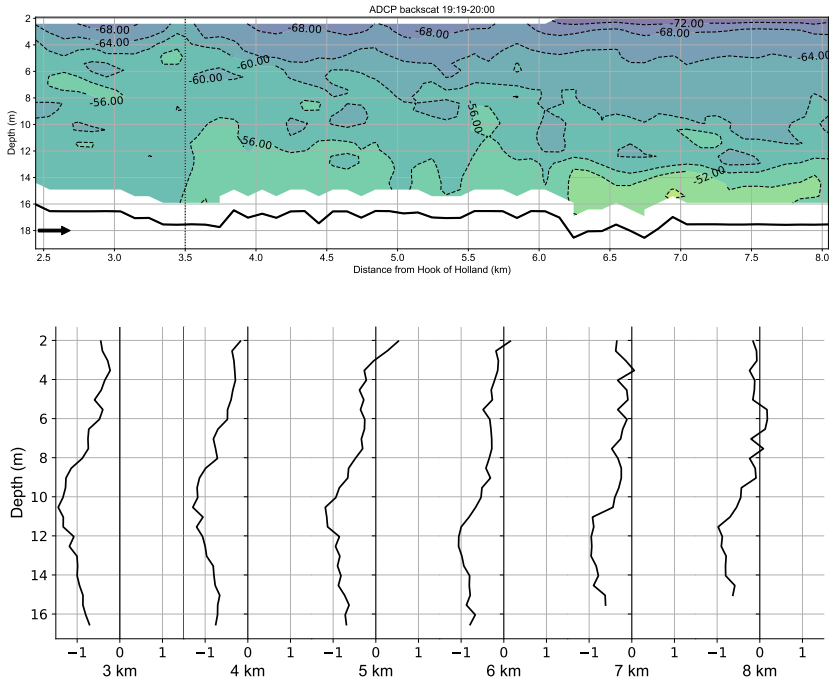

Figure G.15: ADCP backscatter and flow velocity while sailing towards Hook of Holland between 19:20 and 20:00 after disposal.

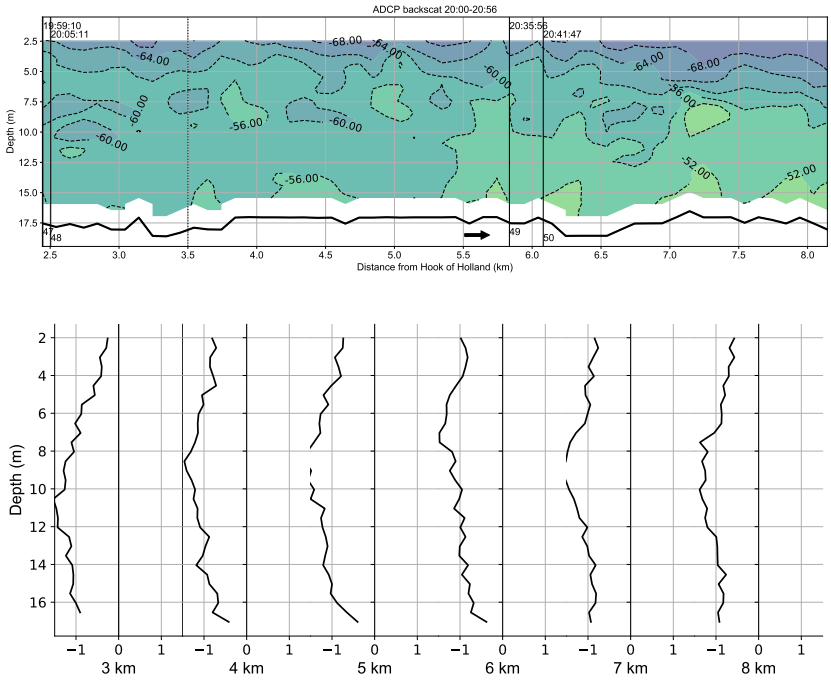

Figure G.16: ADCP backscatter (a) and velocities while sailing towards Hook of Holland between 20:00 and 20:50.

G.3. Long term measurement results

G.3.1. Grab sample

In the following pages the results of the individual grab sample results are displayed for the different times; T_0, T_1, T_2 and T_3.

First the results of the downstream analysis are displayed.

Below are the tables with the composition of the bed at the different times T_0, T_1 and T_2 and the change in bed composition for the downstream locations.

Down1	**Clay**	**Silt**	**Fine**	**Med.**	**Coar.**
T_0	0.89	15.03	53.35	25.51	5.15
T_1	2.62	69.82	20.36	6.68	0.51
T_2	3.96	54.09	39.16	2.80	0.00
$\Delta T_0 - T_1$	1.73	54.79	-32.99	-18.83	-4.64
$\Delta T_1 - T_2$	1.34	-15.73	18.80	-3.88	-0.51
$\Delta T_0 - T_2$	3.07	39.06	-14.19	-22.71	-5.15

(a) Grain size distribution of bed sample at *'Down1'*

Down2	**Clay**	**Silt**	**Fine**	**Med.**	**Coar.**
T_0	3.10	50.22	33.02	13.32	0.34
T_1	4.52	81.64	10.87	2.78	0.20
T_2	1.50	29.19	50.94	18.37	0.00
$\Delta T_0 - T_1$	1.42	31.42	-22.15	-10.54	-0.14
$\Delta T_1 - T_2$	-3.02	-52.45	40.07	15.59	-0.20
$\Delta T_0 - T_2$	-1.60	-21.03	17.92	5.05	-0.34

(b) Grain size distribution of bed sample at *'Down2'*

Down3	**Clay**	**Silt**	**Fine**	**Med.**	**Coar.**
T_0	2.80	38.88	41.78	16.10	0.43
T_1	2.32	58.80	32.63	6.07	0.18
T_2	2.62	47.87	37.84	11.08	0.58
$\Delta T_0 - T_1$	-0.48	19.92	-9.15	-10.03	-0.25
$\Delta T_1 - T_2$	0.30	-10.93	5.21	5.01	0.40
$\Delta T_0 - T_2$	-0.18	8.99	-3.94	-5.02	0.15

(c) Grain size distribution of bed sample at *'Down3'*

Down4	**Clay**	**Silt**	**Fine**	**Med.**	**Coar.**
T_0	2.50	35.82	37.78	22.97	0.91
T_1	2.85	54.81	28.07	14.09	0.18
T_2	2.75	62.92	27.69	6.62	0.03
$\Delta T_0 - T_1$	0.35	18.99	-9.71	-8.88	-0.73
$\Delta T_1 - T_2$	-0.10	8.11	-0.38	-7.47	-0.15
$\Delta T_0 - T_2$	0.25	27.10	-10.09	-16.35	-0.88

(d) Grain size distribution of bed sample at *'Down4'*

Down5	**Clay**	**Silt**	**Fine**	**Med.**	**Coar.**
T_0	3.85	78.46	14.23	3.44	0.01
T_1	2.62	74.34	16.38	6.56	0.10
T_2	3.89	78.51	12.70	4.86	0.05
$\Delta T_0 - T_1$	-1.23	-4.12	2.15	3.12	0.09
$\Delta T_1 - T_2$	1.27	4.17	-3.68	-1.70	-0.05
$\Delta T_0 - T_2$	0.04	0.05	-1.53	1.42	0.04

(e) Grain size distribution of bed sample at *'Down5'*

Figure G.17: The grain size distributions of the bed samples taken at the downstream locations at T_0, T_1 and T_2. *'Fine'*, *'Med.'* and *'Coar.'* refer to Fine sand, medium coarse sand and coarse sand.

Disposal area

In the following pages the results of the individual grab sample results are shown for the samples taken close to the disposal area at different times; T_0, T_1, T_2 and T_3.

Disp1	Clay	Silt	Fine	Med.	Coar.
T_0	2.21	30.15	48.95	18.52	0.17
T_1	2.03	29.28	45.55	22.90	0.23
T_2	2.82	60.12	28.80	7.05	1.20
$\Delta T_0 - T_1$	-0.18	-0.87	-3.40	4.38	0.06
$\Delta T_1 - T_2$	0.79	30.84	-16.75	-15.85	0.97
$\Delta T_0 - T_2$	0.61	29.97	-20.15	-11.47	1.03

(a) Grain size distribution of bed sample at *'Disp1'*

Disp2	Clay	Silt	Fine	Med.	Coar.
T_0	1.17	13.48	57.09	28.27	0.00
T_1	4.50	72.82	11.42	10.11	1.15
T_2	1.82	32.69	48.95	16.55	0.00
$\Delta T_0 - T_1$	3.33	59.34	-45.67	-18.16	1.15
$\Delta T_1 - T_2$	-2.68	-40.13	37.53	6.44	-1.15
$\Delta T_0 - T_2$	0.65	19.21	-8.14	-11.72	0.00

(b) Grain size distribution of bed sample at *'Disp2'*

Disp3	Clay	Silt	Fine	Med.	Coar.
T_0	0.43	10.68	69.72	19.17	0.00
T_1	4.13	79.76	12.68	3.36	0.06
T_2	2.58	52.25	33.40	11.52	0.26
$\Delta T_0 - T_1$	3.70	69.08	-57.04	-15.81	0.06
$\Delta T_1 - T_2$	-1.55	-27.51	20.72	8.16	0.20
$\Delta T_0 - T_2$	2.15	41.57	-36.32	-7.65	0.26

(c) Grain size distribution of bed sample at *'Disp3'*

Disp4	Clay	Silt	Fine	Med.	Coar.
T_0	3.23	42.05	36.45	17.98	0.29
T_1	3.08	60.67	26.82	9.01	0.41
T_2	2.76	51.20	36.06	9.91	0.06
$\Delta T_0 - T_1$	-0.15	18.62	-9.63	-8.97	0.12
$\Delta T_1 - T_2$	-0.32	-9.47	9.24	0.90	-0.35
$\Delta T_0 - T_2$	-0.47	9.15	-0.39	-8.07	-0.23

(d) Grain size distribution of bed sample at *'Disp4'*

Figure G.18: The grain size distributions of the bed samples taken at close to the disposal area at T_0, T_1 and T_2. *'Fine'*, *'Med.'* and *'Coar.'* refer to Fine sand, medium coarse sand and coarse sand.

Upstream

Up1	Clay	Silt	Fine	Med.	Coar.
T_0	3.36	58.55	30.75	7.26	0.09
T_1	3.30	63.58	26.57	6.43	0.12
T_2	4.04	73.48	19.63	2.85	0.00
$\Delta T_0 - T_1$	-0.06	5.03	-4.18	-0.83	0.03
$\Delta T_1 - T_2$	0.74	9.90	-6.94	-3.58	-0.12
$\Delta T_0 - T_2$	0.68	14.93	-11.12	-4.41	-0.09

(a) Grain size distribution of bed sample at *'Up1'*

Up2	Clay	Silt	Fine	Med.	Coar.
T_0	4.68	43.83	41.44	10.06	0.00
T_1	4.57	77.17	15.39	2.79	0.09
T_2	5.00	73.69	17.69	3.56	0.05
$\Delta T_0 - T_1$	-0.11	33.34	-26.05	-7.27	0.09
$\Delta T_1 - T_2$	0.43	-3.48	2.30	0.77	-0.04
$\Delta T_0 - T_2$	0.32	29.86	-23.75	-6.50	0.05

(b) Grain size distribution of bed sample at *'Up2'*

Up3	Clay	Silt	Fine	Med.	Coar.
T_0	3.47	52.82	32.21	11.49	0.00
T_1	4.04	78.68	14.52	2.45	0.31
T_2	3.15	71.14	22.20	3.51	0.00
$\Delta T_0 - T_1$	0.57	25.86	-17.69	-9.04	0.31
$\Delta T_1 - T_2$	-0.89	-7.54	7.68	1.06	-0.31
$\Delta T_0 - T_2$	-0.32	18.32	-10.01	-7.98	0.0

(c) Grain size distribution of bed sample at *'Up3'*

Up4	Clay	Silt	Fine	Med.	Coar.
T_0	3.29	42.63	36.04	16.72	1.31
T_1	2.81	58.00	28.94	9.28	0.97
T_2	2.81	60.71	27.05	8.67	0.76
$\Delta T_0 - T_1$	-0.48	15.37	-7.10	-7.44	-0.34
$\Delta T_1 - T_2$	0.00	2.71	-1.89	-0.61	-0.21
$\Delta T_0 - T_2$	-0.48	18.08	-8.99	-8.05	-0.55

(d) Grain size distribution of bed sample at *'Up4'*

Figure G.19: The grain size distributions of the bed samples taken at the locations upstream of the disposal area at T_0, T_1 and T_2. *'Fine'*, *'Med.'* and *'Coar.'* refer to Fine sand, medium coarse sand and coarse sand.

Dredging location

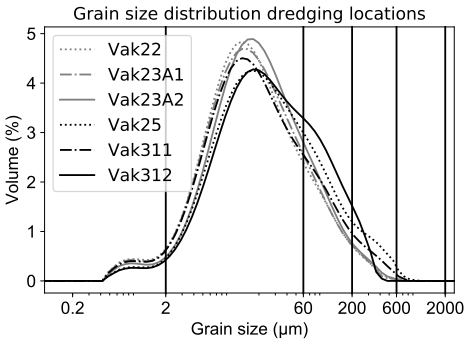

(a) Grain size distribution of bed samples at the dredging sites

	Clay	Silt	Fine	Med.	Coar.
Vak22	4.51	78.72	14.22	2.53	0.02
Vak23A,1	4.31	78.49	14.67	2.47	0.05
Vak23A,2	3.51	77.48	16.18	2.81	0.02
Vak25	2.89	70.95	19.38	6.44	0.34
Vak31,1	4.13	74.90	16.42	4.42	0.13
Vak31,2	2.73	69.78	23.14	4.35	0.00

(b) Grain size distribution of bed samples at the dredging sites

Figure G.20: The grain size distributions of the bed samples taken at the dredging locations or sediment source at T_0, T_1 and T_2. *'Fine'*, *'Med.'* and *'Coar.'* refer to Fine sand, medium coarse sand and coarse sand.

Vak 22 until Vak25 are located in the Waalhaven and Vak 31,1 and Vak 31,2 are located in the Waalhaven.

		Clay	Silt	Sand	Gravel
2018					
	NMS9,1	11.9	25.0	45.1	18.0
	NMS9,2	11.7	28.7	42.6	17.0
2019					
	NMS9,1	10.8	24.7	47.5	17.0
	NMS9,2	11.7	22.4	43.4	22.5
	Average:	11.5	25.2	44.7	18.6

Table G.5: Grain size distribution of the samples taken from the New Meuse. [van Bruchem, 2019]

G.3.2. Flocculation

To determine the tendency of suspended matter to flocculate the ζ-potential can be used as an parameter. In Mohan [2019] this is done for all samples. In fig. G.21 it can be seen that none of the samples has a ζ-potential above -10; which is the threshold for flocculation. Therefore it is concluded that flocculation will not occur.

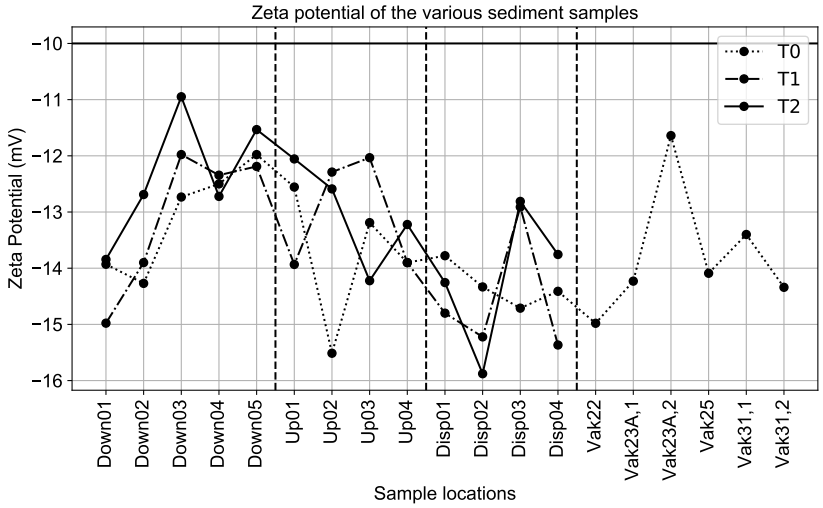

Figure G.21: The Zeta potential of the various samples.

This is confirmed by Eisma et al. [1991b] who investigated the tendency of Rhine sediment to flocculate. Moreover the consistency in zeta potential of the samples confirm another conclusion of Eisma et al. [1991b]; *There is no consistent evidence that salt flocculation is an important factor in river mouths.*

As flocculation does not occur it can be neglected in the determination of e.g. sediment settling velocities.

H

Model results

H.1. Short term model validation

In the following section the results of the hydrodynamic model are compared to the measurements. This is done for the measuring stations as well as the measurements from the survey.

H.1.1. Measuring stations

A comparison with the measuring stations is done to verify the hydrodynamic performance on the day of interest.

Hook of Holland

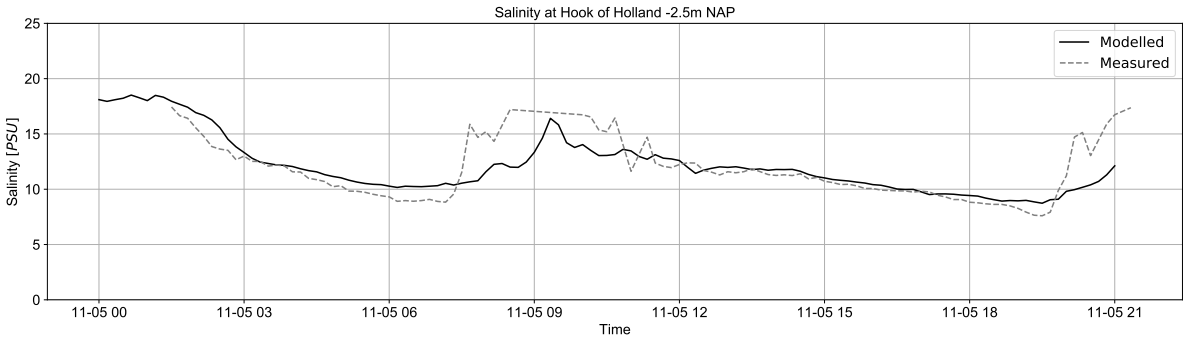

Figure H.1: Comparison of measured and modelled salinity at Hook of Holland at -2.5m NAP on November 5.

Lekhaven

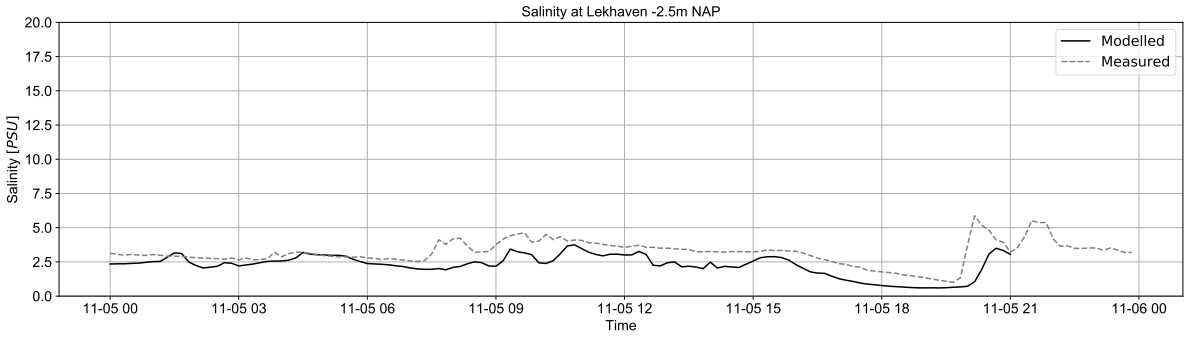

Figure H.2: Comparison of measured and modelled salinity at Lekhaven at -2.5m NAP between on November 5.

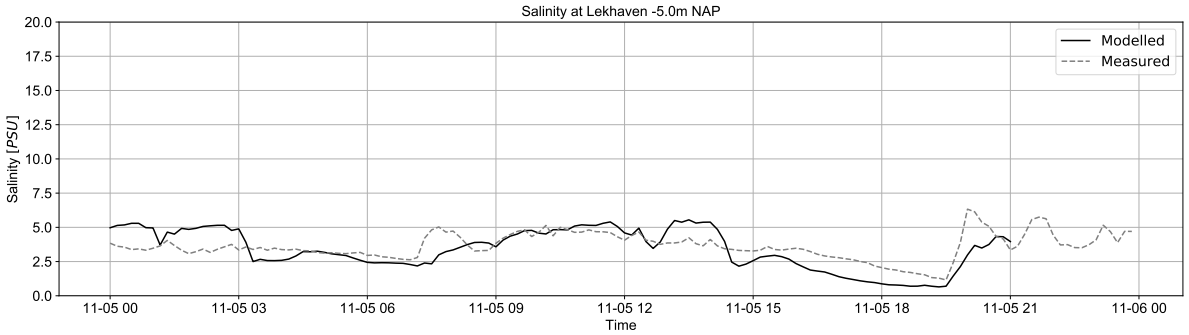

Figure H.3: Comparison of measured and modelled salinity at Lekhaven at -5.0m NAP on November 5.

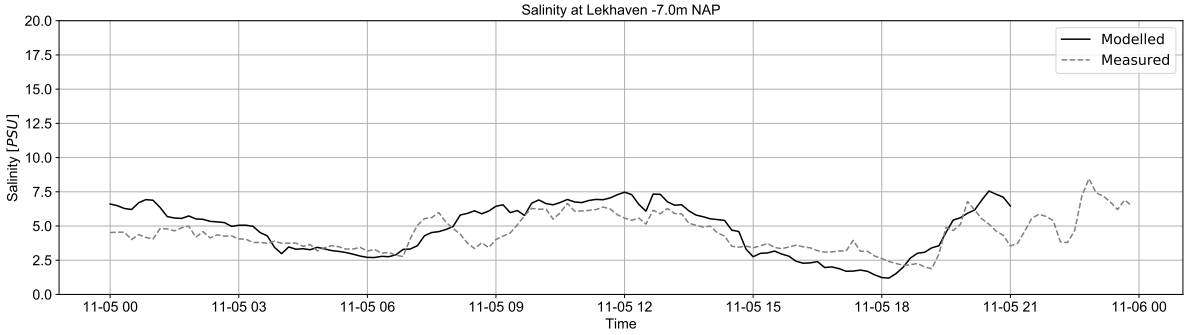

Figure H.4: Comparison of measured and modelled salinity at Lekhaven at -7.0m NAP on November 5.

Spijkenisserbrug

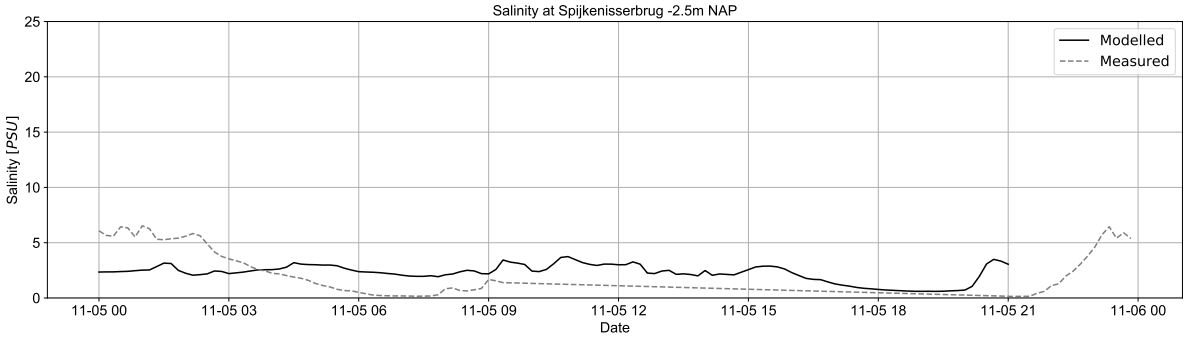

Figure H.5: Comparison of measured and modelled salinity at Spijkennisserbrug at -2.5m NAP on November 5.

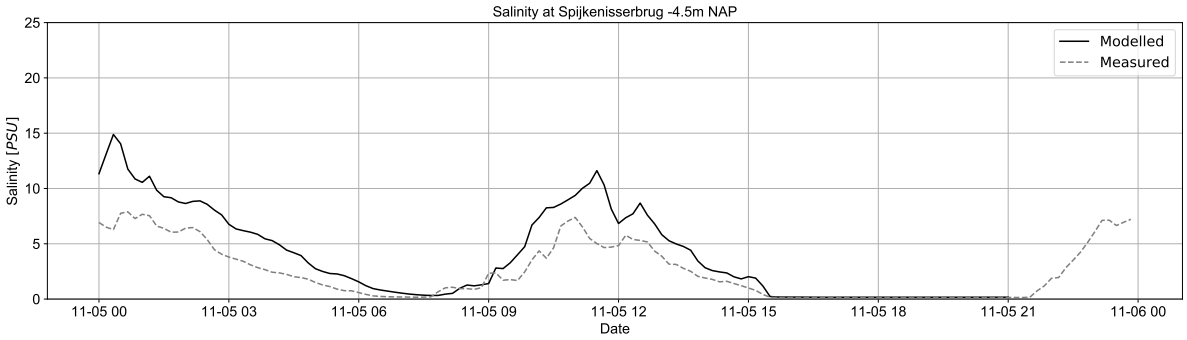

Figure H.6: Comparison of measured and modelled salinity at Spijkennisserbrug at -4.5m NAP on November 5.

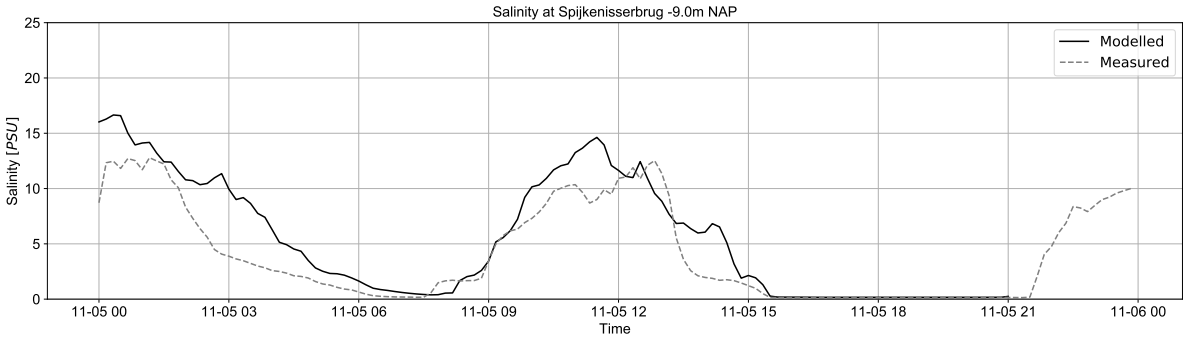

Figure H.7: Comparison of measured and modelled salinity at Spijkennisserbrug at -9.0m NAP on November 5.

H.1.2. Water level validation

In the following figures, appendix H.1.2 the water level as computed by Simona is compared with the measuring stations in and outside our area of interest. In general it can be concluded that the water level prediction is very good and consistent in time. Only around HW and LW small discrepancies occur, especially at Vlaardingen. Moreover, the tidal asymmetry is evident with HW at 8:10, 8:30 and 9:00 and LW at 14:40, 14:50 and 15:20, at Hook of Holland, Maassluis and Vlaardingen.

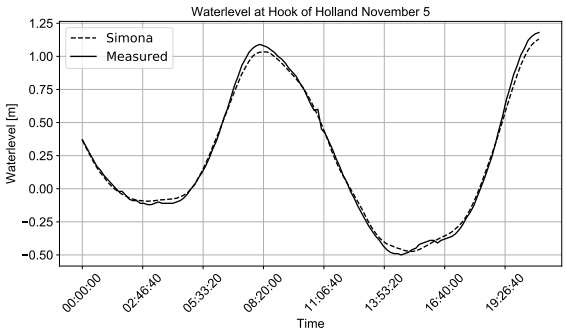

(a) The measured and modelled (SIMONA) water level at Hook of Holland

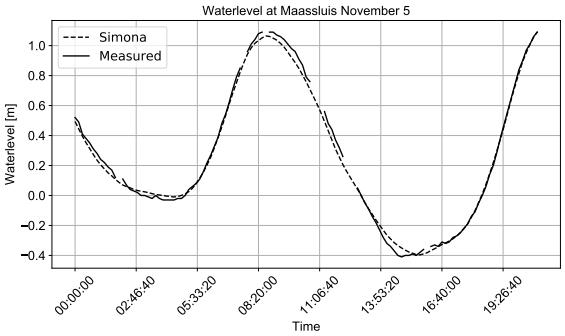

(b) The measured and modelled (SIMONA) water level at Maassluis

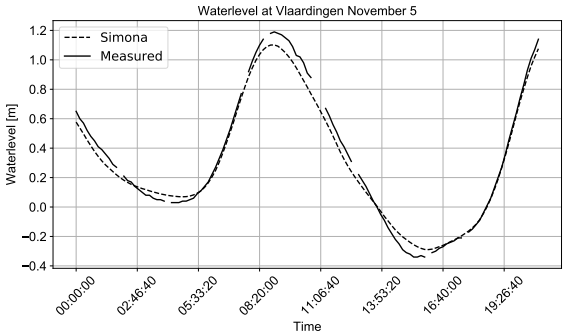

(c) The measured and modelled (SIMONA) water level at Vlaardingen

Figure H.8: Comparison of the measured and modelled water level at the measuring stations Hook of Holland, Maassluis and Vlaardingen (moving up estuary) on November 5, 2019.

H.1.3. Vertical salinity profiles

For the validation of the vertical salinity profiles the same structure with periods is used as in section 7.3, the periods are repeated below;

- **Period I (8:00 - 11:00):** These measurements are taken prior to the 11:00 disposal to measure incoming SPM during flood.
- **Period II (11:00 - 13:00):** These measurements are taken around the vessel and while sailing towards Hook of Holland following the plume.
- **Period III (13:00 - 16:00):** These measurements are taken after the signal of the plume is lost until Low Water Slack.
- **Period IV (16:00 - 21:00):** The last measurements are taken during rising tide to measure the amount of incoming SPM after flow reversal.

Period I: 8:00 - 11:00 Flood and HWS

A positive value for the difference between the measured and modelled value indicates an underestimation of the model, a negative value indicates an overestimation of the model.

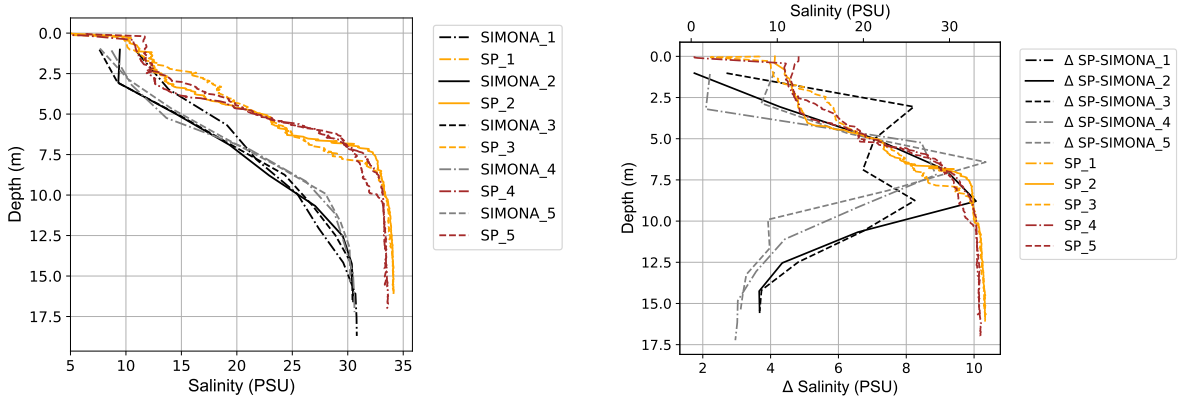

(a) The measured (SP) and modelled (SIMONA) vertical salinity profiles

(b) Difference in the measured (SP) and modelled (SIMONA) vertical salinity profiles

Figure H.9: Comparison of SIMONA output and Siltprofiler measurement 1 - 5. *'SP'* refers to the measured salinity by the silt profiler which is an average value of upcast and downcast. Δ *SP-SIMONA* refers to the difference between the measured (SP) value and the modeled value by SIMONA.

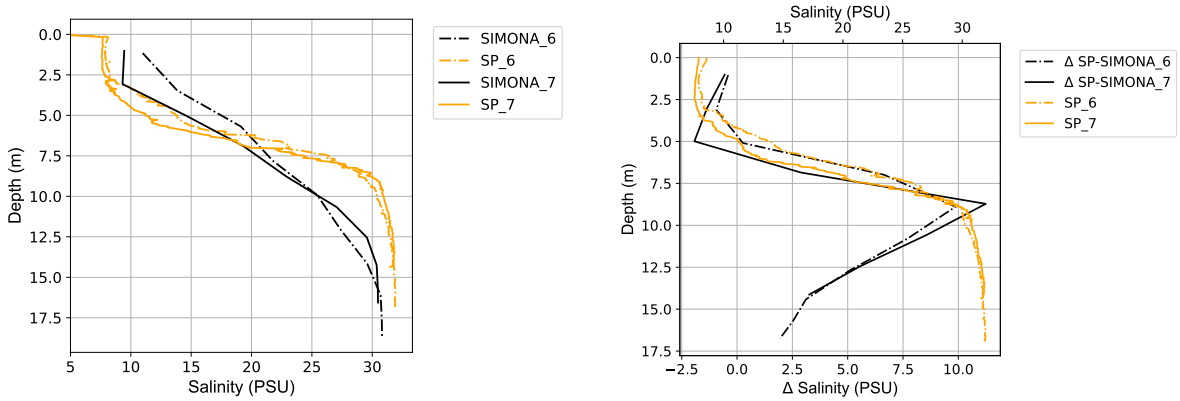

(a) The measured (SP) and modelled (SIMONA) vertical salinity profiles

(b) Difference in the measured (SP) and modelled (SIMONA) vertical salinity profiles

Figure H.10: Comparison of SIMONA output and Siltprofiler measurement 6 - 7. *'SP'* refers to the measured salinity by the silt profiler which is an average value of upcast and downcast. Δ *SP-SIMONA* refers to the difference between the measured (SP) value and the modeled value by SIMONA

Period II: 11:00 - 13:00 Eb

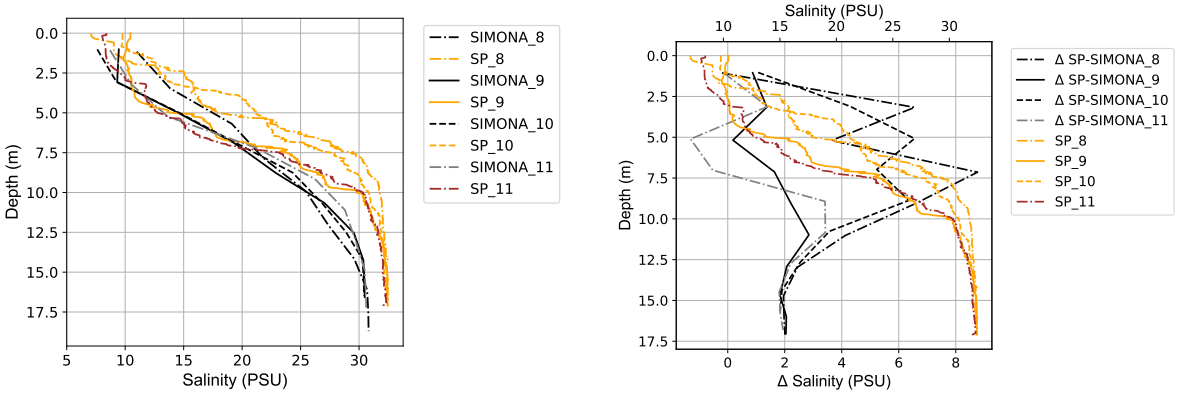

(a) The measured (SP) and modelled (SIMONA) vertical salinity profiles

(b) Difference in the measured (SP) and modelled (SIMONA) vertical salinity profiles

Figure H.11: Comparison of SIMONA output and Siltprofiler measurement 8 - 11. *'SP'* refers to the measured salinity by the silt profiler which is an average value of upcast and downcast. Δ *SP-SIMONA* refers to the difference between the measured (SP) value and the modeled value by SIMONA

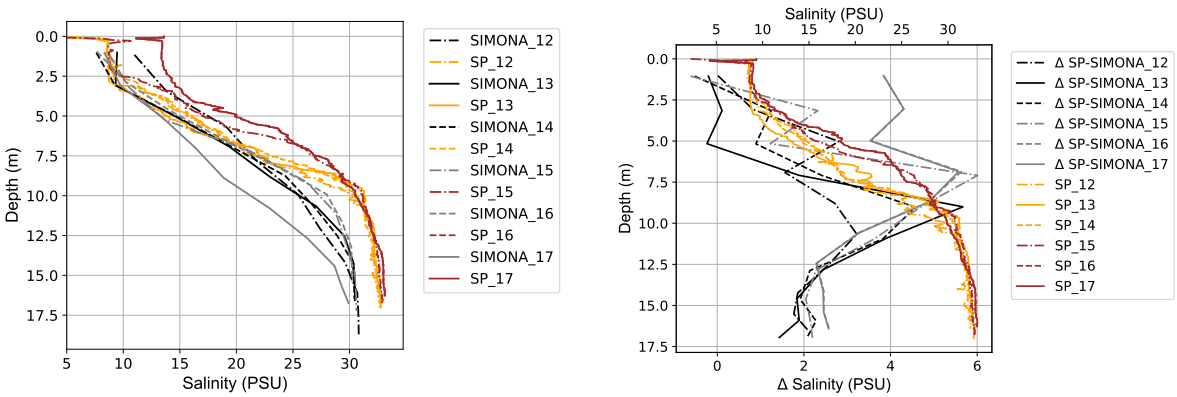

(a) The measured (SP) and modelled (SIMONA) vertical salinity profiles

(b) Difference in the measured (SP) and modelled (SIMONA) vertical salinity profiles

Figure H.12: Comparison of SIMONA output and Siltprofiler measurement 12 - 17. *'SP'* refers to the measured salinity by the silt profiler which is an average value of upcast and downcast. Δ *SP-SIMONA* refers to the difference between the measured (SP) value and the modeled value by SIMONA

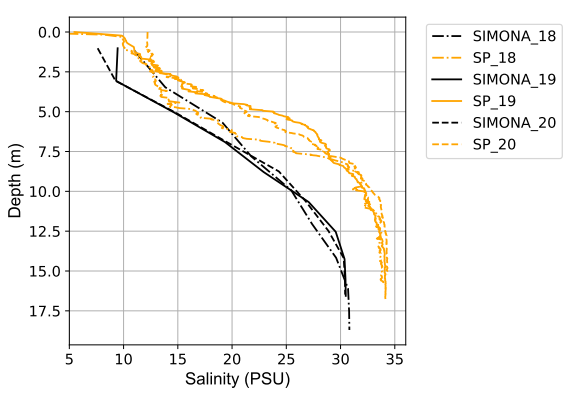

(a) The measured (SP) and modelled (SIMONA) vertical salinity profiles

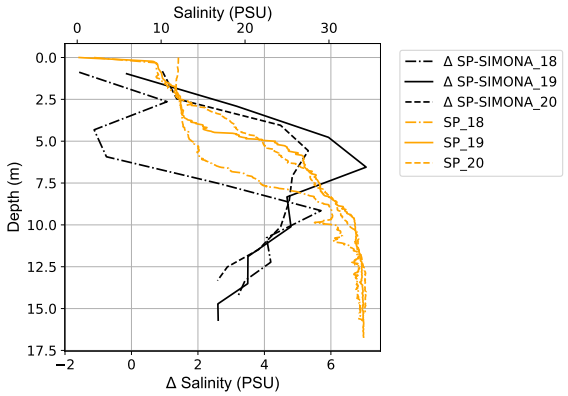

(b) Difference in the measured (SP) and modelled (SIMONA) vertical salinity profiles

Figure H.13: Comparison of SIMONA output and Siltprofiler measurement 18 - 20. *'SP'* refers to the measured salinity by the silt profiler which is an average value of upcast and downcast. Δ *SP-SIMONA* refers to the difference between the measured (SP) value and the modeled value by SIMONA

Period III: 13:00 - 16:00 Ebb

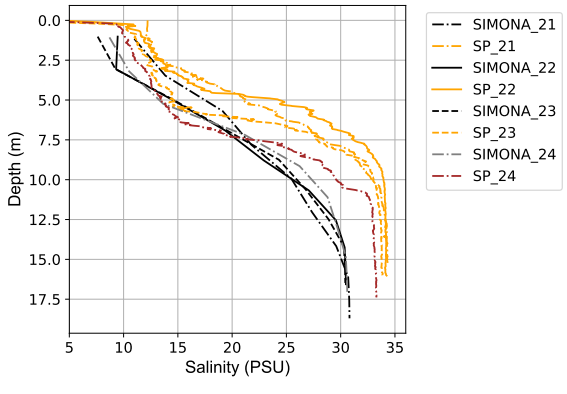

(a) The measured (SP) and modelled (SIMONA) vertical salinity profiles

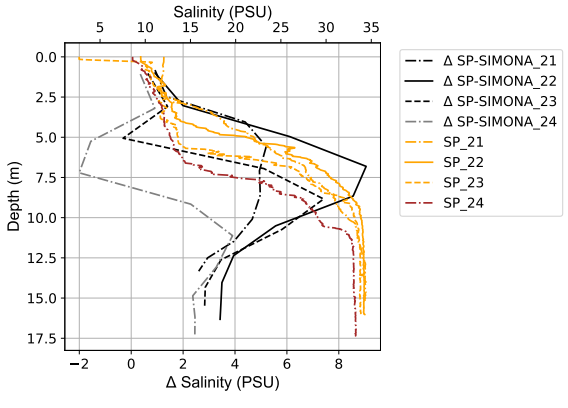

(b) Difference in the measured (SP) and modelled (SIMONA) vertical salinity profiles

Figure H.14: Comparison of SIMONA output and Siltprofiler measurement 18 - 20. *'SP'* refers to the measured salinity by the silt profiler which is an average value of upcast and downcast. Δ *SP-SIMONA* refers to the difference between the measured (SP) value and the modeled value by SIMONA

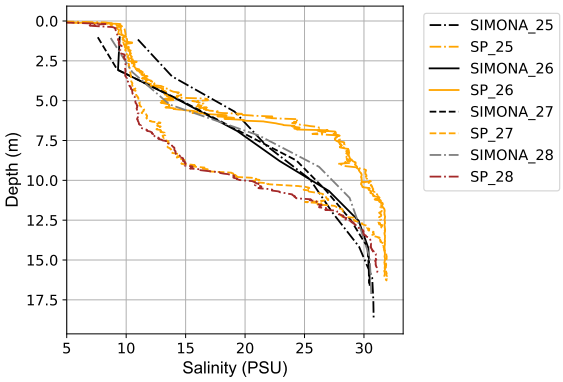

(a) The measured (SP) and modelled (SIMONA) vertical salinity profiles

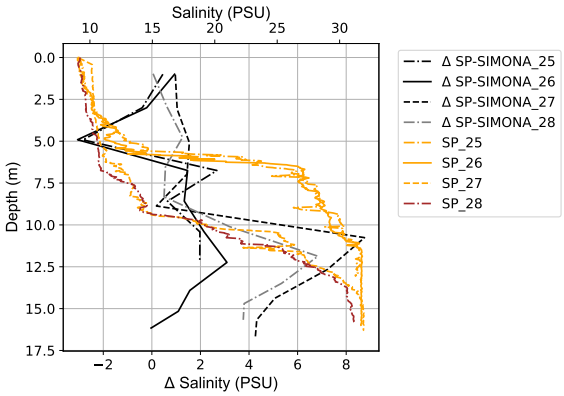

(b) Difference in the measured (SP) and modelled (SIMONA) vertical salinity profiles

Figure H.15: Comparison of SIMONA output and Siltprofiler measurement 25 - 28. *'SP'* refers to the measured salinity by the silt profiler which is an average value of upcast and downcast. Δ *SP-SIMONA* refers to the difference between the measured (SP) value and the modeled value by SIMONA

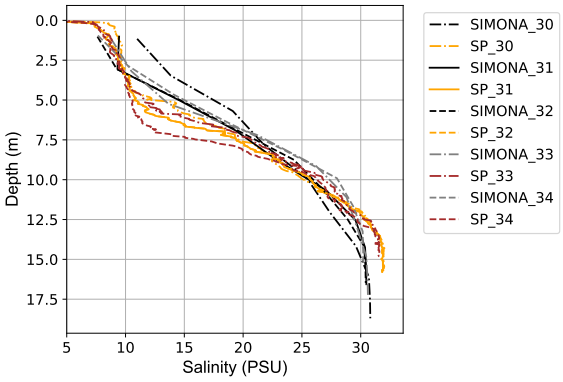

(a) The measured (SP) and modelled (SIMONA) vertical salinity profiles

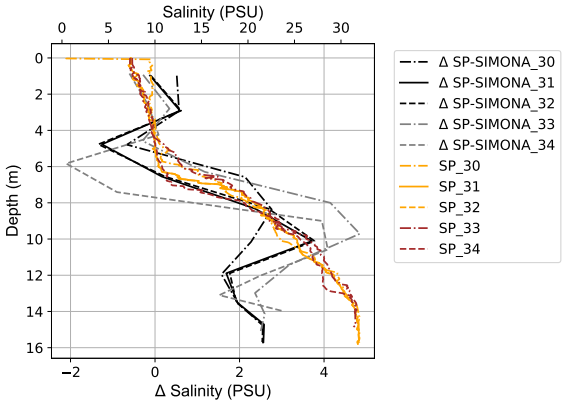

(b) Difference in the measured (SP) and modelled (SIMONA) vertical salinity profiles

Figure H.16: Comparison of SIMONA output and Siltprofiler measurement 30 - 34. *'SP'* refers to the measured salinity by the silt profiler which is an average value of upcast and downcast. Δ *SP-SIMONA* refers to the difference between the measured (SP) value and the modeled value by SIMONA

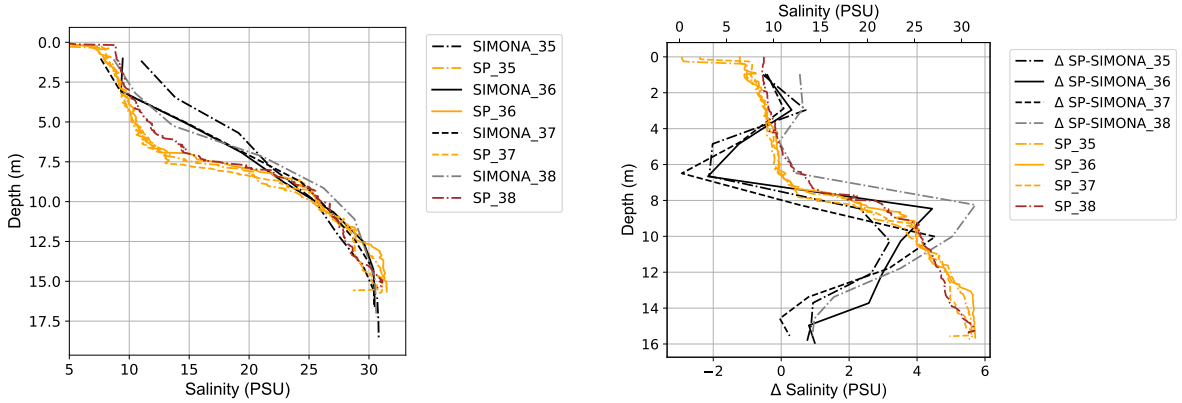

(a) The measured (SP) and modelled (SIMONA) vertical salinity profiles

(b) Difference in the measured (SP) and modelled (SIMONA) vertical salinity profiles

Figure H.17: Comparison of SIMONA output and Siltprofiler measurement 35 - 38. *'SP'* refers to the measured salinity by the silt profiler which is an average value of upcast and downcast. Δ *SP-SIMONA* refers to the difference between the measured (SP) value and the modeled value by SIMONA

Period IV: 16:00 - 21:00 LWS to Flood

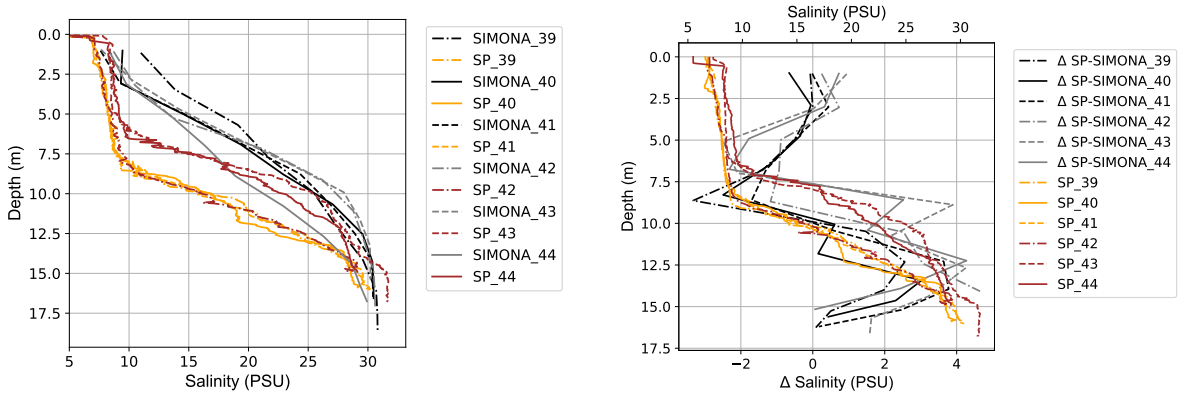

(a) The measured (SP) and modelled (SIMONA) vertical salinity profiles

(b) Difference in the measured (SP) and modelled (SIMONA) vertical salinity profiles

Figure H.18: Comparison of SIMONA output and Siltprofiler measurement 39 - 44. *'SP'* refers to the measured salinity by the silt profiler which is an average value of upcast and downcast. Δ *SP-SIMONA* refers to the difference between the measured (SP) value and the modeled value by SIMONA

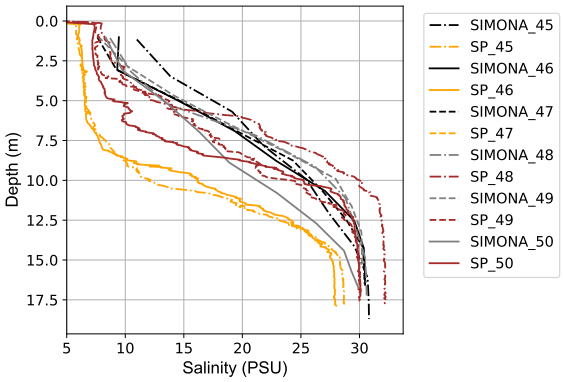

(a) The measured (SP) and modelled (SIMONA) vertical salinity profiles

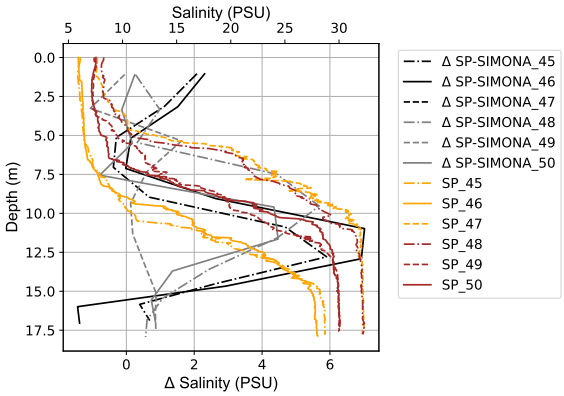

(b) Difference in the measured (SP) and modelled (SIMONA) vertical salinity profiles

Figure H.19: Comparison of SIMONA output and Siltprofiler measurement 45 - 50. *'SP'* refers to the measured salinity by the silt profiler which is an average value of upcast and downcast. Δ *SP-SIMONA* refers to the difference between the measured (SP) value and the modeled value by SIMONA

CTD vs Siltprofiler August 13

On November 5 only the silt profiler has been deployed to measure the salinity over the vertical. However on August 13, during fairly similar conditions both the silt profiler and CTD have been used to determine the salinity over the vertical. From the two profiles below it can be seen that a small difference arises between the silt profiler and CTD measurement taken during ebb, appendix H.1.3 a) (9:10) and flood appendix H.1.3 b) (14:22)

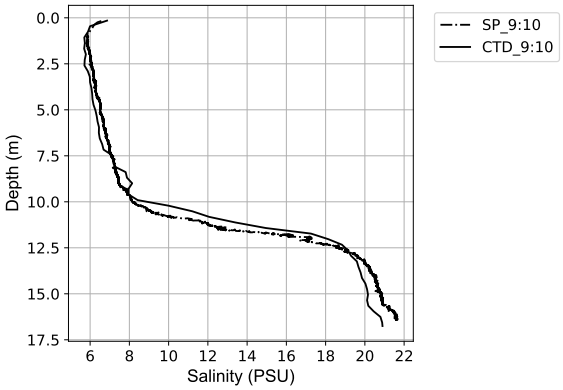

(a) The salinity according to the CTD and silt profiler measured at August 13, 9:10

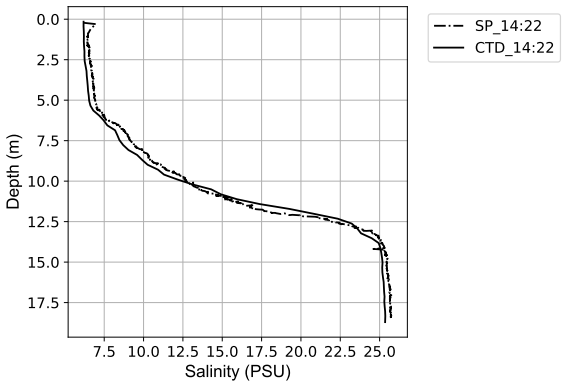

(b) The salinity according to the CTD and silt profiler measured at August 13, 14:22

Figure H.20: Comparison of the measured salinity by the CTD and silt profiler during ebb a) (9:10) and flood b) (14:22) on August 13, 2019.

H.1.4. Sensitivity disposal rate

As stated in section 3.1.1 the majority of the sediment is released by drawing the bottom doors instead of using the bow coupling. The main difference between these two methods is the depth of disposal (which is discussed above) and rate of disposal; the average rate of disposal using bow coupling is approximately 1.3 m^3/s (0.47 TDM / s), whereas this yields 22.1 m^3/s (7.9 TDM / s) for a disposal by bottom door.

As can be seen in table H.1 the effect of the disposal rate itself is negligible on the mass balances of the areas considered.

	Maasmond				Disposal Area			
	NWW in & out	NWW - Beer	NS net.	NS flux	Ups.	Down.	Susp.	Settle
Base case	11%	7%	13%	13%	18%	41%	5%	39%
Long dur.	11%	7%	13%	13%	18%	40%	4%	40%

Table H.1: Composition of the plume for different model runs, varying in grain size distribution.

However, it is expected that the rate of disposal merely influences near field effects and sediment induced buoyancy effects. When a high disposal rate is used, local sediment concentrations can be significantly increased. This may alter the turbulence field. However, these effect are not resolved by the model used.

H.2. Long term model validation

H.2.1. Measuring stations

For the long term modelling the hydrodynamics from August 30 - September 13 are used and repeated. In the following section the hydrodynamics are validated based on the fixed measuring stations at Hook of Holland (-2.5m NAP), Lekhaven (-2.5m, -5m, -7.0m NAP) and Spijkenisserbrug (-2.5m, -4.5m, -9.0m NAP). To do so, time series of water level and salinity are compared;

Hook of Holland

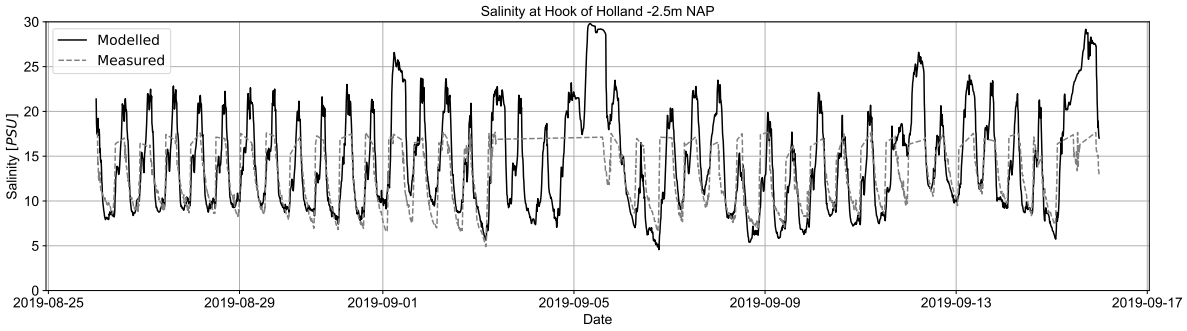

Figure H.21: Comparison of measured and modelled salinity at Hook of Holland at -2.5m NAP between August 26 and September 16.

Lekhaven

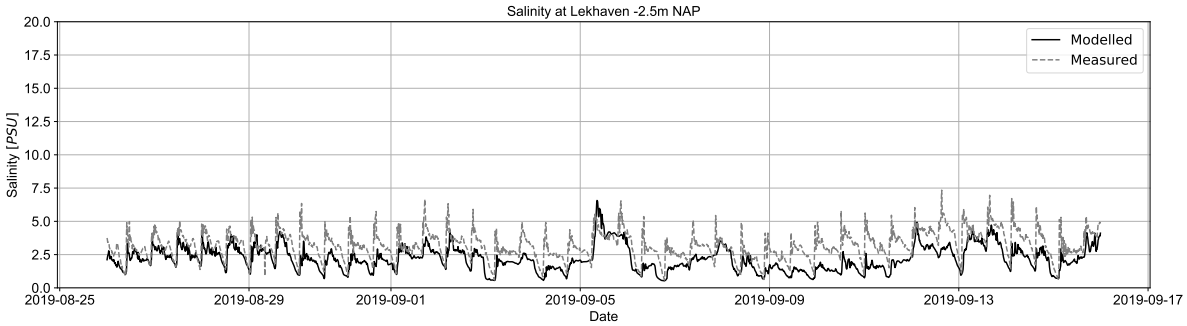

Figure H.22: Comparison of measured and modelled salinity at Lekhaven at -2.5m NAP between August 26 and September 16.

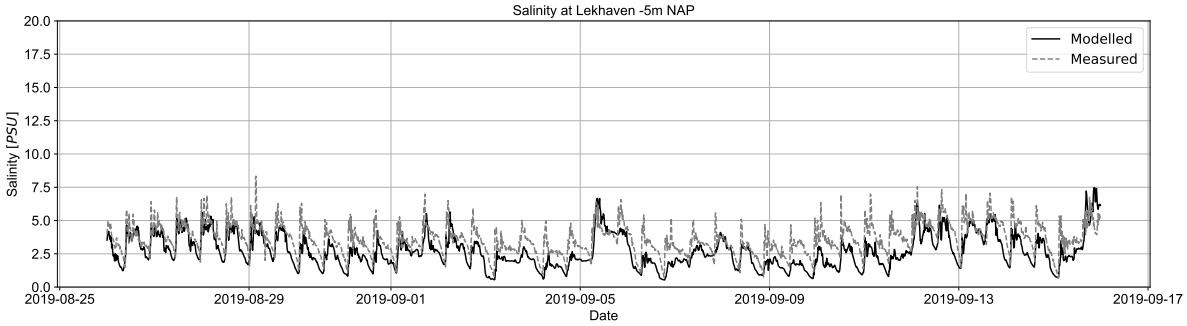

Figure H.23: Comparison of measured and modelled salinity at Lekhaven at -5.0m NAP between August 26 and September 16.

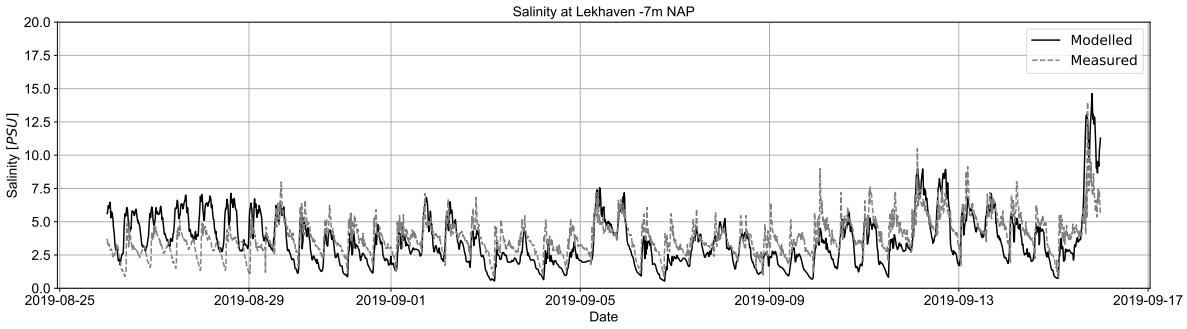

Figure H.24: Comparison of measured and modelled salinity at Lekhaven at -7.0m NAP between August 26 and September 16.

Spijkenisserbrug

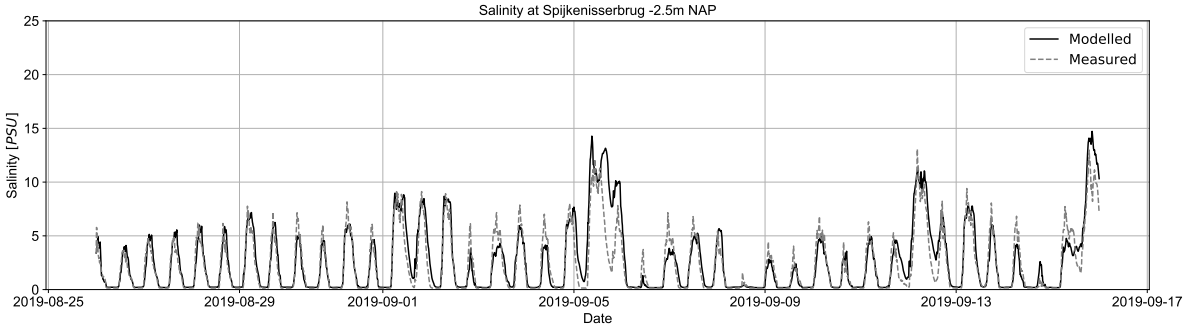

Figure H.25: Comparison of measured and modelled salinity at Spijkennisserbrug at -2.5m NAP between August 26 and September 16.

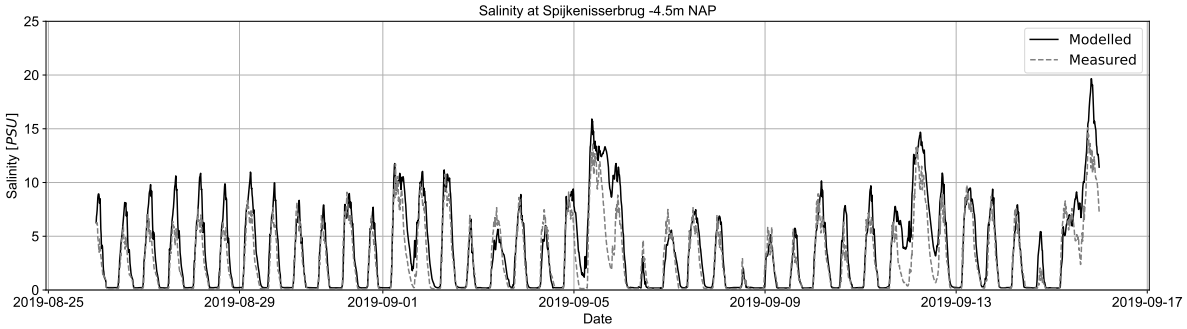

Figure H.26: Comparison of measured and modelled salinity at Spijkennisserbrug at -4.5m NAP between August 26 and September 16.

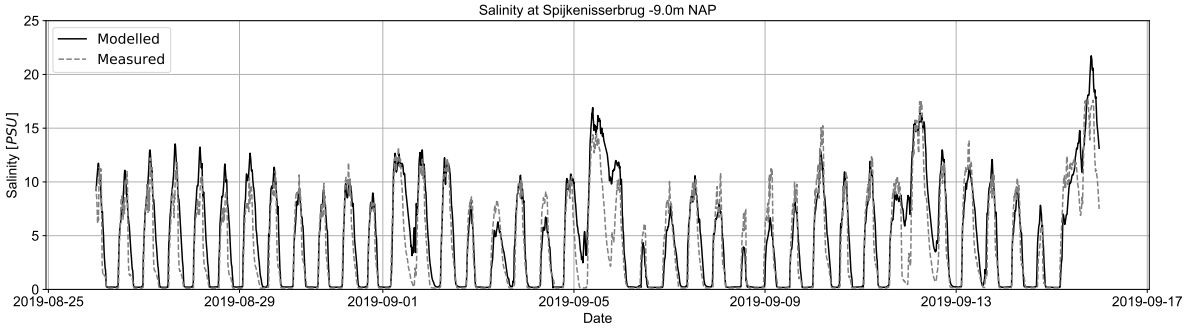

Figure H.27: Comparison of measured and modelled salinity at Spijkennisserbrug at -9.0m NAP between August 26 and September 16.

H.2.2. Modelling results

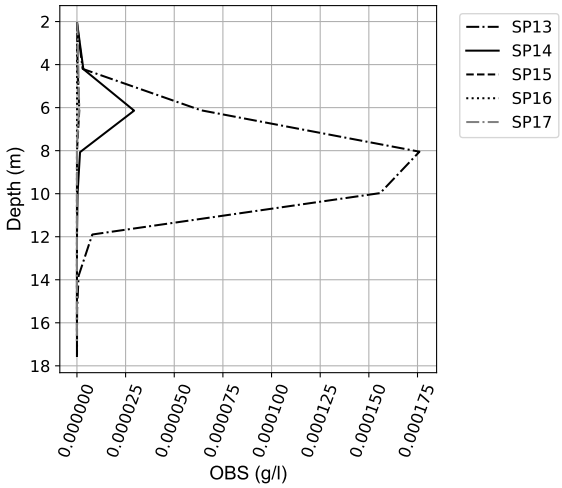

Figure H.28: Model results at location and time of silt profiler measurements 13 - 17. The location and time of the vertical profiles agrees with the location and time of the measurement shown in chapter 6.

H.2.3. Sensitivity analysis

In the following paragraph the supporting plots are provided for the tentative conclusion on the sensitivity for the grain-size of the fractions IM1 and IM2. To do so the amount of sediment of each fraction (IM1,IM2) at the end of the run is displayed for the surface layer (layer 1), a layer halfway the water column (layer 5) and the bed layer (layer 10).

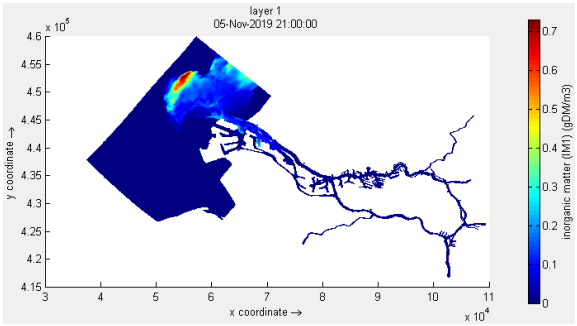

(a) Amount of IM1 in suspension in layer 1

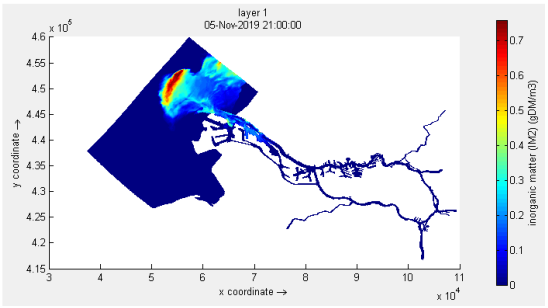

(b) Amount of IM2 in suspension in layer 1

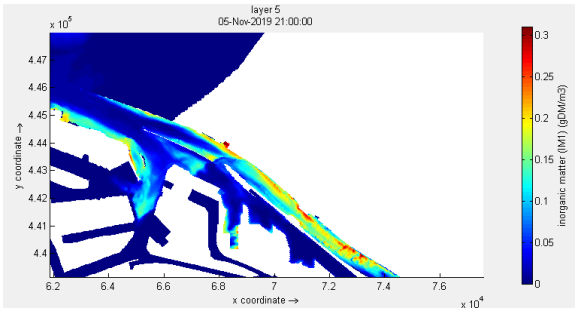

(c) Amount of IM1 in suspension in layer 5

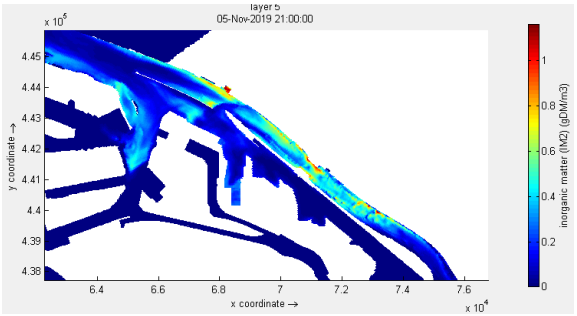

(d) Amount of IM2 in suspension in layer 5

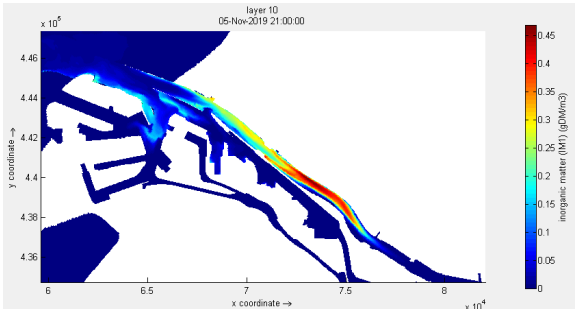

(e) Amount of IM1 in suspension in layer 10

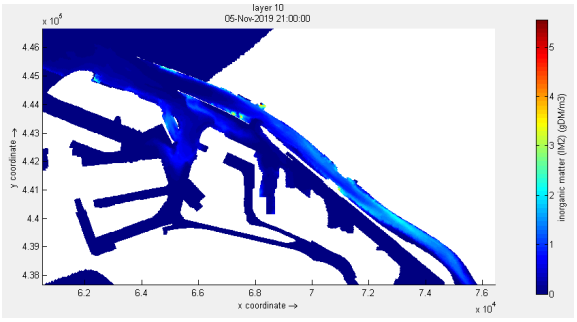

(f) Amount of IM2 in suspension in layer 10

Figure H.29: The amount of sediment in suspension at the end of the simulation 21:00 for the different layers; surface layer 1, halfway the water column layer 5 and close to the bed layer 10.

H.2.4. Eulerian perspective

The measurements executed in chapter 6 are from an Lagrangian perspective with a frame of reference moving with the assumed advection of the plume. However, e.g. de Nijs [2012] used a combination of a Lagrangian and Eulerian frame of reference (FOR) to determine the advection of the salt wedge. It is therefore investigated, if a Eulerian FOR is suitable to determine the sediment plume dynamics. These results are shown from an Eulerian FOR to verify whether the Eulerian FOR is suitable to evaluate the plume behaviour, as well as the performance of the models. This is done by determining the SPM concentration at Maassluis, the disposal site, the Maeslantkering and Hook of Holland.

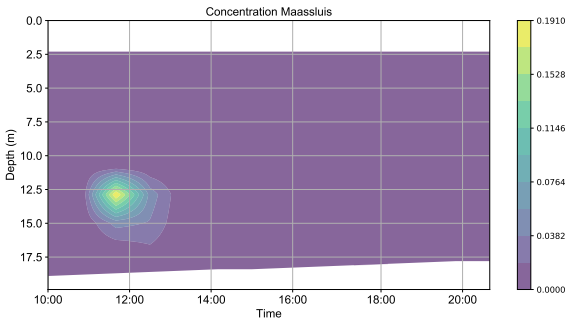

(a) Concentration SPM (g/l) at Maassluis in time

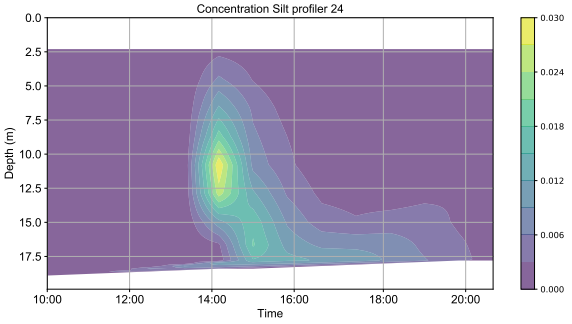

(b) Concentration SPM (g/l) at Maeslantkering in time

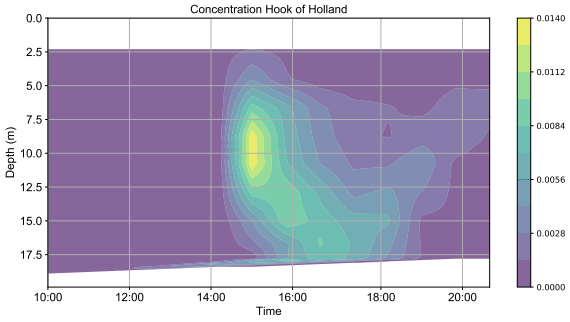

(c) Concentration SPM (g/l) at Hook of Holland in time

Figure H.30: Potential locations for Eulerian measurements to assess the mid field behaviour of the plume released by bow coupling.

In fig. H.30 it can be seen that the sediment plume is subject to significant dispersion. In fig. H.30 a) at the site of disposal the peak concentration is 0.19 g/l, which is significantly larger than the background concentration. However two hours later, at 14:00 at the Maeslantkering (fig. H.30 b)) which is 4.5 km downstream of the disposal site, the plume has spread over the entire vertical and the peak concentration is limited to 0.03 g/l. 1 hour later, the peak concentration is noticeable at Hook of Holland ((fig. H.30 c)) which is 3.5 km downstream of the Maeslantkering. This peak concentration has been subject to more dispersion as the peak concentration is limited to 0.01 g/l.

For the base case, which represents a disposal by bottom door, the concentration of SPM in time at the same locations is extracted from the model results. In fig. H.31 these model results of the base case modelling are shown in an Eulerian FOR at Bocht van Maassluis, Maeslantkering and Hook of Holland.

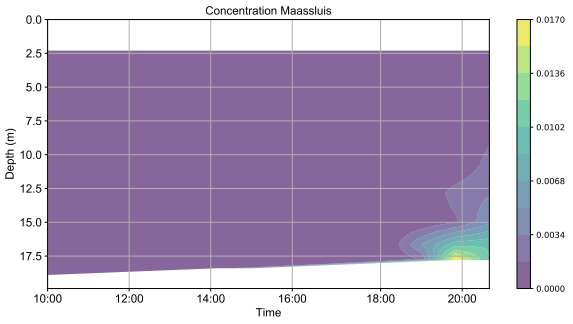

(a) Concentration in (g/l) at Maassluis in time

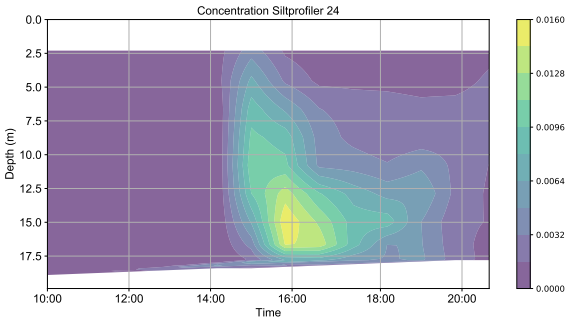

(b) Concentration in (g/l) at Maeslantkering in time

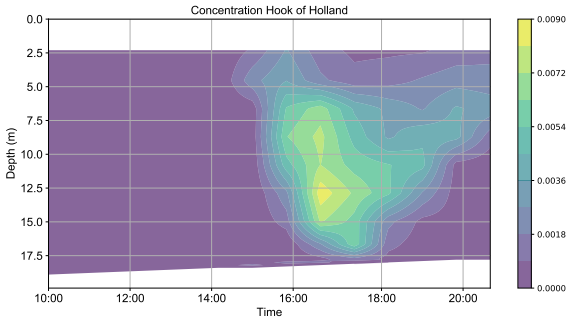

(c) Concentration in (g/l) at Hook of Holland in time

Figure H.31: Potential locations for Eulerian measurements to assess the mid field behaviour of the plume released by bottom door.

From the modelling results in an Eulerian perspective it becomes clear that for the base case, plume related concentrations are even smaller and therefore harder to be distinguished from the background concentration. As shown in chapter 2 and chapter 6 the background concentration close to the bed is at least $\mathcal{O}(0.05\ g/l)$, with peak values of 1 g/l and concentrations above the pycnocline around $\mathcal{O}(0.02\ g/l)$. .

Therefore, the plume related concentrations lie within a range of expected variation in background concentration and can therefore not be excluded. From table 7.2 it is known that 39 % of the sediment disposed for the base case settles within the vicinity of the disposal site. This explains the peak at 20:00 at Maassluis, which is eroded sediment from the 11:00 - 11:50 disposal.

Due to the significant dispersion, plume related concentrations SPM decrease significantly in a limited period of time and space both for the base case (fig. H.31) and the Nov 5 modelling (fig. H.30). Therefore, plume related concentrations will be difficult to distinguish from the background concentration. Based on this latter statement, measurements from an Eulerian perspective will not lead to more reliable results.

H.3. Long term model results

In the following two figures the amount of settled sediment and total amount of sediment in suspension is shown. The amount of sediment in suspension seems more or less in equilibrium at various locations, see (). The amount of settled sediment in the disposal area and Botlek is shown (). In this figure it can be seen that the amount of sediment in the bed is not yet in equilibrium.

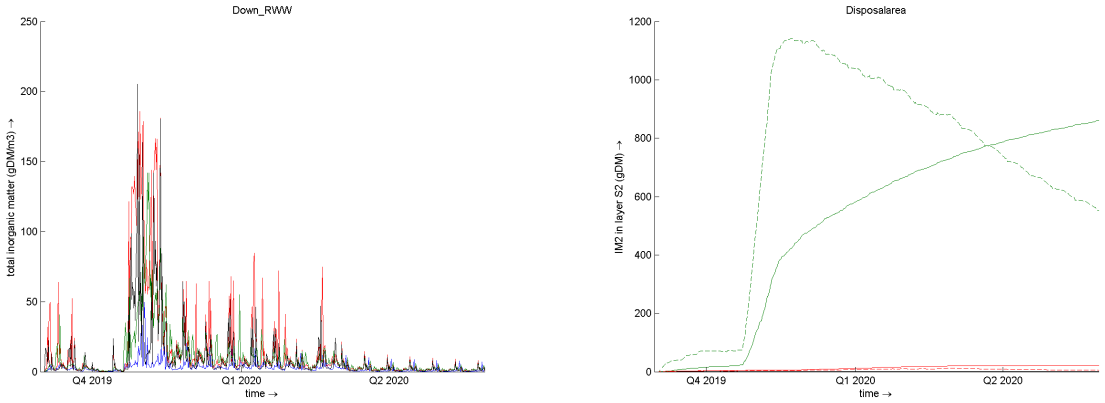

(a) (b)

Figure H.32: a) The total amount of sediment in suspension at the disposal location (black) , upstream (green) and downstream (red) of the disposal location and in the Botlek (blue). b) The amount of settled sediment in the bed at Botlek (straight lines) and disposal area (dashed lines) per sediment fraction (IM1S2 black, IM2S2 red, IM3S2 green).